ISSN 0012-1606
Volume 183, Number 1, March 1, 1997

DEVELOPMENTAL BIOLOGY

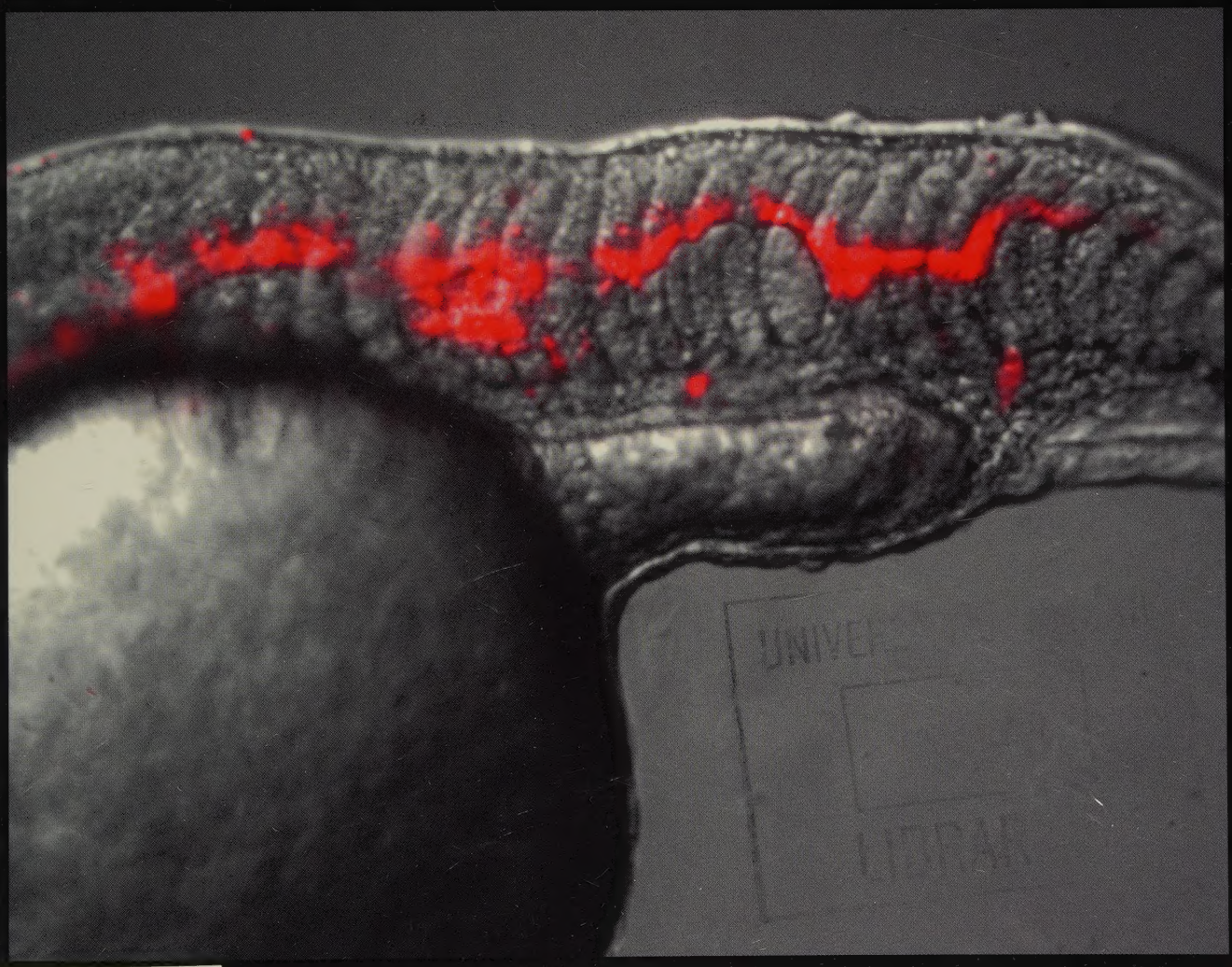

QH
301
D492

MIC PRESS

http://www.idealibrary.com/ http://www.europe.idealibrary.com/
Academic Press
Online Journal Library
IDEAL
Full-text journals on the Internet!

Cover photo. Mosaic analysis of *flh* embryos transplanted with wild-type cells. Composite rhodamine epifluorescence (red) and Nomarski (gray) videomicrograph of the trunk of a 25 somite *flh* mutant embryo that was transplanted at the blastoderm stage.

See the article by Fouquet *et al.*, pages 37–48, in this issue.

DEVELOPMENTAL BIOLOGY

(ISSN 0012-1606)

Published semimonthly by Academic Press, 6277 Sea Harbor Drive, Orlando, FL 32887-4900

1997: Volumes 181–192. Price: $2350.00 U.S.A. and Canada; $2850.00 all other countries.
All prices include postage and handling.

Information concerning personal subscription rates may be obtained by writing to the Publishers. All correspondence and subscription orders should be addressed to the office of the Publishers at 6277 Sea Harbor Drive, Orlando, FL 32887-4900. Send notices of change of address to the office of the Publishers at least 6 to 8 weeks in advance. Please include both old and new addresses. POSTMASTER: Send changes of address to *Developmental Biology*, 6277 Sea Harbor Drive, Orlando, FL 32887-4900.
Periodicals postage paid at Orlando, FL, and at additional mailing offices.

COPYRIGHT © 1997 BY ACADEMIC PRESS

DEVELOPMENTAL BIOLOGY is a registered trademark
of Academic Press (a division of Harcourt Brace & Company)

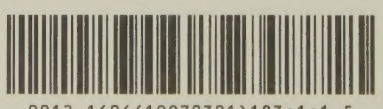

DEVELOPMENTAL BIOLOGY

Editor-in-Chief **Eric N. Olson**

Consulting Editor Helen M. Blau (Stanford, CA)

Editors

Marianne Bronner-Fraser (Pasadena, CA)
Eric H. Davidson (Pasadena, CA)
Scott Fraser (Pasadena, CA)
Richard Harland (Berkeley, CA)
Philip Ingham (London, U.K.)
Laurinda Jaffe (Farmington, CT)
Robb Krumlauf (London, U.K.)
Andrew P. McMahon (Cambridge, MA)
Gary Ruvkun (Boston, MA)
Matthew P. Scott (Stanford, CA)

Editorial Board

David Anderson (Pasadena, CA)
Kathryn Anderson (New York, NY)
Spyros Artavanis-Tsakonas (New Haven, CT)
Michael Bate (Cambridge, U.K.)
Richard R. Behringer (Houston, TX)
Allan Bradley (Houston, TX)
Peter J. Bryant (Irvine, CA)
Jose A. Campos-Ortega (Köln, Germany)
Mario R. Capecchi (Salt Lake City, UT)
Sean Carroll (Madison, WI)
Pierre Chambon (Strasbourg, France)
Bodo Christ (Freiburg, Germany)
Nam-Hai Chua (New York, NY)
Stephen Cohen (Heidelberg, Germany)
Igor B. Dawid (Bethesda, MD)
Edward M. De Robertis (Los Angeles, CA)
Wolfgang Driever (Freiburg, Germany)
Gregor Eichele (Houston, TX)
Anne Ephrussi (Heidelberg, Germany)
Richard A. Firtel (La Jolla, CA)
John Peter Gergen (Stony Brook, NY)
Iva Greenwald (New York, NY)
Ernst Hafen (Zurich, Switzerland)
Peter W. H. Holland (Reading, U.K.)
Yuh Nung Jan (San Francisco, CA)
Lawrence C. Katz (Durham, NC)
Rolf Kemler (Freiburg, Germany)
Cynthia Kenyon (San Francisco, CA)
Daniel P. Kiehart (Durham, NC)
William H. Klein (Houston, TX)
William J. Lennarz (Stony Brook, NY)
Maria Leptin (Köln, Germany)
Sharon R. Long (Palo Alto, CA)
David R. McClay (Durham, NC)
Barbara J. Meyer (Berkeley, CA)
Diana G. Myles (Davis, CA)
Drew M. Noden (Ithaca, NY)
Bradley B. Olwin (Boulder, CO)
Charles P. Ordahl (San Francisco, CA)
Stuart Orkin (Boston, MA)
Luis Parada (Dallas, TX)
Norbert Perrimon (Boston, MA)
James W. Posakony (La Jolla, CA)
Michael G. Rosenfeld (La Jolla, CA)
Nadia Rosenthal (Charlestown, MA)
Josh R. Sanes (St. Louis, MO)
Robert Schwartz (Houston, TX)
Barry D. Shur (Atlanta, GA)
Hermann Steller (Cambridge, MA)
Paul W. Sternberg (Pasadena, CA)
Masatoshi Takeichi (Kyoto, Japan)
Steve Wasserman (Dallas, TX)
David Wilkinson (London, U.K.)
Debra J. Wolgemuth (New York, NY)
William B. Wood (Boulder, CO)
Martin Yanofsky (La Jolla, CA)

Published under the Auspices of the Society for Developmental Biology

4 498HI XL 1368 9/97 31249-200 NULE

DEVELOPMENTAL BIOLOGY

Volume 183, Number 1, March 1, 1997

http://www.apnet.com

Copyright © 1997 by Academic Press. All Rights Reserved

No part of this publication may be reproduced or transmitted in any form, or by any means, electronic or mechanical, including photocopy, recording, or any information storage and retrieval system, without permission in writing from the Publisher.

The appearance of the code at the bottom of the first page of an article in this journal indicates the Publisher's consent that copies of the article may be made for personal or internal use, or for the personal or internal use of specific clients. This consent is given on the condition, however, that the copier pay the stated per copy fee through the Copyright Clearance Center, Inc. (222 Rosewood Drive, Danvers, Massachusetts 01923), for copying beyond that permitted by Sections 107 or 108 of the U.S. Copyright Law. This consent does not extend to other kinds of copying, such as copying for general distribution, for advertising or promotional purposes, for creating new collective works, or for resale. Copy fees for pre-1997 articles are as shown on the article title pages; if no fee code appears on the title page, the copy fee is the same as for current articles.

0012-1606/97 $25.00

MADE IN THE UNITED STATES OF AMERICA

This journal is printed on acid-free paper. ♾

DEVELOPMENTAL BIOLOGY is a registered trademark
of Academic Press (a division of Harcourt Brace & Company)

DEVELOPMENTAL BIOLOGY

Volume 183, Number 1, March 1, 1997

Contents

Stimulation of Tentacle and Bud Formation by the Neuropeptide Head Activator in *Hydra magnipapillata*	**Bert Hobmayer, Thomas W. Holstein, and Charles N. David**	**1**
Localization of MAP Kinase Activity in Early *Xenopus* Embryos: Implications for Endogenous FGF Signaling	**C. LaBonne and M. Whitman**	**9**
GATA-5: A Transcriptional Activator Expressed in a Novel Temporally and Spatially-Restricted Pattern during Embryonic Development	**Edward E. Morrisey, Hon S. Ip, Zhihua Tang, Min M. Lu, and Michael S. Parmacek**	**21**
Vessel Patterning in the Embryo of the Zebrafish: Guidance by Notochord	**Bernadette Fouquet, Brant M. Weinstein, Fabrizio C. Serluca, and Mark C. Fishman**	**37**
Branchial HOX Gene Expression and Human Craniofacial Development	**Isabelle Vieille-Grosjean, Paul Hunt, Massimo Gulisano, Edoardo Boncinelli, and Peter Thorogood**	**49**
tbx6, a *Brachyury*-Related Gene Expressed by Ventral Mesendodermal Precursors in the Zebrafish Embryo	**Barbara Hug, Virginia Walter, and David Jonah Grunwald**	**61**
Characterisation of Amphioxus HNF-3 Genes: Conserved Expression in the Notochord and Floor Plate	**Sebastian M. Shimeld**	**74**
Regeneration of *Sarcophaga* Imaginal Discs *in Vitro:* Implication of 20-Hydroxyecdysone	**Takekazu Kunieda, Shoichiro Kurata, and Shunji Natori**	**86**
Steroid Hormones Act Directly to Trigger Segment-Specific Programmed Cell Death of Identified Motoneurons *in Vitro*	**Laura C. Streichert, Jonathan T. Pierce, Julie A. Nelson, and Janis C. Weeks**	**95**
SOX9 Binds DNA, Activates Transcription, and Coexpresses with Type II Collagen during Chondrogenesis in the Mouse	**Ling-Jim Ng, Susan Wheatley, George E. O. Muscat, John Conway-Campbell, Jo Bowles, Edwina Wright, Donald M. Bell, Patrick P. L. Tam, Kathryn S. E. Cheah, and Peter Koopman**	**108**
Features		**f-1**

NOTICE

Academic Press is pleased to announce that this journal (and all 178 journals published by Academic Press) is now available electronically from our International Digital Electronic Access Library (IDEAL).

IDEAL, a three-year pilot project, exploits the World Wide Web on the Internet to significantly expand and improve access to scientific journals. It uses an efficient no-nonsense approach based on an open, nonproprietary modular architecture. Starting with the 1996 issues, an average 2000 articles published in Academic Press journals will be added to IDEAL every month.

To create this IDEAL environment, Academic Press has formed an alliance with Fujitsu/ICL, a major international technology provider. To ensure efficient access from all points of the globe, so-called "mirror sites" — identical databases — have been set up in the United States and Europe. Other sites will be set up later in Japan and elsewhere.

Anyone with access to the Internet will be able to browse the IDEAL database of journal tables of contents with any standard World Wide Web browser, such as Netscape, at no charge. For a limited time, searching and browsing of abstracts will also be free.

In addition, Academic Press has developed a group licensing scheme called APPEAL (Academic Press Print and Electronic Access License) for libraries. The ultimate aim is to allow convenient access to many more people than is currently possible with the print product only. As part of this license, authorized users at sites within licensed library networks will be able to view, print, and download complete articles using a PDF viewer, such as Adobe's ACROBAT (currently available via the AP WWW home page, for free). There are no restrictions for personal use, but license conditions do apply for other uses.

If you are at a site that does not (yet) have a license, please ask your librarian to contact us at one of the addresses listed below to determine whether a convenient consortium can be found and a license issued.

We invite you to visit IDEAL through AP's home page at http://www.apnet.com.

For further information, please contact:

Ken Metzner
Academic Press
San Diego, U.S.A.
kmetzner@acad.com

or

Chris Gibson
Academic Press Ltd.
London, UK
cgibson@apuk.co.uk

DEVELOPMENTAL BIOLOGY 183, 1–8 (1997)
ARTICLE NO. DB968491

Stimulation of Tentacle and Bud Formation by the Neuropeptide Head Activator in *Hydra magnipapillata*

Bert Hobmayer,*,[1] Thomas W. Holstein,* and Charles N. David†

**Johann Wolfgang Goethe-Universität, Zoologisches Institut, AK Zell- und Entwicklungsbiologie, Theodor-Stern-Kai 7 - Haus 75, 60590 Frankfurt am Main, Germany; and †Ludwig-Maximilians-Universität, Zoologisches Institut, Luisenstr. 14, 80333 München, Germany*

Stimulation of epithelial cell cycling by the neuropeptide head activator was analyzed in *Hydra magnipapillata* and compared with the action of head activator on bud formation and tentacle formation during head regeneration. The results obtained indicate that head activator treatment stimulates epithelial cell division and induces the formation of more tentacle-specific epithelial cells. The number of additional epithelial cells which undergo mitosis during head activator treatment accounts for the increased number of epithelial cells present in the regenerated tentacles. Therefore, the head activator stimulation of tentacle formation can be explained by the mitogenic action of head activator on tentacle cell precursors. To analyze stimulation of bud formation by head activator, polyps of different developmental age were tested under conditions of long-term treatment, and effects on bud formation were compared with effects on epithelial cell proliferation. Head activator treatment strongly stimulated bud formation, but had no detectable effect on epithelial cell numbers. Bud formation occurs at smaller polyp size as a result of head activator treatment, indicating that head activator significantly interferes with the patterning system in hydra. © 1997 Academic Press

INTRODUCTION

Head regeneration in hydra is stimulated by a neuropeptide, the head activator (pGlu-Pro-Pro-Gly-Gly-Ser-Lys-Val-Ile-Leu-Phe), isolated from hydra tissue (Bodenmüller and Schaller, 1981). Treatment of regenerating polyps for several hours with p*M* concentrations of head activator leads to regeneration of about 15% more tentacles per animal after several days (Schaller, 1973; Javois and Tombe, 1991). Head activator also acts as a mitogen. Treatment of intact animals increased the number of S phase cells after about 12 hr (Schaller, 1976a). At present, it is unclear whether the mitogenic effect is related to the increase in tentacle number. However, major changes in mitotic index have been reported in regenerating tips (Park *et al.*, 1970; Holstein *et al.*, 1991). Thus, it is possible that head activator perturbs the mitotic behavior of cells at the regenerating tip and hence the size of the precursor pool for tentacle formation.

Recent experiments have also shown that treatment of intact hydra with head activator can increase the amount of tentacle tissue (Hobmayer *et al.*, 1990). This effect was restricted to apical tissue in the tentacle formation zone at the base of tentacles and did not occur in proximal tissue. In the experiments presented here, we have examined the mitogenic action of head activator in more detail. In particular, we have directly compared mitogenic effects on epithelial cells with the stimulation of tentacle formation in the same tissue. We have investigated both intact and regenerating animals.

We have also analyzed the effect of head activator on bud formation. During bud formation, tissue from the lower gastric region evaginates, differentiates a head at its tip, and finally detaches as a small polyp from the mother animal. It is generally assumed that head formation during budding and head regeneration are governed by the same molecular mechanisms, since both processes are stimulated by head activator (Schaller, 1973), and inhibited by an inhibitor extracted from hydra tissue (Berking, 1977, 1979). Head activa-

[1] To whom correspondence should be addressed at Johann Wolfgang Goethe-Universität, Zoologisches Institut, AK Zell- und Entwicklungsbiologie, Theodor-Stern-Kai 7 - Haus 75, 60590 Frankfurt am Main, Germany. Fax: (49)-69-6301-7639. E-mail: Hobmayer @zoology.uni-frankfurt.d400.de.

0012-1606/97 $25.00
Copyright © 1997 by Academic Press
All rights of reproduction in any form reserved.

tor effects on bud formation were previously analyzed only after short-term treatments (Schaller, 1973, 1976b; Schaller *et al.*, 1979), and mitogenic head activator effects were not measured in these experiments. Thus, the role of head activator in bud formation is not clear at present.

In a new set of experiments we have attempted to distinguish effects on bud formation from effects on epithelial cell proliferation under conditions of long-term head activator treatment. In particular, we have analyzed polyps of different developmental age in order to determine the generality of head activator effects, since previous work had emphasized the importance of examining narrowly defined developmental stages. Our results demonstrate a striking stimulation of bud formation in head activator-treated animals. The extent of the effect depends on developmental age and duration of treatment. It is independent of effects on epithelial cell proliferation, suggesting that head activator interferes with the endogenous patterning system in hydra.

MATERIALS AND METHODS

Hydra Culture

Wildtype strain 105 of *Hydra magnipapillata* (Sugiyama and Fujisawa, 1977) was used for all experiments. Hydra were mass-cultured according to Loomis and Lenhoff (1956) in 1 m*M* $CaCl_2$, 0.1 m*M* $MgCl_2$, 0.1 m*M* KCl, and 1 m*M* $NaHCO_3$ at 18°C and fed daily with freshly hatched *Artemia* nauplii. The medium was changed 6–8 hr after feeding; 24 hr after feeding, experimental animals were selected. Polyps showing their first bud protrusion (stage 1–3, Otto and Campbell, 1977) and large, nonbudding polyps were used as indicated. In order to designate regions within experimental animals, the bodies of budding and nonbudding hydra were considered to consist of five equal parts starting below the whorl of tentacles. All experiments were carried out at a constant temperature of 18 ± 1°C.

Head Activator

Synthetic head activator (BACHEM, Switzerland) was solubilized in trifluoroethanol, lyophilized in 5-nmol samples, and stored at −20°C. One sample was solubilized in 250 μl 3 *M* $(NH_4)_2SO_4$ and 250 μl distilled water and further diluted with 1% BSA (bovine serum albumin) in PBS (phosphate-buffered saline). Final dilution (1:1000) to the end concentration (1 p*M*) was done with hydra medium. All steps were done on ice.

For continuous head activator treatment, experimental animals were incubated in 1 p*M* synthetic head activator at a density of 1 hydra/ml for a period of 4 days. Treatment was started 24 hr after the last feeding. During the treatment, freshly prepared head activator solution was supplied in fresh hydra medium at 12-hr intervals. Hydra medium was also changed in controls.

Cell Cycling

In intact animals, epithelial cell cycling was analyzed by continuous labeling with the thymidine analog 5′-bromo-2′-deoxyuridine (BrdU, Sigma Chemicals; Plickert and Kroiher, 1988). Experimental animals were incubated in hydra medium containing 5 m*M* BrdU. Since epithelial cells in hydra have no G1 phase, both postmitotic cells immediately enter S phase (David and Campbell, 1972). Thus, the number of S phase cells provides a direct measure for the rate of mitosis. To identify S phase cells, pieces of labeled tissue (regions 1 and 3; also referred to as upper and midgastric regions) were excised, dissociated into single cells by maceration (David, 1973), spread onto gelatin-coated slides, and stained with anti-BrdU antibody (Gratzner, 1982; Becton–Dickinson).

In regenerating hydra, epithelial cell cycling was measured by pulse labeling with BrdU. At different times during head regeneration, regenerating tips were isolated and incubated in hydra medium containing 5 m*M* BrdU. After 45 min exposure to BrdU, the regenerating tips were macerated into single cells, spread onto gelatin-coated slides, and stained with anti-BrdU antibody.

Visualization of nuclei stained with anti-BrdU antibody was done as described by Holstein *et al.* (1991) using an alkaline phosphatase reaction. The labeling index in each sample was determined by examination of about 250 epithelial cells under phase-contrast optics.

Quantitative Assay for Tentacle Formation

The effect of head activator on tentacle cell differentiation was investigated during head regeneration. Head activator treatment was performed for 18 hr either in intact hydra, before head regeneration was started, or in head regenerates immediately after head removal. Head regeneration itself was initiated by bisecting the polyps below the whorl of tentacles or in the midgastric region (between regions 2 and 3). After 96 hr of regeneration, all regenerates were anesthetized in 2% urethane in hydra medium (maximum 1 min) to elongate tentacles and fixed with Lavdowski's fixative (ethanol:Formalin:acetic acid:water, 50:10:4:40). Then, the polyps were stained with the DNA-specific fluorochrome DAPI (Leeman and Ruch, 1982) to identify and count individual epithelial cell nuclei in the regenerated tentacles.

Determination of Epithelial Cell Numbers

To determine epithelial cell numbers, hydra were macerated into single cells in a maceration solution containing glycerin:acetic acid:water (1:1:7). Single cell suspensions were then fixed in 4% Formalin and spread onto gelatin-coated microscope slides. Maceration as well as identification of epithelial cells was carried out according to David (1973). Total numbers of epithelial cells per hydra were determined under phase-contrast optics. At least 1000 epithelial cells were counted in each sample.

RESULTS

Head Activator Stimulates Epithelial Cell Cycling in Regenerating Tips

Immediately following removal of the head, there is a dramatic decrease in the number of S phase cells in the regenerating tip (Holstein *et al.*, 1991). Since hydra epithelial cells enter S phase directly from mitosis (no G1 phase; David and Campbell, 1972), these results indicate that re-

Copyright © 1997 by Academic Press. All rights of reproduction in any form reserved.

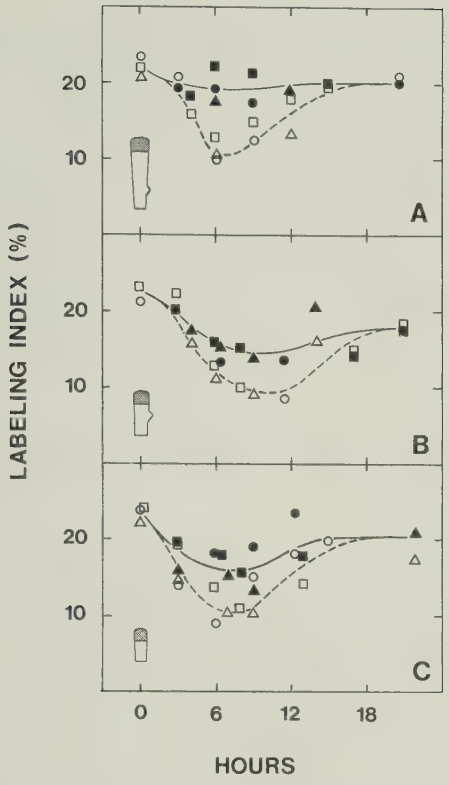

FIG. 1. BrdU pulse labeling of epithelial cells in the distal tip of head regenerating hydra. At t_0, head regeneration was initiated by cutting below the whorl of tentacles (A) and in the midgastric region (B) in budding hydra; in (C), nonbudding hydra were cut in the midgastric region. Head activator treatment began immediately after the surgery. Solid symbols: head activator-treated regenerates; open symbols: untreated controls. Each symbol represents analysis of 5–6 regenerating tips. Different symbols indicate independent experiments.

generation causes a transient block to mitosis (see also Park *et al.*, 1970).

To investigate the effect of head activator on this mitotic inhibition in regenerating tips, head regeneration was initiated and the body columns allowed to regenerate for 18 hr. At various times, the regenerating tips were excised, pulse labeled with BrdU, and macerated to score the labeling index.

The results in Fig. 1 indicate that the labeling index in regenerating tips of untreated controls decreased for the first 6–9 hr of regeneration, in agreement with previous observations (Park *et al.*, 1970; Holstein *et al.*, 1991). The decrease was essentially the same irrespective of whether head regeneration occurred in the upper or the midgastric region (Figs. 1A and 1B); it also occurred in nonbudding hydra (Fig. 1C). Thereafter, the labeling index increased to a normal level of about 20% by 18 hr. Head activator-treated regenerates, by comparison, showed a strikingly different pattern of labeling. Head activator treatment either completely blocked (Fig. 1A) or strongly reduced (Figs. 1B and 1C) the mitotic inhibition occurring in regenerating tips. Thus, head activator appears to act on epithelial cells in late G2 just prior to mitosis.

Effect of Head Activator on Epithelial Cell Cycling in Intact Hydra

To investigate the action of head activator on epithelial cell cycling in normal intact hydra, we labeled budding animals continuously with BrdU during head activator treatment. At various times during treatment, regions 1 and 3 were isolated and the labeling index of epithelial cells was determined in maceration preparations.

The labeling index increased continuously from about 24% to about 30% by 18 hr in untreated control animals. In the upper gastric region of head activator-treated polyps, the labeling index increased rapidly during the first 6 hr (Fig. 2A). Since hydra cells lack G1, this rapid increase indicates that head activator stimulates cells in late G2 to enter mitosis. The number of responding cells appears to be limited since the increase in S phase cells levels off after about 6–9 hr (Fig. 2A).

In the midgastric region of budding animals, there was a strikingly different result (Fig. 2B). Head activator treatment caused no increase in the number of S phase cells compared to untreated controls. Hence, G2 epithelial cells in the proximity of developing buds do not respond to head activator treatment. By comparison, in the equivalent area in nonbudding animals (Fig. 2C), head activator does stimulate epithelial cell mitosis.

Effect of Head Activator on Tentacle Formation

Previous work has shown that head activator stimulates tentacle formation in both intact and regenerating animals (Schaller, 1973; Schaller *et al.*, 1989, 1990; Hobmayer *et al.*, 1990; Javois and Tombe, 1991). To what extent mitogenic stimulation of precursor cells plays a role in this stimulation is unknown. To investigate this question, we measured the number of regenerated tentacle epithelial cells in the same animals used above to test the effects of head activator on cell proliferation.

The results in Table 1 indicate that head activator treatment during regeneration increased the number of regenerated tentacle epithelial cells by about 20–30%. This increase occurred in both budding and nonbudding animals and was independent of the site at which regeneration occurred (cut below tentacles or cut at lower gastric region). Since head activator treatment also stimulated epithelial cell cycling in these animals (Fig. 1), it appears likely the increase is due to mitogenic stimulation of tentacle precursor cells.

Intact animals treated with head activator before regeneration was initiated responded differently. Formation of increased numbers of tentacle epithelial cells occurred in upper gastric regenerates from budding animals and in midgas-

Copyright © 1997 by Academic Press. All rights of reproduction in any form reserved.

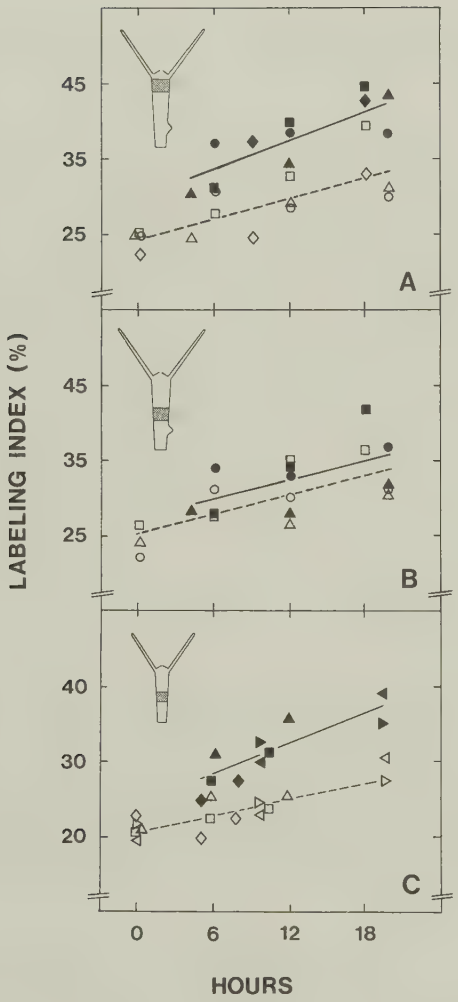

FIG. 2. Labeling kinetics of epithelial cells continuously labeled with BrdU in the upper gastric region of budding hydra (A) and the midgastric region of budding (B) and nonbudding (C) hydra. BrdU labeling and head activator treatment both began at t_0. Solid symbols: head activator-treated polyps; open symbols: untreated controls. Each symbol represents analysis of 6–10 tissue explants. Different symbols indicate independent experiments. Lines were derived from linear regression analysis.

tric regenerates from nonbudding animals (Table 1). Epithelial cell cycling was also stimulated by head activator in both these tissues (Figs. 2A and 2C). By comparison, midgastric regenerates from budding animals did not form more tentacle epithelial cells following head activator treatment (Table 1) and epithelial cell cycling was not stimulated by head activator treatment in such animals (Fig. 2B). Thus, formation of additional tentacle tissue is correlated with mitogenic stimulation of potential tentacle precursor cells.

To estimate whether the mitogenic effect is sufficient to explain the increase in regenerated tentacle cells, we estimated the number of additional precursor cells quantitatively. Regenerating tips (shaded area in Fig. 1A) contain 4200 ± 460 epithelial cells (analysis of 15 explants), of which about 20% are in S phase in head activator-treated animals (Fig. 1A). By comparison, the number of S phase cells transiently decreases in untreated regenerates (Fig. 1A). To quantify this difference, the area under the curves in Fig. 1A was integrated. Assuming a S phase length of about 12 hr (David and Campbell, 1972), the difference in the two curves corresponds to about 300 additional epithelial cells in S phase as a result of head activator treatment. This is roughly equal to the increase in regenerated tentacle epithelial cells induced by head activator treatment (Table 1).

Effect of Continuous Head Activator Treatment on Bud Formation

It is generally assumed that head formation during budding and head regeneration are governed by the same molecular mechanisms, since both processes are stimulated by head activator (Schaller, 1973), and inhibited by an inhibitor extracted from hydra tissue (Berking, 1977, 1979). To what extent mitogenic effects play a role in this stimulation is unknown. We therefore analyzed the relationship between effects of head activator treatment on bud formation and epithelial cell proliferation by long-term head activator treatment using animals of different developmental age. To obtain animals of different developmental age, large budding hydra were separated from the mass culture, fed daily, and allowed to produce buds. Freshly dropped buds were harvested daily. These buds constituted cohorts of polyps of defined age. The cohorts were cultured further under daily feeding. Polyps of the oldest cohort began to produce bud protrusions on the fourth day, at which point feeding was stopped and all cohorts were subjected to continuous treatment with 1 p*M* synthetic head activator for 4 additional days. Untreated control groups were incubated in hydra medium. The number of newly formed bud protrusions was counted during the period of head activator treatment; simultaneously, groups of hydra—including all their buds—were macerated at t_0 and t_4 to determine changes in epithelial cell number.

Bud formation in the different groups is outlined in Figs. 3A–3D. The largest animals (Fig. 3A) continued to produce buds over the course of 4 days, reaching levels of 1.0 buds per mother animal in untreated controls. Smaller animals (Fig. 3B or 3C), by comparison, only started to form buds after 1–2 days and produced fewer total buds. The smallest animals (freshly detached, Fig. 3D) did not bud at all.

Continuous head activator treatment had a dramatic effect on bud formation. In all cohorts, buds were formed faster and more total buds were produced than in controls. For the groups of larger animals (Figs. 3A–3C), the difference in bud formation amounted to an increase of roughly 0.5–1 bud per mother animal after 4 days of head activator treatment. In the youngest group, in which untreated con-

Copyright © 1997 by Academic Press. All rights of reproduction in any form reserved.

TABLE 1
Effect of Head Activator on Tentacle Size in Head Regenerating Hydra

HA treatment	Budding hydra		Nonbudding hydra cut at lower gastric region (cells × 100)
	Cut below tentacles (cells × 100)	Cut at lower gastric region (cells × 100)	
Before regeneration[a]	20 ± 4 (26)*	11 ± 2 (0)	8.0 ± 1.6 (18)*
During regeneration[b]	19 ± 4 (20)*	14 ± 4 (29)*	8.3 ± 1.7 (23)*
Control	16 ± 2	11 ± 2	6.7 ± 1.2

Note. After 96 hr of regeneration, the number of regenerated tentacle epithelial cells per polyp was determined. Data are given as means ± one standard deviation from 14–39 regenerates. Percent increase in epithelial cell number in head activator-treated hydra over untreated controls is shown in parenthesis. Asterisks indicate means of head activator-treated hydra that are significantly different from untreated controls at a 95% confidence limit (Student's *t* test).

[a] Intact hydra were incubated in 1 p*M* head activator for 18 hr. Then, head regeneration was initiated and the regenerates were transferred to hydra medium.

[b] Head regenerates were incubated in 1 p*M* head activator for 18 hr immediately after head removal and then transferred to hydra medium.

trols produced no buds, the effect of head activator treatment was comparatively small (Fig. 3D).

Figures 3E–3H indicate the size of the animals in the four cohorts at t_0 and changes in epithelial cell number during the experiment. As a result of different developmental age, there are clear differences in cell number at t_0. Freshly dropped buds had only 15,000 epithelial cells, while polyps with a first bud protrusion had about 30,000 epithelial cells. During the 4 days of bud formation, the total number of epithelial cells (per mother animal including buds) remained nearly constant due to the lack of feeding. Head activator treatment had no significant effect on cell numbers. The cell numbers in the three smallest groups at t_4 were ± 10% the same as those at t_0. Only in the largest animals were the changes in cell number larger than 10%. These results indicate that in such long-term experiments there is no cumulative effect of head activator on mitotic activity. Thus, the striking stimulation of bud formation by head activator can not be due to stimulation of mitotic activity.

DISCUSSION

Head activator has been shown to act as a mitogen on proliferating epithelial cells and to enhance head-specific differentiation processes during head regeneration and budding. The experiments presented here examine possible relationships between mitogenic stimulation and morphogenetic stimulation of tentacle formation and budding.

In Schaller's original characterization of head activator (1973), only a minor effect on head regeneration was found, i.e., the number of regenerating tentacles increased by 10–15% following head activator treatment. Javois and Tombe (1991) confirmed this result and found that the increase in tentacle number occurred only transiently, i.e., tentacles evaginated earlier than in control animals, but no extra tentacles differentiated as a result of head activator treatment. By comparison, in our experiments, head activator caused a 20–30% increase in the number of regenerated tentacle epithelial cells (Table 1). This increase occurred in both budding and nonbudding animals, as well as in regenerates of the upper and midgastric region (Table 1), and was always correlated with a stimulation of epithelial cell cycling in the corresponding tissues (Figs. 1 and 2). Thus, formation of additional tentacle tissue is directly correlated with mitogenic stimulation of potential tentacle precursor cells.

A quantitative estimate indicates that the number of additional precursor cells as a result of mitogenic stimulation is roughly the same as the observed number of additional tentacle cells in regenerating hydra. The difference in the pulse-labeling kinetics between treated and untreated regenerates in Fig. 1A corresponds to about 300 additional epithelial cells in S phase as a result of head activator treatment.

These cells can differentiate directly to an equivalent number of tentacle cells since tentacle cells complete differentiation in G2 without further division (Dübel and Schaller, 1990). An equivalent calculation made for intact animals leads to the same conclusion (data not shown).

Head activator responsive cells could be precursors which are already committed to tentacle epithelial cells and which undergo a further round of cell division as a result of head activator treatment. Alternatively, they could be uncommitted epithelial cells which are induced to divide, thus creating additional cells in S phase as potential precursors able to respond to endogenious signals for tentacle formation. It seems likely to us that the second possibility is correct since midgastric tissue from nonbudding hydra also responds to head activator. This tissue lacks tentacle cell precursors as revealed by *in situ* hybridization with ks1, an early tentacle battery cell-specific transcript (Weinziger *et al.*, 1994). By comparison, ks1-positive cells are common in the distal gastric tissue at the base of tentacles (tentacle

Copyright © 1997 by Academic Press. All rights of reproduction in any form reserved.

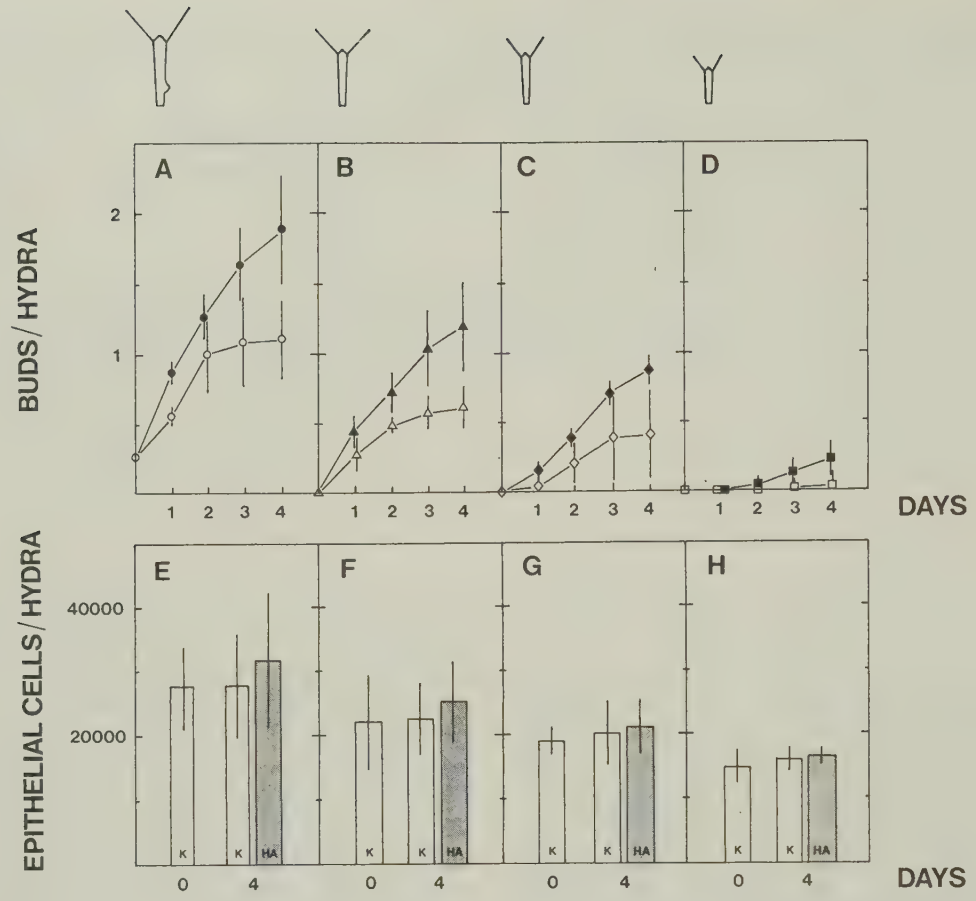

FIG. 3. (A–D) Cumulative number of buds per hydra (±SD) produced in polyps of different developmental age. Solid symbols: continuous head activator treatment; open symbols: untreated controls. Sample size: 90–140 polyps from three independent experiments. (E–H) Changes in epithelial cell number in polyps of different developmental age. Shaded bars: continuous head activator treatment; open bars: untreated controls. Each bar represents analysis of 90 macerated hydra from three independent experiments (±SD).

formation zone). Nevertheless, midgastric tissue from nonbudding hydra responds to head activator treatment with increased tentacle cell differentiation. This response is presumably due to head activator-stimulated mitosis of epithelial cells and hence to an increase in the pool of precursors available for commitment to tentacle cell differentiation.

Midgastric regenerates from budding animals did not form more tentacle epithelial cells following head activator treatment prior to the initiation of regeneration (Table 1). This failure is due to the failure of this tissue to respond mitogenically to head activator treatment (Fig. 2B). The reason for this unresponsiveness is at present unclear, but presumably is related to the presence of a developing bud.

The above experiments reveal that head activator-stimulated tentacle formation in regenerates can be explained by head activator-stimulated epithelial cell mitosis. However, we actually do not know whether this effect is direct or indirect, and we cannot rule out that head activator treatment could also interfere with the endogenous patterning system. According to such an alternative hypothesis, head activator treatment results in the formation of a morphogenetically "activated" regenerating apical end. Since the apical end exerts an inductive influence on tentacle formation (Meinhardt, 1993; Technau and Holstein, 1995), an activated apical regenerating dome gives rise to more tentacles and more tentacle epithelial cells than the apical dome in an untreated regenerate. A transient increase in the absolute number of tentacles in head activator-treated regenerates (data not shown; Javois and Tombe, 1991) could reflect such a transiently altered patterning system.

Our results on bud formation demonstrate that head activator effects the patterning system in hydra. We found a striking stimulation of bud formation in head activator-treated animals (Figs. 3A–3D). The extent of the effect depends on developmental age and duration of treatment, and it is independent of effects on epithelial cell proliferation (Figs. 3E–3H).

To demonstrate the relationship between budding and

Copyright © 1997 by Academic Press. All rights of reproduction in any form reserved.

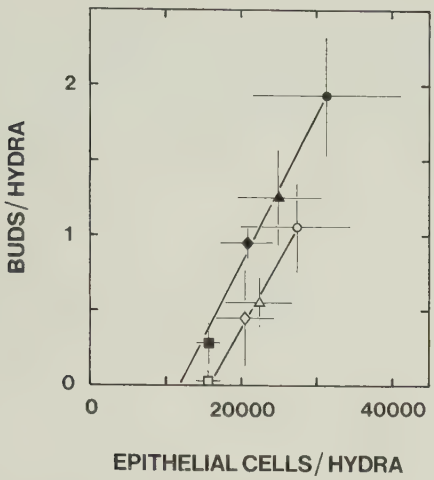

FIG. 4. Relationship between bud formation and number of epithelial cells per hydra after 4 days of continuous head activator treatment. Data were taken from Fig. 3. Different symbols indicate the different cohorts as used in Figs. 3A–3D. Solid symbols: continuous head activator treatment; open symbols: untreated controls. Lines were derived from linear regression analysis.

cell numbers in more detail, the number of buds per hydra on Day 4 was plotted against the corresponding number of epithelial cells per hydra for the different cohorts (Fig. 4). The results were taken from Fig. 3. As expected, bud production was directly correlated with the amount of tissue. In untreated hydra, the number of buds increased with the total number of epithelial cells. Head activator-treated hydra exhibited basically the same correlation. However, the line is clearly shifted toward smaller cell numbers: mother polyps of head activator-treated animals have about 20,000 epithelial cells at the time of first bud evagination, whereas mother polyps of untreated animals have about 28,000 epithelial cells at the time of first bud evagination.

A similar effect on bud formation is induced by temperature. Animals maintained at 16°C (85,000 total cells per body column) are larger at the time of first bud formation than animals maintained at 20°C (55,000 total cells per body column) (Bode *et al.*, 1973). Furthermore, shifting 16°C animals to 20°C induces bud formation immediately (David, unpublished data). Thus, raising the temperature has the same effect as head activator treatment: it causes bud formation in polyps of smaller size.

The position of bud formation in the body column is controlled by inhibition from the head of a polyp (Hyman, 1928; Webster and Hamilton, 1972; Berking, 1977). Thus, both the head activator effect and the temperature effect can be formally described as a reduction of head inhibition in the body column. The reduction could be due to reduced inhibitor production by the polyp head or to increased degradation of the inhibitor in the body column. In either case the threshold level of inhibition, below which bud formation can occur, will be closer to the head. Hence, head activator-treated or temperature-treated polyps will be smaller at the time of bud formation. An alternative explanation for the head activator effect is to assume that head activator activates bud formation. Under this assumption head activator-treated tissue becomes more resistant to inhibition and thus can form buds at inhibitor levels which still inhibit bud formation in untreated tissue.

The fact that head activator stimulates bud formation is not new (Schaller, 1973, 1976b; Schaller *et al.*, 1979). The results presented here, however, differ from the previous measurements. We have assayed effects in whole animals, whereas Schaller assayed head activator effects primarily in regenerating animals (animals lacking heads and thus head inhibition). Our experiments represent long-term treatments, whereas most of the Schaller observations were made on animals treated for only a few hours. Nevertheless, the results are comparable. Schaller obtained the strongest stimulation of bud formation in big budless polyps which are roughly equivalent to polyps in Figs. 2B and 2C. These polyps do not form buds under control conditions, whereas bud formation is induced by head activator treatment. Assuming that there was no effect of head activator treatment on the size of tissue pieces, Schaller's observation is equivalent to bud formation at smaller size, which we observed as a result of head activator treatment.

ACKNOWLEDGMENTS

We thank Dr. T. Sugiyama for supplying wildtype strain 105 of *Hydra magnipapillata* and Drs. H. C. Schaller, S. Berking, and H. K. MacWilliams for helpful comments on the manuscript. This study was supported by the Deutsche Forschungsgemeinschaft (Da 163/1-2, Ho 1088/1-3).

REFERENCES

Berking, S. (1977). Bud formation in hydra: Inhibition by an endogenous morphogen. *Roux's Arch. Dev. Biol.* **181,** 215–225.

Berking, S. (1979). Analysis of head and foot formation in hydra by means of an endogenous inhibitor. *Roux's Arch. Dev. Biol.* **186,** 189–210.

Bode, H., Berking, S., David, C. N., Gierer, A., Schaller, H. C., and Trenkner, E. (1973). Quantitative analysis of cell types during growth and morphogenesis in hydra. *Roux's Arch. Dev. Biol.* **171,** 269–285.

Bodenmüller, H., and Schaller, H. C. (1981). Conserved amino acid sequence of a neuropeptide, the head activator, from coelenterates to humans. *Nature* **293,** 579–580.

David, C. N. (1973). A quantitative method for maceration of hydra tissue. *Roux's Arch. Dev. Biol.* **171,** 259–268.

David, C. N., and Campbell, R. D. (1972). Cell cycle kinetics and development of *Hydra attenuata.* I. Epithelial cells. *J. Cell Sci.* **11,** 557–568.

Dübel, S., and Schaller, H. C. (1990). Terminal differentiation of ectodermal epithelial stem cells of hydra can occur in G2 without requiring mitosis or S phase. *J. Cell Biol.* **110,** 939–945.

Gratzner, H. G. (1982). Monoclonal antibody to 5-bromo- and 5-

Copyright © 1997 by Academic Press. All rights of reproduction in any form reserved.

iododeoxyuridine, a new reagent for detection of DNA replication. *Science* **218,** 474–475.

Hobmayer, E., Holstein, T. W., and David, C. N. (1990). Tentacle morphogenesis in hydra. I. The role of head activator. *Development* **109,** 887–895.

Holstein, T. W., Hobmayer, E., and David, C. N. (1991). Pattern of epithelial cell cycling in hydra. *Dev. Biol.* **148,** 602–611.

Hyman, L. (1928). Miscellaneous observations on Hydra, with special reference to reproduction. *Biol. Bull.* **54,** 65–108.

Javois, L. C., and Tombe, V. K. (1991). Head activator does not qualitatively alter head morphology in regenerates of *Hydra oligactis*. *Roux's Arch. Dev. Biol.* **199,** 402–408.

Leeman, U., and Ruch, F. (1982). Cytofluorometric determination of DNA base content in plant nuclei and chromosomes by the fluorochrome DAPI and Chromomycin A3. *Exp. Cell Res.* **140,** 275–282.

Loomis, W. F., and Lenhoff, H. M. (1956). Growth and sexual differentiation of hydra in mass culture. *J. Exp. Zool.* **132,** 555–574.

Meinhardt, H. (1993). A model for pattern formation of hypostome, tentacles, and foot in hydra: How to form structures close to each other, how to form them at a distance. *Dev. Biol.* **157,** 321–333.

Otto, J. J., and Campbell, R. D. (1977). Budding in *Hydra attenuata:* Bud stages and fate map. *J. Exp. Zool.* **200,** 417–428.

Park, H., Orthmeyer, A. B., and Blankkenbaker, D. P. (1970). Cell division during regeneration in hydra. *Nature* **227,** 617–619.

Plickert, G., and Kroiher, M. (1988). Proliferation kinetics and cell lineages can be studied in whole mounts and macerated tissue by means of BrdU/anti-BrdU technique. *Development* **103,** 791–794.

Schaller, H. C. (1973). Isolation and characterization of a low-molecular-weight substance activating head and bud formation in hydra. *J. Embryol. Exp. Morphol.* **29,** 27–38.

Schaller, H. C. (1976a). Action of the head activator as a growth hormone in hydra. *Cell Differ.* **5,** 1–11.

Schaller, H. C. (1976b). Head regeneration in hydra is initiated by the release of head activator and inhibitor. *Roux's Arch. Dev. Biol.* **180,** 287–295.

Schaller, H. C., Schmidt, T., and Grimmelikhuijzen, C. J. P. (1979). Separation and specificity of four morphogens from hydra. *Roux's Arch. Dev. Biol.* **186,** 139–149.

Schaller, H. C., Hoffmeister, S. A. H., and Dübel, S. (1989). Role of the neuropeptide head activator for growth and development in hydra and mammals. *Development (Suppl.)* **107,** 99–107.

Schaller, H. C., Hofmann, M., and Javois, L. C. (1990). Effect of head activator on proliferation, head-specific determination and differentiation of epithelial cells in hydra. *Differentiation* **43,** 157–164.

Sugiyama, T., and Fujisawa, T. (1977). Genetic analysis of developmental mechanisms in hydra. I. Sexual reproduction of *Hydra magnipapillata* and isolation of mutants. *Dev. Growth Differ.* **19,** 187–200.

Technau, U., and Holstein, T. W. (1995). Head formation in hydra is different at apical and basal levels. *Development* **121,** 1273–1282.

Webster, G., and Hamilton, S. (1972). Budding in hydra: the role of cell multiplication and cell movements in bud initiation. *J. Embryol. Exp. Morphol.* **27,** 301–316.

Weinziger, R., Salgado, L. M., David, C. N., and Bosch, T. C. G. (1994). *Ks1,* an epithelial cell-specific gene, responds to early signals of head formation in *Hydra*. *Development* **120,** 2511–2517.

Received for publication December 1, 1995
Accepted December 6, 1996

Copyright © 1997 by Academic Press. All rights of reproduction in any form reserved.

DEVELOPMENTAL BIOLOGY 183, 9–20 (1997)
ARTICLE NO. DB968497

Localization of MAP Kinase Activity in Early *Xenopus* Embryos: Implications for Endogenous FGF Signaling

C. LaBonne[1] and M. Whitman[2]
Department of Cell Biology, Harvard Medical School, Boston, Massachusetts 02115

We have used a sensitive assay for MAP kinase activity to investigate the role of endogenous fibroblast growth factor (FGF)-activated MAP kinase in early *Xenopus* embryonic patterning. MAP kinase activity is low during cleavage stages and increases significantly during gastrulation. The temporal profile of this activity correlates well with the expression pattern of *Xenopus* eFGF. Spatially, MAP kinase activity is lowest in animal pole tissue and higher in vegetal pole cells and the marginal zone. Endogenous MAP kinase activity is FGF receptor-dependent, demonstrating that FGF signaling is active in all three germ layers of the early embryo. This activity is necessary for normal expression of Mix.1, a meso-endodermal marker, in the endoderm as well as in the mesoderm, indicating that MAP kinase plays a functional role in patterning of both of these germ layers. Spatial and temporal changes in MAP kinase activation during gastrulation also suggest a role for FGF signaling in this process. In addition, we find that embryonic wounding during dissection results in significant stimulation of this pathway, providing a possible explanation for earlier observations of effects of surgical manipulation on cell fate in early embryos. © 1997 Academic Press

INTRODUCTION

The process of mesoderm induction was first described by P. D. Nieuwkoop in experiments in which explants of blastula prospective ectoderm (animal caps) were induced to form mesoderm by coculture with prospective endoderm from the vegetal pole (Nieuwkoop, 1969; Sudarwati and Nieuwkoop, 1971). Since then it has been demonstrated that members of the fibroblast growth factor family (FGF) and members of the TGF-β superfamily can mimic the vegetal pole signal when added to *Xenopus* animal caps (Slack *et al.*, 1987; Kimelman and Kirschner, 1987; Asashima *et al.*, 1990; Smith *et al.*, 1990; Sokol *et al.*, 1990). One interpretation of these experiments is that prospective mesoderm is absent in morula embryos and is subsequently induced in the equatorial zone via interactions with the underlying vegetal mass, a presumed source for TGF-β and/or FGF-like signals (Slack and Tannahill, 1992; Kimelman *et al.*, 1992).

Although members of the TGF-β superfamily are potent in inducing the full range of mesodermal tissues, it is not yet clear which members of this family serve this function endogenously. Activin A and activin B, two of the best characterized and most potent mesoderm inducers in animal cap assays, have not been shown to be present in early embryos (Thomsen *et al.*, 1990; Dohrmann *et al.*, 1993). Activin D, a recently described isotype, is expressed during early *Xenopus* development (Oda *et al.*, 1995); although it is a less potent mesoderm inducer than activin A or B, this is what might be expected of a growth factor responsible for the induction of ventral as well as dorsal mesodermal subtypes. Transcripts for another TGF-β family member, Vg-1, are localized in the prospective endoderm in early embryos (Weeks and Melton, 1987). Experiments with a chimeric Vg1, which is efficiently processed *in vivo*, demonstrate that Vg-1 has potent mesoderm inducing abilities (Thomsen and Melton, 1993; Dale *et al.*, 1993), but mature processed Vg-1 protein has yet to be detected endogenously prior to gastrulation (Tannahill and Melton, 1989).

Two members of the fibroblast growth factor family, basic FGF (bFGF) and *Xenopus* eFGF (XeFGF), are present in early embryos during mesoderm-formation stages, making them candidates for endogenous inducers (Slack *et al.*, 1987; Kimelman *et al.*, 1988; Isaacs *et al.*, 1992). bFGF transcripts are uniformly distributed in all three germ layers, but as

[1] Current Address: Division of Biology, California Institute of Technology, Pasadena CA 91125.
[2] Corresponding Author

0012-1606/97 $25.00
Copyright © 1997 by Academic Press
All rights of reproduction in any form reserved.

bFGF protein lacks a signal sequence, the mechanism by which it could participate in cell–cell signaling events remains unclear (Kimelman *et al.*, 1988). XeFGF is most related to FGF 4 and 6, and like these factors is efficiently secreted. It is expressed maternally, and transcription of it increases significantly during gastrulation when it becomes enriched on the dorsal side of the embryo. As gastrulation proceeds, XeFGF is expressed in a complete circle above the blastopore (Isaacs *et al.*, 1992).

Experiments with dominant inhibitory growth factor receptors have demonstrated that members of the TGF-β superfamily and FGF family are required for mesoderm formation *in vivo* (Amaya *et al.*, 1991, 1993; Hemmati-Brivanlou and Melton, 1992). FGF does not appear to play a sufficient role in mesoderm formation endogenously, however, as embryos overexpressing a dominant inhibitory activin receptor lack mesoderm despite retaining a functional FGF-signaling pathway (Hemmati-Brivanlou and Melton, 1992). Instead, as overexpression of a dominant inhibitory FGF receptor has been found to inhibit mesoderm induction in response to activin or Vg-1, FGF appears to play a essential role in the competence of cells to respond to activin-like mesoderm inducing signals (LaBonne and Whitman, 1994; Cornell and Kimelman, 1994; Schulte-Merker *et al.*, 1994).

Components of the FGF signal transduction pathway required for its mesoderm-inducing ability have been elucidated, and, as has been found for the dominant inhibitory FGF receptor, blocking this pathway by inhibiting the function of RAS, RAF, MEK, or MAP kinase also inhibits activin-mediated mesoderm induction (Whitman and Melton, 1992; LaBonne and Whitman, 1994; LaBonne *et al.*, 1995; Gotoh *et al.*, 1995; Umbhauer *et al.*, 1995; Northrop *et al.*, 1995). In addition, overexpression of constitutively activated mutants of any of these signal transducers is sufficient to induce mesodermal markers in animal pole cells (Whitman and Melton, 1992; MacNicol *et al.*, 1993; LaBonne and Whitman, 1994; LaBonne *et al.*, 1995; Gotoh *et al.*, 1995). Critical targets downstream of activated MAP kinase in early embryos remain to be identified. MAP kinase is known to phosphorylate cytoskeletal targets, which are potential regulators of cell shape and motility, as well as to translocate to the nucleus where it can phosphorylate and regulate members of a number of transcription factor families (Blenis, 1993; Triesman, 1996).

Why activin and Vg-1 require an FGF signal in order to induce a full spectrum of mesodermal responses is unclear. It has recently been suggested that this requirement may help to define the endo-mesodermal boundary in the embryo (Cornell *et al.*, 1995). The model presented by these authors proposes that the activin-like signaling presumed to be present in vegetal pole cells does not lead to mesodermal gene expression in the prospective endoderm because vegetal pole cells lack the required FGF cosignal, while the presence of FGF signaling in the adjacent mesodermal mantle permits mesodermal gene expression in these cells in response to activin-like signals emanating from the vegetal pole. There has, however, been no direct test of whether, as predicted by this model, FGF signals are normally excluded from the prospective endoderm. In order to understand the complex interplay between different growth factors in the early embryo, it is critical to be able to directly measure when and where their signaling pathways become activated endogenously.

It has previously been demonstrated that activation of MAP kinase, a downstream component of FGF signaling, is both necessary and sufficient for mesoderm formation (LaBonne *et al.*, 1995; Gotoh *et al.*, 1995; Umbhauer *et al.*, 1995). Here we demonstrate that endogenous MAP kinase activity can be specifically and sensitively measured in whole embryos and explants, and that this activity is FGF receptor-dependent. We have used this activity as a sensitive marker of where and when FGF signaling is active endogenously during early development. Low levels of MAP kinase activity are detected maternally during cleavage stages, and these levels are found to increase significantly prior to and during gastrulation. Blastula-stage explants of marginal zones and vegetal bottoms have comparable levels of FGF receptor-dependent MAP kinase activity; it therefore appears unlikely that FGF plays a role in excluding mesodermal gene expression from the prospective endoderm. We also find that embryonic wounding leads to significant stimulation of FGF signaling over endogenous levels, and that under some conditions this ectopic activation can be sufficient to activate mesodermal gene expression. We propose that endogenous MAP kinase activation by FGF plays a role in establishing the competence of all three prospective germ layers to respond to early inductive signals, and that ectopic activation of MAP kinase by surgical manipulation may under some circumstances modify the developmental fate of manipulated cells.

MATERIALS AND METHODS

Embryo Manipulations

Embryos were collected from *Xenopus laevis* females and fertilized as previously described (Newport and Kirschner, 1982). Fertilized eggs were kept in 3% Ficoll/1.0× MMR for microinjection and then transferred to 0.1× MMR for culturing. Injection was carried out in both blastomeres at stage 2, in the animal pole, the vegetal pole, or the marginal zone as noted in the text. The truncated type 1 FGF receptor (Amaya *et al.*, 1991) in the plasmid pCS2 (Turner and Weintraub, 1994) was linearized with *Not*I and transcribed with SP6 polymerase. Embryos were injected with 10–15 nl of synthetic mRNA resuspended at a concentration of 0.2 ng/μl.

Staging of embryos is according to Nieuwkoop and Faber (1967). All dissections were performed in 1.0× MMR. Where noted, solutions were precooled to 0°C, and dissections were carried out in dishes resting on a tray of ice. When large numbers of animal caps or vegetal bottoms were explanted for kinase assays, small numbers were dissected and lysed in batches to limit the time between dissection and lysis.

Preparation of STAT-3 Substrate

A plasmid containing the C-terminus of STAT-3 (amino acids 677–750) fused to glutathione *S*-transferase (GST) (between *Bam*HI

Copyright © 1997 by Academic Press. All rights of reproduction in any form reserved.

and *Eco*RI sites of GST-4T1) was a kind gift of J. K. Chung and John Blenis (Harvard Medical School). An overnight culture of bacteria transformed with this plasmid was diluted 1:20 in LB media containing 200 μg/ml ampicillin and incubated at 37°C for 3–4 hr with vigorous shaking. Expression of the fusion protein was induced with 0.1 m*M* IPTG, and incubation was continued for an additional 2–3 hr. Bacteria were harvested by centrifugation, resuspended in PBS/100 m*M* EDTA/1% Triton X-100/1 m*M* DTT/PMSF and lysed by sonication. The lysate was centrifuged to remove cellular debris, and the supernatant was incubated with preswollen glutathione agarose beads (Sigma), with rocking, for 1 hr at 4°C. Beads were washed three times in lysis buffer, twice in PBS/1 *M* NaCl/1% Triton X-100/PMSF, and once in PBS. Protein was eluted with freshly made 20 m*M* Tris, pH 8.0/150 m*M* NaCl/20 m*M* reduced glutathione. Free glutathione was removed by dialysis against 20 m*M* Hepes, pH 7.2/10 m*M* $MgCl_2$/50% Glycerol. The STAT3-GST protein was stored at −20°C.

Immune Complex Kinase Assays

Embryos or explants were lysed in 200 μl of extraction buffer containing 20 m*M* Hepes, pH 7.5/1 m*M* $MgCl_2$/1 m*M* EGTA/1 m*M* DTT/1 m*M* Na vanadate/1 m*M* Na molybdate/100 m*M* β-glycerophosphate/PMSF. The protein concentration in 5 μl of lysate was measured using a standard Bradford reagent assay (Bio-Rad) and for each sample equivalent OD units of lysate were diluted to 300 μl with extraction buffer. Following addition of 4 μl of MAP kinase antiserum (kind gift of Rebecca Hartley and James Maller), samples were incubated on ice for 2 hr. Fifteen microliters of BSA-blocked protein A–Sepharose beads were then added to each sample, and incubation was continued at 4°C with rocking for 1 hr. Beads were washed 2× with 20 m*M* Tris, pH 7.4/5 m*M* EDTA/100 m*M* NaCl/1% Triton X-100, 2× with 20 m*M* Tris, pH 7.4/5 m*M* EDTA/1 *M* NaCl/1% Triton X-100, and 2× with kinase buffer (20 m*M* Hepes, pH 7.5/15 m*M* $MgCl_2$/1 m*M* EGTA/1 m*M* DTT/1 m*M* Na vanadate/1 m*M* Na molybdate/100 m*M* β-glycerophosphate/PMSF. Kinase reactions were carried out in 30 μl of kinase buffer containing 0.2 m*M* ATP and 20–200 μCi [^{32}Pγ]ATP and 2 μl of STAT-3-GST substrate.

Western Blots

Embryos or explants were lysed in 200 μl of extraction buffer, and the protein concentration in 5 μl of lysate was measured using a standard Bradford reagent assay (Bio-Rad). Laemmli loading buffer was added to 1× and samples were electrophoresed on 10% SDS gels. Gels were transferred to nitrocellulose, blocked with casein, and incubated overnight in MAP kinase antiserum (gift of John Blenis) diluted 1:1000 in 1× TBS. Membranes were washed three times for 15 min in 1× TBST and incubated in either ^{125}I-labeled protein A or HRP-conjugated anti-rabbit antibodies diluted in TBS for 1 hr at room temperature. Following washes as above, blots were either exposed to film directly (protein A) or following development with chemiluminescent reagents (HRP).

RT-PCR Analysis

Total RNA was isolated from whole embryos, and first-strand cDNA was synthesized as previously described (LaBonne and Whitman, 1994). PCR reactions were carried out in 25-μl reaction volumes in the presence of trace amounts of α-[^{32}P]dCTP using an annealing temperature of 55°C and 25 cycles. Primer pairs utilized have been described previously (LaBonne and Whitman, 1994).

RESULTS

Sensitive Detection of MAP Kinase Activity in Early Embryos

As it has been demonstrated that MAP kinase is an obligate component of FGF-mediated mesoderm induction, which is itself sufficient to activate mesodermal markers, MAP kinase activity should be a useful tool for investigating endogenous FGF signaling. Previous attempts to measure endogenous MAP kinase activity have utilized whole embryo crushates or in-gel kinase assays using relatively nonspecific peptides as substrates (Hartley *et al.*, 1994; Graves *et al.*, 1994). The resulting measurements have been of limited sensitivity due to the background activity observed in preimmune samples, and therefore the results have been difficult to interpret. Recently the C-terminal portion of STAT-3 has been demonstrated to be a highly specific MAP kinase substrate (Chung *et al.*, submitted). STAT-3 is phosphorylated on serine 727 by activated MAP kinase *in vivo* and *in vitro*, but is not substantially phosphorylated by the ERK-related kinases p38 and JNK. Indeed, STAT-3 appears to be a substantially better substrate for MAP kinase than other previously reported substrates including RSK and MBP. We have used this STAT-3 peptide as a substrate in immune complex kinase assays, following immunoprecipitation of native, active kinase with a MAP kinase-specific antibody. In this way we can sensitively detect and measure endogenous MAP kinase activity. We find that preimmune complexes from blastula stage embryos possess no detectable STAT-3 kinase activity, while a signal is detected in anti-MAP kinase immune complexes at all stages examined (Fig. 1A). This activity is MAP kinase, because it is greatly diminished in embryos in which the MAP kinase phosphatase MKP-1 has been overexpressed (LaBonne *et al.*, 1995). Low residual MAP kinase activity is probably due to cells which did not receive the injected mRNA.

The sensitivity and specificity of this assay appears to be significantly greater than those utilized previously in related experiments (Graves *et al.*, 1994; Hartley *et al.*, 1994; Gotoh *et al.*, 1995). For example, immune complex kinase assays using the relatively nonspecific kinase substrate, myelin basic protein, found only a 2-fold increase in activity at early gastrula stages over the fairly high levels obtained with preimmune serum alone (Gotoh *et al.*, 1995). When STAT-3 is used as a substrate, we find a greater than 30-fold increase over our preimmune sample at this stage. The greater specificity of this substrate may only partially account for the improved sensitivity of the assay, however, as a different anti-MAP kinase antibody has been used in the present study as well.

We find that a low but detectable amount of MAP kinase

Copyright © 1997 by Academic Press. All rights of reproduction in any form reserved.

activity is present during early cleavage stages, and that this level is slightly increased by pre-mid-blastula transition (MBT) blastula stages. After MBT, the time at which zygotic transcription begins, there is a more dramatic increase in activity which peaks at mid-gastrula stages and then declines (Fig. 1A). This increase in kinase activity is not due to an increase in MAP kinase protein expression, as Western blot analysis of the same lysates demonstrates that similar amounts of MAP kinase are present at all of these stages (Fig. 1B). The increase in MAP kinase activity at post-MBT stages does appear to require new protein synthesis, however. When embryos are treated at stage 7 with 5 μg/ml cycloheximide to inhibit translation (Cascio and Gurdon, 1987), the increase in MAP kinase activity noted at post-MBT stages is lost (Fig. 1C). It has previously been demonstrated using less-sensitive assays that treatment of animal caps with activin does not elicit increases in MAP kinase activity at assay times up to 30 min posttreatment, the minimum amount of time required for changes in immediate early gene expression (LaBonne and Whitman, 1994; Graves *et al.*, 1994; Hartley *et al.*, 1994, and data not shown). We find that this is also true when MAP kinase activity is examined using immune complex kinase assays with STAT-3 as a substrate. Embryos injected at the 1-cell stage with activin mRNA show no increase in MAP kinase activity at mid-blastula stages, but a significant increase is noted by late blastula stages (Fig. 1D). This may be due to an increase in XeFGF expression, as this factor is expressed in response to activin treatment in animal cap assays (Issacs *et al.*, 1994). Similarly, overexpression of a dominant inhibitory version of the type IIB activin receptor results in a decrease in endogenous MAP kinase activity at late blastula stages, perhaps by inhibiting the mesoderm-dependent XeFGF expression (Fig. 1D).

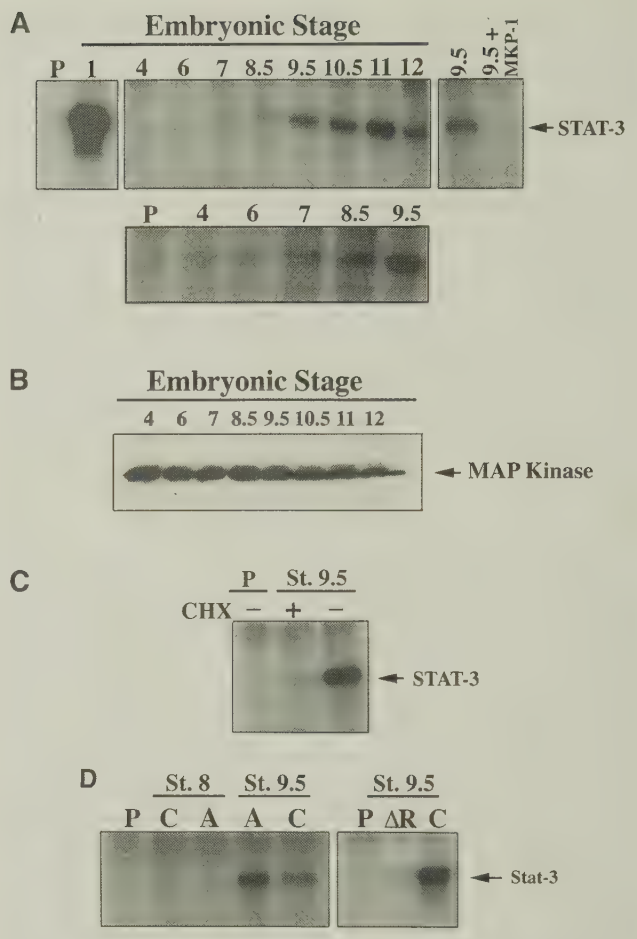

FIG. 1. Detection of endogenous MAP kinase activity during early developmental stages. (A) Equal numbers of embryos from each indicated stage were lysed in extraction buffer, immunoprecipitated with MAP kinase specific antiserum or preimmune serum (P), and assayed for STAT-3 kinase activity. (Bottom) Kinase assay with increased [^{32}P]-ATP to illustrate activity at early cleavage stages. Preimmune precipitates are from stage 10 embryos. Lysates from embryos injected with MKP-1 lack STAT-3 kinase activity, demonstrating the specificity of the assay. (B) Western blot analysis of samples used for kinase assays demonstrates that the changes in MAP kinase activity noted in (A) are not due to differences in the amount of MAP kinase protein present. (C) The increase in MAP kinase activity noted at post-MBT stages is protein synthesis dependent. Embryos were cultured in the presence or absence of 5 μg/ml cycloheximide beginning at stage 7 and were harvested at stage 9 for immune complex kinase assays. (D) Activin overexpression leads to increases in endogenous MAP kinase activity at late but not early blastula stages. Embryos injected with activin βB mRNA at the one cell stage were cultured to stage 8 or stage 9.5 and harvested for immune complex kinase assays. (C) Uninjected controls, (A) activin injected, (ΔR) dominant inhibitory activin receptor injected.

Activation of MAP Kinase by Dissection

Having shown that we can sensitively detect endogenous MAP kinase activity at blastula stages, we examined whether regional differences in MAP kinase activity exist within the blastula. Stage 9 blastulae were dissected into animal, marginal, and vegetal regions (Fig. 2A). The size of explanted animal and vegetal cap regions was kept to a minimum to ensure that they did not contain marginal zone material. Consequently, dissected marginal zone regions contained considerably more tissue than either animal or vegetal regions. To control for this, dissected pieces were lysed in extraction buffer and aliquots were compared for total protein concentration using a standard Bradford assay. Extracts normalized for total cellular protein were found to contain similar amounts of total MAP kinase protein (not shown). Equivalent amounts of protein from each sample were then immunoprecipitated with MAP kinase specific antiserum or preimmune serum. Following stringent washes, immune complexes were assayed for STAT-3 kinase activity.

At stage 9, vegetal and marginal zone explants were found to contain comparable amounts of MAP kinase activity, and these levels were several-fold higher than those found in animal cap explants (Fig. 2A). Surprisingly, however, the sum of these levels was found to be higher than those mea-

Copyright © 1997 by Academic Press. All rights of reproduction in any form reserved.

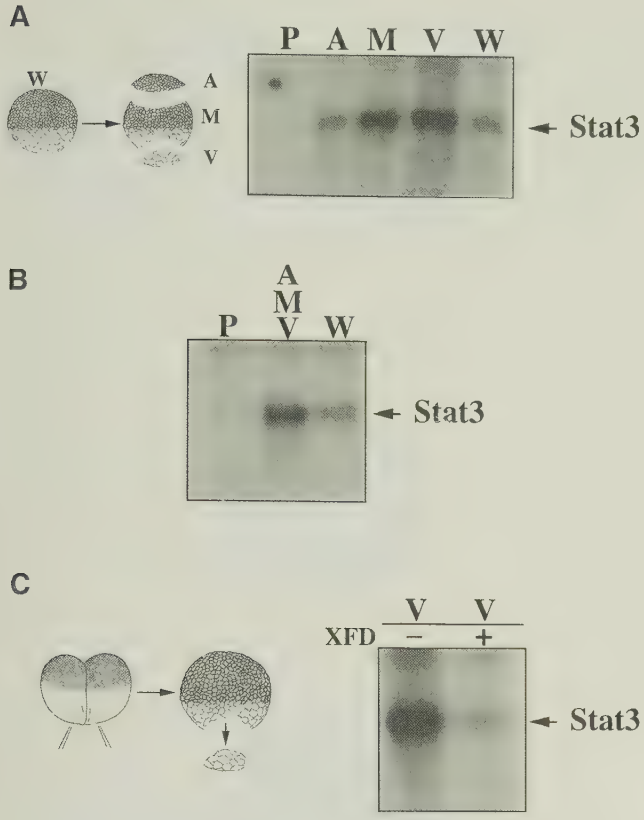

FIG. 2. Spatial localization of MAP kinase activity at blastula stages. (A) Schematic of dissection carried out on blastula stage embryos. Explants from stage 9 embryos dissected as in (A) were lysed in extraction buffer, standardized for total protein, immunoprecipitated with MAP kinase-specific antibodies, and assayed for STAT-3 kinase activity. Note that the average of animal (A), marginal (M), and vegetal (V) samples exceeds activity in whole embryo samples (W). (*P*) preimmune. (B) Stage 9 embryos were dissected into animal, marginal, and vegetal regions and lysed as one sample (AMV) undissected samples (W) were lysed in parallel. Samples were standardized for total protein and assayed for STAT-3 kinase activity. (C) Embryos were injected vegetally at the two-cell stage with mRNA coding for a dominant inhibitory FGF receptor. Vegetal bottoms were explanted from injected and uninjected embryos as depicted, standardized for total protein, and assayed for STAT-3 kinase activity.

sured in undissected whole embryos of the same stage (Fig. 2A). As whole embryo extracts were standardized to contain protein levels equivalent to those present in the dissected samples, differences in MAP kinase protein levels could not explain the discrepancy in MAP kinase activity. In order to more directly compare the relative MAP kinase activities present in dissected and undissected embryos, stage 9 embryos were dissected into animal, marginal, and vegetal regions and the explants were pooled and lysed as one sample. The same number of undissected embryos were lysed separately for immune and preimmune samples, and all three samples were standardized for total protein. Again it was found that the activity present in the sum of the parts was greater than the activity present in whole embryos (Fig. 2B). This suggested that the process of dissecting the embryos was resulting in the activation of MAP kinase to levels above those present endogenously.

The observed increase in activity could be due to the release of peptide growth factors following tissue wounding. As MAP kinase is an obligate component of the signal transduction pathway utilized by FGF during mesoderm induction (Gotoh *et al.*, 1995; LaBonne *et al.*, 1995; Umbhauer *et al.*, 1995), we examined whether the observed increase in MAP kinase activity was FGF dependent. Two-cell stage embryos were microinjected in the vegetal pole of both cells with mRNA encoding a dominant inhibitory version of the type 1 FGF receptor (Amaya *et al.*, 1991). Embryos were allowed to develop to stage 9, when vegetal pole tissue from injected and uninjected embryos were explanted, lysed, and standardized for total protein. Comparable amounts of protein were immunoprecipitated with MAP kinase antibodies and subsequently assayed for STAT-3 kinase activity. The levels of MAP kinase activity present in explants expressing the dominant inhibitory FGF receptor were greatly reduced compared to those in uninjected explants (Fig. 2C), demonstrating that, at least in the vegetal pole, the MAP kinase activity present is FGF dependent. This suggests that there is sufficient endogenous FGF receptor ligand present in the vegetal hemisphere to produce a robust FGF signal in response to dissection. These data do not address, however, to what extent FGF signaling is active in this tissue endogenously.

To accurately determine the endogenous levels of MAP kinase activity in different regions of the blastula, and in order to examine the consequences of ectopic activation of MAP kinase during embryonic dissection it was first necessary to determine conditions under which dissection-induced increases in MAP kinase activity would not occur. As ligand-dependent receptor activation can often be inhibited at 4°C, we hoped that dissection under such conditions might maintain endogenous enzymatic activity at predissection levels. Toward this end, we repeated the experiment in Fig. 2B, this time comparing samples which had been dissected at room temperature to those which had been dissected at 4°C. Again we found that embryos which had been cut into thirds at room temperature prior to lysis had significantly more active MAP kinase than did undissected control embryos. When dissection was carried out at 4°C, however, cut and uncut embryos displayed equivalent levels of MAP kinase activity (Fig. 3). Uncut control embryos held at 4°C during dissection displayed levels of MAP kinase activity comparable to whole embryos maintained at room temperature (Fig. 3, lanes 1 vs lane 3), indicating that cooling did not affect predissection levels of endogenous MAP kinase activity.

To test whether this dissection-induced MAP kinase activation might have significant consequences in a standard mesoderm induction assay, we next examined the levels of

Copyright © 1997 by Academic Press. All rights of reproduction in any form reserved.

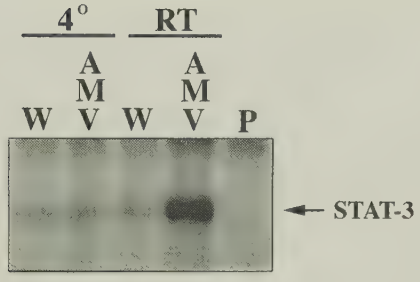

FIG. 3. Dissection at 4°C eliminates wound-induced MAP kinase activation. Stage 9 embryos were dissected into animal (A), marginal (M), and vegetal (V) pieces and lysed as one sample (AMV). Embryos were dissected at room temperature (RT) or on ice in 1.0× MMR precooled to 4°C. Whole embryos (W) at RT or 4°C were lysed in parallel. Samples were standardized for total protein immunoprecipitated with MAP kinase specific antiserum and assayed for STAT-3 kinase activity. The sample lysed for precipitation with preimmune serum (P) is from embryos dissected at RT. Dissection at 4°C prevents wounding-induced activation of MAP kinase.

MAP kinase activity present in animal caps dissected under conditions that lead to ectopic activation (room temperature) or that prevent ectopic activation (4°C). When animal caps were dissected on ice in precooled solutions, the levels of kinase activity present in these caps were below what could be detected using these assay conditions (Fig. 4C, lane 1). In contrast, the same amount of total protein from animal caps dissected at room temperature displayed low but significant levels of MAP kinase activity (Fig. 4C). MAP kinase activity was found to increase rapidly after dissection and remained at elevated levels for over 60 min (not shown). The increase in MAP kinase activity observed in explanted animal caps is most likely due to FGF release upon wounding, as no MAP kinase activity is observed in animal caps overexpressing a dominant inhibitory FGF receptor (Fig. 4C).

As dissection-induced MAP kinase activation is FGFR dependent, and as activation of MAP kinase has been demonstrated to be sufficient for activation of mesodermal markers (Gotoh *et al.*, 1995; LaBonne *et al.*, 1995; Umbhauer *et al.*, 1995), it seemed possible that embryonic dissection itself could lead to ectopic expression of mesodermal markers. Indeed, such a phenomenon had been previously noted in the course of experiments examining the regionalization of the marginal zone (Dale and Slack, 1987). In these experiments, a higher incidence of muscle formation was noted in ventral-half embryos which were first dissected into animal and vegetal regions and then recombined than in ventral-half embryos that were cultured intact, indicating that the process of dissection can indeed alter cell fate. Animal cap explants are among the most common dissection procedures carried out on early embryos; however, animal cap explants also produce the lowest levels of ectopic MAP kinase activation following dissection (Fig. 2). We expected, therefore, that ectopic activation of mesodermal markers would be least likely to occur in this tissue. To test this, small and large animal caps (Fig. 4A) were dissected from stage 8.5 (mid-late blastula) embryos and cultured to early gastrula stages (stage 10), when they were harvested for RT-PCR analysis. As expected, small animal caps dissected from blastulae and cultured in isolation did not express *Xbra*, an immediate early mesodermal response gene (Smith *et al.*, 1991), when assayed at

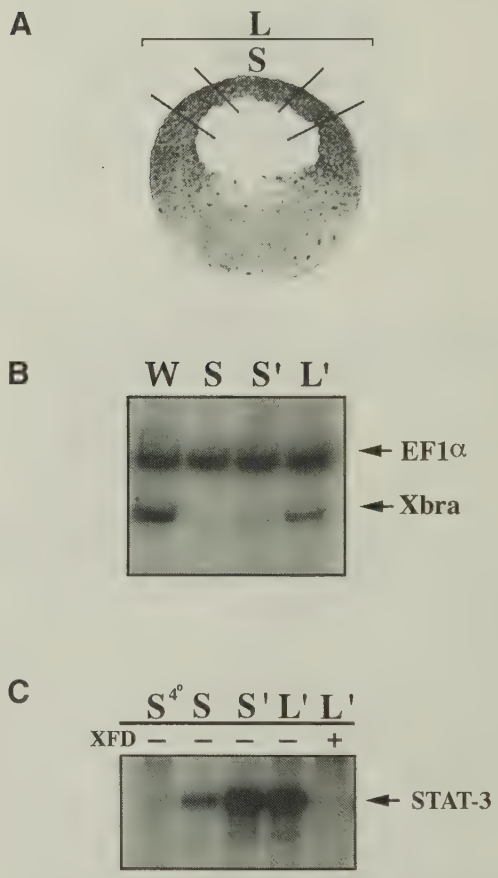

FIG. 4. Dissection-induced MAP kinase activation can lead to *Xbra* expression. (A) Schematic of large (L) and small (S) animal caps from blastula stage embryos. (B) Small animal caps (S) were dissected at stage 9, small and large animal caps were dissected at stage 9 and cut into quarters (S′ and L′). All caps were cultured in 1.0× MMR until stage 10 when they were harvested for RT-PCR analysis. EF1α serves as an internal loading control. Xbra expression is seen weakly in S′ and more strongly in L′. (C) Small animal caps dissected at 4°C (lane 1), small animal caps dissected at room temperature (RT) (lane 2), and small and large animal caps dissected at room temperature and then quartered (lanes 3 and 4) were lysed in extraction buffer, standardized for total protein, immunoprecipitated with MAP kinase-specific antiserum, and assayed for STAT-3 kinase activity. Dissection induced increases in MAP kinase activity were due to increases in FGF signaling as they are absent in animal caps overexpressing a dominant inhibitory FGF receptor (+XFD).

Copyright © 1997 by Academic Press. All rights of reproduction in any form reserved.

early gastrula stages (Fig. 4B). This correlates with the relatively low levels of dissection-mediated MAP kinase activation observed in such caps (Fig. 4C). When animal caps were subjected to additional damage by quartering them prior to lysis, measured levels of MAP kinase activity were found to increase more than 10-fold (Fig. 4C). This increase in MAP kinase activity correlates with a low level induction of *Xbra* expression under these conditions (Fig. 4B). This *Xbra* expression appeared to be transient, however, as it was not observed when caps were harvested at stage 12 (not shown). When large animal caps were dissected, quartered, and cultured under the same conditions, expression of *Xbra* was both stronger (Fig. 4B) and maintained (data not shown). Note that even these larger caps did not contain prospective mesoderm, unless subjected to the additional wounding, and subsequent MAP kinase activation associated with quartering. Interestingly, when the MAP kinase activity immunoprecipitated from quartered large caps which had been standardized for total protein was measured, it was not found to differ significantly from levels observed in similarly treated small caps (Fig. 4C). This suggests that the increased *Xbra* expression noted in large caps in Fig. 4B may be due to cooperation with factors which do not activate MAP kinase and which may be present at higher levels in cells more proximal to the marginal zone.

Measurement of Regional Distribution of Endogenous MAP Kinase Activity

The experiments in Figs. 3 and 4 demonstrate that if dissection is carried out at 4°C, the endogenous levels of MAP kinase activity present in different regions of the embryo can be preserved and accurately compared. They also demonstrated that endogenous levels of MAP kinase activity were low compared to the levels induced by dissection. Consequently, the sensitivity of the assay needed to be improved, both by increasing the amount of total protein added to immunoprecipitations and by increasing the amount of labeled ATP in the kinase reactions, if low endogenous signals were to be detected. To examine actual endogenous levels of activity, approximately 100 animal caps, 130 vegetal bottoms, and 35 marginal zones were dissected at 4°C from stage 7.5 or stage 9 embryos and were standardized for total protein against whole embryos of the same stage. Following immunoprecipitation and stringent washes, immune complexes were assayed for STAT-3 kinase activity in the presence of 200 μCi of γ-[^{32}P]ATP, representing a 30-fold increase in specific activity relative to previous experiments. At early blastula stages, activity measured in marginal zones and vegetal bottoms were comparable and several-fold higher than the barely detectable signal in animal caps (Fig. 5A, stage 7). By stage 9, levels of MAP kinase activity had increased in all regions of the blastula. Animal caps contained the lowest levels of activated MAP kinase. Levels observed in vegetal bottoms were consistently higher than those in the marginal zone (Fig. 5A, stage 9).

It has been proposed that FGF signaling may normally be

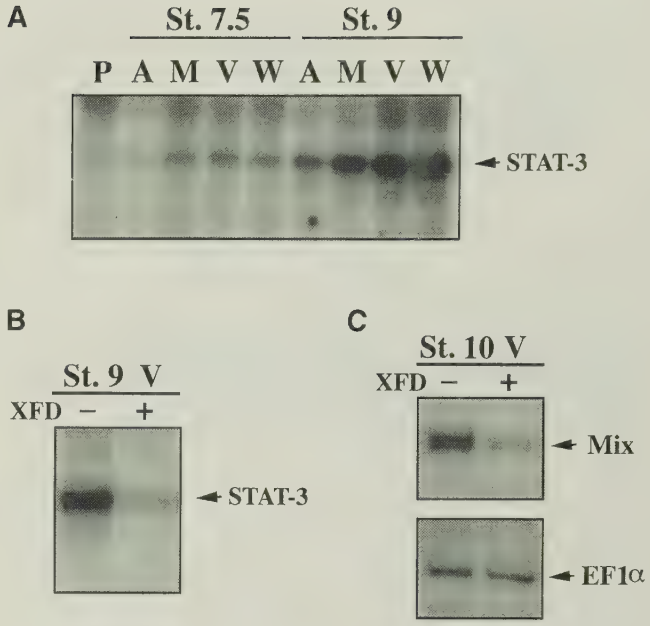

FIG. 5. MAP kinase activity is present in all three germ layers at blastula stages. (A) Stage 7.5 and stage 9 embryos were dissected into animal (A), marginal (M), and vegetal (V) pieces as depicted in Fig. 2A and dissected on ice in solutions precooled to 4°C. Whole embryos of the same stage were cooled to 4°C and lysed in parallel. Lysates were standardized for total protein, immunoprecipitated with MAP kinase specific antiserum and assayed for STAT-3 kinase activity. Active MAP kinase is found in animal, marginal, and vegetal regions. (B) Embryos were injected with mRNA for a dominant inhibitory FGF receptor and vegetal bottoms were explanted at stage 9. Explants were lysed in extraction buffer, standardized for total protein and assayed for STAT-3 kinase activity. MAP kinase activity present in vegetal bottoms is FGF receptor dependent. (C) Vegetal bottoms were explanted at stage 9.5 from uninjected embryos or embryos injected with mRNA encoding dominant inhibitory FGF receptor and harvested for RT-PCR analysis with primers specific for EF1 alpha and Mix.1.

excluded from the vegetal pole of the embryo. It was therefore of interest to determine if the endogenous MAP kinase activity present in vegetal bottoms was FGF receptor dependent (Cornell *et al.*, 1995). Embryos were injected vegetally with mRNA encoding the dominant inhibitory FGF receptor in both cells at the 2-cell stage and allowed to develop until stage 9. Vegetal bottoms were explanted on ice from receptor-injected and uninjected embryos, standardized for total protein and immunoprecipitated with MAP kinase-specific antibodies (Fig. 5B). As was found for dissection-mediated MAP kinase activation, endogenous MAP kinase activity present in immune complexes from dominant inhibitory FGF receptor injected embryos was greatly reduced relative to control embryos. This demonstrates that the vegetal pole MAP kinase activity is due to FGF receptor activity. The residual MAP kinase activity noted in vegetal bottoms from dominant inhibitory receptor-injected embryos

Copyright © 1997 by Academic Press. All rights of reproduction in any form reserved.

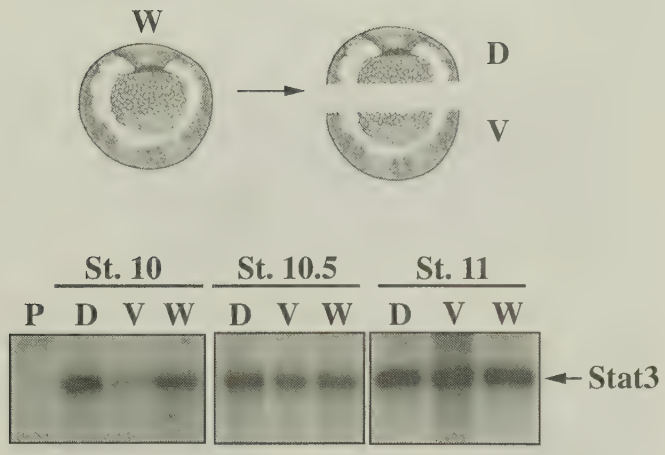

FIG. 6. Increases in MAP kinase activity precede blastopore lip formation. Gastrula stage embryos were dissected into dorsal (D) and ventral (V) halves as depicted at stages 10, 10.5, and 11. Dissections were performed on ice in solutions precooled below 0°C. Lysates from dorsal and ventral half embryos were standardized for total protein with same stage control embryos (W) and immunoprecipitated with MAP kinase specific antiserum and assayed for STAT-3 kinase activity.

may result from nonuniform distribution of the injected mRNA. Consistent with a role for MAP kinase signaling in the prospective endoderm, expression of a meso-endodermal marker normally expressed in vegetal bottoms, Mix-1, is inhibited in vegetal bottoms overexpressing a dominant inhibitory FGF receptor (Fig. 5C). This is consistent with results obtained previously with mesoderm inducing factors in animal cap assays (Labonne and Whitman, 1994; Huang *et al.*, 1995). Endogenous MAP kinase activity in animal caps and marginal zones is also FGF receptor dependent (not shown).

FGF-Dependent MAP Kinase Activity at Gastrulation

In addition to its role in mesoderm formation, FGF signaling is also thought to be required for gastrulation (Isaacs *et al.*, 1994). As MAP kinase activity is regionally localized in blastulae, and as it increases significantly at gastrula stages, it was of interest to determine whether this increase was uniform throughout the embryo, or also displayed regional localization. Prechilled embryos were dissected on ice into dorsal and ventral halves, lysed, and standardized for total protein with undissected embryos of the same stage. Immune complex kinase assays indicated that at stage 10.5, MAP kinase activity was slightly higher on the dorsal side of the embryo than on the ventral side (Fig. 6). As it has been reported that XeFGF is initially enriched dorsally before being expressed in a ring around the blastopore (Isaacs *et al.*, 1992), it seemed possible that some or all of this MAP kinase activity may be XeFGF dependent. If this were the case, dorso-ventral differences in MAP kinase activity might be more dramatic at earlier stages. Accordingly, the experiment was repeated at stage 10+, when bottle cells are visible but no lip has yet formed. At this stage MAP kinase activity was found to be several-fold higher on the dorsal side of the embryo (Fig. 6). Indeed, this difference was already measurable at stage 9.5, before any external evidence of gastrulation could be observed (not shown). By stage 11, MAP kinase activity was fairly equal in both dorsal and ventral regions (Fig. 6). This activity may represent XeFGF activity, as it correlates closely with the dorso-ventral expression of this gene in the marginal zone (Isaacs *et al.*, 1992, 1994). As it has been proposed that XeFGF may play a role in the cell movements and shape changes which underlie gastrulation (Isaacs *et al.*, 1994), the observation that MAP kinase activation precedes lip formation on both the dorsal and ventral sides of the embryo suggest that XeFGF-dependent MAP kinase activation could mediate these effects.

DISCUSSION

Temporal and Spatial Distribution of MAP Kinase Activity in Early Embryos

FGF-dependent activation of MAP kinase has previously been demonstrated to be both necessary and sufficient for mesoderm induction, and as such it is a useful marker of endogenous FGF activity. In this report we examine the spatial and temporal distribution of MAP kinase activity within the early embryo in order to gain insight into the role of FGF during mesoderm induction and axial patterning. Using a highly sensitive immune complex kinase assay, we find that MAP kinase activity is low during early cleavage stages and increases significantly during gastrulation. Interestingly, this is not unlike the expression pattern of one member of the FGF family, XeFGF (Isaacs *et al.*, 1992, 1994). The increase in MAP kinase activity noted at post-MBT stages is dependent upon protein synthesis, as it fails to occur in embryos which have been treated with cycloheximide. This is not surprising as this treatment would prevent zygotic expression of XeFGF. Like XeFGF expression, gastrula stage MAP kinase activity is initially, but transiently, concentrated on the dorsal side of the embryo. As gastrulation proceeds, MAP kinase activity becomes more evenly distributed across dorsal and ventral regions. Similarly, by mid-gastrula stages XeFGF is expressed in a ring around the blastopore. Our results suggest that XeFGF expression and activation of MAP kinase may precede involution in both dorsal and ventral regions, suggesting that FGF signaling could play a role in this process. Consistent with this, when a dominant inhibitory FGF receptor is overexpressed in the vegetal pole, dorsal lip formation and gastrulation movements can be completely inhibited (LaBonne, 1996). An argument for the involvement of XeFGF in gastrulation movements has been made pre-

Copyright © 1997 by Academic Press. All rights of reproduction in any form reserved.

viously (Isaacs *et al.*, 1994). As MAP kinase is an obligate component of FGFR signaling during gastrulation, and as it is known to have cytoskeletal substrates which could mediate changes in cell shape and motility, MAP kinase may mediate any role FGFR signaling plays in gastrulation movements. Consistent with this, downregulation of MAP kinase activity by overexpression of a MAP kinase phosphatase, MKP-1, causes gastrulation defects indistinguishable from those caused by overexpression of a dominant inhibitory FGF receptor (LaBonne *et al.*, 1995).

At blastula stages, MAP kinase activity is found in all three germ layers and activity is lowest in the animal pole. The detection of MAP kinase activity in animal pole cells reinforces the idea that FGF signaling may be acting "upstream" of activin and similar mesoderm inducers in animal cap assays. The MAP kinase activity detected in unstimulated animal caps may be the target of the dominant inhibitory FGF receptor in experiments where immediate early transcriptional responses to activin such as *Xbra* expression are inhibited (LaBonne and Whitman, 1994; Cornell and Kimelman, 1994; LaBonne *et al.*, 1995). It remains possible that the basal FGFR activity noted in unstimulated animal caps is supplemented by a slow activin-mediated pretranscriptional release of sequestered FGF, and it is this increase that is required for mesoderm induction. An activin-dependent increase in MAP kinase activity prior to the activation of immediate early gene expression has not been observed (LaBonne and Whitman, 1994; Graves *et al.*, 1994; Hartley *et al.*, 1994). However, overexpression of activin mRNA can lead to increased levels of endogenous MAP kinase activity at blastula stages, possibly due to increased levels of eFGF expression associated with activin mediated mesoderm induction (Fig. 1D).

Tyrosine Phosphorylation vs Activity of MAP Kinase

Using immune complex kinase assays, MAP kinase activity in marginal zones and vegetal bottoms is found to be several-fold higher than the activity present in animal caps. This differs from what had been observed previously by measuring tyrosine phosphorylation of MAP kinase in these regions (LaBonne *et al.*, 1995). It is possible that the immunoprecipitation/Western blotting procedure which was used to measure tyrosine phosphorylation is not linear enough to detect these differences. Alternatively, tyrosine phosphorylated MAP kinase may not be an accurate predictor of MAP kinase activation in this system. MAP kinase requires phosphorylation on both tyrosine and threonine in order to be active (reviewed in Blenis, 1993). MEK, also known as MAP kinase kinase, is a dual specificity kinase which can phosphorylate both of these sites (Kyriakis *et al.*, 1992), while dual specificity phosphatases such as MKP-1 inactivate MAP kinase by dephosphorylating both of these sites (Sun *et al.*, 1993). If either site is dephosphorylated independently, however, the kinase is rendered inactive (Sarcevic *et al.*, 1993; Alessi *et al.*, 1995). It is possible that an inactive, tyrosine-phosphorylated form of MAP kinase is present in embryos. This would suggest that one mechanism of MAP kinase regulation utilized during embryonic development may involve removal of the regulatory threonine phosphate. A protein phosphatase capable of removing this phosphate is present in early embryos. (Alessi *et al.*, 1995).

Dissection and MAP Kinase Activation

The dramatic increase in MAP kinase activity noted following embryonic wounding indicates that this pathway has the capacity to be activated to much higher levels than are actually observed endogenously. As this increase occurs rapidly and can be inhibited by overexpression of a dominant inhibitory FGF receptor, a likely explanation for this phenomenon is that total levels of endogenous FGFR-ligand are significantly higher than the amount being actively secreted, and that cellular damage permits release of a portion of this excess ligand. This suggests that in *Xenopus* the FGF pathway is regulated, at least in part, at the level of ligand secretion. One member of the FGF family present in early embryos, bFGF, lacks a signal sequence (Kimelman *et al.*, 1988) and as such is not efficiently released from cells which express it. Novel mechanisms of bFGF release are thought to exist (Mason, 1994) and might be active during early *Xenopus* development. Wounding of embryos may allow for a massive and unregulated release of this ligand from cells, resulting in a subsequent burst of MAP kinase activity. This increase in activity is lowest in animal caps and no mesoderm is induced when small animal caps are explanted. Additional wounding can result in expression of *Xbra*, a marker of immediate early mesodermal responses, possibly by increasing the amount of FGF released (Fig. 4B). Effects of embryonic dissection on cell fate have been previously noted. For example, it has been found that dorsal inductive potency can be activated in latero- and ventro-vegetal blastomeres from early cleavage stage embryos by operative procedures (Dale and Slack, 1987). Similarly, in his experiments on the vegetalizing action of lithium, Nieuwkoop noted that lithium's effects were more dramatic on dissected embryos than on those treated intact (Nieuwkoop, 1970). Such experiments highlight the importance of using noninvasive experimental techniques where possible to confirm findings based largely on surgical methods. Recent advances in transgenic and antisense technologies should facilitate these endeavors.

Role of Endogenous FGF-Dependent MAP Kinase Activation in Early Patterning

Endogenous MAP kinase activity measured under conditions where wound-dependent inductions are negligible also appear to be FGF receptor dependent. Contrary to previous models (Cornell *et al.*, 1995), FGF signaling is found to be relatively high within the prospective endoderm. Consistent with this, it has been reported that expression of a marker of dorsal endoderm, XLHbox8, can be inhibited in

Copyright © 1997 by Academic Press. All rights of reproduction in any form reserved.

cells overexpressing a dominant inhibitory FGF receptor (Henry *et al.*, 1996) although this has not been observed by all groups (Gamer and Wright, 1995). Expression of this marker is also inhibited when levels of FGF signaling are increased following treatment with exogenous FGF, however, and are restored by concurrent treatment with activin (Gamer and Wright, 1995). Similarly, we have found that the v-*ras*-induced increase in *Xbra* expression in explanted vegetal bottoms is decreased by coinjection with bVg-1 (LaBonne and Whitman, unpublished). This suggests a model in which relative levels of FGF and TGF-β-like signals may be important for determining embryonic fate. Levels of other growth factors are likely to play instructive roles as well. For example, Nieuwkoop found that treatment of prospective mesoderm with lithium could cause it to adopt an endodermal fate (Nieuwkoop, 1970). As lithium is thought to mimic a wnt-like signaling pathway (Christian and Moon, 1992), it is possible that a member of the wnt family is involved in endoderm specification endogenously. Xwnt-11, whose maternal message is vegetally localized, is an obvious candidate for such a factor (Ku and Melton, 1993).

Despite the progress which has been made in determining the components of FGFR signal transduction required for mesoderm induction, it is as yet unclear how this requirement manifests itself at the molecular level. One possibility is that transcription factors necessary for the immediate early mesoderm response require phosphorylation by both FGF-dependent and TGF-β-dependent kinases in order to be activated. Consistent with this, a regulatory element required for activation of the zebrafish goosecoid promoter has been found to respond only to a combination of activin and FGF (Joore *et al.*, 1996). The immediate early mesodermal response factor brachyury, as well as other T-box family members, contains consensus MAP kinase phosphorylation sites, although FGF-dependent phosphorylation of these sites has yet to be demonstrated. In addition, members of the ETS and Jun families of transcription factors are known MAP kinase substrates in other systems (Triesman, 1996). *Xenopus* ETS-1 has been shown to be a MAP kinase substrate which can modulate mesodermal gene expression in *Xenopus* (C. LaBonne and M. Whitman, in preparation). It has also been reported that c-*Jun* may play an important role downstream of the RAS/MAP kinase pathway during mesoderm induction (Xu *et al.*, 1996). In *Xenopus*, activin induction of Mix-1 expression requires FGF signaling, despite FGF's inability to induce transcription of this gene (LaBonne and Whitman, 1994; Huang *et al.*, 1995). A regulatory element has been identified in the Mix.1 promoter which is both necessary and sufficient for activin induction of this gene (Huang *et al.*, 1995). Interestingly, an ETS DNA binding site is located just upstream of this activin responsive element. The Mix.1 promoter also contains multiple binding sites for c-*Jun*. The necessity of these ETS and Jun sites for Mix-1 promoter function has yet to be determined.

FGF-dependent MAP kinase activity appears to have multiple roles in early patterning. Its presence, and requirement for endogenous or induced meso-endodermal gene expression, in all three germ layers indicates that some level of FGF signaling is ubiquitously required for patterning throughout the early embryo. FGF-dependent MAP kinase activity is found to be lower in animal pole regions than in the vegetal pole or marginal zone, however, and this spatial difference may play an important role in cell fate decisions. For example, maintaining lower FGF signaling levels at the animal pole might help prevent mesodermal gene expression in this region of the embryo. FGF signaling is also thought to be important for maintenance of mesodermal gene expression and may be part of a process through which cell–cell communication translates an initially stochastic cellular response into a coherent patterning of the mesodermal mantle (Wilson and Melton, 1994; Green *et al.*, 1994) and, indeed, all three germ layers. In addition, the dynamic spatial localization of FGF signaling during gastrula stages suggests that this pathway may also play a required role in the complex movements which underlie gastrulation. Clearly there is still much work to be done before the role of FGF signaling during early *Xenopus* development is completely understood.

ACKNOWLEDGMENTS

The authors gratefully acknowledge Jonkyeung Chung and John Blenis for providing STAT-3 substrate and sharing results prior to publication and Rebecca Hartley and Jim Maller for MAP kinase specific antibodies. We thank Anna Philpott, Jeremy Green, Karen Symes, and Adrian Gross for helpful discussions. We are grateful to Karen Symes, Jeremy Green, and Ellen Weisberg for critical reading of the manuscript. C.L. was supported, in part, by an NSF predoctoral fellowship. M.W. is a scholar of the Lucille P. Markey Charitable Trust. This work was also supported by a grant from the NIH.

REFERENCES

Alessi, D. R., Gomez, N., Moorhead, G., Lewis, T., Keyse, S. M., and Cohen, P. (1995). Inactivation of p42 MAP kinase by protein phosphatase 2A and a protein tyrosine phosphatase, but not CL100, in various cell lines. *Curr. Biol.* **5,** 283–295.

Amaya, E., Musci, T. J., and Kirschner, M. W. (1991). Expression of a dominant negative mutant of the FGF receptor disrupts mesoderm formation in *Xenopus* embryos. *Cell* **66,** 257–270.

Amaya, E., Stein, P., Musci, T., and Kirschner, M. W. (1993). FGF signaling in the early specification of mesoderm in *Xenopus*. *Development* **118,** 477–487.

Asashima, M., Nakano, H., Shimada, K., Kinoshita, K., Ishii, K., Shibai, H., and Ueno, N. (1990). Mesodermal induction in early amphibian embryos by activin A (erythroid differentiation factor). *Roux's Arch. Dev. Biol.* **198,** 330–335.

Asashima, M., Nakano, H., Uchiyama, H., Sugino, H., Nakamura, T., Eto, Y., Ejima, D., Nishimatsu, S., Ueno, N., and Kinoshita, K. (1991). Presence of activin (erythroid differentiation factor) in unfertilized eggs and blastulae of *Xenopus laevis*. *Proc. Natl. Acad. Sci. USA* **88,** 6511–6514.

Copyright © 1997 by Academic Press. All rights of reproduction in any form reserved.

Blenis, J. (1993). Signal transduction via the MAP kinases: Proceed at your own RSK. *Proc. Natl. Acad. Sci. USA* **90,** 5899–5892.

Cascio, S., and Gurdon, J. B. (1987). The initiation of new gene transcription during *Xenopus* gastrulation requires immediately preceding protein synthesis. *Development* **100,** 297–305.

Christian, J. L., and Moon, R. T. (1993). Interactions between the Xwnt-8 and Spemann organizer signalling pathways generate dorsoventral pattern in the embryonic mesoderm of *Xenopus. Genes Dev.* **7,** 13–28.

Cornell, R. A., and Kimelman, D. (1994). Activin-mediated mesoderm induction requires FGF. *Development* **120,** 453–462.

Cornell, R. A., Musci, T. J., and Kimelman, D. (1995). FGF is a prospective competence factor for early activin-type signals in *Xenopus* mesoderm induction. *Development* **121,** 2429–2437.

Dale, L., Matthews, G., and Colman, A. (1993). Secretion and mesoderm inducing activity of the TGFβ related domain of *Xenopus* Vg1. *EMBO J.* **12,** 4471–4480.

Dale, L., and Slack, J. M. W. (1987). Regional specification within the mesoderm of early embryos of *Xenopus laevis. Development* **100,** 279–295.

Dohrmann, C. E., Hemmati-Brivanlou, A., Thomsen, G. H., and Fields, A. (1993). Expression of activin mRNA during early development in *Xenopus laevis. Dev. Biol.* **157,** 474–483.

Fukui, A., Nakamura, T., Uchiyama, H., Sugino, K., Sugino, H., and Asashima, M. (1994). Identification of activins A, AB, and B and follistatin proteins in *Xenopus* embryos. *Dev. Biol.* **163,** 279–281.

Gamer, L. W., and Wright, C. V. (1995). Autonomous endodermal determination in *Xenopus:* Regulation of expression of the pancreatic gene X1Hbox 8. *Dev. Biol.* **171,** 240–251.

Gotoh, Y., Masuyama, N., Suzuki, A., Ueno, N., and Nishida, E. (1995). Involvement of the MAP kinase cascade in *Xenopus* mesoderm induction. *EMBO J.* **14,** 2491–2498.

Graves, L. M., Northrup, J. L., Potts, B. C., Krebs, E. G., and Kimelman, D. (1994). Fibroblast growth factor, but not activin, is a potent activator of mitogen-activated protein kinase in *Xenopus* explants. *Proc. Natl. Acad. Sci. USA* **91,** 1662–1666.

Green, J. B., Smith, J. C., and Gerhart, J. C. (1994). Slow emergence of a multithreshold response to activin requires cell-contact-dependent sharpening but not prepattern. *Development* **120,** 2271–2278.

Hartley, R. S., Lewellyn, A. L., and Maller, J. L. (1994). Map kinase is activated during mesoderm induction in *Xenopus laevis. Dev. Biol.* **163,** 521–524.

Hemmati-Brivanlou, A., and Melton, D. A. (1992). A truncated activin receptor dominantly inhibits mesoderm induction and formation of axial structures in *Xenopus* embryos. *Nature* **359,** 609–614.

Henry, G. L., Brivanlou, I. H., Kessler, D. S., Hemmati-Brivanlou, A., and Melton, D. A. (1996). TGF-β signals and a prepattern in *Xenopus laevis* endodermal development. *Development* **122,** 1007–1015.

Huang, H. C., Murtaugh, L. C., Vize, P., and Whitman, M. (1995). Identification of a potential regulator of early transcriptional responses to activin in the frog embryo. *EMBO J.* **14,** 5965–5973.

Isaacs, H. V., Pownall, M. E., and Slack, J. M. W. (1994). eFGF regulates Xbra expression during *Xenopus* gastrulation. *EMBO J.* **13,** 4469–4481.

Isaacs, H. V., Tannahill, D., and Slack, J. M. W. (1992). Expression of a novel FGF in the *Xenopus* embryo: A New candidate inducing factor for mesoderm formation and anteroposterior specification. *Development* **114,** 711–720.

Joore, J., Fasciana, C., Speksnijder, J., Kruijer, W., Destree, O. H. J., van den Eijnden-van Raaij, A. J. M., de Laat, S. W., and Zivkovic, D. (1996). Regulation of the zebrafish goosecoid promoter by mesoderm inducing factors and Xwnt1. *Mech. Dev.* **55,** 3–18.

Kimelman, D., Abraham, J. A., Haaparanta, T., Palishi, T. M., and Kirschner, M. W. (1988). The presence of fibroblast growth factor in the frog egg: Its role as a natural mesoderm inducer. *Science* 1053–1056.

Kimelman, D., Christian, J. L., and Moon, R. T. (1992). Synergistic principles of development: Overlapping patterning systems in *Xenopus* mesoderm induction. *Development* **116,** 1–9.

Kimelman, D., and Kirschner, M. (1987). Synergistic induction of mesoderm by FGF and TGFβ and the identification of FGF in the early *Xenopus* embryo. *Cell* **51,** 869–877.

Ku, M., and Melton, D. A. (1993). Xwnt-11: A maternally expressed wnt gene. *Development* **119,** 1161–1173.

Kyriakis, J. M., App, H., Zhang, X.-F., Banerjee, P., Brautigan, D. L., Rapp, U. R., and Avruch, J. (1992). Raf-1 activates MAP kinase-kinase. *Nature* **358,** 417–421.

LaBonne, C., Burke, B., and Whitman, M. (1995). Role of MAP kinase in mesoderm induction and axial patterning during *Xenopus* development. *Development* **121,** 1475–1486.

LaBonne, C., and Whitman, M. (1994). Mesoderm induction by activin requires FGF mediated intracellular signals. *Development* **120,** 463–472.

LaBonne, C. (1996). "FGF Generated Signals During Mesoderm Formation in *Xenopus*." Doctoral Thesis, Harvard University.

MacNicol, A. M., Muslin, A. J., and Williams, L. T. (1993). Raf-1 kinase is essential for early *Xenopus* development and mediates the induction of mesoderm by FGF. *Cell* **73,** 571–584.

Mason, I. J. (1994). The ins and outs of fibroblast growth factors. *Cell* **78,** 547–552.

Newport, J., and Kirschner, M. (1982). A major developmental transition in early *Xenopus* embryos. 1. Characterization and timing of cellular changes at the midblastula transition. *Cell* **30,** 675–686.

Nieuwkoop, P. D. (1969). The formation of mesoderm in urodelean amphibians. I. Induction by the endoderm. *Roux Arch. EntwMech. Org.* **162,** 341–373.

Nieuwkoop, P. D. (1970). The formation of the mesoderm in urodelean amphibians. III. The vegetalizing action of the Li^+ ion. *Roux' Archiv.* **166,** 105–123.

Nieuwkoop, P. D., and Faber, J. (1967). "Normal Table of *Xenopus laevis* (Daudin)," 2nd ed. North-Holland, Amsterdam.

Northrop, J., Woods, A., Seger, R., Suzuki, A., Ueno, N., Krebs, E., and Kimelman, D. (1995). BMP-4 regulates the dorsal-ventral differences in FGF/MAPKK-mediated mesoderm induction in *Xenopus. Dev. Biol.* **172,** 242–252.

Oda, S., Nishimatsu, S., Murakami, K., and Ueno, N. (1995). Molecular cloning and functional analysis of a new activin β subunit: a Dorsal mesoderm-inducing activity in *Xenopus. Biochem. Biophys. Res. Commun.* **210,** 581–588.

Sarcevic, B., Erikson, E., and Maller, J. L. (1993). Purification and characterization of a mitogen-activated protein kinase tyrosine phosphatase from *Xenopus* eggs. *J. Biol. Chem.* **268,** 25075–25083.

Schulte-Merker, S., Smith, J. C., and Dale, L. (1994). Effects of truncated activin and FGF receptors and of follistatin on the inducing activities of BVg1 and activin: Does activin play a role in mesoderm induction? *EMBO J.* **13,** 3533–3541.

Slack, J. M. W., Darlington, B. G., Heath, J. K., and Godsave, S. F.

Copyright © 1997 by Academic Press. All rights of reproduction in any form reserved.

(1987). Mesoderm induction in early *Xenopus* embryos by heparin-binding growth factors. *Nature* **326,** 197–200.

Slack, J. M. W., and Tannahill, D. (1992). Mechanism of anteroposterior axis specification in vertebrates: Lessons from the amphibians. *Development* **114,** 285–302.

Smith, J. C., Price, B. M. J., Green, J. B. A., Weigel, D., and Herrmann, B. G. (1991). Expression of a *Xenopus* homolog of *Brachyury* (*T*) is an immediate–early response to mesoderm induction. *Cell* **67,** 79–87.

Smith, J. C., Price, B. M. J., Van Nimmen, K., and Huylebroeck, D. (1990). Identification of a potent *Xenopus* mesoderm-inducing factor as a homolog of activin A. *Nature* **345,** 729–731.

Sokol, S., Wong, G. G., and Melton, D. A. (1990). A mouse macrophage factor induces head structures and organizes a body axis in *Xenopus*. *Science* **249,** 561–564.

Sudarwati, S., and Nieuwkoop, P. D. (1971). Mesoderm formation in the anuran *Xenopus laevis* (Daudin). *Roux' Archiv.* **166,** 189–204.

Sun, H., Charles, C., Lau, L., and Tonks, N. (1993). MKP-1 (3CH134) an immediate early gene product, is a dual specificity phosphatase that dephosphorylates MAP kinase in vivo. *Cell* **75,** 487–493.

Takasaki, H., and Yagura, M. (1975). Remarks on dorso-ventral gradients in the mesoderm formation *Xenopus laevis*. *Mem. Osaka Kyoiku Univ. Ser. III* **24,** 145–158.

Tannahill, D., and Melton, D. A. (1989). Localized synthesis of the Vg1 protein during early *Xenopus* development. *Development* **106,** 775–785.

Thomsen, G., and Melton, D. (1993). Processed Vg1 protein is an axial mesoderm inducer in *Xenopus*. *Cell* **74,** 433–441.

Thomsen, G., Woolf, T., Whitman, M., Sokol, S., Vaughan, J., Vale, W., and Melton, D. A. (1990). Activins are expressed early in *Xenopus* embryogenesis and can induce axial mesoderm and anterior structures. *Cell* **63,** 485–493.

Triesman, R. (1996). Regulation of MAP kinase cascades. *Curr. Opin. Cell Biol.* **8,** 205–215.

Turner, D. L., and Weintraub, H. (1994). Expression of achaete-scute homolog 3 in *Xenopus* embryos converts ectodermal cells to a neural fate. *Genes Dev.* **8,** 1434–1447.

Umbhauer, M., Marshall, C. J., Mason, C. S., Old, R. W., and Smith, J. C. (1995). Mesoderm induction in *Xenopus* caused by activation of MAP kinase. *Nature* **376,** 58–62.

Weeks, D. L., and Melton, D. A. (1987). A maternal mRNA localized to the vegetal hemisphere in *Xenopus* eggs codes for a growth factor related to TGF-β. *Cell* **51,** 861–867.

Whitman, M., and Melton, D. (1992). Involvement of p21 ras in *Xenopus* mesoderm induction. *Nature* **357,** 252–255.

Wilson, P. A., and Melton, D. A. (1994). Mesodermal patterning by an inducer gradient depends on secondary cell–cell communication. *Curr. Biol.* **4,** 676–686.

Xu, R.-H., Dong, Z., Maeno, M., Kim, J., Suzuki, A., Ueno, N., Sredni, D., Colburn, N., and Kung, H.-F. (1996). Involvement of ras/raf/AP-1 in BMP-4 signaling during *Xenopus* embryonic development. *Proc. Natl. Acad. Sci. USA* **93,** 834–838.

Received for publication December 4, 1996
Accepted December 19, 1996

Copyright © 1997 by Academic Press. All rights of reproduction in any form reserved.

DEVELOPMENTAL BIOLOGY 183, 21–36 (1997)
ARTICLE NO. DB968485

GATA-5: A Transcriptional Activator Expressed in a Novel Temporally and Spatially-Restricted Pattern during Embryonic Development

Edward E. Morrisey, Hon S. Ip, Zhihua Tang, Min M. Lu, and Michael S. Parmacek

Department of Medicine, University of Chicago, Chicago, Illinois 60637

Members of the GATA family of zinc finger transcription factors regulate critical steps of cellular differentiation during vertebrate development. In the studies described in this report, we have isolated and functionally characterized the murine GATA-5 cDNA and protein and defined the temporal and spatial pattern of GATA-5 gene expression during mammalian development. The amino terminus of the mouse GATA-5 protein shares high level amino acid sequence identity with the murine GATA-4 and -6 proteins, but not with other members of the GATA family. GATA-5 binds to the functionally important CEF-1 nuclear protein binding site in the cardiac-specific slow/cardiac troponin C (cTnC) transcriptional enhancer and overexpression of GATA-5 transactivates the cTnC enhancer in noncardiac muscle cell lines. During embryonic and postnatal development, the pattern of GATA-5 gene expression differs significantly from that of other GATA family members. In the primitive streak embryo, GATA-5 mRNA is detectable in the precardiac mesoderm. Within the embryonic heart, the GATA-5 gene is expressed within the atrial and ventricular chambers (ED 9.5), becomes restricted to the atrial endocardium (ED 12.5), and is subsequently not expressed in the heart during late fetal and postnatal development. Moreover, coincident with the earliest steps in lung development, only the GATA-5 gene is expressed within the pulmonary mesenchyme. Finally, the GATA-5 gene is expressed in tissue-restricted subsets of smooth muscle cells (SMCs), including bronchial SMCs and SMCs in the bladder wall. These data are consistent with a model in which GATA-5 performs a unique temporally and spatially restricted function in the embryonic heart and lung. Moreover, these data suggest that GATA-5 may play an important role in the transcriptional program(s) that underlies smooth muscle cell diversity. © 1997 Academic Press

INTRODUCTION

The GATA family of zinc finger transcription factors play important roles in regulating cell lineage differentiation during vertebrate development (for review see (Orkin, 1992; Simon, 1995; Weiss and Orkin, 1995a). Six GATA family members have been identified in vertebrate species. These six proteins have been classified into two subfamilies based on common amino acid sequence identities and patterns of expression (Arceci *et al.*, 1993; Dorfman *et al.*, 1992; Evans *et al.*, 1988; Heikinheimo *et al.*, 1994; Ho *et al.*, 1991; Jiang and Evans, 1996; Joulin *et al.*, 1991; Kelley *et al.*, 1993; Ko *et al.*, 1991; Laverriere *et al.*, 1994; Lee *et al.*, 1990; Morrisey *et al.*, 1996; Tsai *et al.*, 1989; Wilson *et al.*, 1990; Yamamoto *et al.*, 1990; Zon *et al.*, 1991). Each GATA family member contains a conserved C-X_2-C-X_{17}-C-X_2-C (type IV) zinc finger DNA-binding domain that recognizes a consensus sequence motif (WGATAR) located within transcriptional regulatory elements that control sets of lineage-specific genes (Ho *et al.*, 1991; Ko and Engel, 1993; Merika and Orkin, 1993; Omichinski *et al.*, 1993; Yang *et al.*, 1994). In addition to activating transcription directly, recent studies have revealed that GATA-1 may directly, or indirectly, be involved in regulating programmed cell death during development (Weiss and Orkin, 1995b; Blobel and Orkin, 1996). Gene targeting experiments have revealed that while the GATA-1, -2, and -3 proteins are expressed in overlapping patterns in the hematopoietic cell lineages, mice harboring null mutations in each of these genes exhibit distinct phenotypes (Pandolfi *et al.*, 1995; Pevny *et al.*, 1991; Simon *et al.*, 1992; Tsai *et al.*, 1994; Weiss *et al.*, 1994). These data are consistent with a model wherein each GATA family member regulates unique lineage-restricted developmental programs.

0012-1606/97 $25.00
Copyright © 1997 by Academic Press
All rights of reproduction in any form reserved.

Previous studies have suggested that the GATA-4/5/6 subfamily of transcription factors may direct tissue-specific gene expression during development of the vertebrate heart (Jiang and Evans, 1996; Kelley *et al.*, 1993; Laverriere *et al.*, 1994; Tamura *et al.*, 1993). Functionally important GATA binding sites have been identified within the promoters of multiple cardiac-specific genes, including slow/cardiac troponin C, α-myosin heavy chain, B-type natriuretic peptide (BNP), and cardiac troponin I, and each of these cardiac-specific transcriptional regulatory elements can be transactivated by overexpression of GATA-4 (and in some cases GATA-6) in noncardiac muscle cell lines (Grepin *et al.*, 1994; Ip *et al.*, 1994; Molkentin *et al.*, 1994; Morrisey *et al.*, 1996). In addition, expression of GATA-4 antisense transcripts in pluripotent P19 embryonal carcinoma cells blocks the development of beating cardiac myocytes and interferes with expression of cardiac-specific contractile protein isoforms (Grepin *et al.*, 1995). Moreover, ectopic expression of *Xenopus* GATA-4, -5, or -6 during embryogenesis is capable of prematurely activating expression of the genes encoding α-cardiac actin and α-myosin heavy chain (Jiang and Evans, 1996).

In avian and *Xenopus* species the genes encoding GATA-4, -5, and -6 are expressed in an overlapping pattern in the heart and gut epithelium (Jiang and Evans, 1996; Laverriere *et al.*, 1994). Thus, it remains unclear whether each of these GATA subfamily members subserves unique or redundant developmental functions. In this regard, it is noteworthy that in mammalian species, significant differences in the developmentally regulated, tissue-restricted patterns of GATA-4 and -6 gene expression have been identified that are not present, or were not appreciated, in lower vertebrates (Heikinheimo *et al.*, 1994; Morrisey *et al.*, 1996). For example, coincident with the onset of vasculogenesis, the murine GATA-6 gene is expressed in arterial and venous smooth muscle cells (SMCs), while the GATA-4 gene is not (Morrisey *et al.*, 1996). Moreover, a mammalian GATA-5 homologue has not, as yet, been described. However, in avian species, the GATA-5 gene is expressed at least as early as stage 7 within the heart and the gene continues to be expressed at high levels within both the endocardium and myocardium throughout postnatal development (Laverriere *et al.*, 1994). Taken together, these data suggest that although the GATA-4, -5 and -6 genes are expressed in an overlapping pattern during embryogenesis and postnatal development, fine differences in the spatial and temporal pattern of expression of each family member may impact profoundly on their developmental function.

In the studies described in this report, we have isolated the murine GATA-5 cDNA and compared the structure of the deduced murine GATA-5 protein to each of the previously characterized GATA family members. We have demonstrated that forced expression of GATA-5 transactivates a cardiac-specific transcriptional regulatory element in noncardiac muscle cell lines. In addition, the mouse GATA-5 cDNA was used as a molecular probe to map the temporal and spatial patterns of GATA-5 gene expression in the embryonic mouse and during postnatal development. These data are consistent with a model wherein GATA-5 serves as a transcriptional activator that regulates a novel developmental program within the embryonic heart and lung. In addition, these data suggest that GATA-5 may play an important role in the transcriptional program(s) that underlies smooth muscle cell diversity.

MATERIALS AND METHODS

Isolation of Murine GATA-5 cDNA Clones

To isolate the murine GATA-5 cDNA, 10^6 recombinant clones from a Day 13 mouse embryonic heart λZAP cDNA library (Stratagene) were screened under moderate stringency conditions (0.5X SSC, 0.1% SDS at 50°C) with a radiolabeled murine GATA-4 cDNA probe encoding the two zinc fingers and adjacent basic domain (bp 1173–1547) as described previously (Parmacek and Leiden, 1989). Replicate filters were hybridized to murine GATA-4 3′-untranslated (3′UTR) and GATA-6 3′UTR cDNA probes in order to identify recombinant clones encoding each of these previously characterized cDNAs (Arceci *et al.*, 1993; Morrisey *et al.*, 1996) and these clones were not characterized further. Two positively hybridizing clones (λmG5-A and λmG5-B), which were approximately 1.8- and 3.2-kb in size, respectively, were isolated, purified to homogeneity, and sequenced with an ABI 377 Automated DNA Sequencer using the Sequencher computer program (Gene Codes, Ann Arbor, MI). The deduced murine GATA-4, -5, and -6 amino acid sequences were aligned using the MAP Multiple Sequence Alignment computer program (Huang, 1994).

Northern Blot Analyses

Northern blot analyses were performed as described previously (Solway *et al.*, 1995). Two nonoverlapping GATA-5 cDNA probes were utilized in these analyses. The mouse GATA-5 ORF cDNA probe (bp 253–707) encodes 52-bp of the 5′UTR and 403-bp of the GATA-5 open reading frame (ORF); while the mouse GATA-5 3′UTR cDNA (bp 2262–2740) is derived exclusively from the 3′UTR (see Fig. 1). Quantitative image analyses were performed using a Molecular Dynamics PhosphorImager (Sunnyvale, CA).

Plasmids

The murine GATA-5 expression plasmid, pcDNAG5, was subcloned by digesting the λmG5-A cDNA clone with *Eco*RI and *Kpn*I to isolate the 1828-bp insert (see Fig. 1A) and subcloning the resultant cDNA fragment encoding the 404-aa GATA-5 protein into the *Eco*RV site of the eukaryotic expression plasmid, pcDNA3 (Invitrogen). The murine GATA-4 expression plasmid, pcDNAG4, has been previously described (Morrisey *et al.*, 1996). The p-124cTnCGH and p-124cTnCGHμCEF-1 growth hormone (GH) reporter plasmids contain the 124-bp cTnC cardiac-specific cTnC promoter-enhancer and the 124-bp cTnC promoter-enhancer with a five nucleotide mutation within the CEF-1 nuclear protein binding site, respectively, subcloned into the p0GH human GH reporter plasmid (Nichol's Institute) and have been described previously

Copyright © 1997 by Academic Press. All rights of reproduction in any form reserved.

(Morrisey *et al.*, 1996). The pCEF-1GH and pμCEF-1GH expression plasmids contain a single copy of the murine cTnC CEF-1 nuclear protein binding site or a copy of the cTnC CEF-1 nuclear protein binding site containing a mutation in the GATA motif, respectively, subcloned immediately 5′ of the minimal rabbit β-globin promoter in the p0GH plasmid and have been described previously (Morrisey *et al.*, 1996).

Cell Culture and Transfections

NIH 3T3 and COS-7 cells were grown as described previously (Parmacek *et al.*, 1994; Parmacek and Leiden, 1989; Solway *et al.*, 1995) For transient cotransfection experiments, 10^6 NIH 3T3 cells were cotransfected with 25 μg of the appropriate GATA expression plasmid, 1 μg of pMSVβgal reference plasmid, 2.5 μg of the appropriate GH reporter plasmid, and 20 μl of Lipofectin Reagent (Gibco). Forty-eight hours following transfection, cell supernatants were assayed for GH by radioimmunoassay (Nichol's Institute) and cell lysates were prepared and analyzed for β-galactosidase activity and protein content as described previously (Ip *et al.*, 1994). Data are expressed as normalized growth hormone ± SEM. All experiments were repeated at least three times to ensure reproducibility.

Electrophoretic Mobility Shift Assays (EMSAs)

Nuclear extracts were prepared from COS-7 cells 48 hr following transient transfection with the pcDNAG5, pcDNAG4, or pcDNA3 expression plasmids as described (Ip *et al.*, 1994). The following complementary oligonucleotides were synthesized with *Bam*HI/*Bgl*II overhanging ends:

cTnC CEF-1 5′ CCAGCCT**GAGATTA**CA**GGGAG** 3′
cTnC μCEF-1 5′ CCAGCCTG**GGGCCC**CAGGGAG 3′
αMHC-GATA 5′ CCAAAGGGCCGATGGGC**AGATAG**AGGA-GAGACAGGA 3′

The native and mutated GATA sites are shown in bold font. EMSAs were performed as described previously (Ip *et al.*, 1994). Antibody supershifts were performed by preincubating nuclear extract with 1 μl of goat polyclonal α-GATA-4 affinity purified IgG (that was raised against an epitope corresponding to amino acids 420–439 of the mouse GATA-4 protein (Santa Cruz, Biotech., Cat. No. sc-1237)) for 20 min at 25°C prior to performing the binding reaction as described previously (Ip *et al.*, 1994). This antiserum does not cross-react with the mouse GATA-1, -2, or -3 proteins.

In Situ Hybridization of Staged Murine Embryos

In situ hybridization was performed essentially as described by Eichele and coworkers (Kuratani *et al.*, 1994). The murine GATA-5 (bp 253–707), GATA-4 (bp 486–936), GATA-6 (bp 589–1119), and SM22α cDNAs (bp 333–1102) were subcloned into pGEM7Z or pGEM11Z and were *in vitro*-transcribed using T7 or SP6 polymerase in the presence of ^{35}S-labeled UTP to generate sense and antisense cRNA probes, respectively. Sections were processed for emulsion autoradiography and were poststained with Hoecht 33258 and visualized by epifluorescence and darkfield microscopy on a Zeiss Axiophot microscope. To detect nonspecific background, hybridizations were performed with the radiolabeled sense riboprobe to alternate sections under identical conditions.

RESULTS

Isolation and Structural Characterization of Murine GATA-5 cDNA Clones

To isolate the murine GATA-5 cDNA, 10^6 recombinant clones from an Embryonic Day (ED) 13 mouse heart cDNA library were screened under moderate stringency conditions with a subfragment of the murine GATA-4 cDNA encoding the evolutionarily conserved zinc finger domains. In addition, replicate filters were hybridized to murine GATA-4 3′-untranslated (3′UTR) and GATA-6 3′UTR cDNA probes in order to identify recombinant clones encoding each of these previously characterized cDNAs (Arceci *et al.*, 1993; Morrisey *et al.*, 1996). Two plaques that hybridized to the mouse GATA-4 zinc finger cDNA probe, but not the murine GATA-4 or GATA-6 3′UTR cDNA probes, designated λmG5-A and λmG5-B, were identified using this screening strategy. The λmG5-A and λmG5-B clones contained overlapping cDNA inserts of approximately 1.8- and 3.2-kb, respectively (Fig. 1A). Each clone contained a 1212-bp open reading frame (ORF) that encoded a predicted 404-amino acid polypeptide with a calculated molecular mass of 42.1 kDa (Fig. 1A). The initiation codon conforms to the consensus sequence described by Kozak (1984). The 1.4-kb difference in the length of the two cDNA clones resulted from differences in the length of their respective 3′UTRs (Fig. 1A). Notably, neither cDNA contained a consensus polyadenylation signal.

Comparison of the deduced amino acid sequence of the murine GATA-5 protein with the previously isolated chicken and *Xenopus* GATA-5 proteins (Jiang and Evans, 1996; Laverriere *et al.*, 1994) revealed 62 and 53% amino acid sequence identity, respectively. In contrast, comparison of the deduced amino acid sequence of the murine GATA-5 protein with the chicken GATA-4 and -6 proteins (Laverriere *et al.*, 1994) revealed 44 and 48% amino acid sequence identity. Despite the relatively low level of amino acid sequence identity between the *Xenopus*, chicken, and murine GATA-5 proteins, multiple amino acid residues were identified that are identical in the chicken, *Xenopus*, and murine GATA-5 proteins that are not conserved in the GATA-4 and -6 proteins (data not shown); suggesting that these cDNAs encode the murine homologue of the GATA-5 protein. Of note, comparison of the deduced amino acid sequence of the murine GATA-5 protein with the previously isolated murine GATA-4 and GATA-6 proteins (Arceci *et al.*, 1993; Morrisey *et al.*, 1996) did reveal high level amino acid sequence identity across the two zinc finger domains and adjacent C-terminal basic domain (Fig. 2, shaded gray). In addition, discrete regions located within the amino terminus of the mouse GATA-5 protein, that

Copyright © 1997 by Academic Press. All rights of reproduction in any form reserved.

A

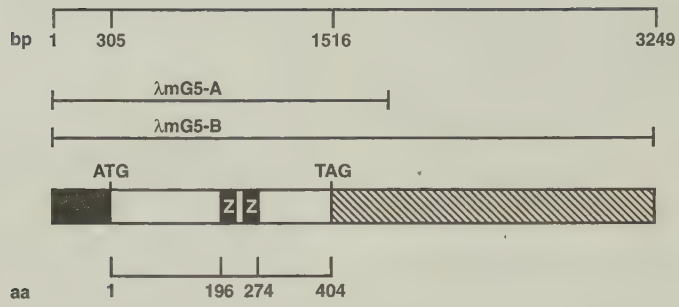

B

```
                                                                                                                ACAACCCACCGGTCACCCTCCCTGGGCCAACGCCGCGCCTTCC
TGTGAGGGCTTTGGCTGGCGATCTCTGCGCAAGGCAAGGACCTCGTTCCTAGGGTCCTGCGCCTCATCTAACCCTGTCATTCCACCC
AGAGGAGCCCGGGACCTGCCCTGGTGAACCGACTCAAAAAAGTGGAGTGCCCAAGCGGAGCAGCAGCACCTGCCCCGGGCGAGCGCA
AGAGCTGATGGAGGGGGCCCAGTGATCCTGCCCTAGACGTCTGCCCGTCTTTCTTCTCTGCAGGTCAAGCTCGCGCGGGGAAAAAAA

ATG TAC CAA AGC TTG GCG TTA GCC CAG AGC CCC GGC CAG GGC ACT TAC GCC GAC TCC GGA GCC TTT
 M   Y   Q   S   L   A   L   A   Q   S   P   G   Q   G   T   Y   A   D   S   G   A   F
CTG CAC TCT TCG GGA ACC GGC TCC CCG GTG TTC GTG GCA CCC ACT CGC ATG CCC TCC ATG CTG CCG
 L   H   S   S   G   T   G   S   P   V   F   V   A   P   T   R   M   P   S   M   L   P
TAC CTG CCT TCG TGT GAG CCG GGC TCG CAG GCT CCC GCG CTC GCC GCG CAC TCC AGC TGG ACA CAA
 Y   L   P   S   C   E   P   G   S   Q   A   P   A   L   A   A   H   S   S   W   T   Q
ACA GTT GCC GCT GAT TCC TCA GCC TTC GGC TCC GGA AGC CCG CAC CCG CCA GCC GCA CAC CCA CCG
 T   V   A   A   D   S   S   A   F   G   S   G   S   P   H   P   P   A   A   H   P   P
GGA GCC ACC ACC TTC CCG TTC GCT CAC AGC CCT CCG GGG TCG GGC AGC GGC GGC AGC GCG GGG GTC
 G   A   T   T   F   P   F   A   H   S   P   P   G   S   G   S   G   G   S   A   G   V
CGG GAC GGC GGC GCC TTC CAG GGC GCG CTG CTG GCT CGC GAA CAG TAC CCG ACC CCG CTC GGG AGA
 R   D   G   G   A   F   Q   G   A   L   L   A   R   E   Q   Y   P   T   P   L   G   R
CCC ATG GGC GCC TCG TAC CCC ACA ACC TAC CCA GCA TAC ATG AGT TCC GAC GTA GCC CCT TCG TGG
 P   M   G   A   S   Y   P   T   T   Y   P   A   Y   M   S   S   D   V   A   P   S   W
ACC TCC GGA GCC TTC GAC AGC AGC ATC CTG CAC GGT CTG CAA GCT CGC CCT GGT GGC CTC CCT GGC
 T   S   G   A   F   D   S   S   I   L   H   G   L   Q   A   R   P   G   G   L   P   G
CGC AGG ACC AGC TTC GTA CCT GAC TTC TTG GAG GAG TTC CCT GGT GAG GGC CGG GAG TGC GTC AAC
 R   R   T   S   F   V   P   D   F   L   E   E   F   P   G   E   G   R   E   C   V   N
TGT GGA GCC CTG TCT ACA CCA CTG TGG CGC AGG GAC GGC ACC GGA CAC TAT CTA TGC AAT GCC TGC
 C   G   A   L   S   T   P   L   W   R   R   D   G   T   G   H   Y   L   C   N   A   C
GGC CTC TAT CAC AAG ATG AAC GGG GTC AAC CGA CCG CTA GTG AGG CCC CAA AAG CGT CTG TCC TCA
 G   L   Y   H   K   M   N   G   V   N   R   P   L   V   R   P   Q   K   R   L   S   S
TCC CGA AGA TCC GGC CTA TGC TGC TCC AAC TGC CAT ACT GCC ACC ACC ACC CTC TGG AGG CGC AAC
 S   R   R   S   G   L   C   C   S   N   C   H   T   A   T   T   T   L   W   R   R   N
TCG GAG GGC GAA CCA GTG TGC AAC GCC TGT GGC CTC TAC ATG AAG CTC CAT GGG GTG CCA AGG CCA
 S   E   G   E   P   V   C   N   A   C   G   L   Y   M   K   L   H   G   V   P   R   P
CTG GCA ATG AAA AAG GAG AGT ATC CAG ACA AGA AAA CGG AAG CCA GAG AAC CCT GCC AAA ATC AAG
 L   A   M   K   K   E   S   I   Q   T   R   K   R   K   P   E   N   P   A   K   I   K
GGC TCC TCA GGA TCC ACA GCA AAC ACC ACA GCC TCT TCT CCC ACT CTC CTC AAC TCT GAG AGC TCA
 G   S   S   G   S   T   A   N   T   T   A   S   S   P   T   L   L   N   S   E   S   S
GCC ACC ACT TTG AAG GCA GAG TCC AGT CTG GCA TCT CCA GTG TGT GCT GGG CCC ACT ATC ACC TCC
 A   T   T   L   K   A   E   S   S   L   A   S   P   V   C   A   G   P   T   I   T   S
CAG GCC TCC AGC CCA GCG GAC GAA TCC CTG GCC TCC AGC CAT TTG GAG TTC AAG TTC GAA CCT GAA
 Q   A   S   S   P   A   D   E   S   L   A   S   S   H   L   E   F   K   F   E   P   E
GAC TTT GCC TTC ACC TCC TCG TCC ATG AGC CCC CAG GCT GGT CTC AGT GGG GTC CTA CGT CAG GAG
 D   F   A   F   T   S   S   S   M   S   P   Q   A   G   L   S   G   V   L   R   Q   E
ACC TGG TGT GCT CTG GCC TTG GCC TAG GTGCTCAGGAAACTGTCACCACAGTACATCCCAGGAACAGAAGTTAGTTCC
 T   W   C   A   L   A   L   A
TGTGTCAGCAGCCCCAGAAGTCCCTCACCACTATGCTGGCGAAATTTTCTGTGCTGATTGCCTGGAGAAAGAACAGGCTGGTGGATG
AAGGGTTGGAGCCTCAGCCGGGGTAGTAATGGACTCCCTAGACCCCTCATGGACCTCTCTGCAGCCAAGATGACTGGAGATATCCAC
CAATTACTTGAATTTAGCTCTTGACATCGATCGTCAAAATTTACAGTTTGTAGCAGCTGGCAAAGGTTCATAGTATCCCACAGTAAA
ATCTGATCCAAGTGAAACAAACATACTCCAGGCAGGCAATAAGAAATAGGGCCTCTGGGCCCTCGTCGTCTTCATTTCCCGTGTTTG
ACTCTGTACGACTGAGAGAGCACACTCTTGCTTACAGACGCAGGACTGCCAGAGACCAGTGTACAGGTTGAGCACTGTACCAGGACA
CCGCCCCAAGGCAAACGCATCCCTCCGGCCCATCATCGCAGACTTCTGTATTTATTTGTATGTTTGTTTCCAGGCCAGGCAGTAAAG
GGCCTTGTTCTGGCAATCTGCGTACTAAGGTGTTTGCTAGTGGGCAGACCTGCAGAGACACTGTTGGAATTGGGTGATGTGTGACCT
TGTGGCCTAGCTCAGCCATTATTCCAGCAGTTGGCAACACAGCCCTATTTGTTAGCATCTTTTTCACCCAGGTCACATCAGCTGGTG
GTGACTTTGCCCAAGGCCTGCAGGTCAGTTCTAGGGCCCTGGTACAGGGAGGTGACAGGCAACAAAAGACAGGTGTTCTATATGCCG
CATTCCCACAGTTTTAGCTCAACGGGTAATTCCTGGCCATCCCAGGTTTCCATTCCCCAGTGAGGAAACCAAGAAGCAAGGGAGTCA
GGGATCATCCACCCATGAAGGTCACCCCTAACCTGTCTCCTGCGTGGACCCTCAATCCTTCCTTCCAGTTCAGCTTGAGGGAGAGGC
AGTAGGCCCTGGTTAGAAGGAAATCAAGAGGCAGTAGCCTGCAGCATTTGCAGGCATCGCAGGGGCAAAGGCAAGACATGCTCTTGT
AACTAGCTCCAAGCAGGCATACCTCACCACCCGTGTATCTGTGGAAGAAAGCCAGCTGCCTAGGTGTCTGTTATCACATCCCAGAGG
CTGGAGTAAGGAGAGGAGGGGACTAGAGACCTGGACACAGGCAACACCGTGTGAGCATCTCCAAGCACCCATACCCCAAGTGTGCAC
AGATGCAGACAGGACCACAGCTGTGCACAAGGTCATAGCACCATGTTCTCGATACAGTGCTGTTCCTAGGAGCTCTGTGTGTTCCTA
GTGTCCTAGCCTCAGTTTCCCCTTCTGTGATTAGAGAGGTGTCTGTGAGCACATCCGTAATTCATGTACCTTTGAGGTGGTTCAAGG
CACTCACCAACCTAGGAAGGCTTCCTGGAGACAGCCACAGTGTTAAGGCACAAGGCAGATGGCACCCCCTTGAATGGAGAGGAAGGG
AACTCGGGAAGAGAGGGGCATGAAGACATAAGATCCCTTCCACGTTGGTTTCTCTGCCTTTCTTTGTTTCATTCGTTTGTTTTTTGT
TGTTGTTATTTTGTTTTGTTTTGTTTTTTGAGACAGGGCCTTACTATGTAGCTCTGGCTGTCCTGGAACTCATTATGTAGACCAGGC
TGGCCTCAAACTCACAGAGACCTGCC
```

Copyright © 1997 by Academic Press. All rights of reproduction in any form reserved.

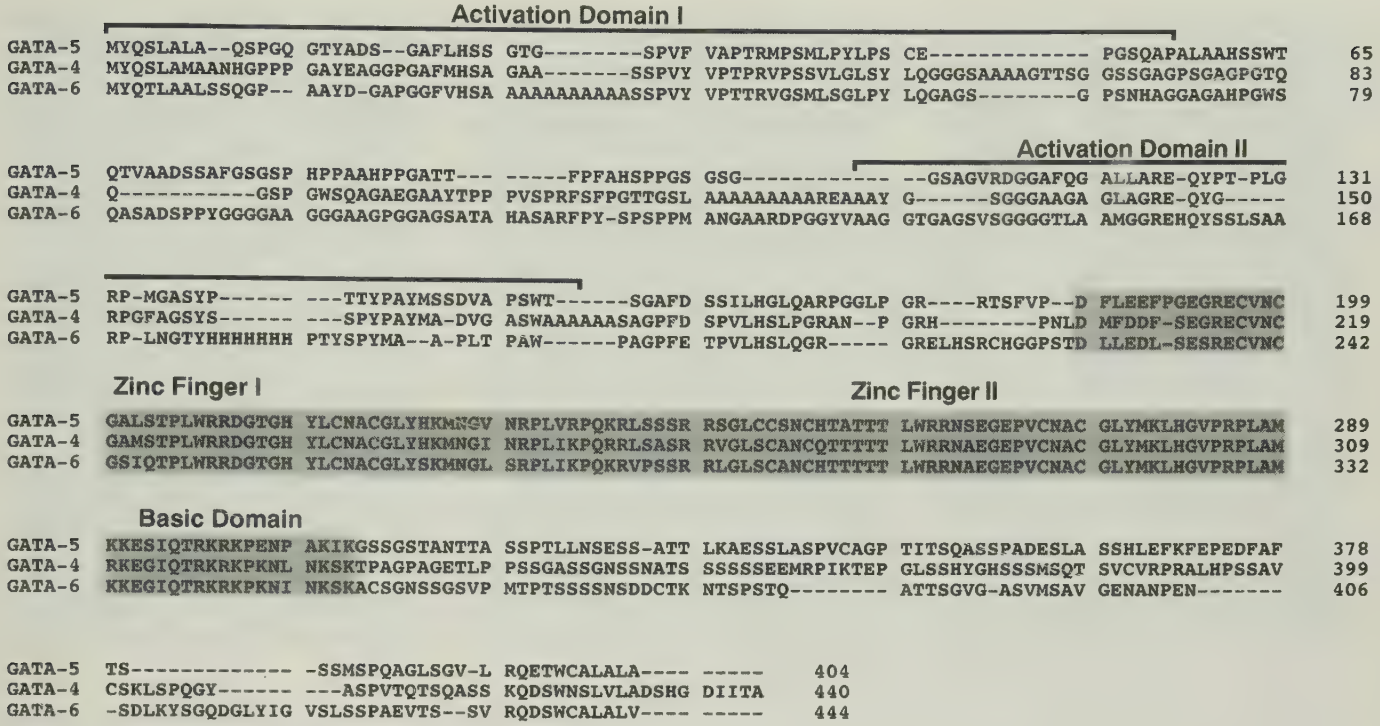
Activation Domain I
Activation Domain II
Zinc Finger I
Zinc Finger II
Basic Domain
GATA-5 MYQSLALA--QSPGQ GTYADS--GAFLHSS GTG--------SPVF VAPTRMPSMLPYLPS CE---------- PGSQAPALAAHSSWT 65
GATA-4 MYQSLAMAANHGPPP GAYEAGGPGAFMHSA GAA-------SSPVY VPTPRVPSSVLGLSY LQGGGSAAAAGTTSG GSSGAGPSGAGPGTQ 83
GATA-6 MYQTLAALSSQGP-- AAYD-GAPGGFVHSA AAAAAAAAAASSPVY VPTTRVGSMLSGLPY LQGAGS--------G PSNHAGGAGAHPGWS 79
GATA-5 QTVAADSSAFGSGSP HPPAAHPPGATT--- -----FPFAHSPPGS GSG---------- --GSAGVRDGGAFQG ALLARE-QYPT-PLG 131
GATA-4 Q----------GSP GWSQAGAEGAAYTPP PVSPRFSFPGTTGSL AAAAAAAAAREAAAY G------SGGGAAGA GLAGRE-QYG----- 150
GATA-6 QASADSPPYGGGGAA GGGAAGPGGAGSATA HASARFPY-SPSPPM ANGAARDPGGYVAAG GTGAGSVSGGGGTLA AMGGREHQYSSLSAA 168
GATA-5 RP-MGASYP------ ---TTYPAYMSSDVA PSWT------SGAFD SSILHGLQARPGGLP GR----RTSFVP--D FLEEFPGEGRECVNC 199
GATA-4 RPGFAGSYS------ ---SPYPAYMA-DVG ASWAAAAAAASAGPFD SPVLHSLPGRAN--P GRH--------PNLD MFDDF-SEGRECVNC 219
GATA-6 RP-LNGTYHHHHHHH PTYSPYMA--A-PLT PAW------PAGPFE TPVLHSLQGR----- GRELHSRCHGGPSTD LLEDL-SESRECVNC 242
GATA-5 GALSTPLWRRDGTGH YLCNACGLYHKMNGV NRPLVRPQKRLSSSR RSGLCCSNCHTATTT LWRRNSEGEPVCNAC GLYMKLHGVPRPLAM 289
GATA-4 GAMSTPLWRRDGTGH YLCNACGLYHKMNGI NRPLIKPQRRLSASR RVGLSCANCQTTTTT LWRRNAEGEPVCNAC GLYMKLHGVPRPLAM 309
GATA-6 GSIQTPLWRRDGTGH YLCNACGLYSKMNGL SRPLIKPQKRVPSSR RLGLSCANCHTTTTT LWRRNAEGEPVCNAC GLYMKLHGVPRPLAM 332
GATA-5 KKESIQTRKRKPENP AKIKGSSGSTANTTA SSPTLLNSESS-ATT LKAESSLASPVCAGP TITSQASSPADESLA SSHLEFKFEPEDFAF 378
GATA-4 RKEGIQTRKRKPKNL NKSKTPAGPAGETLP PSSGASSGNSSNATS SSSSSEEMRPIKTEP GLSSHYGHSSSMSQT SVCVRPRALHPSSAV 399
GATA-6 KKEGIQTRKRKPKNI NKSKACSGNSSGSVP MTPTSSSSNSDDCTK NTSPSTQ-------- ATTSGVG-ASVMSAV GENANPEN------- 406
GATA-5 TS---------- -SSMSPQAGLSGV-L RQETWCALALA---- ----- 404
GATA-4 CSKLSPQGY------ ---ASPVTQTSQASS KQDSWNSLVLADSHG DIITA 440
GATA-6 -SDLKYSGQDGLYIG VSLSSPAEVTS--SV RQDSWCALALV---- ----- 444

FIG. 2. Comparison of the amino acid sequences of the murine GATA-4, GATA-5, and GATA-6 proteins. The protein sequences were aligned using the MAP multiple protein sequence alignment algorithm (Huang, 1994). The conserved zinc fingers and basic domain are shown in gray. Activations Domains I and II of the mouse GATA-4 protein (Morrisey *et al.*, submitted) are shown above the amino acid sequences. Amino acid residue numbers are shown to the right of each sequence.

have been demonstrated previously to encode independent transcriptional activation domains in the mouse GATA-4 protein (Morrisey *et al.*, submitted), were also conserved in the predicted mouse GATA-5 protein (Fig. 2). In contrast, the amino terminus of the mouse GATA-5 protein does not share identifiable sequence homology with either the GATA-1, -2, or -3 proteins (data not shown). Outside of the zinc fingers, C-terminal basic domain and short regions within the amino terminus of the murine GATA-5 protein, the amino acid sequences of the GATA-4, -5, and -6 proteins have diverged significantly (Fig. 2).

Tissue-Specificity of GATA-5 Gene Expression

To determine the tissue-specificity of GATA-5 gene expression during postnatal development, a murine GATA-5 cDNA probe, derived from the 5′UTR and open reading frame (ORF) (bp 253–707), was radiolabeled and used to probe Northern blots containing RNA prepared from adult murine tissues. As shown in Fig. 3 (upper panel), the GATA-5 ORF cDNA probe hybridized to three transcripts approximately 1.8, 3.2, and 8.0 kb (arrows) in size. GATA-5 mRNA was detected in the small intestine, stomach, and bladder and at very low levels within the lung (arrows, Fig. 3, upper panel, lanes 3, 4, 7, and 8). In the stomach and small intestine the 3.2-kb transcript was most abundant, while in the bladder the 1.8- and 8.0-kb transcripts predominated. Even upon prolonged autoradiographic exposure GATA-5 mRNA was not detected within the adult heart (Fig. 3, upper panel, lane 1). In addition, GATA-5 mRNA was not detected in RNA prepared from the adult aorta, skeletal muscle, kidney, liver, spleen, thymus, uterus, and brain (Fig. 3, upper panel,

FIG. 1. The structure and deduced amino acid sequence of the mouse GATA-5 cDNA and protein encoded by clones λmG5-A and λmG5-B. (A) A schematic representation of the structure of the λmG5-A and λmG5-B cDNA clones. The size of the two cDNA clones (λmG5-A and λmG5-B) encoding the murine GATA-5 protein is shown above the map. The 5′-untranslated region is shaded. The protein coding region is shown as an open box with the two evolutionarily conserved zinc finger domains indicated (Z). The 3′-untranslated region is hatched. The size of the deduced mouse GATA-5 protein in amino acids (aa) is shown below the map. (B) The nucleotide sequence and deduced amino acid sequence of the murine GATA-5 protein encoded by λmG5-A and λmG5-B. The deduced amino acid sequence of the murine GATA-5 protein is shown below the nucleotide sequence.

Copyright © 1997 by Academic Press. All rights of reproduction in any form reserved.

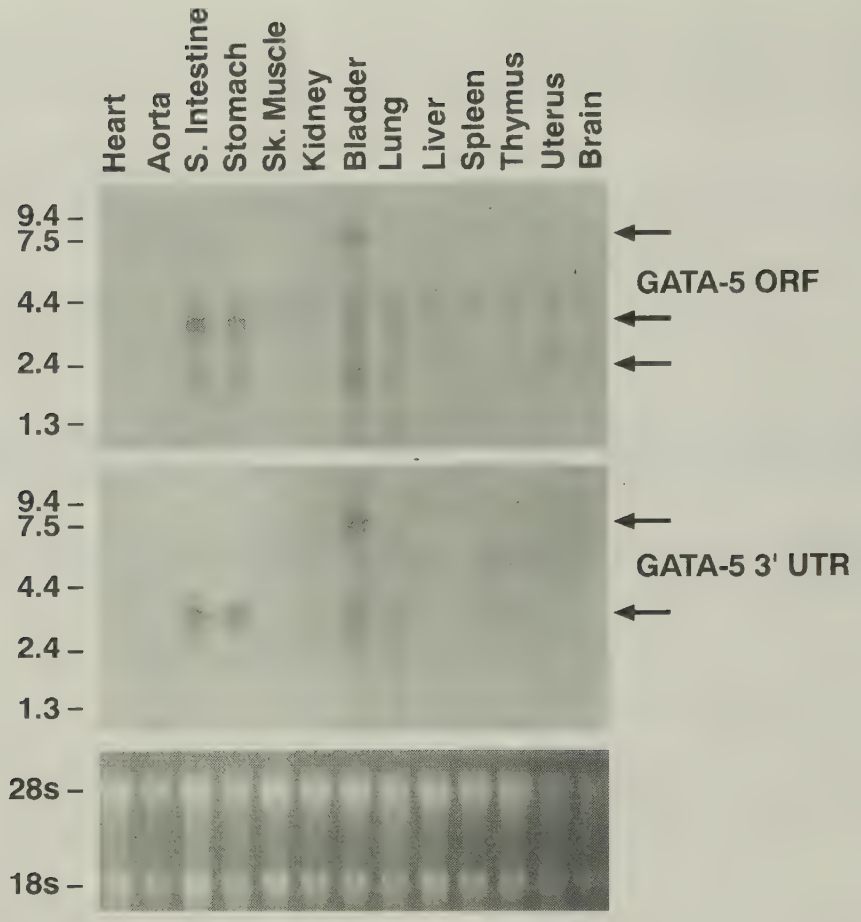

FIG. 3. The *in vivo* tissue distribution of GATA-5 gene expression during postnatal development. The top panel shows a Northern blot analysis of RNA samples isolated from adult murine tissues hybridized to the radiolabeled GATA-5 cDNA probe (bp 253–707) which includes 52 bp of the 5′ UTR and 403 bp of the GATA-5 open reading frame (GATA-5 ORF). This GATA-5 cDNA probe hybridized to 1.8-, 3.2-, and 8.0-kb transcripts (arrows), which were present in the small intestine, stomach, bladder, and lung (at very low levels). RNA size markers are shown in kilobases to the left of the blot. The middle panel shows the same Northern blot hybridized to the radiolabeled GATA-5 3′-untranslated region cDNA probe (bp 2262–2740) (GATA-5 3′ UTR). This GATA-5 cDNA probe hybridized exclusively to the 3.2- and 8.0-kb transcripts (arrows). The bottom panel shows the ethidium bromide-stained gel prior to membrane transfer of RNA. The locations of the 28S and 18S ribosomal RNA bands are indicated to the left of the gel.

lanes 2, 5, 6, 9–13). Of note, the 1.8- and 3.2-kb GATA-5 transcripts that were identified by Northern blot analyses corresponded in size to the λmG5-A and λmG5-B cDNA clones, respectively. In order to determine which, if any, of the three GATA-5 transcripts contain the 1.4 kb of distal 3′ sequence that was present only in the λmG5-B cDNA clone (see Fig. 1A), the Northern blot analysis was repeated using a mouse GATA-5 cDNA probe derived from the distal 3′UTR (bp 2262–2740) (Fig. 3, middle panel). In contrast to the GATA-5 ORF cDNA probe that hybridized to all three GATA-5 transcripts (upper panel), the 3′UTR probe hybridized exclusively to the 3.2- and 8.0-kb transcripts (arrows, Fig. 3, middle panel). Taken together, during postnatal development GATA-5 gene expression is restricted to the gut, bladder, and lung (at low levels). In this regard, the tissue-restricted pattern of expression of the GATA-5 gene during postnatal development differs markedly from that of the GATA-4 which is expressed in the heart, gut, testes, and ovary, and GATA-6 which is expressed in the heart, gut, bladder, and vasculature (Heikinheimo *et al.*, 1994; Morrisey *et al.*, 1996).

The GATA-5 Gene Has a Unique Lineage-Restricted Pattern of Expression during Embryonic Mammalian Development

To determine the temporal and spatial pattern of GATA-5 gene expression during mammalian development, a series

Copyright © 1997 by Academic Press. All rights of reproduction in any form reserved.

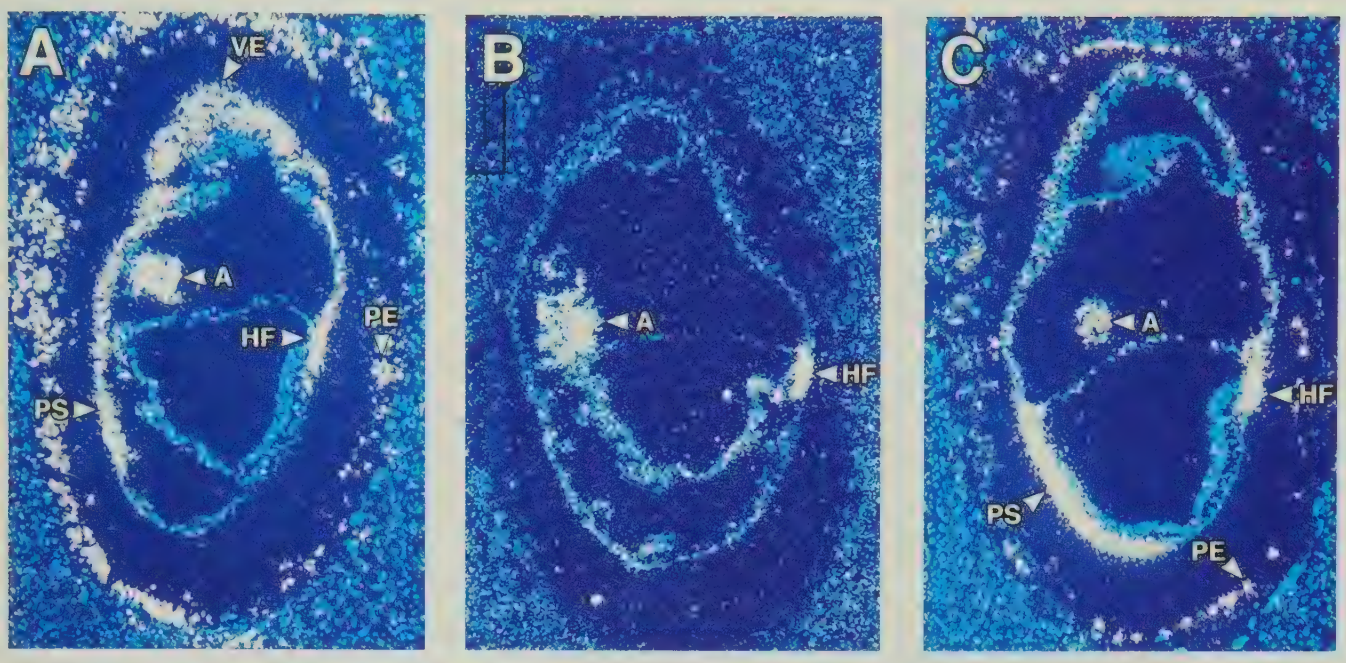

FIG. 4. Expression of the GATA-4, -5, and -6 genes in the primitive streak embryo. *In situ* hybridization analyses were performed using radiolabeled GATA-4 (A), GATA-5 (B), and GATA-6 (C) antisense riboprobes on sections of ED 7.0-staged murine embryos. (A) Specific hybridization (white) of the GATA-4 antisense riboprobe to the embryonic mesoderm in the primitive streak (PS) region and mesoderm subjacent to the headfold (HF) was visualized. Extra-embryonic hybridization of the GATA-4 riboprobe to the allantois (A), visceral endoderm (VE), and parietal endoderm (PE) was also observed. Original magnification, 12.5X. (B) Specific hybridization of the GATA-5 antisense riboprobe to the embryonic mesoderm subjacent to the headfold region (HF) containing the cardiogenic plate and the allantois (A) was visualized. (C) Specific hybridization of the GATA-6 antisense riboprobe to the embryonic mesoderm in the primitive streak (PS) region and mesoderm subjacent to the headfold (HF) was observed. Extra-embryonic hybridization of the GATA-6 riboprobe to the allantois (A) and parietal endoderm (PE) was also observed.

of *in situ* hybridization experiments were performed on staged murine embryos using GATA-4-, -5-, and -6-specific riboprobes. Within the primitive streak embryo (ED 7.0), the GATA-5 riboprobe hybridized exclusively to the embryonic mesoderm subjacent to the future headfold (HF) region which contains the cardiogenic plate (Fig. 4B). In contrast, to this restricted pattern of expression, the GATA-4 and -6 riboprobes hybridized to the lateral plate mesoderm of the primitive streak (PS) region, as well as, the mesoderm subjacent to the headfold (HF) region (Figs. 4A and 4C). Previous studies have suggested that GATA-4 may play an important role in formation of extra-embryonic membranes (Soudais *et al.*, 1995). Thus, it is noteworthy that in contrast to the GATA-4 gene which was expressed at high levels within the visceral endoderm (VE) and the GATA-4 and -6 genes which were expressed within the parietal endoderm (PE) (Figs. 4A and 4C and (Morrisey *et al.*, 1996)), GATA-5 mRNA was only observed within the allantois (A) (Fig. 4B). In summary, in primitive streak embryos, the GATA-5 gene was expressed in a more restricted pattern than either the GATA-4 or -6 genes in both the precardiac mesoderm and within extra-embryonic tissues.

In the ED 9.5 embryo, GATA-5 mRNA was detected within both the common atria (A) and ventricle (V) as well as within the cardiac outflow tract or truncus arteriosus (TA) (Fig. 5A). High power epifluorescence exposures revealed that the GATA-5 riboprobe hybridized more intensely to the common atrial chamber (A) than the common ventricle (V) and most intensely to the underlying septum transversum (Fig. 6A). In contrast, the GATA-4 and -6 riboprobes hybridized at equal intensity to the common atrial and ventricular chambers (data not shown and (Morrisey *et al.*, 1996)). By midgestation (ED 12.5), the spatial pattern of expression of the mouse GATA-5 gene within the heart (Figs. 5B and 6B) diverged significantly from that of the GATA-4 and -6 genes. Coincident with cardiac septation, GATA-5 mRNA was detected exclusively within the atria and was restricted primarily to endocardial cells (white arrowheads) lining the atria and endocardial cushions (EC) (Fig. 6B). In contrast, both the GATA-4 and -6 genes were expressed throughout the atrial and ventricular myocardium and endocardium at this developmental stage (Morrisey *et al.*, 1996). Moreover, by ED 16.5, GATA-5 mRNA was no longer detected within the heart (Fig. 5C). Of note,

Copyright © 1997 by Academic Press. All rights of reproduction in any form reserved.

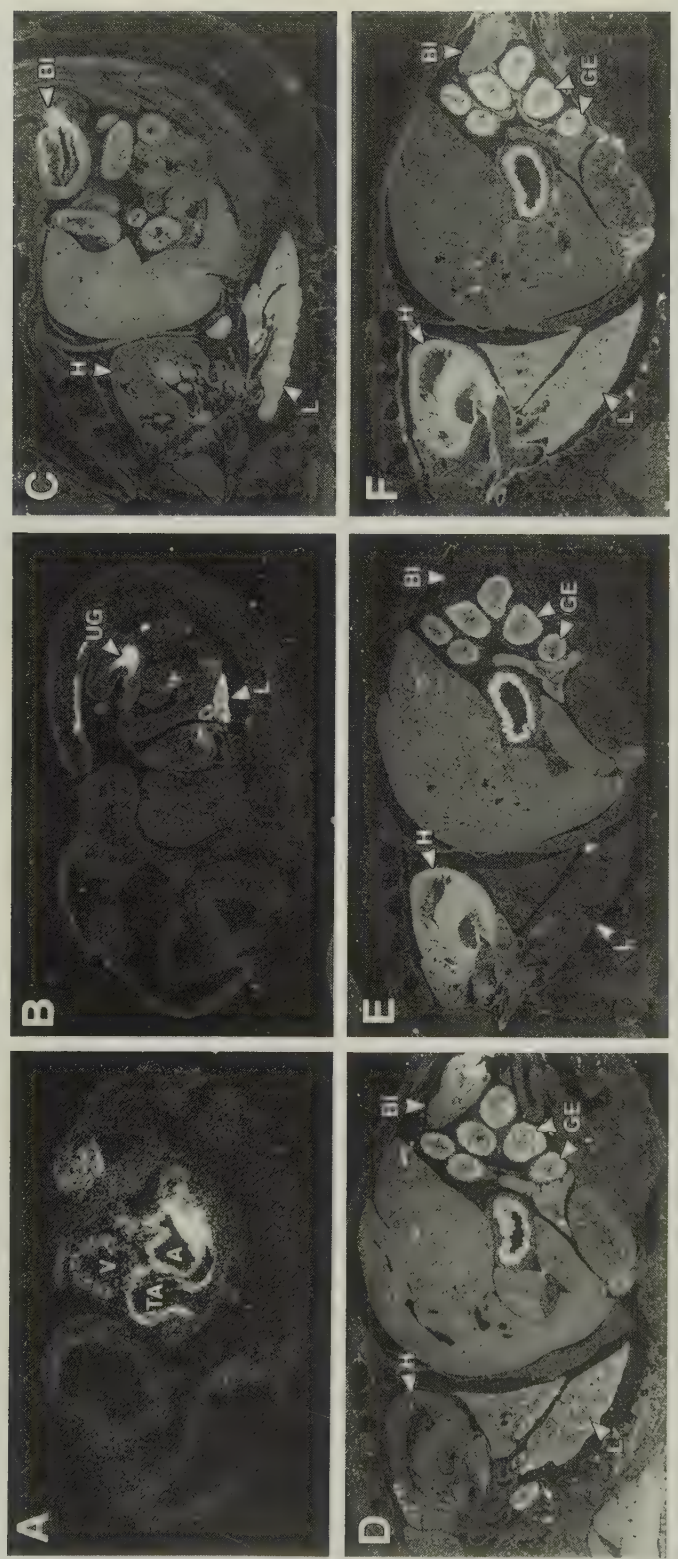

FIG. 5. The temporal and spatial pattern of GATA-5 gene expression during embryonic development of the mouse. *In situ* hybridization analyses were performed on a staged series of murine embryos using the GATA-5 antisense riboprobe (A–D) or the GATA-4 (E) or GATA-6 (F) antisense riboprobes as described under Materials and Methods. (A) Hybridization of the GATA-5 antisense riboprobe to an ED 9.5 embryo. The GATA-5 riboprobe hybridized (white signal) to the common atria (A), ventricle (V) (at low levels), and truncus arteriosus (TA) (see also Fig. 6A). In addition, hybridization of the GATA-5 riboprobe to the cells lining the primitive mid- and hindgut was also observed (not shown). Original magnification, 5X. (B) Hybridization of the GATA-5 antisense riboprobe to an ED 12.5 embryo. The GATA-5 riboprobe hybridized to the lung bud (L) (see also Fig. 7A), urogenital ridge (UG) (see also Fig. 6C), gut epithelium (see also Fig. 6E), and at low levels to the atrial endocardium (see also Fig. 6B). Original magnification, 3.1X. (C) Hybridization of the GATA-5 antisense riboprobe to an ED 16.5 embryo. The GATA-5 riboprobe hybridized to the bladder wall (B1), gut epithelium, and lung (L). Of note, the GATA-5 riboprobe did not hybridize to the heart (H) at this stage of embryonic development. Original magnification, 3.1X. (D) Hybridization of the GATA-5 riboprobe to an ED 18.5 embryo. The GATA-5 riboprobe hybridized to the bladder wall (B1), intestinal (GE) and stomach epithelium, and lung parenchyma (L). Original magnification, 3.1X. (E and F) Hybridization of the GATA-4 antisense riboprobe (E) and the GATA-6 antisense riboprobe (F) to ED 18.5 embryos. In contrast to the pattern of GATA-5 gene expression in the late fetal embryo, the GATA-4 (E) and the GATA-6 (F) riboprobes hybridized to the heart (H). The GATA-4 and -6 genes were also expressed in the gut epithelium (GE). Only GATA-6 mRNA was detected in the bladder wall (B1), the lung (L) (see also Figs. 7E and 7H), and the arteries and veins. Original magnification, 3.1X.

Copyright © 1997 by Academic Press. All rights of reproduction in any form reserved.

the low grade signal observed in the atria is artefactual and emanates from trapped RBCs along the atrial wall. In contrast to the absence of GATA-5 gene expression within the heart at ED 18.5 (Fig. 5D), the GATA-4 (Fig. 5E) and GATA-6 (Fig. 5F) genes were expressed at high levels throughout the atrial and ventricular myocardium and endocardium during late fetal development. Thus, within the heart, the GATA-5 gene has a temporally and spatially restricted pattern of expression which is distinct from that of both the GATA-4 and -6 genes during embryonic and postnatal development.

At midgestation (ED 12.5), the GATA-5 gene is expressed most abundantly within the lung bud (L) and urogenital sinus (UG) (Fig. 5B). Within the nascent lung bud at ED 12.5, GATA-5 gene expression was restricted to pulmonary mesenchyme (Fig. 7A). In contrast, at this developmental stage (ED 12.5), the GATA-6 gene was expressed within epithelial cells lining the bronchi and bronchioles (Fig. 7B, Br), while the GATA-4 gene was not expressed within the lung (data not shown). The pattern of GATA-5 gene expression within the lung parenchyma overlaps with, but is much more diffuse than, that of the smooth muscle cell marker, SM22α gene, which was expressed exclusively within bronchial (Br) and pulmonary arterial SMCs (Fig. 7C). In the fetal lung at ED 18.5, the GATA-5 riboprobe hybridized intensely to the smooth muscle cells surrounding the large airways (Figs. 7D and 7G, open arrowheads (Br)), while low level hybridization was observed throughout the lung parenchyma. Conversely, GATA-6 gene expression was detected within pulmonary arterial SMCs (Figs. 7E and 7H, white arrowheads (A)), and at low levels throughout the lung parenchyma (Fig. 7H). In contrast to the arterial SMC-specific or bronchial SMC-specific pattern of GATA-5 and -6 gene expression, respectively, within the fetal lung the SM22α gene was expressed in both bronchial (Br) and pulmonary arterial (A) SMCs (Figs. 7F and 7I). These data demonstrate that the GATA-5 and -6 genes are expressed in distinct, complementary, lineage-restricted patterns in the embryonic lung.

During postnatal development, GATA-5 gene expression was detected within the gastrointestinal tract and bladder (see Fig. 3). During embryogenesis, intense hybridization of the GATA-5 riboprobe to the dorsal aspect of the urogenital ridge can be appreciated at least as early as ED 12.5 (Figs. 5B and 6C, white arrowheads). Over the next 48 hr, the pattern of hybridization expands circumferentially to surround the epithelial cells lining the urogenital sinus (Fig. 6D). Subsequently by ED 18.5, the GATA-5 gene is expressed at high levels within the wall of the embryonic bladder (Bl) (Fig. 5D) where the gene continues to be expressed throughout postnatal development. Within the developing gastrointestinal tract, the GATA-5 riboprobe hybridized to cells lining the embryonic mid- and hindgut at least as early as ED 9.5 (data not shown). Of note, despite the fact that the GATA-5 gene is expressed in bronchial SMCs (Figs. 7D and 7G) and SMCs of the bladder wall (Figs. 6D and 7D), within the gut GATA-5 gene expression is restricted to the epithelial cells (Fig. 6E, white arrowheads). This epithelial-specific pattern of expression within the gastrointestinal tract continues as the intestinal crypts and villi differentiate during the fetal period (ED 18.5) (Fig. 6F). These data demonstrate that the GATA-5 gene is an early developmental marker of the gut epithelium and of bladder smooth muscle cells where the gene continues to be expressed throughout postnatal development.

GATA-5 Binds to the Cardiac-Specific cTnC Transcriptional Enhancer

GATA-4 and -6 have been demonstrated to bind to the cardiac-specific cTnC transcriptional enhancer and transactivate the cTnC gene in noncardiac muscle cell lineages (Ip *et al.*, 1994; Morrisey *et al.*, 1996). The developmentally regulated, cell- and chamber-specific pattern of GATA-5 gene expression suggested the hypothesis that GATA-5 might recognize a unique set of transcriptional targets. Therefore, to determine whether GATA-5 binds to the functionally important nonconsensus CEF-1/GATA motif located within the cTnC promoter-enhancer (Ip *et al.*, 1994), EMSAs were performed using nuclear extracts prepared from COS-7 cells transiently transfected with the GATA-5 expression plasmid, pcDNAG5. As shown in Fig. 8, the radiolabeled cTnC CEF-1 oligonucleotide probe bound two nuclear protein complexes (arrows) that were not identified in nuclear extracts prepared from COS-7 cells transfected with the pcDNA3 control expression plasmid (Fig. 8, lanes 1 and 2). Each of these complexes was abolished by the addition of unlabeled cTnC CEF-competitor oligonucleotide or by an unlabeled oligonucleotide corresponding to the functionally important consensus GATA motif identified within the α-cardiac myosin heavy chain promoter (Molkentin *et al.*, 1994) (Fig. 8, lanes 3 and 4), but not by nonspecific oligonucleotide competitor (Fig. 8, lane 5). Of note, neither nuclear protein complex was supershifted following preincubation with α-GATA-4-specific IgG (Fig. 8, lane 6). In addition, three nuclear protein complexes were identified in binding reactions containing nuclear extracts prepared from COS-7 cells transfected with the mouse GATA-4 expression plasmid, pcDNAG4, and the radiolabeled CEF-1 probe (Fig. 8, lane 7). Each of these nuclear protein complexes were ablated and supershifted (dashed arrows) following preincubation with α-GATA-4-specific IgG (Fig. 8, lane 8). These data demonstrate that GATA-5 can bind specifically to DNA, and that GATA-5 binds to the functionally important nuclear protein binding site in the cTnC cardiac-specific promoter-enhancer.

GATA-5 Transactivates the cTnC Cardiac-Specific Transcriptional Enhancer in Noncardiac Muscle Cells

To determine whether forced expression of GATA-5 can transactivate the cardiac-specific cTnC promoter-enhancer

Copyright © 1997 by Academic Press. All rights of reproduction in any form reserved.

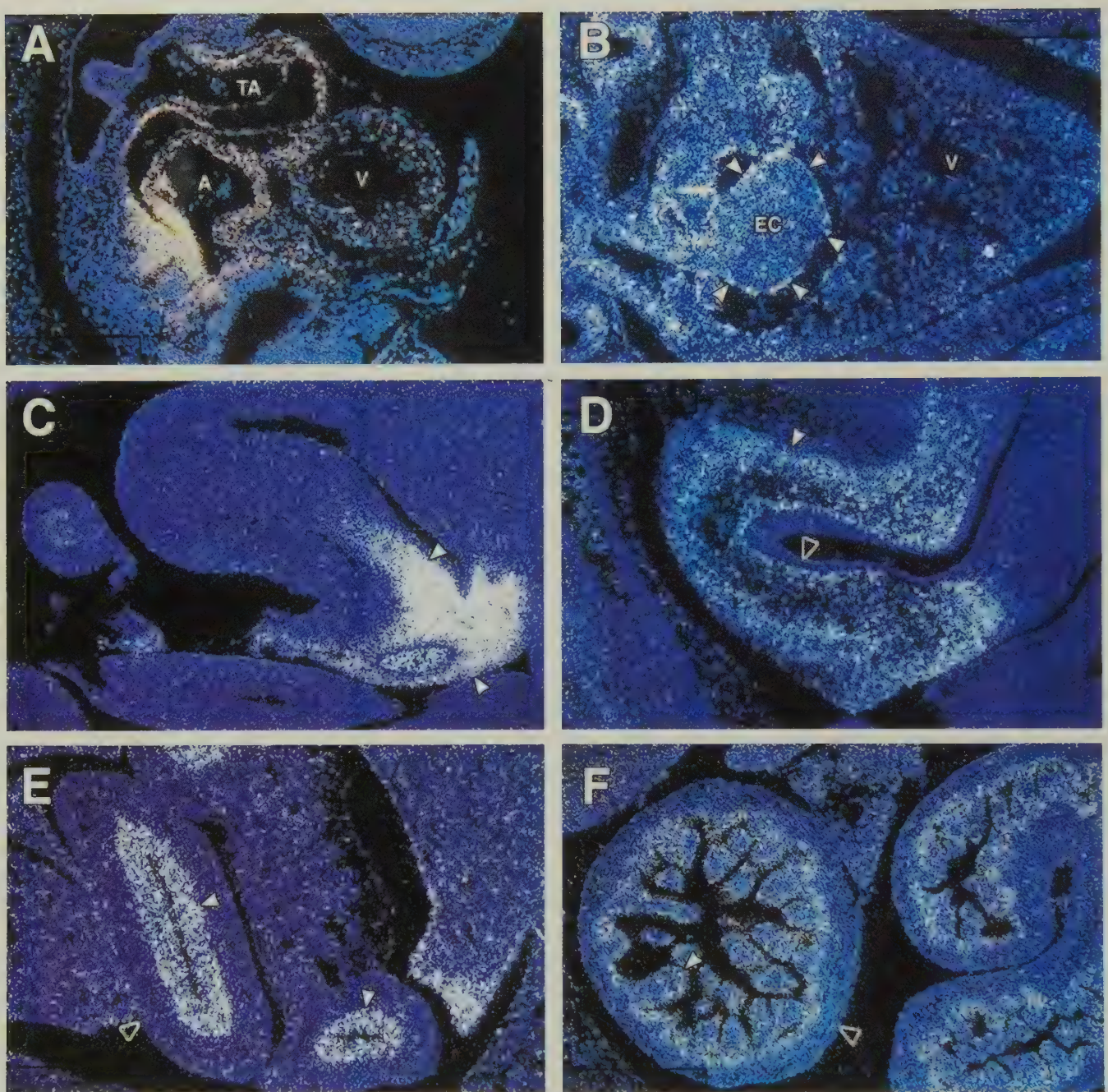

FIG. 6. The GATA-5 gene is expressed in the embryonic heart, the urogenital ridge, and the gut epithelium in a developmentally regulated fashion. *In situ* hybridization analyses were performed using a GATA-5 antisense riboprobe and sections through staged ED 9.5 (A), 12.5 (B, C and E), 14.5 (D), and 18.5 embryos (F). (A) Within the primitive heart (ED 9.5), abundant hybridization (white signal) to the atrial (A) myocardium and endocardium and truncus arteriosus (TA) was visualized. In contrast, only low level hybridization to the ventricular chamber (V) was observed. Original magnification, 10X. (B) At ED 12.5, hybridization to the atrial endocardium (arrowheads) and endocardium lining the endocardial cushion (EC) was visualized. In contrast, the GATA-5 riboprobe did not hybridize to the ventricular myocardium or endocardium. Original magnification, 10X. (C) At ED 12.5, intense hybridization to the dorsal aspect of the urogenital ridge was observed (arrowheads). Original magnification, 10X. (D) At ED 14.5, GATA-5 mRNA can be detected in cells of the urogenital ridge (white arrowhead) surrounding the epithelial cells lining the urogenital sinus (open arrowhead). Original magnification, 10X. (E) At ED 12.5, hybridization to the epithelial cells (white arrowhead) lining the midgut is visualized. Hybridization to the lamina propria was not observed (open arrowhead). Original magnification, 10X. (F) At ED 18.5, hybridization to the epithelial cells (white arrowhead) lining the crypts and villi of the intestine, but not the lamina propria (open arrowhead), was observed. Original magnification, 5X.

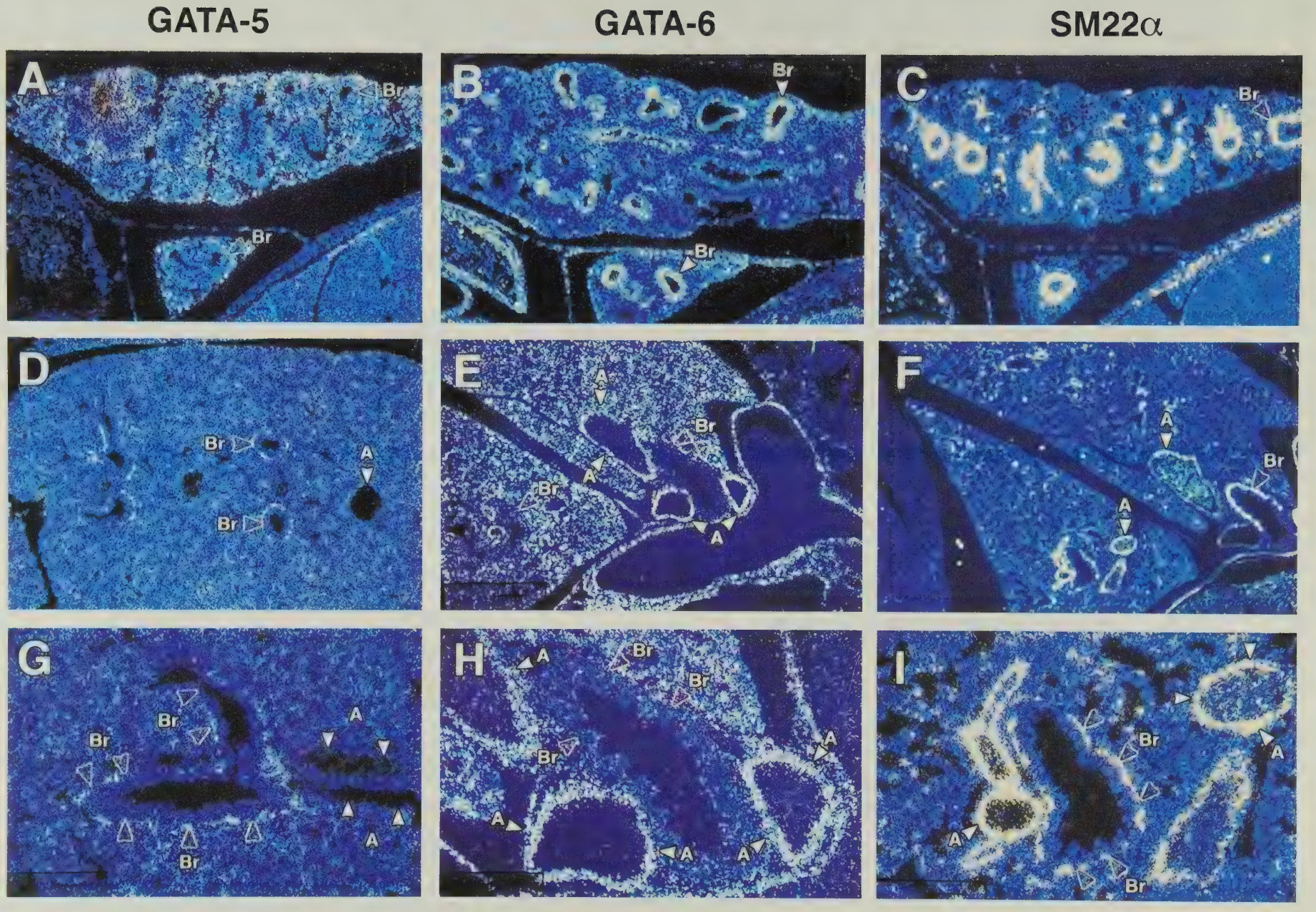
GATA-5
GATA-6
SM22α
A
B
C
D
E
F
G
H
I
Br
A

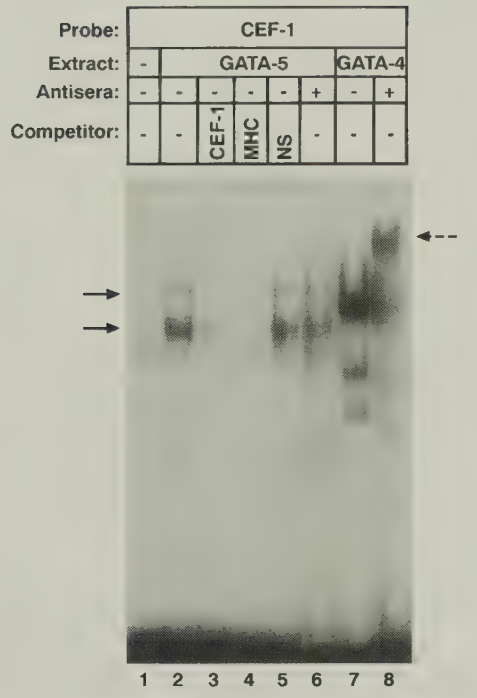

FIG. 8. Binding of GATA-5 and GATA-4 to the CEF-1 site of the cTnC transcriptional enhancer. Radiolabeled CEF-1 oligonucleotides were used in EMSAs with nuclear extracts prepared from COS-7 cells transiently transfected with either the negative control expression plasmid, pcDNA3 (lane 1), or expression plasmids encoding the murine GATA-5 (lanes 2–6) or GATA-4 (lanes 7–8) proteins. Where indicated, binding reactions were preincubated with either 100 ng of indicated unlabeled competitor oligonucleotides or with goat polyclonal α-GATA-4 IgG (+). The bands corresponding to the GATA-5 nuclear protein complexes are shown by arrows to the left of the autoradiogram. The GATA-4 antibody-supershifted complex is indicated with a dashed arrow to the right of the autoradiogram.

in noncardiac muscle cells, NIH 3T3 cells were transiently cotransfected with a GH reporter plasmid driven by the 124-bp cardiac-specific cTnC promoter-enhancer (Parmacek *et al.*, 1992) and an eukaryotic expression plasmid encoding the murine GATA-5 protein. As demonstrated previously (Ip *et al.*, 1994), the negative control plasmid, pcDNA3, failed to transactivate the p-124GH reporter plasmid in NIH 3T3 cells (Fig. 9A, column 1). In contrast, forced expression of GATA-5 resulted in approximately a 275-fold increase in GH reporter activity (Fig. 9A, column 2). To determine whether this increase in transcriptional activity was dependent upon binding of GATA-5 to the CEF-1 motif within the cTnC transcriptional enhancer, the GATA-5 expression plasmid was transiently cotransfected with the p-124GHμCEF-1 reporter plasmid, that contains a mutation within the CEF-1/GATA element that abolishes binding of GATA-5 (data not shown). Mutation of the CEF-1/GATA motif resulted in approximately a 60% reduction in normalized GH activity (Fig. 9A, column 4), demonstrating that most, but not all, of the transcriptional activation of the cTnC promoter was dependent upon an intact CEF-1/GATA motif.

The finding that overexpression of GATA-5 transactivated the p-124GHμCEF-1 plasmid above levels obtained with the negative control expression plasmid, pcDNA3 (Fig. 9A, columns 3 and 4), suggested that GATA-5 might be capable of indirectly activating the cTnC cardiac-specific promoter enhancer. In this regard it is noteworthy that several recent studies have demonstrated that GATA family members can activate transcription either by binding directly to DNA, or alternatively, by binding directly to other transcription factors (Crossley *et al.*, 1995; Osada *et al.*, 1995). Therefore, to determine whether the ability of GATA-5 to transactivate the p-124GHμCEF-1 reporter plasmid was dependent upon any of the other previously characterized *cis*-acting regulatory elements within the cTnC promoter-enhancer (Parmacek *et al.*, 1992), the GATA-5 expression plasmid was transiently cotransfected with the pCEF-1GH reporter plasmid, containing a single copy of the CEF-1 motif upstream of the minimal rabbit β-globin promoter (Morrisey *et al.*, 1996), and the pμCEF-1GH reporter plasmid, containing a mutated copy of the CEF-1 motif subcloned upstream of the minimal β-globin promoter, into NIH 3T3 cells. Forced expression of GATA-5 in NIH 3T3 cells transactivated the pCEF-1GH reporter

FIG. 7. The temporal and spatial patterns of GATA-5, GATA-6, and SM22α gene expression in the murine embryonic and fetal lung. *In situ* hybridization analyses were performed using GATA-5 (A, D, and G), GATA-6 (B, E, and H), and SM22α (C, F, and I) antisense riboprobes on staged ED 12.5 (A–C) and ED 18.5 (D–I) embryonic lung sections. (A–C) At ED 12.5, the GATA-5 riboprobe (A) hybridized diffusely to the pulmonary mesenchyme, but not to the bronchial epithelial cells (Br). In contrast, the GATA-6 riboprobe (B) hybridized to the bronchial epithelial cells (Br), but not to the pulmonary mesenchyme. The SM22α riboprobe (C), a marker of the smooth muscle cell lineage, hybridized to bronchial (Br) and pulmonary arterial SMCs. Original magnification, 10X. (D and G) At ED 18.5, the GATA-5 riboprobe hybridized to the bronchial SMCs (Br, open arrowheads), but not the pulmonary arterial SMCs (A, white arrowheads). In addition, diffuse low level hybridization of the GATA-5 riboprobe to the lung parenchyma was visualized. Original magnification, 5X and 20X. (E and H) At ED 18.5, the GATA-6 riboprobe hybridized to pulmonary arterial SMCs (A, white arrowheads) and to the lung parenchyma. GATA-6 gene expression was not observed in the epithelial cells lining the large airways (Br, open arrowheads). Original magnification, 5X and 20X. (F and I) At ED 18.5, the SM22α riboprobe hybridized exclusively to bronchial (Br) and pulmonary arterial (A) SMCs. Original magnification, 5X and 20X.

Copyright © 1997 by Academic Press. All rights of reproduction in any form reserved.

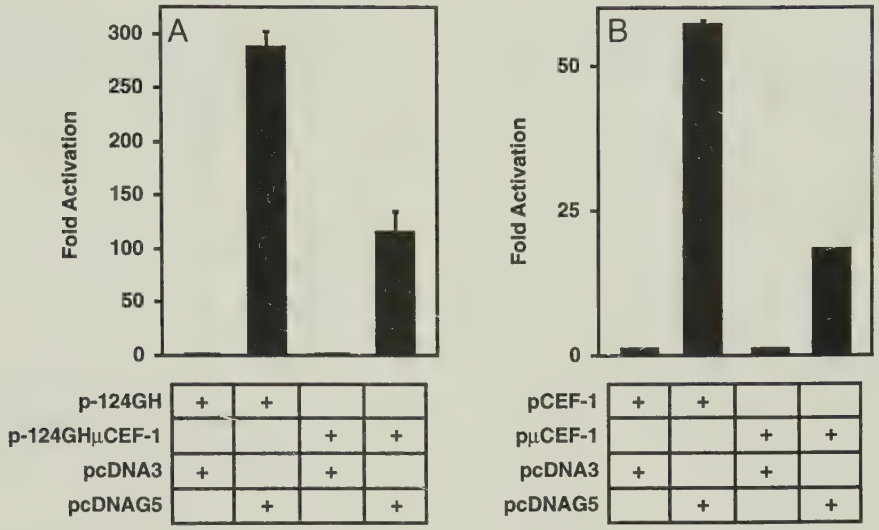

FIG. 9. GATA-5-mediated activation of the cTnC promoter and a minimal CEF-1-containing promoter in noncardiac muscle cells. (A) NIH 3T3 cells were transfected with either 2.5 μg of the p-124cTnCGH (p124GH +) or the p-124cTnCGHμCEF-1 (p-124GHμCEF-1 +) reporter plasmids and either 25 μg of the control expression plasmid (pcDNA3 +) or the GATA-5 expression plasmid (pcDNAG5 +). All transfections contained 1 μg of the pMSVβgal reference plasmid. Forty-eight hours following transfection, the amount of growth hormone in the media and the β-galactosidase activities were determined. Relative GH activity was determined by correcting for differences in transfection efficiencies and normalizing to the amount of growth hormone obtained following transfection of the p-124cTnCGH plasmid with the pcDNA3 expression plasmid. The data are presented as relative GH activity ± SEM. (B) Transient cotransfections were performed as described above with the exception that the pCEF-1GH or pμCEF-1GH reporter plasmids were utilized which contain a single CEF-1 nuclear protein binding site or a mutant CEF-1 nuclear protein binding site, respectively, subcloned immediately 5′ of the minimal rabbit β-globin promoter.

construct 55-fold above levels in cells cotransfected with the negative control expression plasmid, pcDNA3 (Fig. 9B, columns 1 and 2). In contrast, only an 18-fold induction in normalized GH activity was demonstrated with the pμCEF-1GH plasmid (Fig. 9B, columns 2 and 3). Taken together, these data demonstrate that GATA-5 is a potent transcriptional activator that is capable of activating the cardiac-specific cTnC promoter enhancer in noncardiac muscle cells. The majority of the transcriptional activation is dependent upon an intact GATA motif within the cTnC CEF-1 nuclear protein binding site and the residual induction in transcriptional activity results from the indirect activation of the cTnC CEF-1 element.

DISCUSSION

Members of the GATA family of transcription factors play important roles in transducing nuclear events that regulate cell lineage differentiation during vertebrate development. In this report, we have isolated and structurally and functionally characterized the mouse GATA-5 protein. In addition, we have determined the temporal and spatial patterns of GATA-5 gene expression during mouse embryonic development. Structural comparison of the mouse GATA-5 protein with the previously characterized mouse GATA-4 and -6 proteins identified specific regions within two N-terminal activation domains that have been conserved across the GATA-4/5/6 subfamily (Morrisey *et al.*, submitted). In addition, GATA-5 binds to the functionally important CEF-1 nuclear protein binding site in the cardiac-specific cTnC transcriptional enhancer and over-expression of GATA-5 is sufficient to transactivate the cTnC promoter-enhancer in noncardiac muscle cells. In contrast to the GATA-4 and -6 genes, which are developmentally coexpressed in the embryonic and adult heart, the GATA-5 gene is expressed in a temporally and spatially restricted pattern during early embryonic cardiac development. Moreover, coincident with expansion of the embryonic lung bud, the GATA-5 gene is expressed at high levels within the pulmonary mesenchyme in a cell lineage-restricted pattern which is complementary to that of the GATA-6 gene. Finally, the GATA-5 gene is expressed in tissue-restricted subsets of SMCs, including bronchial SMCs and SMCs of the bladder wall. These data are consistent with a model wherein GATA-5 regulates a novel molecular program in the mammalian embryo and serves to identify GATA-5 as a candidate regulator of the transcriptional program(s) that underlies smooth muscle cell diversity.

Previous studies have suggested that GATA-4 may play

Copyright © 1997 by Academic Press. All rights of reproduction in any form reserved.

an important role in formation and/or specification of extra-embryonic tissues (Soudais *et al.*, 1995; Bielinska *et al.*, 1996). Soudais *et al.* (1995) reported that embryonic stem (ES) cells containing a homozygous null mutation in the GATA-4 gene exhibit gross defects in membranous structures including the visceral and parietal endoderm. While these data are consistent with the high levels of GATA-4 mRNA that were observed in these extra-embryonic tissues, the finding that the GATA-5 gene is not expressed either within the visceral or parietal endoderm suggests that the functional repertoire of GATA-5 is restricted in extra-embryonic tissues and limited to the allantois. Moreover, in the primitive streak embryo, the murine GATA-5 gene is expressed exclusively within the mesoderm subjacent to the headfold region which contains the cardiogenic plate. In contrast, the GATA-4 and -6 genes were developmentally coexpressed in the ED 7.0 embryo both within the primitive streak mesoderm as well as the cardiogenic plate. Once again, this suggests that the function of GATA-5 in the precardiac mesoderm is more restricted than that of either the GATA-4 or -6 genes. In this regard it is noteworthy that within the embryonic heart, the GATA-5 gene has a temporally and spatially restricted pattern of expression that is distinct from that of the GATA-4 and -6 genes (see below). Thus, identification of the subpopulation of cells within the lateral plate mesoderm that express GATA-5 may serve to define previously unrecognized sublineages within the primitive heart that give rise to atria versus ventricle and/or cardiac myocytes versus endocardial cells.

Several independent groups have suggested that the GATA-4/5/6 subfamily of transcription factors may play an important role in directing tissue-specific gene expression within the heart during embryonic and postnatal development (Jiang and Evans, 1996; Kelley *et al.*, 1993; Laverriere *et al.*, 1994; Grepin *et al.*, 1994; Ip *et al.*, 1994; Tamura *et al.*, 1993). In avian and *Xenopus* species the GATA-4, -5, and -6 genes are developmentally coexpressed within the precardiac mesoderm and embryonic and adult heart (Jiang and Evans, 1996; Laverriere *et al.*, 1994). Thus, it was somewhat surprising to find that in the mammalian species, the GATA-5 gene is expressed in a developmentally regulated, spatially restricted pattern that differs significantly from that of the mouse GATA-4 and -6 genes. Within the primitive heart tube, the GATA-5 gene is expressed at higher levels in the common atrial chamber than in the ventricle. In contrast, the GATA-4 and -6 genes are expressed at relatively equal levels in both the atria and ventricles (Morrisey *et al.*, 1996). Coincident with cardiac septation and formation of the endocardial cushions (ED 12.5), GATA-5 gene expression becomes restricted to the atrial endocardium, while the GATA-4 and -6 genes are expressed at high levels throughout the embryonic heart. Subsequently, during fetal and postnatal development, the GATA-5 gene is not expressed in the heart, whereas the GATA-4 and -6 genes continue to be expressed at high levels in both cardiac chambers (Heikinheimo *et al.*, 1994; Morrisey *et al.*, 1996). The unique pattern of GATA-5 gene expression within the mouse heart coupled with the demonstration that GATA-5 can transactivate a cardiac-specific transcriptional regulatory element in noncardiac muscle cells suggests that GATA-5 gene may play an important role in chamber-specification and/or establishment of the endocardium and/or endocardial cushions. These data support the emerging hypothesis that distinct transcriptional programs may direct atrial versus ventricular-specificity and left/right asymmetry within the vertebrate heart (Li *et al.*, 1996; Ross *et al.*, 1996; Tsuda *et al.*, 1996).

Fine differences in the patterns of expression of the GATA-1, -2, and -3 proteins in the hematopoietic cell lineages have translated into marked differences in the phenotypes of mice harboring null mutations in each of these family members (Pandolfi *et al.*, 1995; Pevny *et al.*, 1991; Simon *et al.*, 1992; Tsai *et al.*, 1994; Weiss *et al.*, 1994). Thus, the demonstration that the GATA-5 gene was expressed in the embryonic pulmonary mesenchyme and bronchial SMCs suggests that GATA-5 may mediate important, and unanticipated, functions in the embryonic lung. During expansion of the embryonic lung bud, the GATA-5 and -6 genes are expressed in complementary, cell lineage-restricted patterns; GATA-5 gene expression is restricted to the pulmonary mesenchyme and GATA-6 gene expression is restricted to the bronchial epithelial cells. Of note, the embryonic lung contains cells derived both from gut epithelium (bronchial epithelial cells), as well as lateral mesoderm (mesenchymal cells, endothelial cells, and smooth muscle cells). The finding that both the GATA-5 and -6 genes are expressed in the gut epithelium and lateral mesoderm, while these genes are differentially expressed in a cell lineage-specific pattern within the embryonic lung, suggests that GATA-5 and -6, in concert with other transcription factors, may play important roles in regulating the differentiation of distinct cell lineages during embryonic lung development.

Relatively little is currently understood about the molecular mechanisms that control SMC identity and differentiation (for review see Owens, 1995). Thus, the observation that GATA-5 is expressed in bronchial and bladder SMCs, but not in arterial or gut SMCs, suggests that GATA-5 may activate transcription in tissue-restricted subsets of the SMC lineage. Of note, we have reported recently that the GATA-6 gene is expressed within arterial, venous, and bladder SMCs (Morrisey *et al.*, 1996). Taken together, these data support and extend our hypothesis that distinct transcriptional programs may underlie SMC diversity and serve to identify GATA-5 (and GATA-6) as potential regulators of this program. As such, identification of the transcriptional targets of GATA-5 (and GATA-6) in the different SMC lineages should increase understanding of the molecular mechanisms that regulate SMC development and differentiation.

ACKNOWLEDGMENTS

We thank Jeff Leiden, Celeste Simon, and Beth McNally for reviewing the manuscript and providing helpful suggestions. We

Copyright © 1997 by Academic Press. All rights of reproduction in any form reserved.

thank Lisa Gottschalk for expert preparation of the figures and Amy Murphy for expert secretarial assistance. This work was supported in part by Public Health Service Grant R01HL51145 and an American Heart Association Grant-In-Aid to M.S.P. M.S.P. is an Established Investigator of the American Heart Association.

REFERENCES

Arceci, R. J., King, A. A., Simon, M. C., Orkin, S. H., and Wilson, D. B. (1993). Mouse GATA-4: A retinoic acid-inducible GATA-binding transcription factor expressed in endodermally derived tissues and heart. *Mol. Cell. Biol.* **13,** 2235–2246.

Bielinska, M., Narita, N., Heikinheimo, M., Porter, S. B., and Wilson, D. B. (1996). Erythropoiesis and vasculogenesis in embryoid bodies lacking visceral yolk sac endoderm. *Blood* **88,** 3720–3730.

Blobel, G. A., and Orkin, S. H. (1996). Estrogen-induced apoptosis by inhibition of erythroid transcription factor GATA-1. *Mol. Cell. Biol.* **16,** 1687–1694.

Crossley, M., Merika, M., and Orkin, S. H. (1995). Self-association of the erythroid transcription factor GATA-1 mediated by its zinc finger domains. *Mol. Cell. Biol.* **15,** 2448–2456.

Dorfman, D. M., Wilson, D. B., Bruns, G. A., and Orkin, S. H. (1992). Human transcription factor GATA-2: Evidence for regulation of preproendothelin-1 gene expression in endothelial cells. *J. Biol. Chem.* **267,** 1279–1285.

Evans, T., Reitman, M., and Felsenfeld, G. (1988). An erythrocyte-specific DNA-binding factor recognizes a regulatory sequence common to all chicken globin genes. *Proc. Natl. Acad. Sci. USA* **85,** 5976–5980.

Grepin, C., Dagnino, L., Robitaille, L., Haberstroh, L., Antakly, T., and Nemer, M. (1994). A hormone-encoding gene identifies a pathway for cardiac but not skeletal muscle gene transcription. *Mol. Cell. Biol.* **14,** 3115–3129.

Grepin, C., Robitaille, L., Antakly, T., and Nemer, M. (1995). Inhibition of transcription factor GATA-4 expression blocks in vitro cardiac muscle differentiation. *Mol. Cell. Biol.* **15,** 4095–4102.

Heikinheimo, M., Scandrett, J. M., and Wilson, D. B. (1994). Localization of transcription factor GATA-4 to regions of the mouse embryo involved in cardiac development. *Dev. Biol.* **164,** 361–373.

Ho, I. C., Vorhees, P., Marin, N., Oakley, B. K., Tsai, S. F., Orkin, S. H., and Leiden, J. M. (1991. Human GATA-3: a lineage-restricted transcription factor that regulates the expression of the T cell receptor alpha gene. *EMBO J.* **10,** 1187–1192.

Huang, X. (1994). On global sequence alignment. *Comput. Appl. Biosci.* **10,** 227–235.

Ip, H. S., Wilson, D. B., Heikinheimo, M., Tang, Z., Ting, C. N., Simon, M. C., Leiden, J. M., and Parmacek, M. S. (1994). The GATA-4 transcription factor transactivates the cardiac muscle-specific troponin C promoter-enhancer in nonmuscle cells. *Mol. Cell. Biol.* **14,** 7517–7526.

Jiang, Y., and Evans, T. (1996). The Xenopus GATA-4/5/6 genes are associated with cardiac specification and can regulate cardiac-specific transcription during embryogenesis. *Dev. Biol.* **174,** 258–270.

Joulin, V., Bories, D., Eleouet, J. F., Labastie, M. C., Chretien, S., Mattei, M. G., and Romeo, P. H. (1991). A T-cell-specific TCR delta DNA binding protein is a member of the human GATA family. *EMBO J.* **10,** 1809–1816.

Kelley, C., Blumberg, H., Zon, L. I., and Evans, T. (1993). GATA-4 is a novel transcription factor expressed in endocardium of the developing heart. *Development* **118,** 817–827.

Ko, L. J., and Engel, J. D. (1993). DNA-binding specificities of the GATA transcription factor family. *Mol. Cell. Biol.* **13,** 4011–4022.

Ko, L. J., Yamamoto, M., Leonard, M. W., George, K. M., Ting, P., and Engel, J. D. (1991). Murine and human T-lymphocyte GATA-3 factors mediate transcription through a cis-regulatory element within the human T-cell receptor delta gene enhancer. *Mol. Cell. Biol.* **11,** 2778–2784.

Kozak, M. (1984). Selection of initiation sites by eukaryotic ribosomes: Effects of inserting AUG triplets upstream from the coding sequence for preproinsulin. *Nucleic Acids Res.* **12,** 857–872.

Kuratani, S., Martin, J. F., Wawersik, S., Lilly, B., Eichele, G., and Olson, E. N. (1994). The expression pattern of the chick homeobox gene MHox suggests a role in patterning of the limbs and face and in compartmentalization of somites. *Dev. Biol.* **161,** 357–369.

Laverriere, A. C., MacNeill, C., Mueller, C., Poelmann, R. E., Burch, J. B., and Evans, T. (1994). GATA-4/5/6, a subfamily of three transcription factors transcribed in developing heart and gut. *J. Biol. Chem.* **269,** 23177–23184.

Lee, M.-E., Bloch, K. D., Clifford, J. A., and Quertomous, T. (1990). Functional analysis of the endothelin-1 gene promoter: evidence for an endothelial cell-specific cis-acting sequence. *J. Biol. Chem.* **266,** 16188–16192.

Li, L., Miano, J. M., Mercer, B., and Olson, E. N. (1996). Expression of the SM22α promoter in transgenic mice provides evidence for distinct transcriptional regulatory programs in vascular and visceral smooth muscle cells. *J. Cell Biol.* **132,** 849–859.

Merika, M., and Orkin, S. H. (1993). DNA-binding specificity of GATA family transcription factors. *Mol. Cell. Biol.* **13,** 3999–4010.

Molkentin, J. D., Kalvakolanu, D. V., and Markham, B. E. (1994). Transcription factor GATA-4 regulates cardiac muscle-specific expression of the α-myosin heavy chain gene. *Mol. Cell. Biol.* **14,** 4947–4957.

Morrisey, E. E., Ip, H. S., Lu, M. M., and Parmacek, M. S. (1996). GATA-6: A zinc finger transcription factor that is expressed in multiple cell lineages derived from lateral mesoderm. *Dev. Biol.* **177,** 309–322.

Morrisey, E. E., Ip, H. S., Tang, Z., and Parmacek, M. S. (submitted). GATA-4 activates transcription via two novel domains that are conserved within the GATA-4/5/6 subfamily.

Omichinski, J. G., Clore, G. M., Schaad, O., Felsenfeld, G., Trainor, C., Appella, E., Stahl, S. J., and Gronenborn, A. M. (1993). NMR structure of a specific DNA complex of Zn-containing DNA binding domain of GATA-1. *Science* **261,** 438–446.

Orkin, S. H. (1992). GATA-binding transcription factors in hematopoietic cells. *Blood* **80,** 575–581.

Osada, H., Grutz, G., Axelson, H., Forster, A., and Rabbitts, T. H. (1995). Association of erythroid transcription factors: Complexes involving the LIM protein RBTN2 and the zinc-finger protein GATA1. *Proc. Natl. Acad. Sci. USA* **92,** 9585–9589.

Owens, G. K. (1995). Regulation of differentiation of vascular smooth muscle cells. *Phys. Rev.* **75,** 487–517.

Pandolfi, P. P., Roth, M. E., Karis, A., Leonard, M. W., Dzierzak, E., Grosveld, F. G., Engel, J. D., and Lindenbaum, M. H. (1995). Targeted disruption of the GATA3 gene causes severe abnormalities in the nervous system and in fetal liver haematopoiesis. *Nature Genet.* **11,** 40–44.

Copyright © 1997 by Academic Press. All rights of reproduction in any form reserved.

Parmacek, M. S., Ip, H. S., Jung, F., Shen, T., Martin, J. F., Vora, A. J., Olson, E. N., and Leiden, J. M. (1994). A novel myogenic regulatory circuit controls slow/cardiac troponin C gene transcription in skeletal muscle. *Mol. Cell. Biol.* **14,** 1870–1885.

Parmacek, M. S., and Leiden, J. M. (1989). Structure and expression of the murine slow/cardiac troponin C gene. *J. Biol. Chem.* **264,** 13217–13225.

Parmacek, M. S., Vora, A. J., Shen, T., Barr, E., Jung, F., and Leiden, J. M. (1992). Identification and characterization of a cardiac-specific transcriptional regulatory element in the slow/cardiac troponin C gene. *Mol. Cell. Biol.* **12,** 1967–1976.

Pevny, L., Simon, M. C., Robertson, E., Klein, W. H., Tsai, S. F., D'Agati, V., Orkin, S. H., and Costantini, F. (1991). Erythroid differentiation in chimaeric mice blocked by a targeted mutation in the gene for transcription factor GATA-1. *Nature* **349,** 257–260.

Ross, R. S., Navankasattusas, S., Harvey, R. P., and Chien, K. R. (1996). An HF-1a/HF-1b/MEF-2 combinatorial element confers ventricular specificity and establishes an anterior-posterior gradient of expression. *Development* **122,** 1799–1809.

Simon, M. C. (1995). Gotta have GATA. *Nature Genet.* **11,** 9–11.

Simon, M. C., Pevny, L., Wiles, M. V., Keller, G., Costantini, F., and Orkin, S. H. (1992). Rescue of erythroid development in gene targeted GATA-1-mouse embryonic stem cells. *Nature Genet.* **1,** 92–98.

Solway, J., Seltzer, J., Samaha, F. F., Kim, S., Alger, L. E., Niu, Q., Morrisey, E. E., Ip, H. S., and Parmacek, M. S. (1995). Structure and expression of a smooth muscle cell-specific gene, SM22α. *J. Biol. Chem.* **270,** 13460–13469.

Soudais, C., Bielinska, M., Heikinheimo, M., MacArthur, C. A., Narita, N., Saffitz, J. E., Simon, M. C., Leiden, J. M., and Wilson, D. B. (1995). Targeted mutagenesis of the transcription factor GATA-4 gene in mouse embryonic stem cells disrupts visceral endoderm differentiation. *Development* **121,** 3877–3888.

Tamura, S., Wang, X.-H., Maeda, M., and Futai, M. (1993). Gastric DNA-binding proteins recognize upstream sequence motifs of parietal cell-specific genes. *Proc. Natl. Acad. Sci. USA* **90,** 10876–10880.

Tsai, F. Y., Keller, G., Kuo, F. C., Weiss, M., Chen, J., Rosenblatt, M., Alt, F. W., and Orkin, S. H. (1994). An early haematopoietic defect in mice lacking the transcription factor GATA-2. *Nature* **371,** 221–226.

Tsai, S. F., Martin, D. I. K., Zon, L. I., D'Andrea, A. D., Wong, G. G., and Orkin, S. H. (1989). Cloning of cDNA for the major DNA-binding protein of the erythroid lineage through expression in mammalian cells. *Nature* **339,** 446–451.

Tsuda, T., Philp, N., Zile, M. H., and Linask, K. K. (1996). Left-right asymmetric localization of flectin in the extracellular matrix during heart looping. *Dev. Biol.* **173,** 39–50.

Weiss, M. J., Keller, G., and Orkin, S. H. (1994). Novel insights into erythroid development revealed through in vitro differentiation of GATA-1 embryonic stem cells. *Genes Dev.* **8,** 1184–1197.

Weiss, M. J., and Orkin, S. H. (1995a). GATA transcription factors: key regulators of hematopoiesis. *Exp. Hematol.* **23,** 99–107.

Weiss, M. J., and Orkin, S. H. (1995b). Transcription factor GATA-1 permits survival and maturation of erythroid precursors by preventing apoptosis. *Proc. Natl. Acad. Sci. USA* **92,** 9623–9627.

Wilson, D. B., Dorfman, D. M., and Orkin, S. H. (1990). A nonerythroid GATA-binding protein is required for function of the human preproendothelin-1 promoter in endothelial cells. *Mol. Cell. Biol.* **10,** 4854–4862.

Yamamoto, M., Ko, L. J., Leonard, M. W., Beug, H., Orkin, S. H., and Engel, J. D. (1990). Activity and tissue-specific expression of the transcription factor NF-E1 multigene family. *Genes Dev.* **4,** 1650–1662.

Yang, Z., Gu, L., Romeo, P.-H., Bories, D., Motohashi, H., Yamamoto, M., and Engel, J. D. (1994). Human GATA-3 trans-activation, DNA-binding, and nuclear localization activities are organized into distinct structural domains. *Mol. Cell. Biol.* **14,** 2201–2212.

Zon, L. I., Gurish, M. F., Stevens, R. L., Mather, C., Reynolds, D. S., Austen, K. F., and Orkin, S. H. (1991). GATA-binding transcription factors in mast cells regulate the promoter of the mast cell carboxypeptidase A gene. *J. Biol. Chem.* **266,** 22948–22953.

Received for publication October 22, 1996
Accepted November 25, 1996

Copyright © 1997 by Academic Press. All rights of reproduction in any form reserved.

DEVELOPMENTAL BIOLOGY 183, 37–48 (1997)
ARTICLE NO. DB968495

Vessel Patterning in the Embryo of the Zebrafish: Guidance by Notochord

Bernadette Fouquet, Brant M. Weinstein, Fabrizio C. Serluca, and Mark C. Fishman[1]

Cardiovascular Research Center, Massachusetts General Hospital, Charlestown, Massachusetts 02129; and Department of Medicine, Harvard Medical School, Boston, Massachusetts 02115

We have cloned the zebrafish homolog of the receptor tyrosine kinase *flk-1* to provide us with a tool to study normal vascular pattern formation in the developing zebrafish embryo and to compare it to mutants in which vascular pattern is perturbed. We find that during normal development the first angioblasts arise laterally in the mesoderm and then migrate medially to form the primordia of the large axial vessels, the dorsal aorta (axial artery) and the axial vein. Lumen formation occurs shortly before onset of circulation at 24 hr postfertilization. We examined the specification of vascular progenitors in the mutant *cloche*, which fails to form both vessels and blood. *cloche* lacks all *flk*-expressing cells and therefore appears to lack angioblasts. The axial vessels of the trunk form in close proximity to notochord and endoderm, which may provide cues for their formation. The dorsal aorta is normally just ventral to the notochord; the axial vein is just below the dorsal aorta and above the endoderm. *floating head (flh)* and *no tail (ntl)* mutants both have defects in the formation of notochord. Both are cell-autonomous lesions, *flh* abolishing notochord and *ntl* preventing its differentiation. In both mutants the dorsal aorta fails to form, while formation of the axial vein is less affected. Mosaic analysis of mutant embryos shows that transplanted wild-type cells can become notochord in mutant *flh* embryos. In these mosaic embryos *flh* cells expressing *flk* assemble at the midline, beneath the wild-type notochord, and form an aortic primordium. This suggests that signals from the notochord may guide angioblasts in the fashioning of the dorsal aorta. The notochord seems to be less important for the formation of the vein. © 1997 Academic Press

INTRODUCTION

The major vessels of the body are assembled locally, yet must be integrated into a seamless systemic circulation. It is not known what signals guide the generation of the tubes, assign vascular identities as artery or vein, or coordinate vessel placement with regard to viscera.

Angioblast precursors are dispersed throughout the mesoderm. Some appear to migrate long distances before assembly, whereas others appear to form tubes locally (Pardanaud *et al.*, 1987, 1989; Coffin and Poole, 1988, 1991; Noden, 1991; Couly *et al.*, 1995). The major axial vessels, such as aorta and vena cava, and those to organs derived from endoderm are believed to be formed by local assembly of angioblasts into tubes, a process termed vasculogenesis (Pardanaud *et al.*, 1987, 1989; Coffin and Poole, 1988, 1991; Risau *et al.*, 1988; Poole and Coffin, 1991; Risau, 1991). It is not known whether particular genes control the assembly of different regions of the vasculature.

The endothelial-specific mitogen, vascular endothelial growth factor (VEGF) (Keck *et al.*, 1989; Leung *et al.*, 1989), is expressed in regions appropriate to support vessel growth (Breier *et al.*, 1992; Flamme *et al.*, 1995a). VEGF overexpression *in vivo* in chick embryos causes anomalous vessel formation (Drake and Little, 1995; Flamme *et al.*, 1995b). Receptor tyrosine kinases for VEGF, VEGF R1 (*flt-1*), and VEGF R2 (*flk-1*) are present on angioblasts (Eichmann *et al.*, 1993; Millauer *et al.*, 1993; Yamaguchi *et al.*, 1993; Dumont *et al.*, 1995). Targeted mutation of *flk-1* in mice blocks development of both blood and vessels (Shalaby *et al.*, 1995). *flt-1* mutation interferes with vessel organization, although it does not abolish angioblast generation and vessel tubulogenesis (Fong *et al.*, 1995). The pattern of *flk-1* expression suggests that it is the earliest marker of intraembryonic angioblasts in the mouse, from the time of their appearance in the lateral mesoderm of the trunk and the cardiogenic plate through tubular assembly. After vessel formation *flk-1* expression diminishes, while expression of *flt-1* and other endothelial tyrosine kinases remains high (Dumont *et al.*, 1995).

The notochord, the transient cartilaginous support which

[1] To whom correspondence should be addressed.

0012-1606/97 $25.00
Copyright © 1997 by Academic Press
All rights of reproduction in any form reserved.

characterizes chordates, plays an important role in the establishment of embryonic form. It serves as a prominent source of patterning information to both the adjacent spinal cord and somites. In mutations of the notochord in mice (*brachyury* (Herrmann *et al.*, 1990)) and zebrafish, both neural tube and somites are perturbed. For example, in the zebrafish mutation *floating head* (*flh*), due to mutation in the orthologue of *Xenopus Xnot*, the notochord is absent, somites fuse at the midline and floor plate in the trunk is absent (Halpern *et al.*, 1995; Talbot *et al.*, 1995). The floor plate of the midbrain, hindbrain, and anterior spinal cord is relatively normal, presumably because prechordal plate is not affected by the mutation. In *no tail* (*ntl*), a mutation in *brachyury*, notochord precursors do not complete differentiation, the myotome does not assume its chevron shape, and muscle pioneers are absent, although notochord signals are sufficient to induce floor plate (Halpern *et al.*, 1993; Schulte-Merker *et al.*, 1994). Both *flh* and *ntl* act in a cell-autonomous fashion with regard to notochord precursors and a cell-non-autonomous manner with regard to somite and neural tube (Halpern *et al.*, 1993, 1995).

In order to define the early spatial organization of endothelial primordia, we have cloned a zebrafish homolog of the receptor tyrosine kinase *flk-1*. We have used expression of this receptor tyrosine kinase to follow vessel assembly primarily in the trunk and to examine the role of the notochord in vasculogenesis. We find evidence that notochord regulates assembly of the dorsal aorta, while the axial vein is far less dependent on the notochord.

MATERIAL AND METHODS

Animals

Fish were maintained in the zebrafish facility at the Cardiovascular Research Center at the Massachusetts General Hospital. Embryos were raised at constant 28.5°C and staged according to morphological criteria (somite number) and hours postfertilization (hpf) (Kimmel *et al.*, 1995). Mutations used in this study were *cloche*^{m378} (Stainier *et al.*, 1996), *no tail*^{b195} (Schulte-Merker *et al.*, 1994), and *floating head*^{n1} (Talbot *et al.*, 1995).

cDNA Cloning and Sequencing

Oligonucleotides PTKI and PTKII (Wilks, 1989) were used to amplify zebrafish receptor tyrosine kinase domains from reverse-transcribed RNA from 24 hpf embryos. PCR products were used to construct a "minilibrary" of kinase domains in the TA cloning vector (Invitrogen). Colony hybridization was performed using oligos specific for *flk-1* (BF15: GATTATGTCAGAAAAGGAGATGC and BF16: ATT/CCTCC/TTATCGGAGAAGAAT/CGT) to identify homologous clones out of this minilibrary. Hybridization was carried out at 37°C in 6× SSC, 1% SDS, 1× Denhardt's, 100 μg/ml yeast RNA, and washes of the filters were at 45°C in 6× SSC, 1% SDS (1× SSC is 0.15 *M* NaCl, 0.015 *M* Na citrate, pH 7.4, and 1× Denhardts is 0.02% Ficoll, 0.02% polyvinylpyrrolidone, 0.02% bovine serum albumin). Zebrafish homologs of *flk-1* were identified by sequence comparison and used to screen two different cDNA libraries, a cDNA library from adult zebrafish heart (Chen and Fishman, 1996) and a cDNA library from whole embryos stages 18 to 40 hpf (kindly provided by Professor P. Chambon, INSERM, Strasbourg). Phages (10^6) of each Lambda ZAPII cDNA library were screened. Hybridization was carried out at 42°C in 5× SSC, 50% formamide, 1% SDS, 1× Denhardts, and 100 μg/ml yeast total RNA. Washes of the filters were carried out at 60°C in 0.1× SSC, 1% SDS. One positive clone, h-1, with an insert size of 2051 bp, was isolated from the adult heart library and one positive clone, e-1, with an insert size of 1100 bp, was isolated from the embryonic library. Sequence analysis and database searches was performed using GCG. Sequence analysis revealed that the two clones are identical in their overlapping region except for a 102-bp insertion in the longer clone which is probably due to a cloning artifact. Amino acid sequences were obtained from the open reading frames, which were identical in both clones.

Whole Mount RNA in Situ Hybridization

Whole mount RNA *in situ* hybridization was carried out as described (Jowett and Lettice, 1994). A 1100-bp *Eco*RI/*Hin*dIII fragment of cDNA h-1 spanning the nonconserved intracellular and part of the 3′ UTR region was subcloned and used for *in vitro* transcription. After staining, embryos were observed under an Axiophot Microscope (Zeiss). For histological analysis specimens were refixed in 4% paraformaldehyde, dehydrated, and embedded in plastic (JB-4). Sections were counterstained with Nuclear Fast Red (Sigma) where indicated. Serial sections were analyzed with an Axiophot Microscope (Zeiss).

Cell Transplantation

Transplantations were carried out essentially as described previously (Ho and Kane, 1991; Halpern *et al.*, 1993; Ho and Kimmel, 1993; Lee *et al.*, 1994). Donor embryos were injected with 4% rhodamine–dextran/4% biotin–dextran (Molecular Probes) in 0.15 KCl between the 1k-cell stage and the sphere stage and depending on the age of the embryos between 20 and 100 cells were introduced into the host blastulae. Cells were transplanted from phenotypically wild-type host embryos into *flh* mutant embryos at the blastula stage. Donor and host embryos were phenotyped at the 25 somite stage. Transplanted cells were visualized in the living embryo by epifluorescence. Subsequently, embryos were fixed and processed for *in situ* hybridization. After *in situ* hybridization transplanted cells were detected using peroxidase-coupled antibodies to biotin.

RESULTS

flk cDNA

The deduced amino acid sequence of *flk* cDNA is shown in Fig. 1, aligned with the VEGF receptor 2 homologs in mouse (*flk-1*, (Matthews *et al.*, 1991)), human (*kdr* (Terman *et al.*, 1991)), and quail (*quek-1* (Eichmann *et al.*, 1993)). In all regions of high interspecies identity, *flk* is essentially equally conserved among all species analyzed (77% to *kdr*, 74% to *flk-1*, and 74% to *quek1*) and overall 63% to *kdr* and 60% to *flk-1*. As for other species, there is also a high, but lesser, degree of homology to the other known VEGF receptor tyrosine kinase, *flt-1* (54%, not shown) (Shibuya *et al.*, 1990).

Embryonic Patterns of flk Expression

We have previously analyzed the development of the zebrafish circulation, once the vessels are patent, by the technique

Copyright © 1997 by Academic Press. All rights of reproduction in any form reserved.

```
           1                                                  50
    Flk1   DVEEEEA.SE ELYKDFLTLE HLICYSFQVA KGMEFLASRK CIHRDLAARN
     Kdr   DVEEEEA.PE DLYKDFLTLE HLICYSFQVA KGMEFLASRK CIHRDLAARN
   Quek1   DVEEEDAGSE DLCKNPLTME DLICYSFQVA RGMEFLASRK CIHRDLAARN
     flk   .SEEEEEEQE DLYKKVLTLE DLICYSFQVA KGMEFLASRK CIHRDLAARN
Consensus  --***----* -*-*--**-* -********* -********* **********

           51                                                 100
    Flk1   ILLSEKNVVK ICDFGLARDI YKDPDYVRKG DARLPLKWMA PETIFDRVYT
     Kdr   ILLSEKNVVK ICDFGLARDI YKDPDYVRKG DARLPLKWMA PETIFDRVYT
   Quek1   ILLSDNNVVK ICDFGLARDI YKDPDYVRKG DARLPLKWMA PETIFDRVYT
     flk   ILLSENNVVK ICDFGLARDV YKDPDYVRKG DARLPLKWMA PEAIFDKIYT
Consensus  ****--**** *********_ ********** ********** **-***--**

           101                                                150
    Flk1   IQSDVWSFGV LLWEIFSLGA SPYPGVKIDE EFCRRLKEGT RMRAPDYTTP
     Kdr   IQSDVWSFGV LLWEIFSLGA SPYPGVKIDE EFCRRLKEGT RMRAPDYTTP
   Quek1   IQSDVWSFGV LLWEIFSLGA SPYPGVKIDE EFCRRLKEGT RMRAPDYTTP
     flk   TQSDVWSFGV LMWEIFSLGA SPYPGLHIDE EFCCRLKEGT RMKAPEYSSS
Consensus  -********* *-******** *****--*** ***-****** **-**-*---

           151                                                200
    Flk1   EMYQTMLDCW HEDPNQRPSF SELVEHLGNL LQANAQQDGK DYIVLPMSET
     Kdr   EMYQTMLDCW HGEPSQRPTF SELVEHLGNL LQANAQQDGK DYIVLPISET
   Quek1   EMYQTMLDCW HGDPKQRPTF SELVEHLGNL LQANVRQDGK DYVVLPLSVS
     flk   EIYQTMLDCW HGEPSQRPTF TELVERLGDL LQASVQQEGK HYI..PINTA
Consensus  *-********* *--*-***-* -****-**-* ***---*-** -*---*----

           201                                                250
    Flk1   LSMEEDSGLS LPTSPVSCME EEEVCDPKFH YDNTAGISHY LQNSKRKSRP
     Kdr   LSMEEDSGLS LPTSPVSCME EEEVCDPKFH YDNTAGISQY LQNSKRKSRP
   Quek1   LNMEEDSGLS LPTSPASCKE EEEVCDPKFH YDNTAGISQY RQGSKRKSRP
     flk   LLTKADP... ...SNQSPTE ETSTRPVSLR DSGTA..... ...WNIKIRP
Consensus  *----*---- ---*--*--* *--------- ---**----- ------*-**

           251                                                300
    Flk1   VSVKTFEDIP LEEPEVKVIP DDSQTDSGMV LASEELKTLE DRNK.LSPS.
     Kdr   VSVKTFEDIP LEEPEVKVIP DDNQTDSGMV LASEELKTLE DRTK.LSPS.
   Quek1   VSVKTFEDIP L.VTTVKVVQ EENQTDSGMV LASEELKTLE EQDKQVKIP.
     flk   ESVKTFDEVI LENGTNK.IH EGGQSDSGIG LSSDDLKTLK RLESLARPRS
Consensus  -*****---- *-----*--- ---*-***-- *-*--****- ----------

           301                                                350
    Flk1   .FGGMMPSKS RESVASEGSN QTSGYQSGYH SDDTDTTVYS SDEAGLLKMV
     Kdr   .FGGMVPSKS RESVASEGSN QTSGYQSGYH SDDTDTTVYS SEEAELIKLI
   Quek1   .FSTLAPSKS NESVMSEASN QTSGYQSGYH SDDMDNMVCS SEDTELL...
     flk   FMSRAMKRKS KESVLLEG.. EMDKYPPLVP SLSLED...S SLDSEM....
Consensus  ---------- -***--*--- ----*----- *--------* *---------

           351                                    390
    Flk1   DAAVHADSGT TLQLTSCLNG SGPVPAPPPT PGNHERGAA.
     Kdr   EIGVQTGSTA QILQP...DT GTTLSSPPV. ..........
   Quek1   .CAQEASPTL PRCAWPGIYS PAPVASLPL. ..........
     flk   ....ECHSPP PDYNYVVRYS .....TPPV............
Consensus  ---------- ---------- -------*-- ----------
```

FIG. 1. Amino acid sequence alignment of *flk* to *flk-1*, *kdr*, and *quek-1*. Residues identical in all four sequences are marked with asterisks.

of microangiography (Weinstein *et al.*, 1995). The first vessels formed are the major axial vessels to the trunk, the artery termed the dorsal aorta (or axial artery) and the vein termed the axial vein. Trunk circulation begins at around 24 hpf (30 somites), and cranial circulation is present by 30 hpf.

In the trunk, *flk*-expressing cells are evident at the 10-

Copyright © 1997 by Academic Press. All rights of reproduction in any form reserved.

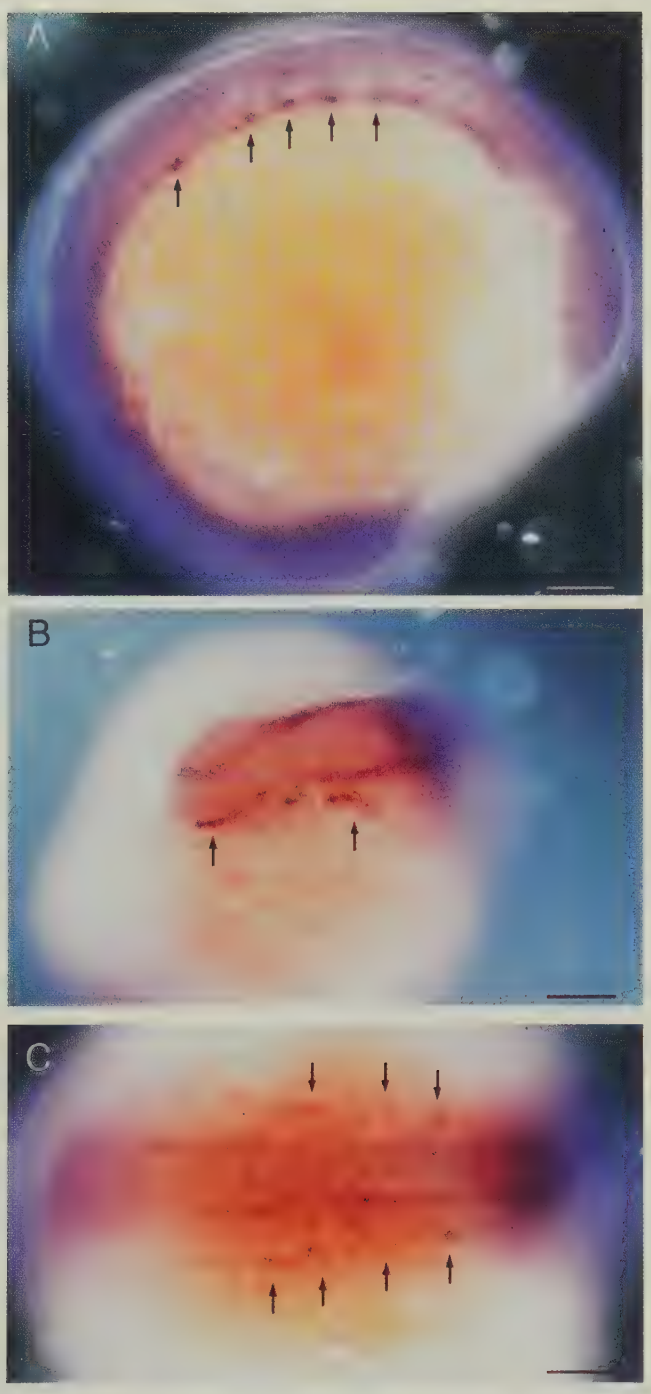

FIG. 2. Whole mount RNA *in situ* hybridization with *flk* performed on 12 somite stage embryos (15 hpf). (A) Lateral view and (C) dorsal view showing the bilateral angiogenic cell clusters in the trunk (arrows). (B) Anterior view showing the endocardial and cephalic angioblasts (arrows). Dorsal is up (A) and anterior is to the left (A). Bars, 100 μm.

somite stage, as patches of three to five cells arrayed in repeating units at the lateral edge of the mesoderm (Figs. 2A and 2C). By the 14 somite stage these *flk*-expressing cells are at the midline, where they form the primordium of the dorsal aorta, just ventral to the notochord (Figs. 3A, 3G, and 3H). Other *flk*-expressing cells are visible laterally, adjacent to the endoderm (Figs. 3H and 3I). These are presumably angioblasts which may be precursors of the axial vein, which assembles between the 14 and 20 somite stages. Both the aorta and the vein appear to assemble in a craniocaudal direction. Anteriorly, the primordia of the paired dorsal aortae that are not yet formed by the 14 somite stage (Fig. 3F) merge at the level of somite 1 to link up with the single dorsal aorta to the posterior trunk and tail by the 24 somite stage (Figs. 4A and 4C). The primordium of the axial vein forms below the dorsal aorta (Figs. 4B and 4D).

Intersomitic vessels, and those to ectodermally derived organs, are believed to form predominantly by sprouting, a process termed angiogenesis (Pardanaud *et al.*, 1987, 1989; Coffin and Poole, 1988, 1991; Risau *et al.*, 1988; Poole and Coffin, 1991; Risau, 1991). The first intersomitic arteries, as evidenced by *flk* expression, sprout from the dorsal aorta by the 26 somite stage (shown at 24 hpf, Figs. 5B and 5C). At this time, while the network of all major vessels is evident by *flk* expression, most vessels are not yet open, although the beginning of lumen formation is evident in the dorsal aorta at the 24 somite stage (Fig. 4D).

In the heart region, the presumptive endocardial precursors lie in two bilateral patches laterally in the mesoderm just anterior to the otic vesicle (Figs. 2B, 3A, and 3B). By the 14 somite stage *flk*-expressing cells are medial, where they coalesce to form the primordium of the endocardium at the midline, as well as the primordia of ventral aorta, the first aortic arch, and the proximal parts of dorsal aortae and internal carotid arteries (Figs. 3B, 3D, and 3E). Between the 20 and 26 somite stages the endocardial precursors are enclosed by the fusing myocardial tubes (not shown) (Stainier *et al.*, 1993).

In the head, the first *flk*-expressing cells reside anteriorly, ventral to the optic vesicles, presumably in the cephalic paraxial mesoderm (Figs. 2B and 3A–3C). At the 14 somite stage these clusters of cells enlarge into two plexi and coalesce with the primordia of the two internal carotid arteries that extend anteriorly from the heart region. The primordia of the large vessels in the head form by the 26 somite stage.

The formation of vessel lumina precedes the onset of trunk circulation at the 30 somite stage (24 hpf). At this time most large vessels are patent, as shown in Fig. 5A for the dorsal aorta, although some, such as the anterior cardinal vein, do not yet possess a lumen. In large vessels, such as the dorsal aorta, *flk* is still expressed at Day 2, although at a lower level. Throughout embryonic development *flk* is highly expressed in newly forming vessels such as capillaries sprouting into the brain or pectoral fin and in vessels forming the aortic arches (not shown).

We have followed this pattern of vessel formation in mutations which appear to be revealing about the generation of angioblasts or their assembly into vessels.

The Mutant cloche Interferes with Specification or Maturation of Angioblasts

In *cloche* mutants, there are no vessels, or very few (in the perianal region of the trunk at 36 hpf), and hematopoiesis is

Copyright © 1997 by Academic Press. All rights of reproduction in any form reserved.

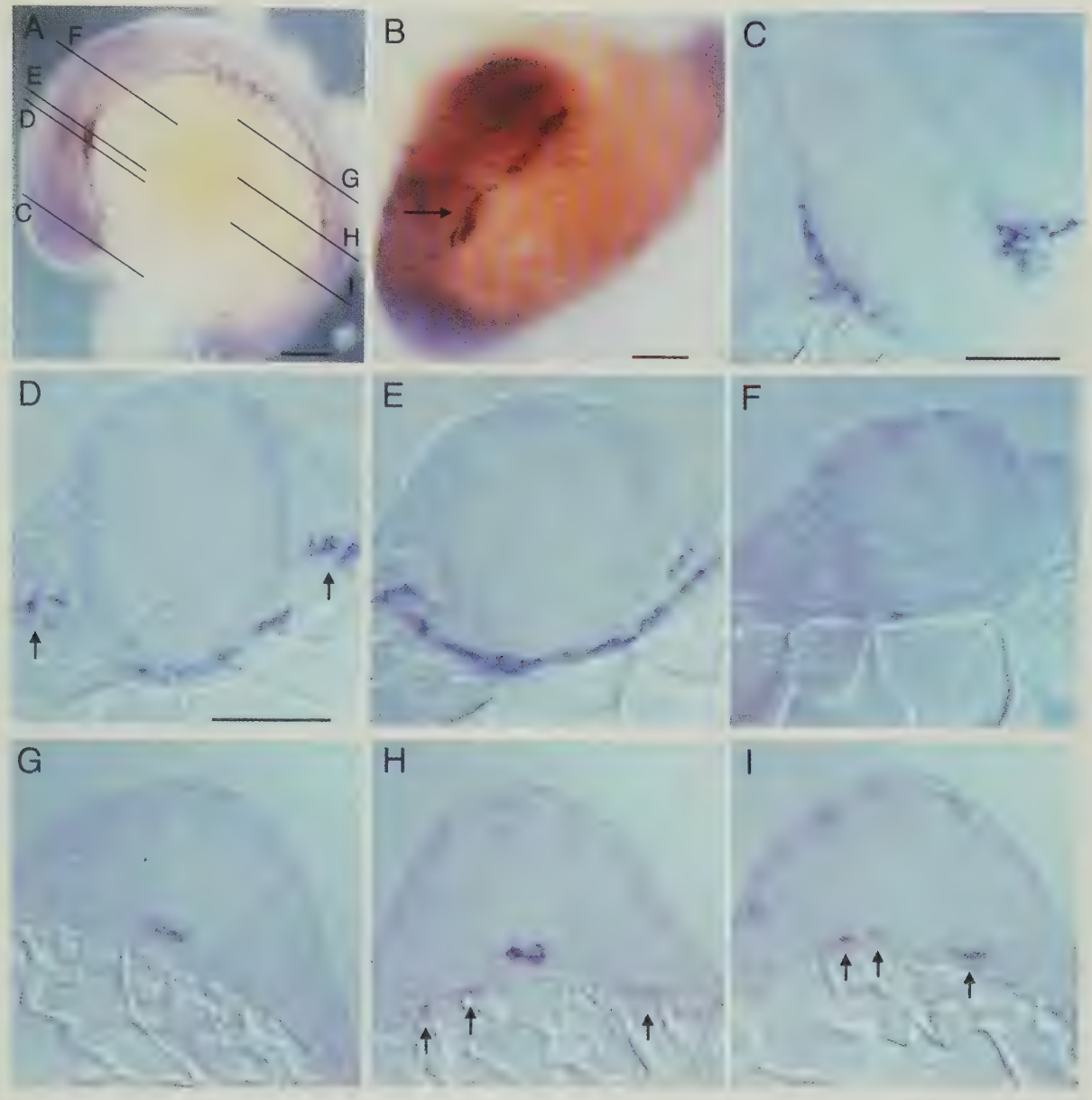

FIG. 3. Whole mount RNA *in situ* hybridization with *flk* performed on 14 somite stage embryos (16 hpf). (A) Lateral view and (B) anterior view showing angioblastic areas in the embryo. Lines in (A) indicate planes of sectioning for panels C through I. Arrow in (B) indicates position of first aortic arch. (C) Section at the level of the forebrain and eye vesicles, showing angioblastic cells in the ventrally to the brain located plexus. (D) Section at the level of the endocardial primordium which has reached the midline by this stage. Arrows indicate the primordia of the internal carotid artery. (E) Section at the level of the aortic arch primordium. (F) Section at the level of the hindbrain, which lacks *flk*-positive cells at this stage. (G–I) Sections at various planes through the trunk. Angioblasts have reached the midline below the notochord (G, H) forming the primordium of the dorsal aorta. Other angioblasts are still located laterally close to the yolk (arrows). (I) In the posterior trunk angioblastic cells have not yet reached the midline (arrows). Dorsal is up (A, C–I) and anterior is to the left (A). Bars, 100 μm (A, B), 50 μm (C–I).

severely reduced. We had speculated that the mutation might interfere with generation of a primitive vessel precursor, perhaps one with a bipotential hemangioblast fate (Stainier *et al.*, 1995). As shown in Fig. 6B, there is no *flk* labeling in *cloche* mutant embryos at the 30 somite stage (24 hpf). This is evident from the time of normal onset of expression (10 somites) through 30 somites (24 hpf) and so does not represent a delay in maturation (similar results are found by (Liao *et al.*, 1997)). These results suggest that angioblasts are not specified in *cloche*.

Copyright © 1997 by Academic Press. All rights of reproduction in any form reserved.

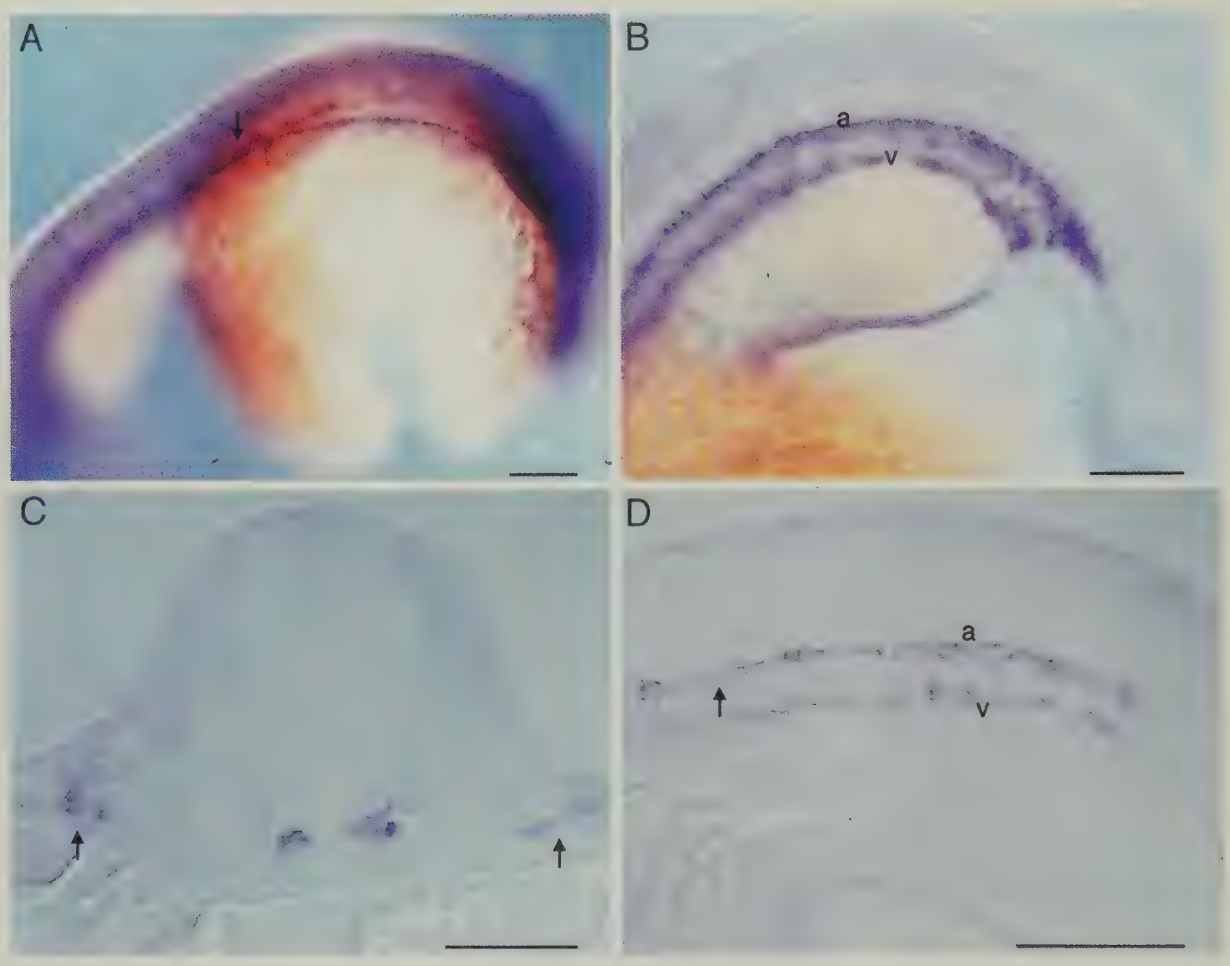

FIG. 4. Whole mount RNA *in situ* hybridization with *flk* on 24 somite stage embryos (21 hpf). (A) Dorsolateral view showing the paired dorsal aortae in the area of the hindbrain and their junction in the anterior trunk (arrow). (B) Lateral view of the posterior trunk and tail showing the primordia of the dorsal aorta (a) and the axial vein (v). (C) Transverse section through the anterior trunk at the level of the first somite. The two primordia of the dorsal aortae lie just beneath the notochord. Laterally located (arrows) are precursors of the bilateral ducti of Cuvier. (D) Sagittal section of the posterior trunk showing the primordia of the dorsal aorta (a) and the ventral vein (v). Arrow indicates beginning lumen formation in the dorsal aorta. No intersomitic vessels are yet formed. Dorsal is up, and anterior is to the right in (A) and to the left in (B, D). Bars, 100 μm (A, B), 50 μm (C, D).

The Mutants floating head and no tail Have Defects in Formation of the Dorsal Aorta

The axial vessels of the trunk form in close proximity to notochord and endoderm, which may provide cues for their formation. The dorsal aorta is normally just ventral to the notochord; the axial vein is just below the dorsal aorta and above the endoderm. We were interested in examining mutations lacking notochord with respect to their vascular phenotype.

flh is a mutation in the orthologue of *Xnot*, a transcription factor expressed in notochord precursors (Gont *et al.*, 1993; von Dassow *et al.*, 1993; Talbot *et al.*, 1995). The mutant lacks notochord and, as a consequence, fails to pattern the neural tube. Somites fuse due to transfating of axial mesoderm to muscle (Halpern *et al.*, 1995; Melby *et al.*, 1996). In *flh*, as shown in Fig. 6C, there is no evidence of an aorta. A single ventral stripe of *flk*-expressing cells is evident along the entire trunk, which assembles into small vessel stretches. The region corresponds to the position of the vein just above the endoderm (Fig. 7B), although whether this vessel is continuous cannot be determined because *flk* expression appears to be extinguished more rapidly in *flh* than in wild-type embryos. In the tail region, the *flk*-expressing cells aggregate into a large ventral endothelial lacuna enclosing red blood cells (Fig. 6C). Mutants never establish a functional circulation to the trunk. Circulation to the head is much less affected, and blood flow is generally established. The pattern of cranial vessels is usually normal although extra sprouts of vessels can be found, possibly related to increased blood pressure. Thus the most prominent vascular deficiency in *flh* is the absence of dorsal aorta.

In *ntl*, notochord precursors are present and adequate to

Copyright © 1997 by Academic Press. All rights of reproduction in any form reserved.

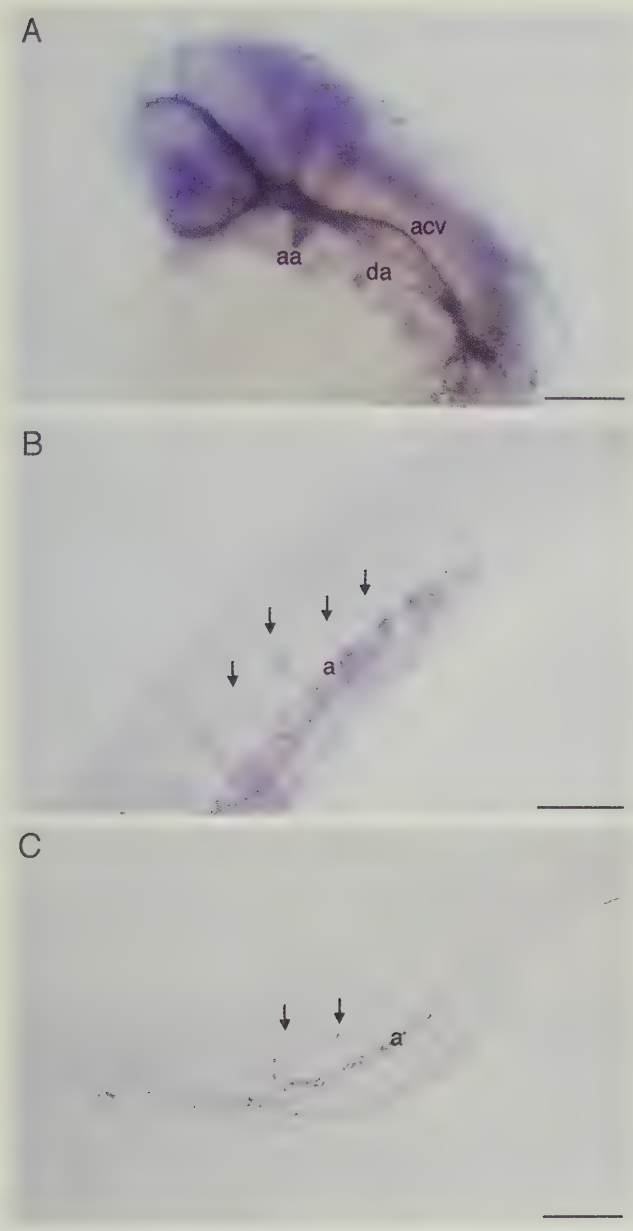

FIG. 5. Whole mount RNA *in situ* hybridization with *flk* on 30 somite stage embryos (24 hpf) showing (A) a view of the head, (B) a lateral view of the trunk, and (C) a sagittal section of the posterior trunk and tail. (A) Clearly visible are the patent first aortic arch (aa) and left dorsal aorta (da). In contrast, the anterior cardinal vein (acv) does not yet possess a lumen. (B, C) In the trunk, intersomitic vessels (arrows) can be seen sprouting from the dorsal aorta (a). Dorsal is up and anterior is to the left. Bars, 100 μm (A), 50 μm (B, C).

generate the signal to floor plate. Somites do not fuse, although they lack the normal chevron shape (Halpern *et al.*, 1993). At 24 hpf circulation to the trunk is not present. As in *flh* mutants, only one stripe of *flk*-expressing cells is present in the trunk of 24 hpf embryos (Fig. 6D). A single tubular structure lined by *flk*-expressing cells forms in *ntl* mutants (Fig. 7C). Because the distance between neural tube and endoderm is small, it is impossible to distinguish, by the relative dorsoventral position, whether the vessel is artery or vein.

Mosaic Analysis of flh: Is There a Signal from Notochord to Vessels?

Genetically mosaic zebrafish embryos may be generated by transplantation between two embryos at the blastula stage. Transplanted cells are incorporated in a manner predicted by the fate map and contribute to host tissues depending upon where they were introduced. Transplanted cells are labeled with both fluorescent and biotinylated dextrans to distinguish them from unlabeled host cells. If the donor and host are genetically different, the analysis of the consequent mosaic permits distinction of whether a mutation acts cell-autonomously in its effects upon different tissues. Here we were particularly interested to use this technique to examine effects of notochord upon vessels of the trunk.

flh is more amenable to analysis of rescue by wild-type notochord than is *ntl* because the distance between neural tube and endoderm permits the distinction of artery from vein and because *flh* is fully expressive. Therefore, we performed transplantation between wild-type donors and mutant host embryos at the blastula stage, allowed the embryos to mature to the 25 somite stage, and scored for the contribution of wild-type cells to notochord. Transplanted cells were visualized in the living embryo using epifluorescence optics (Fig. 8A). Embryos were then examined for *flk* expression by whole mount *in situ* hybridization and transplanted cells were identified by peroxidase-coupled antibodies to biotin. Wild-type cells can form notochord in a *flh* mutant background, as demonstrated previously (Halpern *et al.*, 1995) and shown in Figs. 8A and 8C. Therefore, *flh* acts cell-autonomously with regard to notochord formation.

Most importantly, in *flh* host embryos, a new more dorsal population of *flk*-expressing host cells is detected in the midline immediately beneath areas of the embryo where transplanted wild-type cells have contributed to notochord (Fig. 8C). In areas of the same embryo where wild-type cells contribute only to ventral neural tube (and not to notochord), only the ventral population of *flk*-expressing cells normally found in *flh* is evident (Fig. 8B). As shown in Table 1, all *flh* embryos with transplanted wild-type notochord, as determined morphologically by appearance of clearly identifiable large vacuolated cells characteristic of notochord, evidenced additional *flk*-expressing cells immediately below the wild-type notochord cells ($n = 11$). In contrast, *flh* embryos with wild-type cells found only in other regions (e.g., neural tube, somites) never evidenced additional dorsal *flk*-expressing cells ($n = 26$) in the trunk. Wild-type cells in both anterior and posterior trunk notochord rescued local *flk* expression. Thus, local assembly and/or *flk* expression in the dorsal vessel, presumably the aorta, appears to require the presence of wild-type notochord.

Copyright © 1997 by Academic Press. All rights of reproduction in any form reserved.

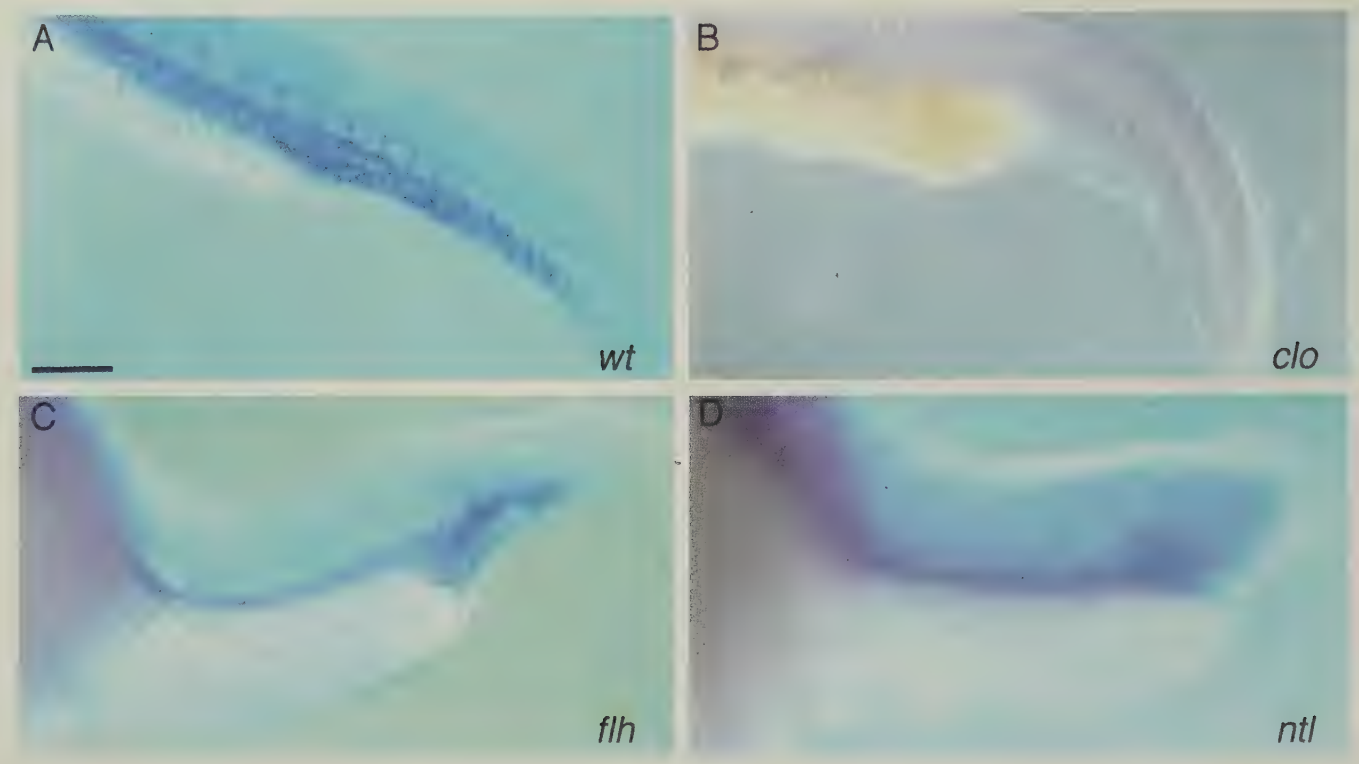

FIG. 6. Whole mount RNA *in situ* hybridization with *flk* performed on 30 somite stage zebrafish mutant embryos (24 hpf). (A) wild-type, (B) *cloche*, (C) *floating head*, (D) *no tail*. (B) In *cloche* no *flk*-expressing cells can be found. (C) *flh* has few *flk*-expressing cells in the trunk, but forms a sinus of endothelial cells in the tail. (D) *ntl* is similar to *flh*. Dorsal is up and anterior is to the left. Bar, 100 μm.

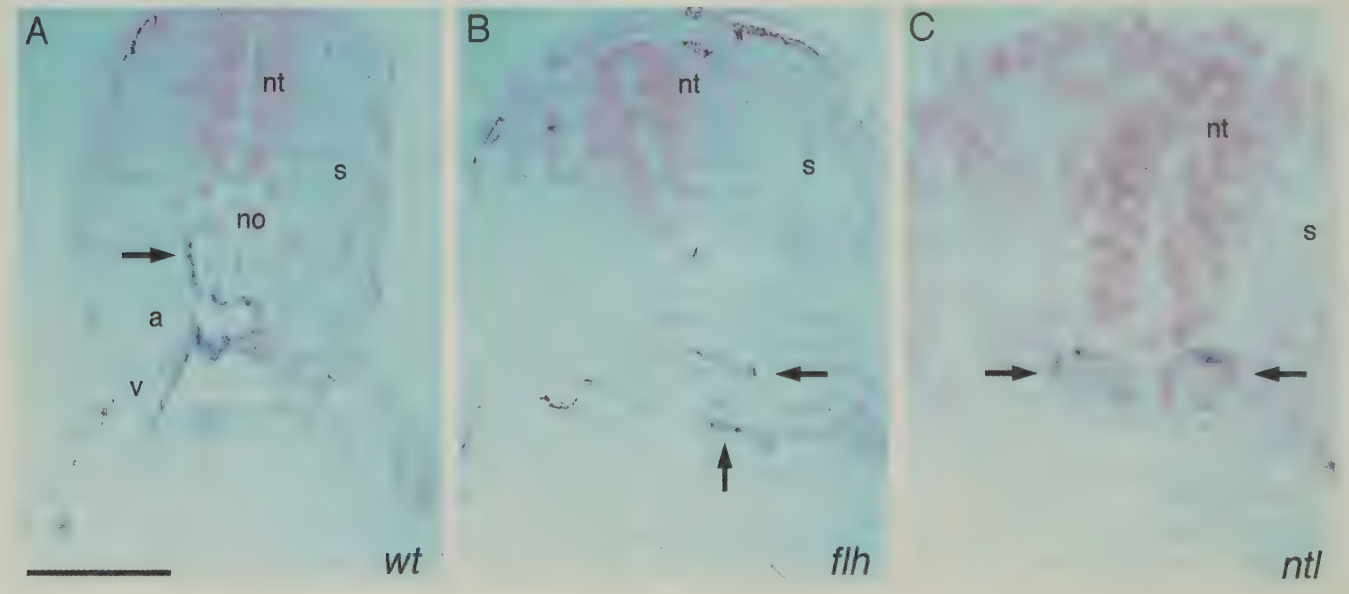

FIG. 7. Histological analysis of whole mount RNA *in situ* hybridization with *flk* performed on 30 somite stage embryos (24 hpf). (A) Wild type, (B) *floating head*, (C) *no tail*. (A) The wild-type embryo clearly shows the two axial vessels, dorsal aorta (a) and axial vein (v) and a sprout of an intersomitic vessel (arrow). (B, C) No axial vessels can be observed in *floating head* or *no tail*. Arrows point to *flk*-expressing cells. Sections were counterstained with Nuclear Fast Red. Dorsal is up. Bar, 50 μm.

Copyright © 1997 by Academic Press. All rights of reproduction in any form reserved.

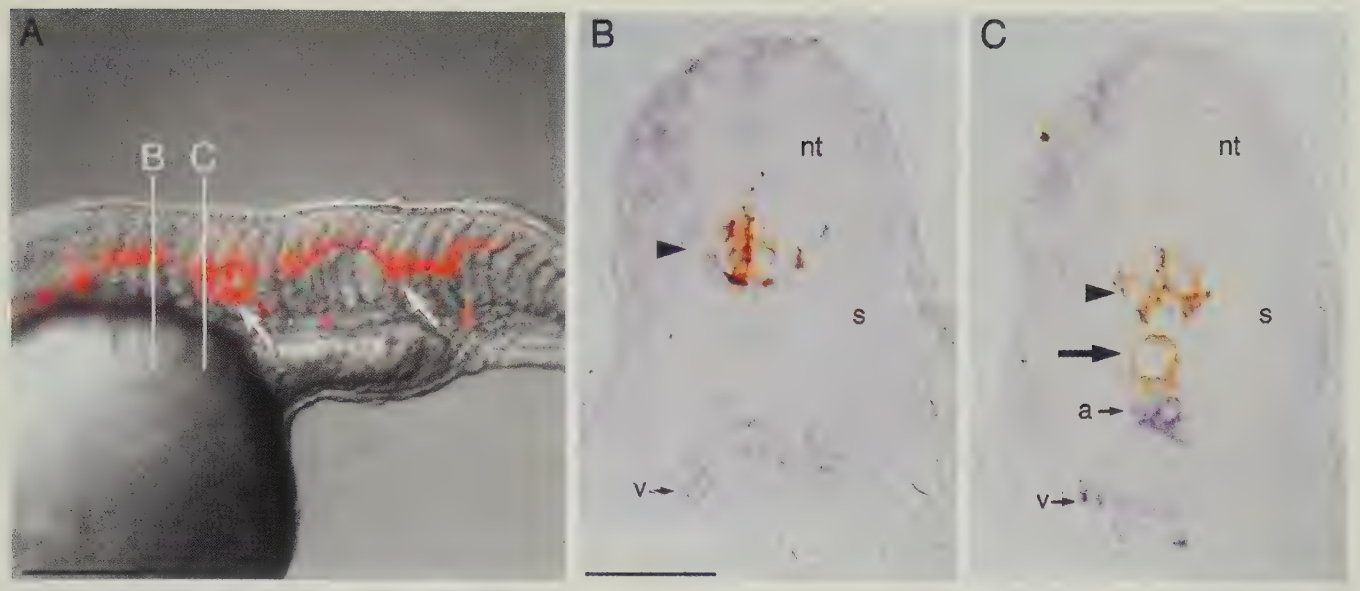

FIG. 8. Mosaic analysis of *flh* embryos transplanted with wild-type cells. (A) Composite rhodamine epifluorescence (red) and Nomarski (gray) videomicrograph of the trunk of a 25 somite *flh* mutant embryo that was transplanted at the blastoderm stage. In this embryo wild-type cells contributed primarily to neural tube and notochord (arrows). B and C indicate planes of cross-sectioning in panels (B) and (C). (B) Cross section of *flh* embryo in plane B. Transplanted wild-type cells labeled with biotin–peroxidase (brown, arrowhead) contributed to ventral neural tube (nt). A single population of *flk*-expressing cells (blue, v) resides ventrally. The somites (s) are fused beneath the neural tube. (C) Cross section of *flh* embryo in plane C. Transplanted wild-type cells contributed both to ventral neural tube (arrowhead) and to notochord (arrow). There are two populations of *flk*-expressing cells, a dorsal one (a) just beneath the notochord and a ventral one (v). Somites (s) are not fused. Dorsal is up, anterior is to the left in (A). Bars, 250 μm (A), 50 μm (B, C).

DISCUSSION

We are interested in the establishment of vascular patterns in the early embryo. How do signals organize vessel assembly in concert with body form? The transparency of the zebrafish and its attractiveness for large-scale genetic screens make it an ideal organism to begin to understand the signals for vessel development. We turned to the *flk* gene as a potential probe to establish the normal timing and pattern of angioblast assembly. We have focused upon the trunk because of its clarity and clear topography of vessels.

TABLE 1

	Ventral stripe of *flk*-expressing cells	Dorsal stripe of *flk*-expressing cells
Wild-type cells not in notochord (n = 26)	26/26	0/26
Wild-type cells in notochord (n = 11)	11/11	11/11

Specification of Angioblasts

The zebrafish *flk* cDNA identifies a putative receptor tyrosine kinase of the *flk-1/flt-1* family. In the tyrosine kinase domain zebrafish *flk* is equally related to *flk-1* or *flt-1*, but overall, it is slightly more related to *flk-1* than to *flt-1*. Both *flk-1* and *flt-1* are markers of angioblasts in mouse (Dumont *et al.*, 1995) and quail (Eichmann *et al.*, 1993). In many vertebrate embryos islands of angioblasts and red blood cells appear first on the yolk sac, but angioblasts of the embryo proper arise from intraembryonic mesoderm (Hahn, 1909; Reagan, 1915; Sabin, 1917; Pardanaud *et al.*, 1987, 1989; Coffin and Poole, 1988). The lineage of some angioblasts may be shared with blood cells. Thus, it is believed that in the paraaortic region (and on the yolk sac) there may be a common progenitor, referred to as a hemangioblast (Dieterlen-Lievre and Marin, 1981; Pardanaud, 1989, 1996). In the targeted mutation of the *flk-1* gene in mice (Shalaby *et al.*, 1995) and in the *cloche* mutant in zebrafish (Stainier *et al.*, 1995) neither endothelium nor blood cells form. Since both mutations affect the endothelium in a cell-autonomous manner, the absence of blood indicates that the mutation perturbs a common progenitor, or that the earliest blood compartment depends upon endothelium, or that the mutation independently affects differentiation of both lineages. *cloche* appears to act upstream of the hematopoietic transcription factors *GATA1* and *GATA2* (Stainier *et al.*,

Copyright © 1997 by Academic Press. All rights of reproduction in any form reserved.

1995). *flk* is absent in *cloche* mutants. This likely reflects absence of angioblasts, but could alternatively indicate a failure of their maturation. It is conceivable that *cloche* could be a mutation which perturbs *flk* signaling, but genetic mapping indicates that it is not linked to the *flk* gene (Fouquet and Fishman, unpublished).

Assembly of Vessels in the Zebrafish

We have focused here upon the trunk vessels. Vessel formation in the trunk, using endothelial markers such as *flk-1*, is similar to that described in other species (His, 1900; Reagan, 1915; Sabin, 1917; Pardanaud *et al.*, 1987, 1989; Coffin and Poole, 1988; Poole and Coffin, 1991) and appears to involve vasculogenesis of the major artery and vein, followed by angiogenic sprouting of intersomitic arteries. The zebrafish is unusual in that it lacks significant yolk sac blood islands and so lacks the early *flk* expression which, in the mouse, is on the ectoplacental cone, the extraembryonic mesoderm of the future yolk sac (Dumont *et al.*, 1995).

There are two other spatially distinctive regions of vessel assembly. One is in the region where the heart will form, just anterior to the otic placode and to the notochord. In this region angioblasts appear first laterally in the mesoderm and then appear to migrate medially to form the endocardial primordium at the midline, where they become enclosed by the myocardial tubes. At the time of fusion of the bilateral primordia, the *flk*-expressing cords of endothelial cells in the cardiac region appear continuous from endocardium to ventral aorta and through the first aortic arches, where the cords branch posteriorly into dorsal aortae and anteriorly into internal carotid arteries. The other spatially separate region of *flk*-expressing cells is anterior and ventral to the forebrain and the optic vesicles. These cells presumably arise from cephalic paraxial mesoderm.

It is not known whether angioblasts in the different sites of expression have distinctly different properties, but it seems unlikely. Transplantation experiments in avians show that angioblasts are derived from throughout the mesoderm, with the exception of notochord and prechordal plate (Noden, 1989). Normally, in the chick, the major vessels are assembled from local angioblasts (Pardanaud *et al.*, 1987, 1989; Coffin and Poole, 1988; Poole and Coffin, 1991; Couly *et al.*, 1995), but there is also evidence for long migrations from angioblast site of origin to vessel (Coffin and Poole, 1988, 1991; Noden, 1989, 1991). Transplanted mesoderm can populate ectopic sites with angioblasts (Noden, 1989). Tissues normally vascularized by sprouting, such as limb or ectodermal derivatives, receive such angiogenic input even after transplantation to a different host (Pardanaud *et al.*, 1989). These observations suggest that assembly of major vessels is driven by local cues. Two tissues in close proximity to the developing trunk vasculature, which are candidates for provision of such signals, are the notochord and the endoderm.

Notochord Generates Signals for Assembly of the Aorta

In the trunk, *flk*-expressing cells are first evident in the mesoderm lateral and ventral to the somites and then appear to migrate to the midline. This region is referred to as the intermediate cell mass and is bounded above by notochord and below by endoderm. Notochord is known to pattern adjacent neurectoderm and somites. In the absence of notochord the floor plate does not differentiate and ventral cell fates are not achieved in the neuroectoderm (Goulding *et al.*, 1993) and sclerotome does not differentiate and myotomes fuse beneath the neural tube (Dietrich *et al.*, 1993; Pourquie *et al.*, 1993; Goulding *et al.*, 1994; Halpern *et al.*, 1995). The mediator of both signaling events is believed to be sonic hedgehog (Fan and Tessier-Lavigne, 1994; Johnson *et al.*, 1994). Recently it has been shown that notochord affects the laterality and migratory behavior of endothelial cells (Klessinger and Christ, 1996).

Vessel formation in zebrafish notochord mutants, *flh* and *ntl*, is abnormal. *flh* lacks notochord due to mutation in the transcription factor *Xnot*, and *no tail* blocks notochord differentiation by mutation in *brachyury*. In *flh*, both somites and neural tube are perturbed, such that somites fuse beneath the notochord and floor plate does not form. In *ntl*, on the other hand, notochord precursors form and generate signals sufficient to pattern floor plate and to prevent somite fusion, although floor plate forms in a wider band and somites lack their normal chevron shape. Hence, it is believed that different signals (either quantitatively or qualitatively) are generated by the notochord during different stages of its differentiation. The effect on vasculogenesis could reflect perturbation in signals from notochord or its precursors. We have no evidence for or against a role in vessel assembly of the best-defined notochord signal, sonic hedgehog, which certainly does pattern somites and ventral neural tube (Fan and Tessier-Lavigne, 1994; Johnson *et al.*, 1994). The ligand for *flk*, VEGF is ubiquitously expressed during development of mouse and quail, (Breier *et al.*, 1992; Flamme *et al.*, 1995a), most prominently in endoderm (Dumont *et al.*, 1995). Since *flk*-expressing cells are present ventrally in both *flh* and *ntl*, and can even form a tubular structure near the yolk, it is possible that the partial assembly of a vessel adjacent to the yolk, presumably pieces of vein, is due to support of vein formation by this or other signals from the endoderm (Weinstein *et al.*, personal communication).

It is conceivable that the failure of *flk*-expressing cells to form aorta in *flh* could be due to physical obstruction by the fused somites, but this seems unlikely because *ntl* mutants also have just one vessel but do not have fused somites in the trunk and because somites themselves contain angioblasts, at least in chick (Wilting *et al.*, 1995). Thus, it appears that normal notochord is needed for maintenance of *flk* expression and for normal axial vessel assembly, especially of the dorsal aorta, and that the vein is less dependent upon notochord. Of course, the signals which directly affect vessels need not be generated by the notochord per se, but could alternatively be derived from somites or other tissues dependent upon notochord.

ACKNOWLEDGMENTS

We thank Chris Simpson for expert technical help and Drs. J.-N. Chen and K. S. Warren for helpful discussions. This work was

Copyright © 1997 by Academic Press. All rights of reproduction in any form reserved.

supported in part by NIH RO1-HL49579. Support for B.F. was from Boehringer Ingelheim Fonds and EMBO and for B.M.W. from Training Grant NIH T32-HL07208. Sequence data from this article have been deposited with the EMBL/GenBank Data Libraries under Accession No. U82383.

REFERENCES

Breier, G., Albrecht, U., Sterrer, S., and Risau, W. (1992). Expression of vascular endothelial growth factor during embryonic angiogenesis and endothelial cell differentiation. *Development* **114,** 521–532.

Chen, J.-N., and Fishman, M. C. (1996). Zebrafish tinman homolog demarcates the heart field and initiates myocardial differentiation. *Development* **122,** 3809–3816.

Coffin, J. D., and Poole, T. J. (1988). Embryonic vascular development: immunohistochemical identification of the origin and subsequent morphogenesis of the major vessel primordia in quail embryos. *Development* **102,** 735–748.

Coffin, J. D., and Poole, T. J. (1991). Endothelial cell origin and migration in embryonic heart and cranial blood vessel development. *Anat. Rec.* **231,** 383–395.

Couly, G., Coltey, P., Eichmann, A., and Le Douarin, N. M. (1995). The angiogenic potentials of the cephalic mesoderm and the origin of brain and head blood vessels. *Mech. Dev.* **53,** 97–112.

Dieterlen-Lievre, F., and Marin, C. (1981). Diffuse intraembryonic hemopoiesis in normal and chimeric avian development. *Dev. Biol.* **88,** 180–191.

Dietrich, S., Schubert, F. R., and Gruss, P. (1993). Altered *Pax* gene expression in murine notochord mutants: The notochord is required to initiate and maintain ventral identity in the somite. *Mech. Dev.* **44,** 189–207.

Drake, C. J., and Little, C. D. (1995). Exogenous vascular endothelial growth factor induces malformed and hyperfused vessels during embryonic neovascularization. *Proc. Natl. Acad. Sci. USA* **92,** 7657–7661.

Dumont, D. J., Fong, G.-H., Puri, M. C., Gradwohl, G., Alitalo, K., and Breitman, M. L. (1995). Vascularization of the mouse embryo: a study of *flk-1, tek, tie* and vascular endothelial growth factor expression during development. *Dev. Dyn.* **203,** 80–92.

Eichmann, A., Marcelle, C., Breant, C., and Le Douarin, N. M. (1993). Two molecules related to the VEGF receptor are expressed in early endothelial cells during avian development. *Mech. Dev.* **42,** 33–48.

Fan, C. M., and Tessier-Lavigne, M. (1994). Patterning of mammalian somites by surface ectoderm and notochord: evidence for sclerotome induction by a hedgehog homolog. *Cell* **79,** 1175–1186.

Flamme, I., Breier, G., and Risau, W. (1995a). Vascular endothelial growth factor (VEGF) and VEGF receptor 2 (*flk-1*) are expressed during vasculogenesis and vascular differentiation in the quail embryo. *Dev. Biol.* **169,** 699–712.

Flamme, I., von Reutern, M., Drexler, H. C., Syed-Ali, S., and Risau, W. (1995b). Overexpression of vascular endothelial growth factor in the avian embryo induces hypervascularization and increased vascular permeability without alterations of embryonic pattern formation. *Dev. Biol.* **171,** 399–414.

Fong, G.-H., Rossant, J., Gertsenstein, M., and Breitman, M. L. (1995). Role of the flt-1 receptor tyrosine kinase in regulating the assembly of vascular endothelium. *Nature* **376,** 66–70.

Gont, L. K., Steinbeisser, H., Blumberg, B., and De Robertis, E. M. (1993). Tail formation as a continuation of gastrulation: The multiple cell populations of the *Xenopus* tailbud derive from the late blastopore lip. *Development* **119,** 991–1004.

Goulding, M., Lumsden, A., and Paquette, A. J. (1994). Regulation of Pax-3 expression in the dermomyotome and its role in muscle development. *Development* **120,** 957–971.

Goulding, M. D., Lumsden, A., and Gruss, P. (1993). Signals from the notochord and floor plate regulate the region-specific expression of two Pax genes in the developing spinal cord. *Development* **117,** 1001–1016.

Hahn, H. (1909). Experimentelle Studien über die Entstehung des Blutes und der ersten Gefässe beim Hühnchen. *Wilhelm Roux' Entwicklungsmech. Org.* **27,** 337–433.

Halpern, M. E., Ho, R. K., Walker, C., and Kimmel, C. B. (1993). Induction of muscle pioneers and floor plate is distinguished by the zebrafish *no tail* mutation. *Cell* **75,** 99–111.

Halpern, M. E., Thisse, C., Ho, R. K., Thisse, B., Riggleman, B., Trevarrow, B., Weinberg, E. S., Postlethwait, J. H., and Kimmel, C. B. (1995). Cell-autonomous shift from axial to paraxial mesodermal development in zebrafish *floating head* mutants. *Development* **121,** 4257–4264.

Herrmann, B. G., Labeit, S., Poustka, A., King, T. R., and Lehrach, H. (1990). Cloning of the T gene required in mesoderm formation in the mouse. *Nature* **343,** 617–622.

His, W. (1900). Lecithoblast und Angioblast der Wirbeltiere. *Abh. Math-phys. Ges Wiss.* **26,** 171–328.

Ho, R. K., and Kane, D. A. (1991). Cell-autonomous action of zebrafish *spt-1* mutation in specific mesodermal precursors. *Nature* **348,** 728–730.

Ho, R. K., and Kimmel, C. B. (1993). Commitment of cell fate in the early zebrafish embryo. *Science* **261,** 109–111.

Johnson, R. L., Laufer, E., Riddle, R. D., and Tabin, C. (1994). Ectopic expression of *sonic* hedgehog alters dorsal-ventral patterning of somites. *Cell* **79,** 1165–1173.

Jowett, T., and Lettice, L. (1994). Whole-mount in situ hybridizations on zebrafish embryos using a mixture of digoxigenin- and fluorescein-labelled probes. *Trends Genet.* **10,** 73–74.

Keck, P. J., Hauser, S. D., Krivi, G., Sanzo, K., Warren, T., Feder, J., and Connolly, D. T. (1989). Vascular permeability factor, an endothelial mitogen related to PDGF. *Science* **246,** 1309–1312.

Kimmel, C. B., Ballard, W. W., Kimmel, S. R., Ullmann, B., and Schilling, T. F. (1995). Stages of embryonic development of the zebrafish. *Dev. Dyn.* **203,** 253–310.

Klessinger, S., and Christ, B. (1996). Axial structures control laterality in the distribution pattern of endothelial cells. *Anat. Embryol.* **193,** 319–330.

Lee, R. K. K., Stainier, D. Y. R., Weinstein, B. M., and Fishman, M. C. (1994). Cardiovascular development in the zebrafish. II. Endocardial progenitors are sequestered in the heart field. *Development* **120,** 3361–3366.

Leung, D. W., Cachianes, G., Kuang, W.-J., Goeddel, D. V., and Ferrara, N. (1989). Vascular endothelial growth factor is a secreted angiogenic mitogen. *Science* **246,** 1306–1309.

Liao, W., Bisgrove, B. W., H., S., Hug, B., Bell, B., Peters, K., Grunwald, D. J., and Stainier, D. Y. S. (1997). The zebrafish gene *cloche* acts upstream of a *flk-1* homologue to regulate endothelial cell differentiation. *Development* **124,** 381–389.

Matthews, W., Jordan, C. T., Gavin, M., Jenkins, N. A., Copeland, N. G., and Lemischka, I. R. (1991). A receptor tyrosine kinase cDNA isolated from a population of enriched primitive hematopoietic cells and exhibiting close genetic linkage c-*kit*. *Proc. Natl. Acad. Sci. USA* **88,** 9026–9030.

Melby, A. E., Warga, R. M., and Kimmel, C. B. (1996). Specification of cell fates at the dorsal margin of the zebrafish gastrula. *Development* **122,** 2225–2237.

Copyright © 1997 by Academic Press. All rights of reproduction in any form reserved.

Millauer, B., Wizigmann-Voos, S., Schürch, H., Martinez, R., Möller, N. P. H., Risau, W., and Ullrich, A. (1993). High affinity VEGF binding and developmental expression suggest *flk-1* as a major regulator of vasculogenesis and angiogenesis. *Cell* **72,** 835–846.

Noden, D. M. (1989). Embryonic origins and assembly of blood vessels. *Am. Rev. Res. Dis.* **140,** 1097–1103.

Noden, D. M. (1991). Origins and patterning of avian outflow tract endocardium. *Development* **111,** 867–876.

Pardanaud, L., Altmann, C., Kitos, P., Dieterlen-Lievre, F., and Buck, C. A. (1987). Vasculogenesis in the early quail blastodisc as studied with a monoclonal antibody recognizing endothelial cells. *Development* **100,** 339–349.

Pardanaud, L., Luton, D., Prigent, M., Bourcheix, L.-M., Catala, M., and Dieterlen-Lievre, F. (1996). Two distinct endothelial lineages in ontogeny, one of them related to hemopoiesis. *Development* **122,** 1363–1371.

Pardanaud, L., Yassine, F., and Dieterlen-Lievre, F. (1989). Relationship between vasculogenesis, angiogenesis and haemopoiesis during avian ontogeny. *Development* **105,** 473–485.

Poole, T. J., and Coffin, J. D. (1991). Morphogenetic mechanisms in avian vascular development. *In* "The Development of the Vascular System" (S. G. Feinberg and R. N. Auerbach, Eds.), pp. 25–36. Issues Biomed., Basel.

Pourquie, O., Coltey, M., Teillet, M.-A., Ordahl, C., and Le Douarin, N. M. (1993). Control of dorsoventral patterning of somitic derivatives by notochord and floor plate. *Proc. Natl. Acad. Sci. USA* **90,** 5242–5246.

Reagan, F. P. (1915). Vascularization phenomena in fragments of embryonic bodies completely isolated from yolk-sac blastoderm. *Anat. Rec.* **9,** 329–341.

Risau, W. (1991). Vasculogenesis, angiogenesis and endothelial cell differentiation during embryonic development. *In* "The Development of the Vascular System" (R. N. Feinberg, G. K. Scherer, and R. Auerbach, Eds.), pp. 58–68. Issues Biomed., Basel.

Risau, W., Sariola, H., Zerwes, H.-G., Sasse, J., Ekblom, P., Kemler, R., and Doetschman, T. (1988). Vasculogenesis and angiogenesis in embryonic-stem-cell-derived embryoid bodies. *Development* **102,** 471–478.

Sabin, F. R. (1917). Origin and development of the primitive vessels of the chick and of the pig. *Contrib. Embryol. Carnegie Inst. Washington* **226,** 61–124.

Schulte-Merker, S., van Eeden, F. J. M., Halpern, M. E., Kimmel, C. B., and Nüsslein-Volhard, C. (1994). *no tail* (*ntl*) is the zebrafish homologue of the mouse *T* (*Brachyury*) gene. *Development* **120,** 1009–1015.

Shalaby, F., Rossant, J., Yamaguchi, T. P., Gertsenstein, M., Wu, X.-F., Breitman, M. L., and Schuh, A. C. (1995). Failure of blood island formation and vasculogenesis in *flk-1* deficient mice. *Nature* **376,** 62–66.

Shibuya, M., Yamaguchi, S., Yamane, A., Ikeda, T., Tojo, A., Matsuhsime, H., and Sato, M. (1990). Nucleotide sequence and expression of a novel human receptor-type tyrosine kinase gene (*flt*) closely related to the *fms* family. *Oncogene* **5,** 519–524.

Stainier, D. Y. R., Fouquet, B., Chen, J.-N., Warren, K. S., Weinstein, B. M., Meiler, S., Mohideen, M.-A. P. K., Neuhauss, S. C. F., Solnica-Krezel, L., Schier, A. F., Zwartkruis, F., Stemple, D. L., Malicki, J., Driever, W., and Fishman, M. C. (1996). Mutations affecting the formation and function of the cardiovascular system in the zebrafish embryo. *Development* **123,** 285–292.

Stainier, D. Y. R., Lee, R. K., and Fishman, M. C. (1993). Cardiovascular development in the zebrafish: I. Myocardial fate map and heart tube formation. *Development* **119,** 31–40.

Stainier, D. Y. R., Weinstein, B. M., Detrich III, H. W., Zon, L. I., and Fishman, M. C. (1995). *Cloche,* an early acting zebrafish gene, is required by both the endothelial and hematopoietic lineages. *Development* **121,** 3141–3150.

Talbot, W. S., Trevarrow, B., Halpern, M. E., Melby, A. E., Farr, G., Postlethwait, J. H., Jovett, T., Kimmel, C. B., and Kimelman, D. (1995). A homeobox gene essential for zebrafish notochord development. *Nature* **378,** 150–157.

Terman, B. I., Carrion, M. E., Kovacs, E., Rasmussen, B. A., Eddy, R. L., and Shows, T. B. (1991). Identification of a new endothelial cell growth factor receptor tyrosine kinase. *Oncogene* **6,** 1677–1683.

von Dassow, G., Schmidt, J. E., and Kimelman, D. (1993). Induction of the *Xenopus* organizer: expression and regulation of *Xnot,* a novel FGF and activin-regulated homeo box gene. *Genes. Dev.* **7,** 355–366.

Weinstein, B. M., Stemple, D. L., Driever, W., and Fishman, M. C. (1995). *gridlock,* a localized heritable vascular patterning defect in the zebrafish. *Nature Med.* **1,** 1143–1147.

Wilks, A. F. (1989). Two putative protein-tyrosine kinases identified by application of the polymerase chain reaction. *Proc. Natl. Acad. Sci. USA* **86,** 1603–1607.

Wilting, J., Brand-Saberi, B., Ruijin, H., Zhi, Q., Köntges, G., Ordahl, C. P., and Christ, B. (1995). Angiogenic potential of the avian somite. *Dev. Dyn.* **202,** 165–171.

Yamaguchi, T. P., Dumont, D. J., Conlon, R. A., Breitman, M. L., and Rossant, J. (1993). *flk-1,* an *flt-1* related tyrosine kinase is an early marker for endothelial cell precursors. *Development* **118,** 489–498.

Received for publication September 24, 1996
Accepted December 13, 1996

Copyright © 1997 by Academic Press. All rights of reproduction in any form reserved.

DEVELOPMENTAL BIOLOGY 183, 49–60 (1997)
ARTICLE NO. DB968450

Branchial HOX Gene Expression and Human Craniofacial Development

Isabelle Vieille-Grosjean,* Paul Hunt,* Massimo Gulisano,† Edoardo Boncinelli,† and Peter Thorogood*

**Developmental Biology Unit, Institute of Child Health (London University), 30 Guilford Street, London WC1N 1EH, Britain; †Dipartimento di Ricerca Biologica e Tecnologica, Istituto Scientifico H San Raffaele, Via Olgettina 58, 20132 Milan, Italy*

Members of the *Antennapedia* class of homeobox genes, known as Hox genes, are believed to be pivotal in vertebrate craniofacial development. Here we show that eight members of paralogous groups 1, 2, 3, and 4 are expressed in the human embryonic hindbrain and branchial arches at 4 weeks of development. The combinatorial patterns of expression of genes representing the first three paralogous groups parallel the patterns described for their homologues in various animal models, demonstrating a high degree of conservation of the branchial Hox code. Arch expression of group 4 genes is defined for the first time in any vertebrate. Furthermore, as development proceeds, individual paralogues of a single paralogous group (group 3), which initially share a common expression domain, are differentially down-regulated in a tissue-, organ-, or site-specific fashion. © 1997 Academic Press

INTRODUCTION

Recent years have seen dramatic progress in identification of genes critically involved in craniofacial development during early embryogenesis and, in particular, recognition of the involvement of homeobox-containing regulatory genes in this process. Although our understanding of craniofacial morphogenesis lacks a unifying hypothesis, one of the most influential models to have emerged to date is based on the expression patterns of the genes of the *Antennapedia* class of homeobox genes, the so-called "Hox" genes, described in various animal model systems, chiefly the mouse. These genes, totalling some 38 in number, are organized in four clusters located on different chromosomes (Fig. 1) and believed to be derived from a common ancestral cluster, from which the single HOM-C complex in *Drosophila* (Manak and Scott, 1994) is also derived. Cluster duplication during the course of evolution has led to the phenomenon of paralogy whereby groups of up to four genes, derived from a common ancestral gene in the primitive cluster, are identifiable across contemporary clusters by virtue of their 3′ to 5′ position and their sequence homologies with each other (McGinnis and Krumlauf, 1992). Such paralogues can display equivalent expression domains and may therefore have common functions during development, resulting in some functional redundancy (Hunt and Krumlauf, 1992). Significantly, Hox genes are expressed in precise patterns during early embryogenesis particularly during critical periods of fate specification within morphogenetic fields, such as the limb and genital tubercle (Duboule, 1992; Dollé *et al.*, 1991). The expression domains of the various groups overlap to different extents within any particular field, leading to the concept that the role of Hox genes is fulfilled by a combinatorial mode of action (Hunt and Krumlauf, 1992). Along the body axis these genes are generally expressed with discrete rostral cutoffs which coincide with either existing or emergent anatomical landmarks and which therefore have been interpreted as serving to specify component parts of the vertebrate body plan. Significantly, the rostro–caudal sequence of these cutoffs maps quite precisely with the 3′ to 5′ sequence of the Hox genes within their respective cluster and with the order in which these genes are expressed, phenomena known as spatial and temporal colinearity, respectively (Duboule and Dollé, 1989).

The existence of such cutoffs at sclerotomal boundaries has been used as the basis of a combinatorial "Hox code" for the developing vertebral column (Kessel and Gruss, 1990). This model has been tested by both transgenic and teratogenic strategies and, in most instances, the resultant changes of the code elicit a homeotic transformation of vertebral phenotype (Lufkin *et al.*, 1992; Kessel and Gruss, 1991). Generally, the phenotypic consequences of transgenic inactivation coincide with the rostral expression boundary, suggesting that this is the critical region of the expression domain. In the embryonic head, the genes of

0012-1606/97 $25.00
Copyright © 1997 by Academic Press
All rights of reproduction in any form reserved.

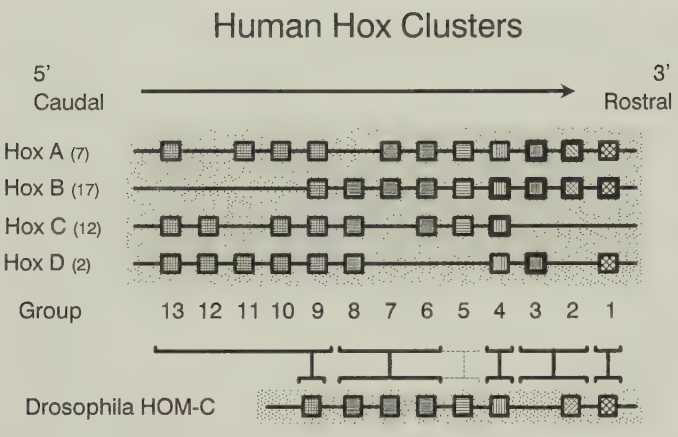

FIG. 1. Schematic representation of human *HOX* genes clusters and their chromosomal locations. Clusters are aligned so that paralogous genes belonging to the same group correspond vertically. The *Drosophila HOM-C* complex and known homologies with vertebrate genes are shown below. Direction of transcription is indicated by the arrow. Genes situated at the 3′ end of the clusters are expressed more rostrally and earlier than genes at the 5′ end. The eight genes from groups 1 to 4 used in this study are indicated in bold outline. All members of groups 2 and 3 have been studied, as well as all *HOXB* genes belonging to the four groups.

the first four paralagous groups have been found to display cutoffs within the hindbrain (rhombencephalon) at the interfaces between the repeating metameric units termed rhombomeres (Wilkinson *et al.*, 1989). Thus, for example, groups 3 and 4 have rostral cutoffs at interfaces between rhombomeres 4/5 and 6/7, respectively. Subsequently, neural crest cells derived from the hindbrain migrate into branchial arches at equivalent axial levels and give rise to much of the facial mesenchyme. Thus, crest cells from rhombomeres 1 and 2 migrate to colonize arch 1 (the mandibular arch), expressing no Hox genes. Caudally, the migrating crest cells maintain the combination of Hox gene expression, which characterized their rhombomere of origin. Cells from rhombomeres 4 and 6 migrate into arches two and three, respectively (Lumsden *et al.*, 1991). A segmental organization of crest migration is ensured by crest cells from rhombomeres 3 and 5 either being lost through apoptosis (Lumsden *et al.*, 1991; Graham *et al.*, 1993) or merging with the streams of cells emigrating from rhombomeres 4 and 6 (Sechrist *et al.*, 1993). Events caudal to arch three are speculative, but the model predicts that cells from rhombomeres 7 and 8 migrate into the fourth arch and possibly the sixth arch (modern convention holds that the fifth arch was lost during evolution), although there is no hard evidence for this. The branchial Hox code defined by the patterns of combinatorial Hox gene expression (Hunt *et al.*, 1991a) has been interpreted as a developmental strategy whereby positional specification made axially within the neural tube is transmitted to the periphery (the arches) via the migrating neural crest, and it is seen as an integral part of the mechanisms whereby a vertebrate embryo builds a head and face (Hunt *et al.*, 1991b). Even though downstream targets are largely unknown, various transgenic (e.g., Gendron-Maguire *et al.*, 1993) and experimental embryological (e.g., Hunt *et al.*, 1995) strategies indicate that this interpretation is largely correct. To date all of this is based on analysis and manipulation of various animal model systems, chiefly the mouse. The assumption has been made, in the absence of any comprehensive data, that the paradigms emerging are applicable to all vertebrates, including humans. However, given the pivotal role proposed for these genes, and for the combinatorial manner in which they are expressed, elucidation of the human expression patterns is an essential prerequisite to understanding the molecular/genetic control of human facial development and indeed to understanding dysmorphogenesis of this complex process. Such data will also facilitate an assessment of the degree to which mouse embryogenesis can justifiably provide a model for human craniofacial development, an assumption which is frequently made but without any genetic foundation to date.

Here, in the first multigene expression study to be carried out using human embryonic tissue, we describe analysis of the human branchial arch Hox code, using specific probes against message from eight *HOX* genes (namely, *HOX B1, A2, B2, A3, B3, D3, B4,* and *C4*) whose mouse homologues have been previously identified as having cutoffs at the relevant axial levels. These genes include not only representatives of each of the first four paralogous groups but also two of those groups (2 and 3) in their entirety. *In situ* hybridization of tissue from two key developmental stages reveals a high degree of conservation of the code and differential down-regulation of members of a single paralogous group in a site-specific manner.

MATERIALS AND METHODS

Collection of Embryos

Human embryos were provided by the MRC-funded Human Embryo Bank maintained at Institute of Child Health/University College Hospital, having been collected with full ethical permission from RU486 terminations. The precise stage of embryonic development was determined by assessment of external morphology (Larsen, 1993).

In Situ Hybridization

Autoradiographic *in situ* hybridization was carried out basically as described by Wilkinson and Green (1990). Embryos were fixed in 4% paraformaldehyde in PBS (phosphate-buffered saline) (pH 7.0) overnight at 4°C, dehydrated through graded alcohols and Histo-Clear (National Diagnostics, Atlanta, GA), and embedded in paraffin wax (Fibrowax). Sections (6 μm) were cut and placed on slides pretreated with 3-aminopropyltriethoxysilane and acetone. The sections were dewaxed in Histo-Clear, rehydrated, and treated with 0.15 *M* NaCl before fixation in paraformaldehyde. Slides were subjected to proteinase K treatment, refixed, and treated with acetic anhydride.

Copyright © 1997 by Academic Press. All rights of reproduction in any form reserved.

RNA riboprobes were prepared with ^{35}S-UTP (Amersham > 1000 Ci/mmol) as run-off transcripts. The cDNA clones were derived from the 3′ untranslated region of *HOX A2, A3, HOX B1–B4, HOX D3,* and *HOX C4* genes (Acampora *et al.*, 1989; Simeone *et al.*, 1991), cloned into pGEM3 vector (Promega). The probes corresponded to the following fragments:

HOX A2	0.20 kb	*Eco*RI/*Taq*I
HOX A3	0.15 kb	*Hinc*II/*Hinc*II
HOX B1	0.20 kb	*Pvu*II/*Pvu*II
HOX B2	0.30 kb	*Taq*I/*Taq*I
HOX B3	0.15 kb	*Bgl*II/*Alu*I
HOX B4	0.30 kb	*Bgl*II/*Hin*dIII
HOX D3	0.30 kb	*Eco*RI/*Eco*RI
HOX C4	0.25 kb	*Xho*I/*Sma*I

The *HOX A2, A3, B1, B2, B3, C4,* and *D3* plasmids were linearized with *Hin*dIII, and the antisense riboprobes were generated using T7 RNA polymerase (Promega). *Eco*RI and Sp6 RNA polymerase (Promega) were used to generate the *HOX B4* antisense riboprobe. Probes were purified through columns of Sephadex G50, dehydrated, and redissolved at a final activity of 1×10^5 cpm/μl in hybridization buffer (50% formamide, 0.3 *M* NaCl, 20 m*M* Tris, 5 m*M* EDTA, pH 8.0, 10% dextran sulfate, 1× Denhardt's solution, 0.5 mg/ml tRNA). Hybridization was overnight at 55°C.

High-stringency washing was performed at 65°C in 50% formamide, 2× SSC, 10 m*M* DTT for 30 min, followed by incubation with RNase A at 20 μg/ml in 0.5 *M* NaCl, 10 m*M* Tris, 5 m*M* EDTA for 30 min. Sections were washed again, at high stringency (65°C), for 30 min, followed by two 15-min washes in 2× SSC and 0.1× SSC. Sections were then dehydrated through alcohol solutions containing 0.3 *M* ammonium acetate. Slides were dipped in Ilford K5 nuclear emulsion in 1% glycerol and kept at 4°C for 5 days, until developed. Sections were stained in 0.5% toluidine blue, dehydrated, and mounted in Permount for documentation.

The protocol for nonradioactive *in situ* hybridization on wax sections was based largely on the whole mount procedure described by Wilkinson (1992). Digoxigenin-labeled *HOX A3* riboprobe was generated using DIG-UTP (Boehringer) and T7 RNA polymerase. After precipitation with LiCl, probe was resuspended at 0.01 μg/μl in TE. Sections were dewaxed, rehydrated, and washed in PBT (0.1% Tween 20 in phosphate buffered saline). At this step, the rest of the procedure was carried out in 12-ml volumes using a slide mailer. Sections were treated 15 min with proteinase K (10 μg/ml) and refixed in 4% paraformaldehyde. Prehybridization was carried out 1 hr at 70°C in 50% formamide, 5× SSC, pH 4.5, 1% SDS, 50 μg/ml heparin, 50 μg/ml yeast tRNA. Hybridization mix containing the probe at 0.3 μg/ml was applied to sections which were then incubated overnight at 70°C. Slides were washed three times at 70°C in 50% formamide, 5× SSC, 1% SDS for 30 min, two times in 50% formamide, 2× SSC, 1% SDS at 70°C for 30 min, and three times at room temperature for 5 min in TBST (0.14 *M* NaCl, 2.7 m*M* KCl, 25 m*M* Tris–HCl, pH 7.5, 0.1% Tween 20). Slides were preblocked in 5% goat serum in TBST and then covered with the preabsorbed antidigoxigenin antibody (anti DIG-AP Fab fragment, Boehringer) at the final dilution of 5×10^{-4} and incubated overnight at 4°C. Slides were then washed three times with TBST for 5 min, five times with TBST for 1 hr, and then overnight in TBST at 4°C. On the following day, slides were washed three times for 10 min in NTMT (100 m*M* NaCl, 100 m*M* Tris–HCl, pH 9.5, 50 m*M* $MgCl_2$, 0.1% Tween 20) and covered with a solution containing 337 μg/ml NBT (nitroblue tetrazolium salt, Boehringer), 175 μg/ml BCIP (5-bromo-4-chloro-3-indolyl phosphate, Boehringer). The color reaction took place in the absence of light, at room temperature, after which slides were washed three times in PBS to stop further reaction. Finally slides were mounted in 50% glycerol for documentation.

Documentation

Slides were examined using an Olympus BH2 microscope and images captured electronically using a Kontron ProgRes3012 digital camera, version 2.0, of the associated software and stored as Adobe Photoshop v3.0 files.

RESULTS

Expression in Rhombomeres and Branchial Arches at 4 Weeks

We have chosen to study the expression of eight genes belonging to the paralogous groups 1, 2, 3, and 4, since it is known that these Hox genes are expressed in the hindbrain and branchial arches during embryogenesis of other vertebrate species, at similar stage of development. At 4 weeks postfertilization, the branchial arches display their maximum development before fusion and remodeling (Larsen, 1993). Four embryos of this stage have been used, aged from 28 to 30/31 days (Fig. 2). Each gene has been tested on sections from at least two embryos and in several independent experiments, with repeatable results (Table 1). Using *in situ* hybridization techniques on wax sections through the hindbrain and through the branchial arches, we have been able to define the expression pattern of *HOX B1, HOX A2, B2, HOX A3, B3, D3, HOX B4,* and *C4.* Figure 3 shows a series of coronal sections of 4-week embryos hybridized with these probes, with plane of section indicated in Fig. 2. Results are presented below, following the order of the four paralogous groups of genes within the clusters, and are summarized diagrammatically in Fig. 4.

The expression of one of the three genes constituting paralogous group 1, *HOX B1,* was studied (Figs. 3a and 3b). In the hindbrain, it was expressed as a single stripe in rhombomere 4. No expression was detected in branchial arches one, two, and three and expression was only detected in the caudal ectoderm of the fourth branchial arch and in the ectoderm lining the fourth cleft and covering the sixth arch. Expression was also detected in the dorsal endoderm of the foregut at the same axial level.

Both paralogues of group 2 were studied (Figs. 3c–3f). Within the hindbrain, expression of *HOX A2* displayed a clear rostral cutoff at the boundary between rhombomeres 1 and 2, whereas the cutoff for *HOX B2* occurred at the boundary between rhombomeres 2 and 3; in fact, *HOX B2* expression was higher in rhomobomeres 3, 4, and 5 than in more caudal rhombomeres. In contrast to these expression differences in the hindbrain, within the branchial arches the two paralogues had equivalent patterns of expression with signal being detected in arches two, three and four.

Copyright © 1997 by Academic Press. All rights of reproduction in any form reserved.

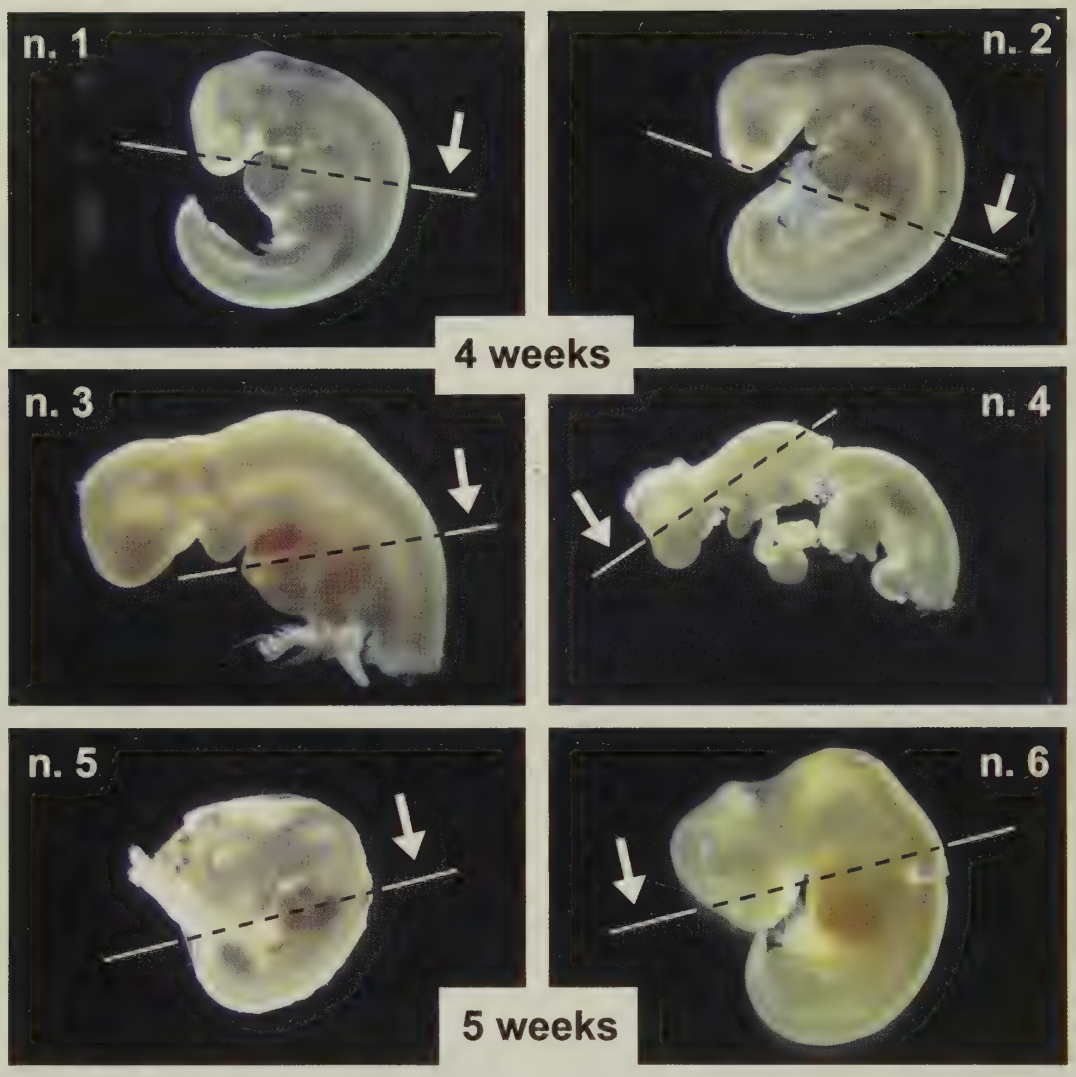

FIG. 2. The human embryos used in this study. Embryos are numbered from the earliest to the latest stage. Four are in the early fifth week of gestation (referred to as "4 weeks old"), and the two others are in the early sixth week (referred to as "5 weeks old"). Exact age is indicated in Table 1. Plane of section is indicated for each.

Group 3 contains three paralogous genes, all of which were examined (Figs. 3g–3l). *HOX A3, B3,* and *D3* presented the same rostral limit of expression in the hindbrain, between rhombomeres 4 and 5 but with some differences in the intensity of expression. Thus, expression of *HOX A3* was higher in rhombomeres 5 and 6 than in the more caudal segments, *HOX B3* was expressed less intensely in rhombomeres 5 and 6, and expression of *HOX D3* hardly detectable at this stage in rhombomere 5. All three genes were expressed in the branchial arches with a rostral limit of expression between arch two and arch three but again displayed regional differences in intensity; for example, the level of expression of *HOX B3* and *D3* was lower in the third arch than in the fourth arch, whereas *A3* was expressed uniformly throughout arches two, three, and four.

Finally, we have studied the expression pattern of two of the four genes belonging to group 4 (Figs. 3m–3p). Both *HOX B4* and *C4* were expressed in the more caudal rhombomeres. The expression pattern of *HOX B4* showed a clear cutoff at the boundary between rhombomere 6 and 7. In contrast, *HOX C4* displayed no equivalent cutoff, with its most rostral and weak expression observed in rhombomere 8 and gradually increasing caudad along the neural tube. At the level of the branchial arches, both genes were expressed in domains caudal to arch four. *HOX B4* was expressed in a large stripe of mesenchyme surrounding the pharyngeal region of foregut and in the surface ectoderm, whereas *HOX C4* expression was only detected in the dorsal endoderm of the foregut and surface ectoderm.

For some of these genes, specifically *HOX B2, HOX A3,*

Copyright © 1997 by Academic Press. All rights of reproduction in any form reserved.

TABLE 1
Developmental Stage of the Embryos Used in This Study

Age:		Embryo 1 28	Embryo 2 28	Embryo 3 29/30	Embryo 4 30/31	Embryo 5 35/36	Embryo 6 37
HOX B1	r	✓			✓		
	ba	✓			✓		
HOX A2	r		✓				
	ba		✓	✓			
HOX B2	r			✓	✓		
	ba	✓	✓		✓		
HOX A3	r			✓	✓	✓	✓
	ba		✓	✓	✓	✓	✓
HOX B3	r	✓	✓	✓	✓	✓	✓
	ba		✓	✓		✓	✓
HOX D3	r			✓	✓		✓
	ba			✓	✓	✓	✓
HOX B4	r		✓	✓	✓		
	ba		✓	✓	✓		
HOX C4	r		✓	✓			
	ba		✓	✓			

Note. The exact stage of development of the embryos used is expressed in days. Ticks indicate, for each gene, which embryos have been used successfully, for both sections through the rhombomeres (r) and sections through the branchial arches (ba).

HOX D3, and *HOX B4,* expression in the marginal layer of the neural tube, as assessed by autoradioactive *in situ* hybridization, appeared stronger than in the mantle layer (Figs. 3e, 3g, 3k, and 3m). To confirm that this was not an artefact due to toluidine blue staining, *HOX A3* expression was examined using a digoxigenin-labeled probe. Equivalent results were obtained with high signal distribution in the marginal layer and with characteristic strong *HOX A3* expression in rhombomere 5 (Fig. 5).

Expression in Rhombomeres and Branchial Arches at 5 Weeks

Since critical events in branchial arch morphogenesis commence during the fifth week of development in human embryos (growth, fusion, and remodelling of the arches as the first stages in face and neck development ensue (Larsen, 1993)), the pattern of expression of selected *HOX* genes was also assessed during this later stage. All three paralogues of group 3 were studied in order to investigate the possibility that members of an individual paralogous group become differentially expressed with time. Expression of *HOX A3, B3,* and *D3* was assessed, using two embryos of 5 weeks, 35/36, and 37 days old (Fig. 2, Table 1) with repeatable results obtained from both embryos (Fig. 6).

Within the hindbrain, expression of the three genes was identical to that defined previously in 4-week embryos, with a rostral limit of expression at rhombomere 5 (Figs. 6d and 6j). Expression of *HOX D3* in rhombomere 5 was more obvious at this stage of development (whereas it had been rather weak earlier), but nevertheless remains less intense than the signal in rhombomere 6 (Fig. 6j). More ventral sections, including those through the branchial arches, revealed that expression of all three genes in the more caudal neural tube was high, with expression also being observed in dorsal root ganglia (not illustrated).

In the branchial arches, the anterior limit of expression of the three genes remained between arches two and three, but differences between *HOX A3* and *D3* were becoming more apparent (Fig. 6). A clear cutoff was observed for both *HOX A3* and *HOX B3* between arch two and three (Figs. 6e and 6o), whereas expression of *HOX D3* was only found in the caudal mesenchyme of the third arch, displayed a poorly defined cutoff, and was absent in all other components of this arch (Fig. 6k). Similarly, in the fourth arch, *HOX D3* was strongly expressed in the mesenchyme but, again, not detectable in the other tissues of the arch.

Given that the thymus and parathyroid glands are both derived from the third branchial pouch (Larsen, 1993) and that *Hoxa-3* has been implicated in the normal development of these derivatives in the mouse (Chisaka and Capecchi, 1991), we analyzed wherever possible the expression of these genes in the different components of the branchial arches at this axial level, namely the surface ectoderm, the ectoderm-lined external clefts, the mesenchyme, and the endoderm-lined branchial pouches (Table 2). Significantly, there was differential expression within the third branchial pouch, with both *HOX A3* and *B3* being expressed by the endodermal epithelium but *HOX D3* not expressed (Figs. 6e, 6k, and 6o). More caudally, within the tracheolaryngeal groove (the site where the tracheal primordium exits from the primitive gut as a diverticulum) and the mesodermal arytenoid swellings (which will subsequently form the arytenoid cartilages), *HOX B3* alone was weakly expressed with no signal found for *A3* or *D3* (Figs. 6f, 6l, and 6p). In the thyroid primodium, limited data revealed that *HOX D3*

Copyright © 1997 by Academic Press. All rights of reproduction in any form reserved.

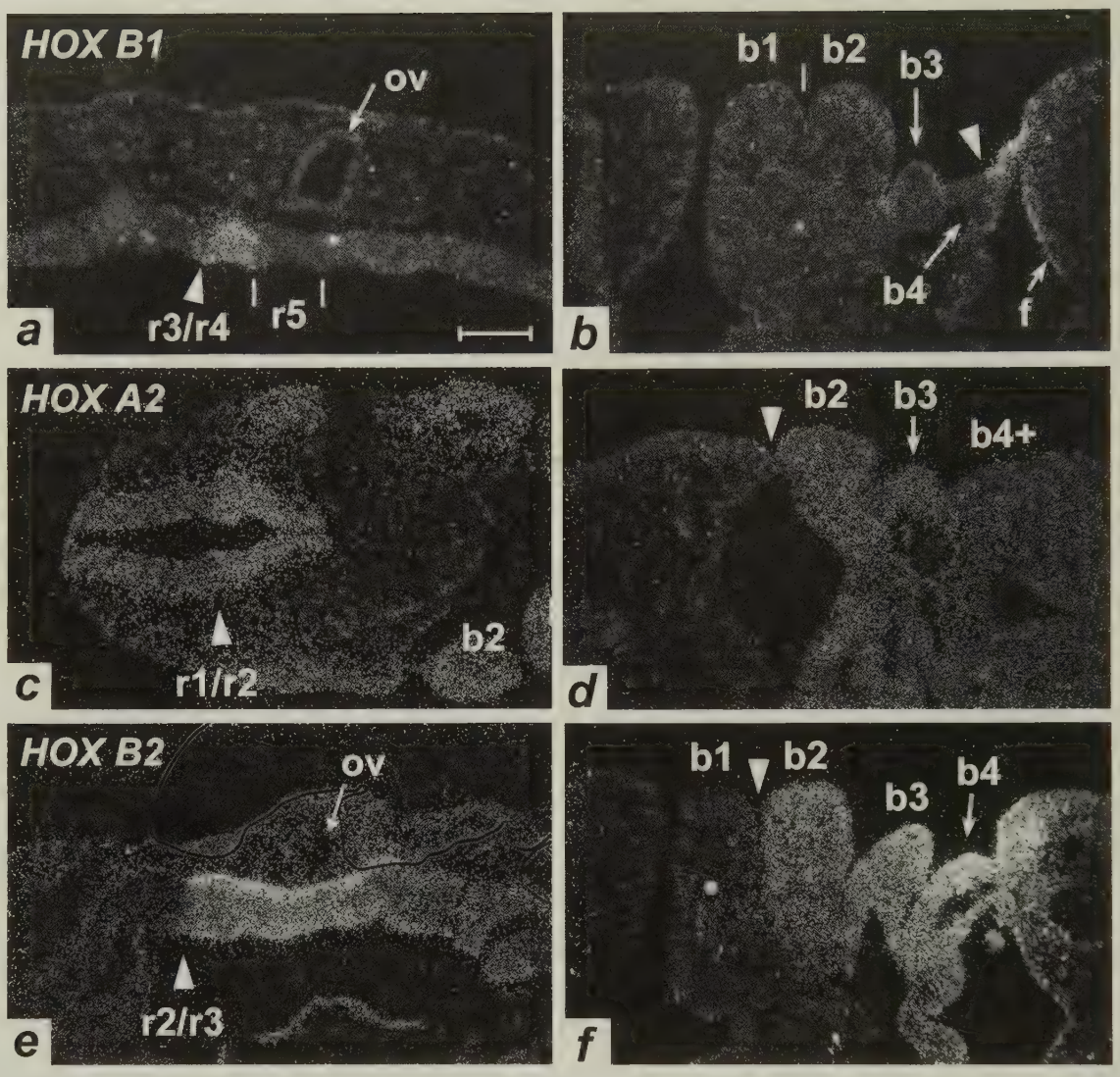

FIG. 3. Expression of *HOX* genes from paralogous groups 1, 2, 3, and 4 in the 4-week human embryos. For each gene, a dark-field image of a section through the rhombencephalon (left) and a section through the branchial arches (right) are shown side by side. Orientation of sections is rostral to the left and caudal to the right. In each panel, a white arrowhead indicates the anterior limit of the gene expression. Embryos used: in a, b, f, i, and j number 1; in c, d, m, n, o, and p number 2, in e, g, and h number 4, and in k and l number 3. Abbreviations: ov, otic vesicle; r3/r4, boundary between rhombomeres 3 and 4; b2/b3, boundary between branchial arches 2 and 3; f, pharyngeal region of foregut; g ix/x, combined superior ganglion of IXth and Xth nerves. Scale bar: 200 μm, for all panels.

was definitely not expressed (Fig. 6k), but we have no data on *A3* or *B3* expression within this structure.

DISCUSSION

The Vertebrate Branchial Hox Code Is Conserved in Humans

The single most striking result to emerge from this analysis is that the basic architecture of *HOX* gene expression is essentially the same in the branchial region of the 4-week human embryo as it is for other vertebrate species at equivalent stages of development (Wilkinson *et al.*, 1989; Hunt *et al.*, 1991a,b). From the genes studied here, this conclusion applies equally to both the rhombomeric region of the hindbrain and the branchial arches which will go on to form much of the face and neck. Clearly the vertebrate branchial "Hox code," as it has been elucidated from work in the mouse (Wilkinson *et al.*, 1989; Hunt *et al.*, 1991a,b) and from incomplete data from avian (Hunt *et al.*, 1995) and amphibian species (Godsave *et al.*, 1994), remains highly conserved in the spatial pattern of expression domains and, as far as we can tell, in the timing of its expression. Al-

Copyright © 1997 by Academic Press. All rights of reproduction in any form reserved.

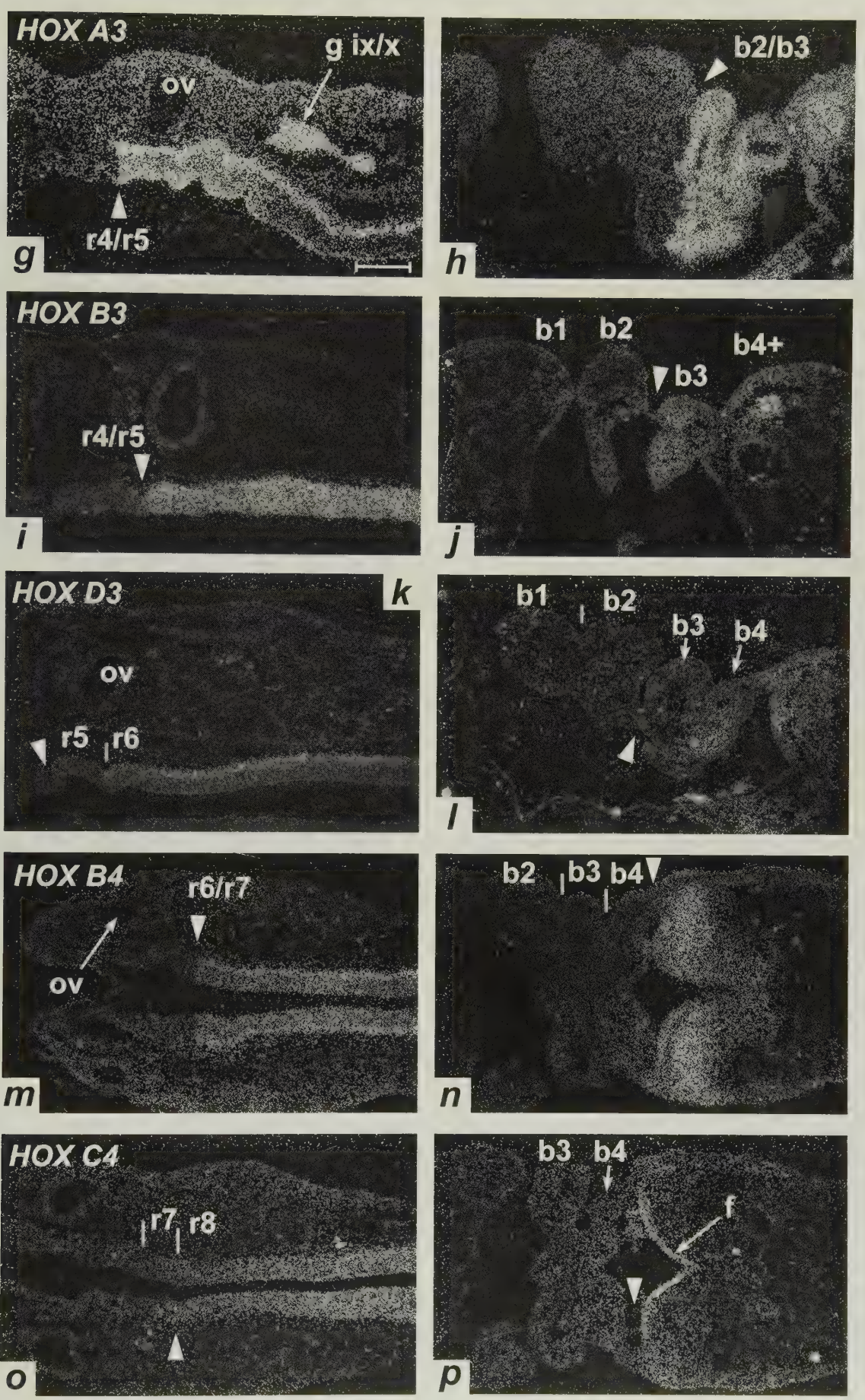

FIG. 3—*Continued*

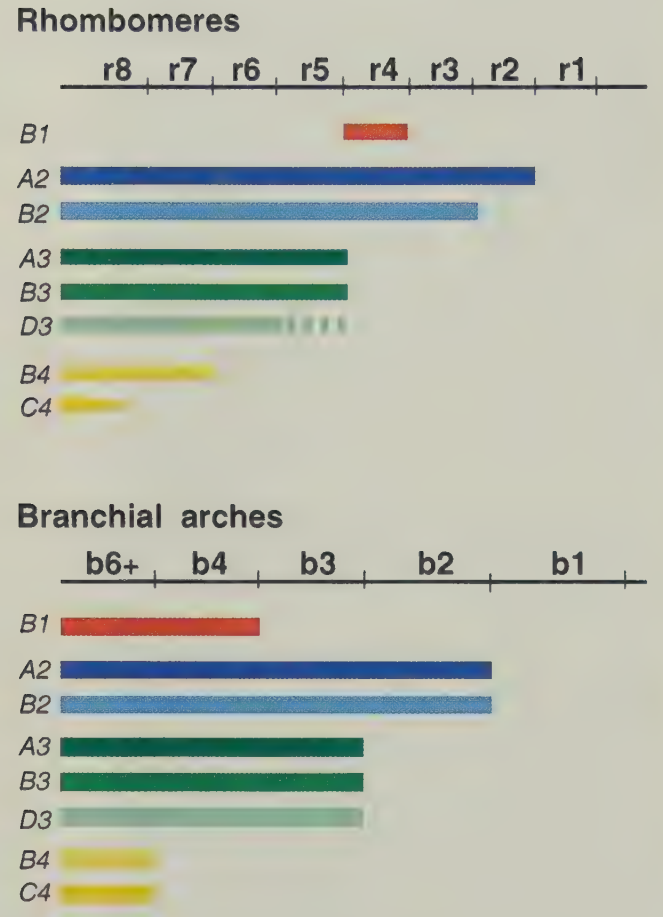

FIG. 4. The Hox code in the human branchial region. This diagram summarizes the results from Fig. 3, both in the rhombencephalon (top) and the branchial arches (bottom). At 4 weeks, the majority of the genes display clear rostral cutoffs along the embryonic axis, at boundaries between adjacent rhombomeres and between adjacent branchial arches. For *HOX B1*, expression in the hindbrain is confined to a single stripe in r4. The dotted line for *HOX D3* expression in r5 indicates a very weak expression; the arrowhead for *HOX C4* expression reflects an increasing intensity from r8 caudad along the neural tube.

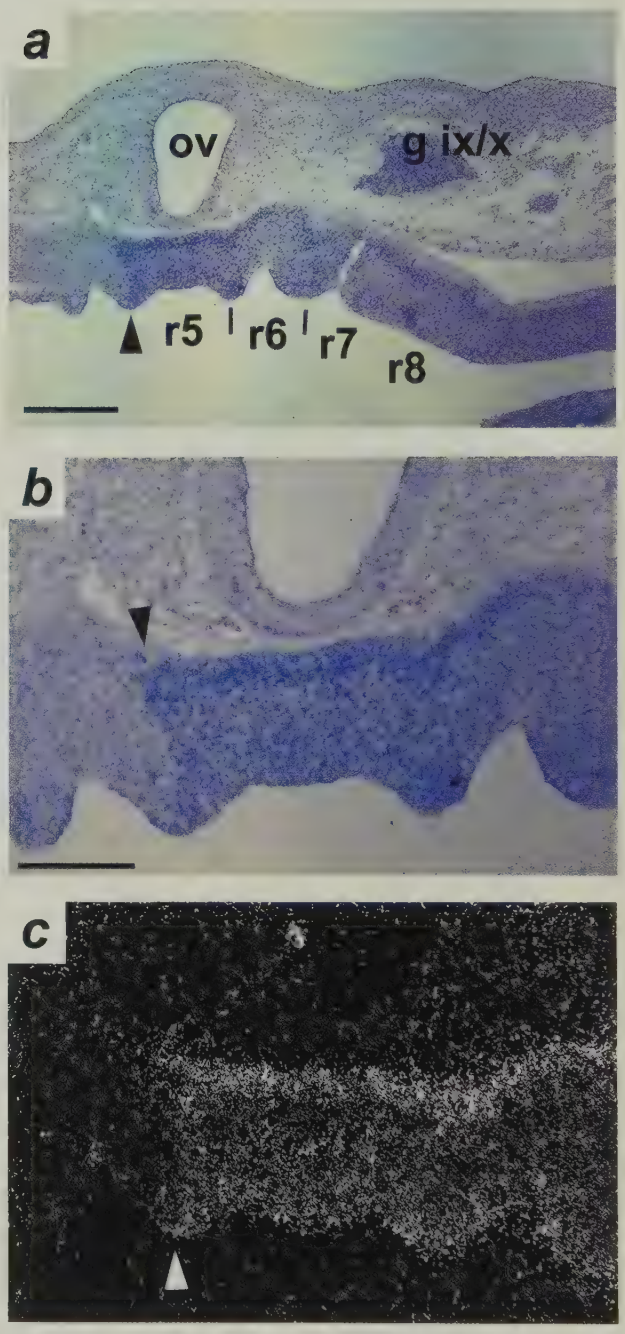

FIG. 5. Expression of *HOX A3* in the marginal layer of neural tube. (a, b) Bright-field images of the same section hybridized with a digoxigenin-labeled probe. (c) Dark-field image of the adjacent section hybridized with a radio-labeled probe. Arrowheads indicate the anterior gene expression cutoff. Sections from embryo number 4 were used throughout. Abbreviations: ov, otic vesicle; g ix/x, combined superior ganglion of IXth and Xth nerves; r, rhombomere. Scale bars: (a) 200 μm; (b) 100 μm.

though the existing data tell us nothing about conservation of function, the tight correlations observed here with the published mouse data suggest that the repertoire of *HOX* gene expression serves an equivalent function in the embryonic assembly of the head and face in the human and the mouse. Given that there appears to be little that is intrinsically different in the human branchial code then attention should now be focused on identity of the downstream target genes and their deployment during development.

Nevertheless, the issue of functional homology remains critical, since for all the current interest in homology, there has been no thorough appraisal of genetic conservation on this scale in humans. Although conservation might be expected, the fact remains that expectation and a rigorous evaluation of gene expression are two different things. Here we provide, for the first time and in any system, the confirmation of that expectation for human development. Fur-

Copyright © 1997 by Academic Press. All rights of reproduction in any form reserved.

thermore, it has to be borne in mind that a single demonstration such as this will not be sufficient since we cannot assume a priori that such assumptions will hold true for all those genes implicated directly or indirectly in human birth defects (and should species-specific differences in expression of any particular genes be found, it will necessitate a reevaluation of the assumptions we make about the validity of the mouse model in that instance).

The Human Data Vindicates the Mouse Model

A less obvious but nevertheless important corollary is that these data allow us to assess the extent to which the mouse can justifiably be used as a model system to understand human craniofacial development and its dysmorphogenesis. On the basis of the similarities in gene expression described here it would seem to be reasonable to assume that models of normal development based on Hox gene function, emerging from mouse work, can safely be extrapolated to the human. This will include data and paradigms emerging from transgenic manipulations but should not necessarily be extended uncritically to transgenic lines being adopted as models for human craniofacial anomalies. Indeed, apart from one notable exception (Chisaka and Capecchi, 1991; Manley and Capecchi, 1995) (see later) there is little evidence to date of a human craniofacial syndrome with a phenotype matching that produced by any mouse Hox knockout, suggesting that loss-of-function mutations in *HOX* genes are unlikely to be a common explanation for dysmorphic syndromes affecting the head and face.

The Human Data Extends the Model Derived from the Mouse

The model of a combinatorial code of Hox gene expression underlying the morphogenetic specification of the branchial arches, and therefore underpinning much of early facial development, is based largely on the orderly migration of crest cells from individual rhombomeres to specific arches as reported from animal studies (e.g., Lumsden *et al.*, 1991) (see earlier). Ironically, the human data presented here allow us to follow up several predictions of that model and to extend it significantly. In the first instance, although data exists for the first three branchial arches, migration of crest cells from rhombomeres 7 and 8 to the fourth arch is ill-defined and largely a prediction based on assumptions about serial homology (Hunt *et al.*, 1991a,b). This qualification applies also to the assumed expression of group 4 Hox genes in the fourth arch (Hunt *et al.*, 1991a). In fact, the analysis reported here extends what is known about the branchial arch hox code by assessing gene expression in the fourth arch. Surprisingly, group 4 genes are not expressed in the fourth arch and we could only find rostral cutoffs for *HOX B4* and *C4* immediately caudal to arch 4. Although it appears from this that assumptions about serial homology break down at the level of the more caudal arches, this may not necessarily be the case. Downregulation of expression of group 4 genes might occur during crest cell migration to, or shortly following, arrival in this arch destination; our data do not allow us to distinguish between these various possibilities. (Similarly, the expression of *HOX B1* in rhombomere 4, but with a rostral cutoff only detectable in arch four and not arch two, as might otherwise be predicted, may be explicable in the same way). Nevertheless, it is interesting that anterior boundaries of expression domains of *HOX* genes belonging to an individual paralogous group coincide in branchial arches, even if not in the neurectoderm (Fig. 4). The significance of this remains unclear.

Paralogous HOX Genes Become Differentially Expressed as Development Proceeds

A second advance is the observation that within a single paralogous group (in this instance, group 3), the various paralogues become differentially expressed as development proceeds. Thus, within days of the entire group being expressed within the branchial arch region and sharing an expression domain, we find modulation of expression domains emerging. For example, the *HOX D3* gene is only expressed in the caudal region of the third arch, unlike its two paralogues, which are expressed throughout. But perhaps more significantly, *HOX A3* and *D3* are differentially expressed within the lining of the third branchial pouch. This is significant not only in terms of what it reveals about normal development. It has fundamental implications for how we interpret dysmorphogenesis, not just in transgenic mouse phenotypes but also how we start to unravel the aetiology of human craniofacial problems. Thus, the transgenic inactivation of *Hoxa-3* in the mouse produces a dysmorphic phenotype which includes thymic aplasia, thyroid hypoplasia, and hypoparathyroidism, and it has been proposed as a model for the Di George syndrome in humans (Chisaka and Capecchi, 1991). Interestingly, the *Hoxd-3* knockout displays a different phenotype in which these tissues are unaffected and the primary defects are in the cervical vertebrae (Condie and Capecchi, 1993). Given that there are major endodermal contributions to both thymus and the parathyroid glands from the third branchial pouch (Larsen, 1993), our finding that of the two human paralogues, only *HOX A3* is expressed within the epithelial lining of this pouch serves two functions. First, it explains why individual inactivation of each of the two paralogues in the mouse produces two completely different phenotypes with regard to branchial pouch derivatives (Condie and Capecchi, 1994). Furthermore, our data, albeit incomplete, showing that *HOX D3* is definitely not expressed in the thyroid primordium, provide an explanation for why inactivation of this paralogue in the mouse leaves thyroid development unaffected. Second, it provides unique evidence supporting the contention that inactivation of *Hoxa-3* is a valuable model for Di George (Chisaka and Capecchi, 1991; Manley and Capecchi, 1995), since here we show that it is indeed expressed in the pouch from which the human thymus and parathyroids are derived. *HOX A3* may serve to regulate the unidentified Di George genes (at 22q11 and 10p13), which is perhaps why the *Hoxa-3* knockout displays some of the

Copyright © 1997 by Academic Press. All rights of reproduction in any form reserved.

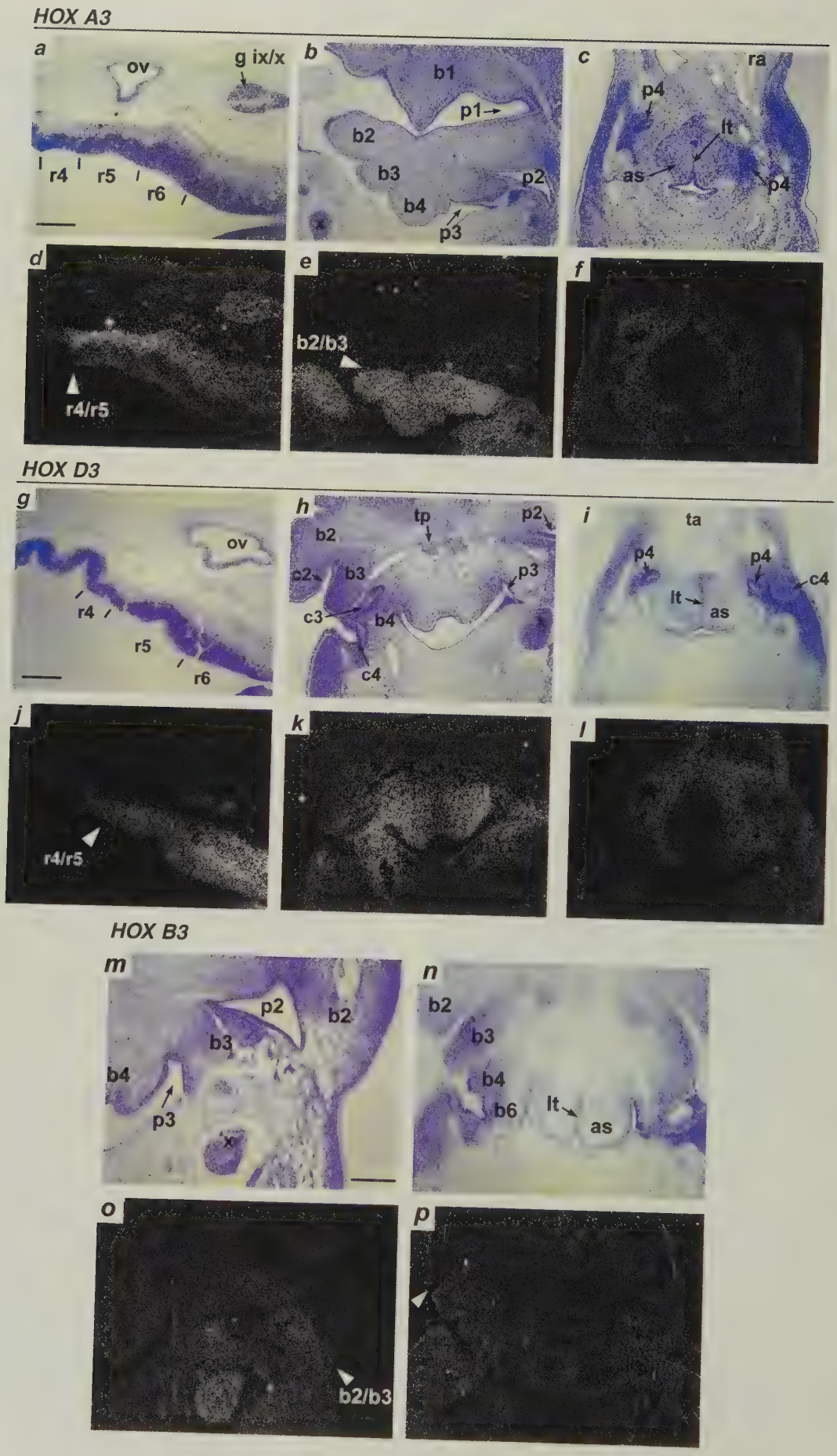
HOX A3
a
ov
g ix/x
r4
r5
r6
b
b1
p1
b2
b3
p2
b4
p3
c
ra
p4
lt
as
p4
d
r4/r5
e
b2/b3
f
HOX D3
g
ov
r4
r5
r6
h
tp
p2
b2
c2
b3
p3
c3
b4
c4
i
ta
p4
p4
c4
lt
as
j
r4/r5
k
l
HOX B3
m
p2
b2
b3
b4
p3
x
n
b2
b3
b4
b6
lt
as
o
b2/b3
p

TABLE 2
Expression of Group 3 *HOX* Genes in Branchial Arch Components

	HOX A3		*HOX B3*		*HOX D3*	
	4w	5w	4w	5w	4w	5w
Second arch						
Second pouch	–	–	–	–	–	–
Third arch						
Surface ectoderm	+	+	+	<+	–	–
Third cleft	+	?	+	<+	–	–
Mesenchyme	+	+	+	<+	+	+
Third pouch	+	+	?	<+	–	–
Fourth arch						
Surface ectoderm	+	+	+	<+	–	–
Fourth cleft	+	?	+	?	–	–
Mesenchyme	+	+	+	<+	+	+
Fourth pouch	+	–	+	?	–	–
Oropharynx	+	<+	+	<+	–	–

Note. Expression of *HOX A3, B3,* and *D3* in branchial arch components, compared between the two stages studied. ("4w" and "5w," 4 weeks and 5 weeks, respectively). –, no expression detected over the background; +, expression; <+, weak expression; ?, no data or equivocal result.

features of the syndrome. Should this be the case, then the noted variation in syndromic phenotype may reflect subtle polymorphisms in a regulatory Hox gene which would not necessarily be apparent when using the mouse model.

The Branchial Hox Code and Human Craniofacial Dysmorphogenesis

Aside from the Di George model, Hox genes haven't been broadly implicated to date as common loci for mutations generating human craniofacial abnormalities. Nevertheless, given the undoubted importance of this family of genes within the genetic hierarchy of craniofacial morphogenesis, delineation of those genes comprising the human branchial Hox code, and of their spatiotemporal patterns of expression, is an essential and integral part of understanding the molecular events underlying craniofacial dysmorphogenesis in humans. This is perhaps exemplified by retinoic acid-induced abnormalities (Morriss-Kay, 1993), where a characteristic phenotype is generated in the human (Lammer *et al.,* 1985). Given the retinoic acid response elements are contained within the enhancer of some Hox genes (Marshall *et al.,* 1994; Ogura and Evans, 1995), such as *Hoxb-1,* and that *in vitro* activation of Hox genes in a 3′ to 5′ sequence can be induced by increasing concentrations of retinoic acid (Simeone *et al.,* 1990), then a more insightful explanation of how elevated retinoid levels operate as craniofacial teratogens becomes possible. A similar rationale can be used regarding known instances of genetic "cross-talk" involving Hox genes and, perhaps eventually, for other craniofacial teratogens.

The Use of Human Embryo Banks

In a strategic sense, completion of this task demonstrates that even within the constraints imposed by the comparative rarity and finite availability of human embryos, judicious use of such material can generate comprehensive and valuable data. Here we provide the first published instance of a multigene expression analysis of human embryonic or fetal tissue at any stage of development, with tissue from any one embryo being used to define the expression of up to six genes. Indeed, this figure itself is in no sense an absolute limit and simply reflects the stage of embryonic development. Thus, the outcome illustrates the value of coordinated use of such rare material and demonstrates the very considerable potential for the use of banked human embryonic tissues in the long term (Burn and Strachan, 1995). We anticipate that with the emergence of data from the Human Genome Project demand for, and use of, such embryo banks will increase dramatically.

ACKNOWLEDGMENTS

We thank our colleagues Paul Buxton, Joe Chan, and Pete Scambler for their comments on a draft manuscript and all staff running the Human Embryo Bank at ICH/UCH for their technical help. This work was supported by grants from the European Union, the Medical Research Council, and the Programme Telethon-Italia.

REFERENCES

Acampora, D., D'Esposito, M., Faiella, A., Pannese, M., Migliaccio, E., Morelli, F., Stornaiuolo, A., Nigro, V., Simeone, A., and Boncinelli, E. (1989). The human HOX gene family. *Nucleic Acids Res.* **17,** 10385–10402.

Burn, J., and Strachan, T. (1995). Human embryo use in developmental research. *Nature Genet.* **11,** 3–6.

FIG. 6. Expression of group 3 genes in the 5-week human embryos. (a–f) *HOX A3,* (g–l) *HOX D3,* m–p, *HOX B3.* For each section, both bright-field (top) and dark-field (bottom) are shown side by side. For *HOX A3* and *HOX D3,* sections through the hindbrain are shown (a, g). For all three genes, two set of sections through the branchial arches are illustrated, (b, h, m) preceeding (c, i, n). Orientation of sections is for (a, g), rostral to the left and caudal to the right; for all other panels, rostral is uppermost. Arrowheads indicate rostral gene expression cutoffs. Embryos used: in a–c, h, i, and n number 5, in g and m number 6. Abbreviations: as, arytenoid swelling; b, branchial arch; c, branchial cleft; g ix/x, combined superior ganglion of IXth and Xth nerves; lt, laryngo-tracheal groove; ov, otic vesicle; p, branchial pouch; r, rhombomere; ra, right atrium; ta, truncus arteriosus; tp, thyroid primordium. Scale bar: 200 μm, for all panels.

Copyright © 1997 by Academic Press. All rights of reproduction in any form reserved.

Chisaka, O., and Capecchi, M. R. (1991). Regionally restricted developmental defects resulting from targeted disruption of the mouse homeobox gene hox-1.5. *Nature* **350,** 473–479.

Condie, B. G., and Capecchi, M. R. (1993). Mice homozygous for a targeted disruption of Hoxd-3 (Hox-4.1) exhibit anterior transformations of the first and second cervical vertebrae, the atlas and the axis. *Development* **119,** 579–595.

Condie, B. G., and Capecchi, M. R. (1994). Mice with targeted disruptions in the paralogous genes hoxa-3 and hoxd-3 reveal synergistic interactions. *Nature* **370,** 304–307.

Dollé, P., Izpisúa-Belmonte, J.-C., Tickle, C., Brown, J., and Duboule, D. (1991). Hox-4 genes and the morphogenesis of mammalian genitalia. *Genes Dev.* **5,** 1767–1776.

Duboule, E., and Dollé, P. (1989). The structural and functional organization of the murine HOX gene family resembles that of Drosophila homeotic genes. *EMBO J.* **8,** 1497–1505.

Duboule, D. (1992). The vertebrate limb: A model system to study the Hox/HOM gene network during development and evolution. *BioEssays* **14,** 375–384.

Gendron-Maguire, M., Mallo, M., Zhang, M., and Gridley, T. (1993). Hoxa-2 mutant mice exhibit homeotic transformation of skeletal elements derived from cranial neural crest. *Cell* **75,** 1317–1331.

Godsave, S., Dekker, E. J., Holling, T., Pannese, M., Boncinelli, E., and Durston, A. (1994). Expression patterns of Hoxb genes in the Xenopus embryo suggest roles in anteroposterior specification of the hindbrain and in dorsoventral patterning of the mesoderm. *Dev. Biol.* **166,** 465–476.

Graham, A., Heyman, I., and Lumsden, A. (1991). Even numbered rhombomeres control the apoptotic elimination of neural crest cells from odd numbered rhombomeres in the chick hindbrain. *Development* **119,** 233–245.

Hunt, P., Gulisano, M., Cook, M., Sham, M.-H., Faiella, A., Wilkinson, D., Boncinelli, E., and Krumlauf, R. (1991a). A distinct Hox code for the branchial region of the vertebrate head. *Nature* **353,** 861–864.

Hunt, P., *et al.* (1991b). The branchial Hox code and its implications for gene regulation, patterning of the nervous system and head evolution. *Development* **Supplement 2,** 63–77.

Hunt, P., and Krumlauf, R. (1992). Hox codes and positional specification in vertebrate embryonic axes. *Annu. Rev. Cell. Biol.* **8,** 227–256.

Hunt, P., Ferretti, P., Krumlauf, R., and Thorogood, P. (1995). Restoration of normal Hox code and branchial arch morphogenesis after extensive deletion of hindbrain neural crest. *Dev. Biol.* **168,** 584–597.

Kessel, M., and Gruss, P. (1990). Murine development control genes. *Science* **249,** 374–379.

Kessel, M., and Gruss, P. (1991). Homeotic transformations of murine vertebrae and concomitant alteration of Hox codes induced by retinoic acid. *Cell* **67,** 89–104.

Lammer, E. J., *et al.* (1985). Retinoic acid embryopathy. *N. Engl. J. Med.* **313,** 837–841.

Larsen, W. J. (1993) "Human Embryology." Churchill Livingstone, New York.

Lufkin, T., Manuel, M., Hart, C. P., Dollé, P., LeMeur, M., and Chambon, P. (1992). Homeotic transformation of the occipital bones of the skull by ectopic expression of a homeobox gene. *Nature* **359,** 835–841.

Lumsden, A., Sprawson, N., and Graham, A. (1991). Segmental origin and migration of neural crest cells in the hindbrain region of the chick embryo. *Development* **113,** 1281–1291.

Manak, J. R., and Scott, M. P. (1994). A class act: Conservation of homeodomain protein functions. *Development* **Supplement,** 61–77.

Manley, N. R., and Capecchi, M. R. (1995). The role of Hoxa-3 in mouse thymus and thyroid development. *Development* **121,** 1989–2003.

Marshall, H., Studer, M., Pöpperl, H., Aparicio, S., Kuroiwa, A., Brenner, S., and Krumlauf, R. (1994). A conserved retinoic acid response element required for early expression of the homeobox gene Hoxb-1. *Nature* **370,** 567–571.

McGinnis, W., and Krumlauf, R. (1992). Homeobox genes and axial patterning. *Cell* **68,** 283–302.

Morriss-Kay, G. M. (1993). Retinoic acid and craniofacial development. *BioEssays* **15,** 9–15.

Ogura, T., and Evans, R. M. (1995). Evidence for two distinct retinoic acid response pathways for HOXB1 gene regulation. *Proc. Natl. Acad. Sci. USA* **92,** 392–396.

Sechrist, J., Serbedzija, G. N., Scherson, T., Fraser, S., and Bronner-Fraser, M. (1993). Segmental migration of the hindbrain neural crest does not arise from segmental generation. *Development* **118,** 691–703.

Simeone, A., Acampora, D., Arcioni, L., Andrews, P. W., Boncinelli, E., and Mavilio, F. (1990). Sequential activation of Hox2 homeobox genes by retinoic acid in human embryonal carcinoma cells. *Nature* **346,** 763–766.

Simeone, A., Acampora, D., Nigro, V., Faiella, A., D'Esposito, M., Stornaiuolo, A., Mavilio, F., and Boncinelli, E. (1991). Differential regulation by retinoic acid of the homeobox genes of the four HOX loci in human embryonal carcinoma cells. *Mech. Dev.* **33,** 215–228.

Wilkinson, D. G., Bhatt, S., Cook, M., Boncinelli, E., and Krumlauf, R. (1989). Segmental expression of Hox-2 homeobox-containing genes in the developing mouse hindbrain. *Nature* **341,** 405–409.

Wilkinson, D. G., and Green, J. (1990). In situ hybridization and the three-dimensional reconstruction of serial sections. *In* "Postimplantation Mammalian Embryos: A Practical Approach" (A. J. Copp and D. L. Cockroft, Ed.), pp. 155–171. IRL Press, Oxford.

Wilkinson, D. G. (1992). Whole mount in situ hybridization of vertebrate embryos. *In* "In Situ Hybridization: A Practical Approach" (D. G. Wilkinson, Ed.), pp. 75–83. IRL Press, Oxford.

Received for publication September 8, 1996
Accepted October 16, 1996

Copyright © 1997 by Academic Press. All rights of reproduction in any form reserved.

DEVELOPMENTAL BIOLOGY **183,** 61–73 (1997)
ARTICLE NO. DB968490

tbx6, a *Brachyury*-Related Gene Expressed by Ventral Mesendodermal Precursors in the Zebrafish Embryo

Barbara Hug, Virginia Walter, and David Jonah Grunwald
Department of Human Genetics, University of Utah, Salt Lake City, Utah 84112

Classical embryology experiments have indicated the existence of dorsal-type and ventral-type mesoderms that arise as a consequence of mesoderm induction during vertebrate development. Here we report that the zebrafish *tbx6* gene, a member of the *Brachyury*-related T-box family of genes, is exclusively expressed by ventral mesendoderm. Three observations link the expression of *tbx6* to ventral mesoderm specification. First, the gene is initially expressed at the onset of gastrulation within a ventrolateral subpopulation of cells that express the pan-mesodermal gene, *no tail* (*Brachyury*). Second, the mesoderm-inducing factors activin and bFGF activate *tbx6* expression in animal caps. Third, dorsalization of the mesendodermal precursor population following exposure of embryos to lithium ions causes down-regulation of *tbx6* transcription. *tbx6* is expressed transiently in the involuting derivatives of the ventral mesendoderm, which give rise to nonaxial mesodermal tissues; its expression is extinguished as tissue differentiation progresses. Transcription of *tbx6* commences about an hour after initiation of expression of the pan-mesendodermal gene *no tail* and the organizer gene *goosecoid*. The dependence of *tbx6* expression on *no tail* activity was examined in *no tail* mutant embryos. The activation of *tbx6* transcription in ventral mesoderm does not depend on *no tail* gene activity. However, *no tail* appears to contribute to the maintenance of normal levels of *tbx6* transcription and may be required for *tbx6* transcription in the developing tail. © 1997 Academic Press

INTRODUCTION

Though cell lineage studies performed in a wide variety of vertebrate embryos have revealed that the precursor cells of specific tissues reside in distinct positions within the embryo at the onset of gastrulation (Dale and Slack, 1987a; Kimmel *et al.*, 1990; Lawson and Pedersen, 1992; reviewed in Tam and Quinlan, 1996), it has been difficult to determine the actual complexity of cell identities present in the early gastrula (Dale and Slack 1987b; Ho and Kimmel, 1993). In the early embryo we know most about the determination of the progenitors of the mesoderm, but few molecular markers that identify stages of their differentiation have been described. Tissue explantation and recombination experiments performed in amphibian embryos have led to the idea that initially only two types of mesoderm, dorsal and ventral, are generated in response to maternally supplied localized signals (Nieuwkoop, 1973; Gerhart *et al.*, 1991; Smith, 1993; Slack, 1994). Subsequent intercellular signaling is thought to be responsible for diversification of the mesodermal precursor population (Smith *et al.*, 1985; Dale and Slack, 1987b; Gerhart *et al.*, 1991; Piccolo *et al.*, 1996; Zimmerman *et al.*, 1996). Dorsal mesoderm cells, known as organizer tissue, play a pivotal role in initiating and coordinating the cell movements and tissue differentiation events that generate the body plan of the vertebrate embryo (Spemann and Mangold, 1924). The cells that comprise the organizer can be recognized by their distinct behaviors during gastrulation, by their ability to give rise to axial tissues such as notochord both in the embryo and when isolated in culture, and by the distinct set of genes they express (Keller and Danilchik, 1988; Gerhart *et al.*, 1991; De Robertis *et al.*, 1992; Beddington and Smith, 1993; Streit *et al.*, 1994; De Robertis, 1995). In contrast, far less is known about the specification and properties of the mesodermal precursors that arise from lateral and ventral positions of the fate map. In the absence of organizer tissue, these latter cells appear to have a homogeneous "ventral-type" specification, giving rise only to blood and mesothelium (Dale and Slack, 1987b; Gerhart *et al.*, 1989). Under the influence of signaling from the organizer, the ventral cells become "dorsalized," developing the capacity to give rise to the intermediate forms of mesoderm found in the fate map, including somites and kidney. We do not know whether the initial ventrolateral cell population is really homogeneous, nor is it clear how many domains of identity exist within this population prior to the overt differentiation of tissues.

One reason to suspect that previously unidentified gene

0012-1606/97 $25.00
Copyright © 1997 by Academic Press
All rights of reproduction in any form reserved.

activities may distinguish domains of mesodermal specification in the early gastrula comes from analysis of the *Brachyury* gene. *Brachyury* has been studied extensively in a variety of vertebrates, where its orthologs have been assigned species-specific names, including *T* in the mouse, *no tail* in the zebrafish, and *Xbra* in *Xenopus* (Herrmann and Kispert, 1994; Herrmann, 1995a,b; Smith *et al.*, 1995; Schulte-Merker, 1995). Transcription of *Brachyury* is activated as an immediate early response to mesoderm induction (Smith *et al.*, 1991) and occurs throughout the entire mesendodermal precursor population (Wilkinson *et al.*, 1990; Schulte-Merker *et al.*, 1992; Smith *et al.*, 1995). *Brachyury* encodes a transcription factor (Kispert *et al.*, 1995; Kispert, 1995), which when expressed in animal cap cells of frog embryos can activate some aspects of mesoderm-specific gene expression (Cunliffe and Smith, 1992). Nevertheless, despite its expression throughout the mesendoderm precursor population, analyses of the expression and function of *Brachyury* indicate that the gene is not required for all of mesodermal development. Among the involuting mesodermal cells, *Brachyury* expression is maintained only in precursors of the notochord (Herrmann, 1995b; Smith *et al.*, 1995; Schulte-Merker, 1995), in which transcription appears to depend on the presence of functional Brachyury protein (Herrmann, 1991, 1995b; Schulte-Merker *et al.*, 1994b). Analyses of the embryonic phenotypes of *T/T* mutant mice and *ntl/ntl* mutant zebrafish indicate that *Brachyury* function is required for the normal gastrulation movements of mesodermal precursors in the mouse (Wilson *et al.*, 1993, 1995) and for the differentiation of notochord in both types of embryos (Chesley, 1935; Halpern *et al.*, 1993). In addition, mutants exhibit defects in the formation of trunk somites and a deficit of posterior tissues. Notably, anterior mesodermal derivatives are spared in both types of mutant embryos. Studies in zebrafish have indicated that the aberrantly formed trunk somites arise as a secondary consequence of the absence of wild-type notochord precursors (Halpern *et al.*, 1993). In sum, although the requirement for *Brachyury* activity may be somewhat more widespread in the mouse than in the zebrafish (Beddington *et al.*, 1992; Wilson *et al.*, 1993, 1995), it appears that in both embryos the function of *Brachyury* in the notochord precursor population is different from its activity elsewhere in the mesoderm.

The finding that *Brachyury* function is not essential for all aspects of mesoderm formation is consistent with the idea that other regulatory genes may specify the fates of specific regional domains of mesodermal precursors (Griffin *et al.*, 1995; Herrmann, 1995b). Indeed, soon after organizer-specific genes such as *goosecoid* are expressed in the dorsal mesoderm of zebrafish embryos, these cells appear to downregulate *no tail* expression (Schulte-Merker *et al.*, 1994a). Thus, the involuting cells that contribute to anterior chordamesoderm do not express *Brachyury*.

Few regulatory genes have been identified as candidates that might be responsible for conferring distinct identities to the mesendodermal precursors that reside in the lateral and ventral positions in the gastrula. These precursors are the cells that normally contribute to nonaxial mesoderm. Here we describe a potential regulatory gene that is expressed throughout gastrulation specifically by mesodermal precursors that originate in ventrolateral positions in the early gastrula. The gene *tbx6* (for *T-box6*) encodes a protein with a domain related to the DNA-binding T-domain of Brachyury (Kispert and Herrmann, 1993; Bollag *et al.*, 1994; Kispert, 1995). Initially *tbx6* is coexpressed with *no tail* in cells that reside at ventral and lateral positions in the early gastrula. However, as these cells enter the hypoblast they maintain *tbx6* expression in the absence of *no tail* activity. Similar to *no tail*, *tbx6* is expressed by intermediates in mesoderm differentiation and its expression is absent from terminally differentiated mesodermal derivatives. The expression pattern of *tbx6* reveals that nonaxial and axial mesodermal precursors have distinct patterns of gene expression and may have distinct identities early in development.

MATERIALS AND METHODS

Fish Stocks and Maintenance

Fish were maintained at 28.5°C on a 14-h light/10-h dark cycle. Embryos were collected from pairwise matings, cultured in Egg Water (Westerfield, 1993), and staged by hours of development at 28.5°C (h) and by morphological criteria (Westerfield, 1993; Kimmel *et al.*, 1995). Wild-type fish were laboratory-maintained stocks originally obtained from Ekkwill, Inc. (Gibsonton, FL). Mutant embryos were obtained from stocks generously supplied by Charles Kimmel and the University of Oregon fish facility. Mutant lines included *spadetail* (*spt*^{b104}) and *no tail* (*ntl*^{b160} or *ntl*^{b195}).

Analysis of cDNA Clones

A clone isolated from a zebrafish gastrula-stage cDNA library (Helde and Grunwald, 1993) was found by *in situ* hybridization to harbor sequences that were expressed in the mesoderm of early gastrulae. These DNA sequences were used to probe poly(dT)-primed embryonic zebrafish cDNA libraries generated from a mix of 4- to 9-h or 10- to 16-h embryos, and multiple hybridizing clones were recovered. Each clone was either partially or entirely sequenced using manual (Sequenase DNA sequencing kit, USB) or automated methods (Taq Dye Primer Cycle sequencing kit, Applied Biosystems). All clones contained portions of the single open reading frame contained in clone 1N, the sequence of which is shown in Fig. 1A (GenBank Accession No. U80951). All clones but 1G contained either of two 3′ UTR sequences, differing only in the use of polyadenylation sites (Fig. 1A) such that one class included an extra 250 bp at the 3′ terminus. In addition, the 3′ UTR sequence of clone 1G diverged from the others at position 1710 (Fig. 1A).

RNA in Situ Hybridization Analysis and Immunohistochemistry

Staged embryos were fixed overnight at 4°C in 4% paraformaldehyde in sucrose fix buffer (Westerfield, 1993), rinsed in PBS, dehydrated through a methanol series, and stored in absolute methanol at −20°C. RNA *in situ* hybridization was carried out as described by Helde and Grunwald (1993) with the following changes: protein-

Copyright © 1997 by Academic Press. All rights of reproduction in any form reserved.

ase K treatment was increased in duration for older embryos, prehybridization was carried out for 24 h, and RNase treatment (7.5 μg/ml RNase A) was performed for 15 min at 20°C. Double RNA *in situ* hybridizations were performed according to Hauptmann and Gerster (1994) with similar modifications. Following *in situ* hybridization, some embryos were processed for immunohistochemistry as described in Stachel *et al.* (1993). For most studies, whole-mount preparations of embryos were cleared in benzyl benzoate:benzyl alcohol (2:1) or in 75% glycerol and photographed using an Olympus SZH dissecting microscope. In some cases, whole-mount stained embryos were embedded in paraffin and sectioned at 8 μm thickness prior to analysis.

Analysis of RNA

RNA was isolated from whole embryos or animal caps using TRIzol reagent (GibcoBRL). For Northern analysis, 10 μg/lane of total RNA was separated by electrophoresis through a 20 m*M* Mops, pH 7.0/1.75 *M* formaldehyde/1% agarose gel. The RNA was then transferred and cross-linked to a membrane (Duralon, Stratagene). Blots were prehybridized overnight at 42°C in 0.25 *M* $NaHPO_4$, pH 7.2, 1 m*M* EDTA, 7% SDS, 40% formamide, 5% dextran and then hybridized for 36–48 h at 42°C in the same solution containing 5×10^5 cpm/ml of probe. ^{32}P-labeled probes were generated from purified fragments representing partial cDNA sequences and were prepared using the Prime-it II kit (Stratagene). Blots were washed (5 min at RT in 4× SSC; 20 min at 60°C in 0.25 *M* $NaHPO_4$, pH 7.2, 1 m*M* EDTA, 2% SDS; and 60 min at 60°C in 0.04 *M* $NaHPO_4$, pH 7.2, 1 m*M* EDTA, 1% SDS) and then exposed to X-ray film for 1–8 days.

Gene probes used in these studies include *cytokeratin8* (B. Hug and D. J. Grunwald, unpublished), *eve1* (Joly *et al.*, 1993), *goosecoid* (Stachel *et al.*, 1993), *no tail* (Schulte-Merker *et al.*, 1992), and *snail1* (Thisse *et al.*, 1993).

Animal Cap Assay

Animal caps were removed from the marginal region and yolk cell of 3.25- to 3.5-h embryos using a fragment of a razor blade and cultured (10 caps/2.4 ml media in agarose-coated 35-mm dishes) for 5 h at 28.5°C in a simple salt solution (88 m*M* NaCl, 1 m*M* KCl, 0.7 m*M* $CaCl_2$, 1 m*M* $MgSO_4$, 2.5 m*M* $NaHCO_3$, 5 m*M* Hepes, pH 7.8) supplemented with 1× chemically defined lipid concentrate (GibcoBRL, Cat. No. 11905-031) and antibiotics (recipe via personal communication from C. Sagerstrom, Y. Grinblat, and H. Sive). In some experiments, the medium was supplemented with activinA, a generous gift from W. Fischer and W. Vale (Salk Institute), or bFGF (Upstate Biotechnology Inc., Cat. No. 01-106). RNA harvested from groups of 10 animal caps served as template for the production of first-strand cDNA using SUPERSCRIPT II RNase H$^-$ reverse transcriptase according to the specifications of the supplier (GibcoBRL). One microliter of the first-strand cDNA product (0.5 animal cap equivalent) was then used as template in a PCR using a nucleotide mix supplemented with [^{32}P]dCTP. Primers used to detect expressed sequences were 5′-CCGCTTCGCTTCCTTCATCG-3′ (forward) and 5′-GAGCCTCGTAGACTGCCCAG-3′ (reverse) for *cytokeratin8*, 5′-ATCAGAATTCAATGTCTGCCTCAAGTCCC-3′ (forward) and 5′-ATCAAGGCCTGTTGTCAGTGCTGTGGTC-3′ (reverse) for *no tail*, and 5′-GACAGCATATGAATCATTTGGCTAATAAC-3′ (forward) and 5′-GACAGCTCGAGCCTGCATCTCTTGGGTCC-3′ (reverse) for *tbx6*. The PCR products were resolved on 3.5 or 5% acrylamide gels that were subsequently dried and exposed to X-ray film.

RESULTS

The Zebrafish tbx6 Gene Is a Member of the T-box Gene Family

The *tbx6* cDNA was isolated in a study aimed at identifying genes whose expression patterns revealed domains of cells in the zebrafish gastrula. By the pattern of its expression in early gastrulae as detected by *in situ* hybridization, one cDNA sequence was determined to be expressed by a subpopulation of mesendodermal precursor cells. A series of partially overlapping gene sequences was isolated from embryonic cDNA libraries. The longest of these cDNA clones, 1N, appears to represent a full-length copy of the mRNA: first, it is 2871 bp in length, in good accord with the apparent size (2700 nt) of the predominant transcript of the embryo detected by Northern analysis (data not shown); second, 5′ RACE of poly(A)-selected embryonic RNA indicated that virtually all of the 5′ region of the endogenous mRNA is accounted for in the cDNA clone (data not shown). Given the absence of an in-frame stop codon upstream of the putative translational start site, there exists a possibility that some 5′ sequences may be missing in the clone. Conceptual translation of the recovered sequence (Fig. 1A) indicates that the gene potentially encodes a protein of 473 amino acids, whose amino-terminal half is closely related to the amino-terminal portion of the zebrafish No Tail protein (Fig. 1B; Schulte-Merker *et al.*, 1992). Extensive similarity between the two proteins does not extend beyond the putative DNA binding domain (Fig. 1B; Kispert and Herrmann, 1993). Comparison of the T-domain (defined as in Agulnik *et al.*, 1995; Fig. 1A) of the protein encoded by the newly isolated zebrafish gene with the available sequences of the T-domains encoded by the mouse *T* gene and each of the six identified murine *Brachyury*-related genes, *Tbx1–Tbx6* (Bollag *et al.*, 1994; Kispert, 1995; Agulnik *et al.*, 1996), indicates that the zebrafish protein shares 47–57% identity over this region and that the zebrafish gene is most closely related to the *Tbx6* gene of the mouse (data not shown; L. Silver, personal communication). In addition to sequence similarities, the pattern of expression of the zebrafish gene throughout development closely parallels that of mouse *Tbx6* (Chapman *et al.*, 1997). We have thus designated the zebrafish gene described here *tbx6* since it appears to be the ortholog of the mouse *Tbx6* gene.

tbx6 Is Expressed by Ventrolateral Mesendodermal Precursors in the Zebrafish Gastrula

Zebrafish *tbx6* is specifically expressed by the subpopulation of mesendodermal precursor cells in the gastrula that gives rise to nonaxial mesodermal derivatives. At the beginning of gastrulation, the zebrafish blastoderm is shaped like an inverted cup covering the animal pole of the yolk cell,

Copyright © 1997 by Academic Press. All rights of reproduction in any form reserved.

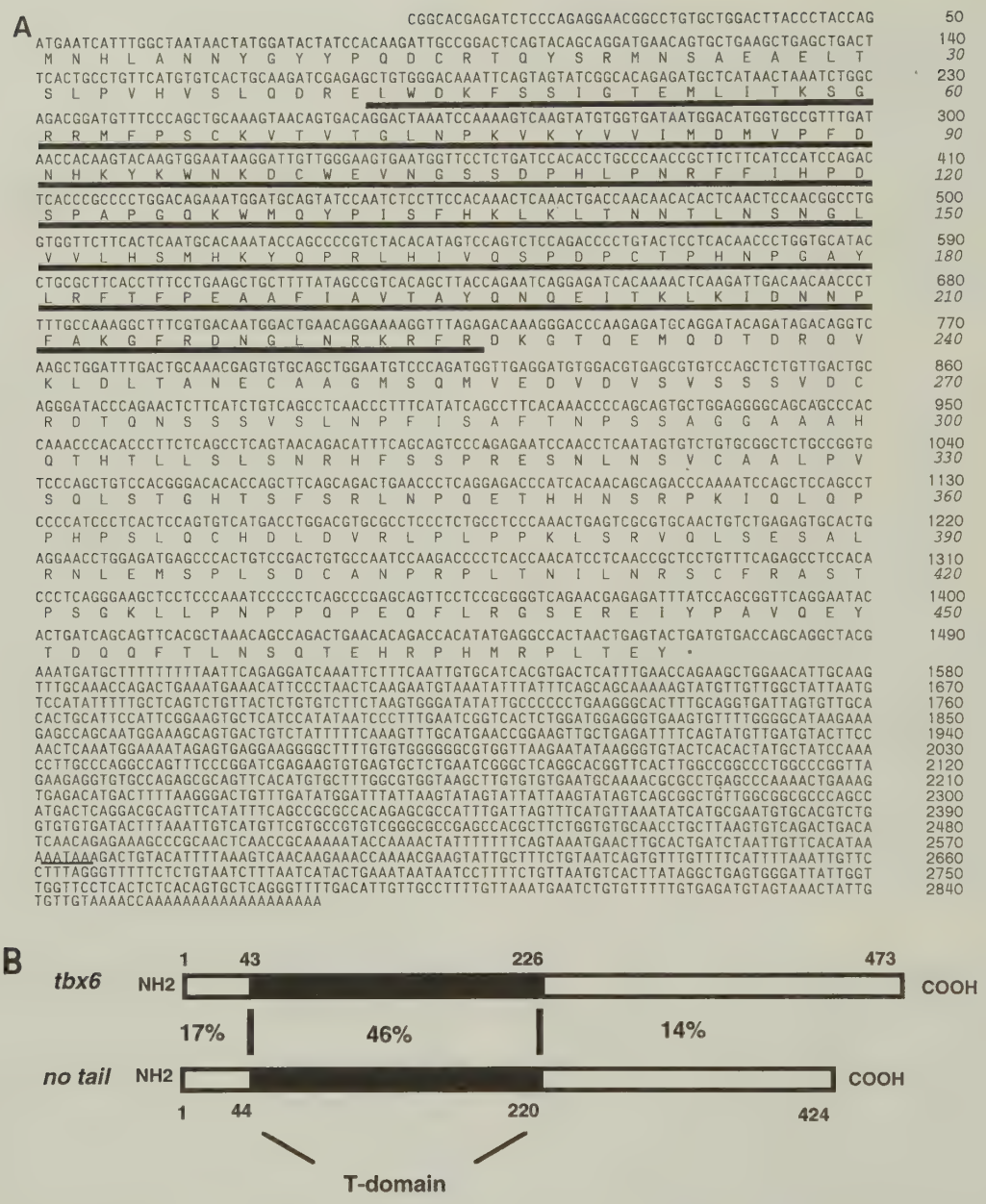

FIG. 1. Sequence analysis of the *tbx6* gene product. (A) The entire sequence contained in clone 1N, a presumed full-length cDNA clone of *tbx6*, is presented. Conceptual translation begins at the first available ATG codon. The boldly underlined 184-amino-acid sequence represents the portion of the protein that is similar to the T-domain of No Tail and other Brachyury-related proteins (Agulnik *et al.*, 1995). * indicates the first in-frame stop codon. Several independent cDNA isolates of *tbx6* shared the entire 3′ UTR with clone 1N, while others contained a shorter 3′ UTR that terminated at position 2595, just 19 bases downstream of the underlined AATAAA sequence. (B) Schematic comparison of the protein products of the *tbx6* and *no tail* genes indicating the amino acid regions that share identity (%). Amino acids 44–220 of No Tail and 43–226 of Tbx constitute the T-domains of these proteins.

and the relative positions of the presumptive primordia of tissues have been described in a fate map for this stage (Fig. 2A; Kimmel *et al.*, 1990). As indicated by the fate map, all of the mesoderm arises as a circumferential belt of cells present at the margin of the blastoderm in the early gastrula. Figures 2B and 2B′ present two lateral views of early gastrula embryos (60% epiboly, 7 h) that have been processed by *in situ* hybridization to reveal the distribution of *tbx6* transcripts. *tbx6* is expressed initially by a continuous arc of cells present at the margin of the blastoderm in the gastrula. Simultaneous detection of *tbx6* transcripts (purple staining) and No Tail protein (brown nuclear staining) indicated that the cells that express *tbx6* are a subpopulation of the *no tail*-expressing mesendodermal precursor population (Fig.

Copyright © 1997 by Academic Press. All rights of reproduction in any form reserved.

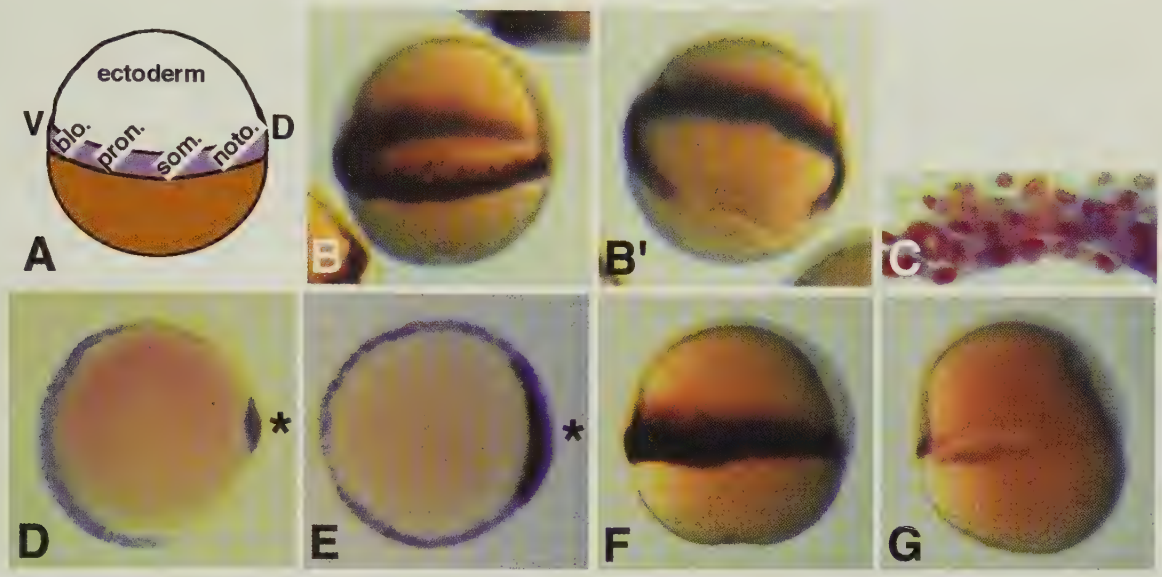

FIG. 2. *tbx6* is expressed by ventrolateral mesendodermal precursors in the early zebrafish gastrula. (A) A simplified fate map of the early zebrafish gastrula (Kimmel *et al.*, 1990). At this stage the blastoderm is shaped as an inverted cup covering the animal pole of the yolk cell (gold). Mesoderm and endoderm arise from involuting cells initially present at the blastoderm margin (purple). The remaining cells give rise to ectoderm. Mesodermal tissues are formed from prospective tissue precursors that are organized in the following dorsal (D) to ventral (V) order: notochord (noto.), somites (som.), pronephros (pron.), blood (blo.). (B and B') Oblique lateral views (animal pole up) of early gastrulae showing the distribution of *tbx6* transcripts revealed by whole-mount *in situ* hybridization. *tbx6* is expressed by a continuous arc of cells at the margin of the blastoderm, corresponding to the mesendodermal precursors. The dorsal view in B' illustrates the absence of the *tbx6* expression in dorsal marginal cells. (C) A section through the margin of an embryo in which *tbx6* transcripts were detected by *in situ* hybridization (purple stain) and the No Tail protein was detected by immunohistochemistry (brown nuclear stain) reveals coexpression of the two genes in marginal cells. (D) *In situ* hybridization to detect transcripts of both *tbx6* and the dorsal-specific gene *goosecoid* indicates that *tbx6* is not expressed in the dorsal mesoderm. In this animal pole view of a midgastrula (7 h) embryo, the recently involuted *goosecoid*-expressing cells (*) appear as a knot of stained cells at the center of the region devoid of *tbx6* gene expression. (E) An animal pole view of an early gastrula (5.5 h) embryo showing the distribution of both *tbx6* and *goosecoid* transcripts. At the onset of gastrulation the domain of *tbx6* expression (light blue arc) is continuous, and perhaps slightly overlapping, with the domain of *goosecoid* expression (dark blue staining, *). (F, G) *tbx6* expression is down-regulated in embryos dorsalized by exposure to lithium ions. (F) A lateral view of *tbx6* transcripts in a control early gastrula. (G) A lateral view of *tbx6* transcripts in an early gastrula of an embryo that had been exposed at the 32- to 64-cell stage to 0.3 *M* LiCl for 10 min.

2C). The approximately 90° arc of cells in the early gastrula that do not express the gene reside on the dorsal side of the embryo, as shown (Fig. 2D) in an animal pole view of a midgastrula stage embryo that had been hybridized with probes specific for both *tbx6* and the organizer-specific gene *goosecoid* (Stachel *et al.*, 1993).

The dynamic nature of the expression patterns of many early acting genes makes it difficult to place the initial domain of *tbx6* expression precisely with respect to other gene markers that indicate the dorsal–ventral polarity of the mesoderm. Examination of the expression of *tbx6* and the dorsal-specific gene *goosecoid* in 50% epiboly (5.5 h) embryos (Fig. 2E) indicates that these genes are expressed in adjoining and perhaps slightly overlapping domains of expression early in development. Thus, in the early gastrula, all marginal cells of the blastoderm express one of these two genes in addition to *no tail*. As gastrulation proceeds, the *goosecoid*-expressing cells converge toward the dorsal midline and involute (Stachel *et al.*, 1993; Schulte-Merker *et al.*, 1994a), separating from the *tbx6*-expressing cells (Fig. 2D) so that at least three domains of mesodermal precursors can be identified by virtue of the expression patterns of *goosecoid, no tail,* and *tbx6*.

To determine whether the domain of *tbx6* expression might be regulated by factors that establish the dorsoventral polarity of the mesoderm, the normal polarity of this population of cells was perturbed by exposure of early cleavage stage embryos to lithium ions, which causes many regions of the margin to assume dorsal mesoderm characteristics (Stachel *et al.*, 1993). Under normal conditions of development, *tbx6* gene expression can be detected in all gastrula embryos as a continuous arc of stained cells at the margin of the blastoderm (Fig. 2F). Following exposure of cleavage stage embryos to 0.3 *M* lithium chloride, treated embryos

Copyright © 1997 by Academic Press. All rights of reproduction in any form reserved.

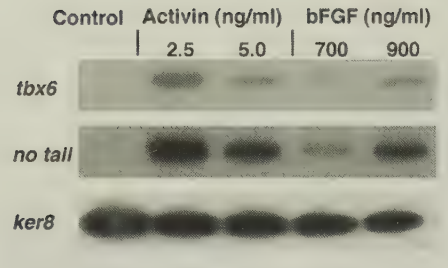

FIG. 3. *tbx6* and *no tail* are transcribed in response to mesoderm induction. Animal caps, removed from 2000- to 4000-cell embryos, were incubated for 5 hr in the absence (Control lane) or the presence of activin or bFGF, provided at the indicated concentrations. RNA was harvested from groups of 10 caps and transcribed genes were detected by RT-PCR. The *ker8* (*cytokeratin 8*) gene is specific to the extraembryonic enveloping layer and serves as a control for the viability of the animal caps and the recovery of RNA.

display varying degrees of dorsalization at the onset of gastrulation (Stachel *et al.*, 1993), and these embryos express greatly diminished levels of *tbx6* gene expression (Fig. 2G).

tbx6 Is Activated in Response to Mesoderm Induction

To examine whether the expression of *tbx6* in marginal cells is likely to be related to a functional role in mesodermal development, we tested the ability of mesoderm-inducing factors to activate its expression ectopically. Animal caps were removed from embryos at the 2000- to 4000-cell stage, during the period when zygotic gene transcription is first activated (Kane and Kimmel, 1993). Groups of 10 caps were cultured in the absence or presence of growth factors, and the expression of *no tail* or *tbx6* was monitored by RT-PCR (see Materials and Methods). As shown in Fig. 3, animal caps incubated in the absence of additional growth factors failed to express either gene, although they appeared to maintain viability and expressed an enveloping layer-specific gene, *cytokeratin 8*, at robust levels. In contrast, both genes were transcribed after caps were exposed to either activin or basic FGF, factors known to elicit a mesoderm-induction response. In these preliminary studies, it appeared that exposure to 2.5 ng/ml activin induced higher levels of *no tail* or *tbx6* expression than did exposure to 5 ng/ml, a finding in accord with previous studies on the induction of *Xbra* in *Xenopus* (Green *et al.*, 1992). We are currently pursuing studies to clarify the dose–response relation between mesoderm-inducing factors and the activation of *tbx6* gene expression.

Relation of the Timing of tbx6 Expression to the Expression of Other Genes in the Early Gastrula

The prevailing models of mesoderm induction (Smith *et al.*, 1985; Dale and Slack, 1987b; Kimelman *et al.*, 1992; De Robertis and Sasai, 1996) suggest that dorsal and ventral identities are established early in development and perhaps independently; however, they do not make specific predictions concerning the relative timing with which these domains are established. To place *tbx6* expression in the context of other genes that are restricted to specific domains at the onset of gastrulation, we examined by Northern analysis the expression of the *no tail, goosecoid, snail1, eve1,* and *tbx6* genes in a single series of developmentally staged embryos (Fig. 4). The genes selected represent a substantial fraction of the characterized zebrafish genes that are expressed within specific domains of the early gastrula embryo. Although *in situ* hybridization may be more sensitive than Northern analysis, the latter permits a direct comparison of the relative time of transcriptional activation of a variety of genes within an identical population of embryos.

Expression of the pan-mesodermal *no tail* gene is an indication of the timing of the response to mesoderm induction. Under the conditions of this experiment, *no tail* RNA was not detected during the first 3.5 h, the pre-midblastula transition (MBT) period. *no tail* RNA was first detected soon after the MBT, at 4.5 h, and its relative abundance in the

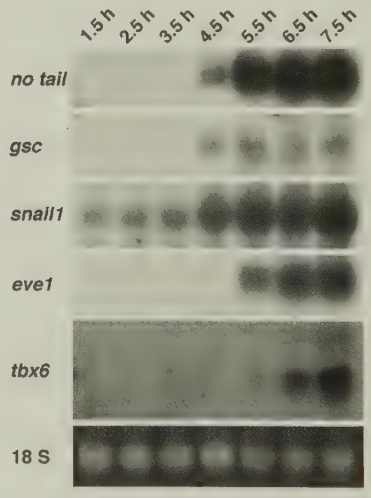

FIG. 4. Northern analysis of the expression of dorsal- and ventral-specific genes at defined developmental time points. Each lane contained RNA harvested from developmentally staged embryos (h, hours of development at 28.5°C). Zygotic gene transcription begins around 3.5 h (Kane and Kimmel, 1993). Transcripts of the pan-mesodermal gene *no tail* (2.5-kb transcript) and the organizer-specific gene *goosecoid* (*gsc*; predominant transcript 1.4 kb) were first detected at 4.5 h. Although *snail1* RNA (1.9-kb transcript) is maternally supplied, a burst of zygotic transcription, corresponding to *snail1* gene expression in dorsal mesoderm (Hammerschmidt and Nusslein-Volhard, 1993; Thisse *et al.*, 1993), was detected at 4.5 h. In contrast, transcripts of the ventrally restricted genes *eve1* (1.4-kb transcript) and *tbx6* (predominant transcript 2.7 kb, additional transcript 3.5 kb) were first detected at 5.5 h. *eve1,* whose domain of expression includes marginal cells of the blastoderm, is maintained in noninvoluting cells of the epiblast. *tbx6* is expressed by marginal cells and their involuting derivatives. A photograph of the 18S ribosomal band of the ethidium bromide-stained Northern gel is shown as a loading control.

Copyright © 1997 by Academic Press. All rights of reproduction in any form reserved.

embryo increased over the next 3 h, during the first half of gastrulation (5.5–7.5 h).

Dorsal-specific gene expression also appears to be activated shortly after the MBT. Although maternal *goosecoid* and *snail1* RNAs can be detected in the early zebrafish embryo, zygotic transcription of these genes is initially restricted to the dorsal portion of the blastoderm margin (Stachel *et al.*, 1993; Hammerschmidt and Nusslein-Volhard, 1993; Thisse *et al.*, 1993). Zygotic expression of both genes was clearly induced by 4.5 h. In contrast, transcripts of the ventrolaterally expressed *eve1* or *tbx6* genes were detected only at later times. *eve1* is initially expressed as a 270° arc of cells along the ventrolateral margin of the blastoderm (Joly *et al.*, 1993) in a pattern very similar to that of *tbx6*. However, *eve1* expression is restricted to the epiblast, whereas *tbx6* is expressed among involuting cells (see below). *eve1* RNA was not detected during the first 4.5 h, consistent with previous *in situ* hybridization studies (Joly *et al.*, 1993). Similarly, transcripts of *tbx6* were first detected at 5.5 h, approximately 1 h after the onset of expression of *no tail* and the dorsal-specific genes examined here. Thus, the currently known dorsally expressed genes appear to be zygotically transcribed significantly earlier than known genes that are activated in ventrolateral domains of the zebrafish embryo. The correlation observed here may reflect the independent timing with which each domain is activated as a consequence of maternally supplied inductive signals or may reflect a requirement for the accumulation of zygotic gene products prior to the transcription of the *eve1* and *tbx6* genes.

tbx6 Is Expressed during Gastrulation by Involuting Nonaxial Precursor Cells

As the blastoderm expands vegetally to cover the yolk cell, and marginal cells become internalized during gastrulation, *tbx6* continues to be expressed specifically by the nonaxial mesodermal precursor population. Figure 5 presents a left side (A) and a dorsal view (A′) of the expression pattern of *tbx6* in a 95% epiboly embryo—in the dorsal view of the embryo, the nonstaining domain of cells corresponds to the presumptive notochord. As illustrated here, nondorsal cells at the margin of the blastoderm continue to express the gene late in gastrulation. In addition, *tbx6* is expressed among cells that appear to be moving rostrally away from the margin while converging toward the dorsal midline. Transverse sections through a similarly staged and processed embryo (Fig. 5B) revealed that expression of *tbx6* rostral to the margin was restricted to the recently involuted hypoblast cells, the precursors of the nonaxial mesoderm and possibly the endoderm. Within the hypoblast, the dorsalmost extent of the domain of *tbx6*-expressing cells abuts the axial mesoderm, identified by the expression of the No Tail protein (Fig. 5C). Thus, *tbx6* expression appears to mark the entire population of cells that will form the nonaxial mesoderm.

Only tissue precursor cells express *tbx6*; we have not observed expression in fully differentiated cell types. As gastrulation proceeds, tissue differentiation progresses in a rostral to caudal manner. Hence, the expression pattern displayed by late gastrula embryos (Fig. 5A) is one indication that only the undifferentiated mesodermal precursors continue to express *tbx6*. At 15 h, when gastrulation is complete and the tail has become the major site of morphogenetic growth and tissue differentiation, *tbx6* is expressed in an arc of ventral tail tissue whose apex coincides with the posterior tip of the tail (Figs. 5D and 6G). As recently demonstrated in the *Xenopus* embryo (Gont *et al.*, 1993), over the course of tail development chordamesoderm and neural ectoderm extend progressively caudally into the undifferentiated region of the tail, which is derived from ventral mesendodermal precursors. Analyses of sectioned material of developing tail tissue in 14- and 17-h zebrafish embryos revealed that *tbx6* is expressed throughout the ventral cells of the most caudal zone and is restricted to lateral cells in regions where axial mesoderm and neurectoderm have extended into the tail (data not shown). Hence, only the most developmentally immature nonaxial mesendodermal cells of the tail express *tbx6*. The region of cells that express *tbx6* grows smaller as the tail differentiates (compare Figs. 5D–5F) until expression becomes undetectable.

The pattern of *tbx6* expression in the hypoblast and the developing tail is consistent with the interpretation that it marks an early stage in the differentiation of nonaxial mesodermal cells. Although nascent paraxial mesoderm expressed the *tbx6* gene, *tbx6* transcripts were not detected in morphologically distinguishable somites. Similarly, *tbx6* is expressed in the blood precursor population of the intermediate cell mass (Figs. 5E and 5F) and in the blood precursors as they migrate first rostrally (Fig. 5F) and then laterally (Fig. 5G) over the yolk cell, but *tbx6* transcripts were not detected in circulating blood. *tbx6*-expressing cells were not observed in the regions of the intermediate cell mass or of the ventral medial trunk of *spadetail* mutant embryos (data not shown), which are deficient in blood (Kimmel *et al.*, 1989). Altogether, these observations indicate that *tbx6* is expressed in mesodermal precursor cells and its expression is down-regulated during the course of mesodermal differentiation. Because of the extensive expression of *tbx6* among mesodermal precursors and the paucity of criteria for discerning endodermal precursors, we have not yet been able to determine unambiguously whether *tbx6* is also expressed in the endoderm.

Activation of tbx6 Expression Is Independent of No Tail Gene Activity

Two lines of evidence suggest the possibility that *tbx6* expression is dependent on *no tail* gene function: (1) *tbx6* transcription is activated in cells that already express *no tail*, and (2) *Brachyury* has been shown to regulate the expression of some downstream mesoderm-specific genes (Cunliffe and Smith, 1992). To examine this possibility, expression of *tbx6* was analyzed in embryos homozygous for a null mutation in *no tail* and in their wild-type siblings. Embryos from matings between *ntl*/+ heterozygotes were

Copyright © 1997 by Academic Press. All rights of reproduction in any form reserved.

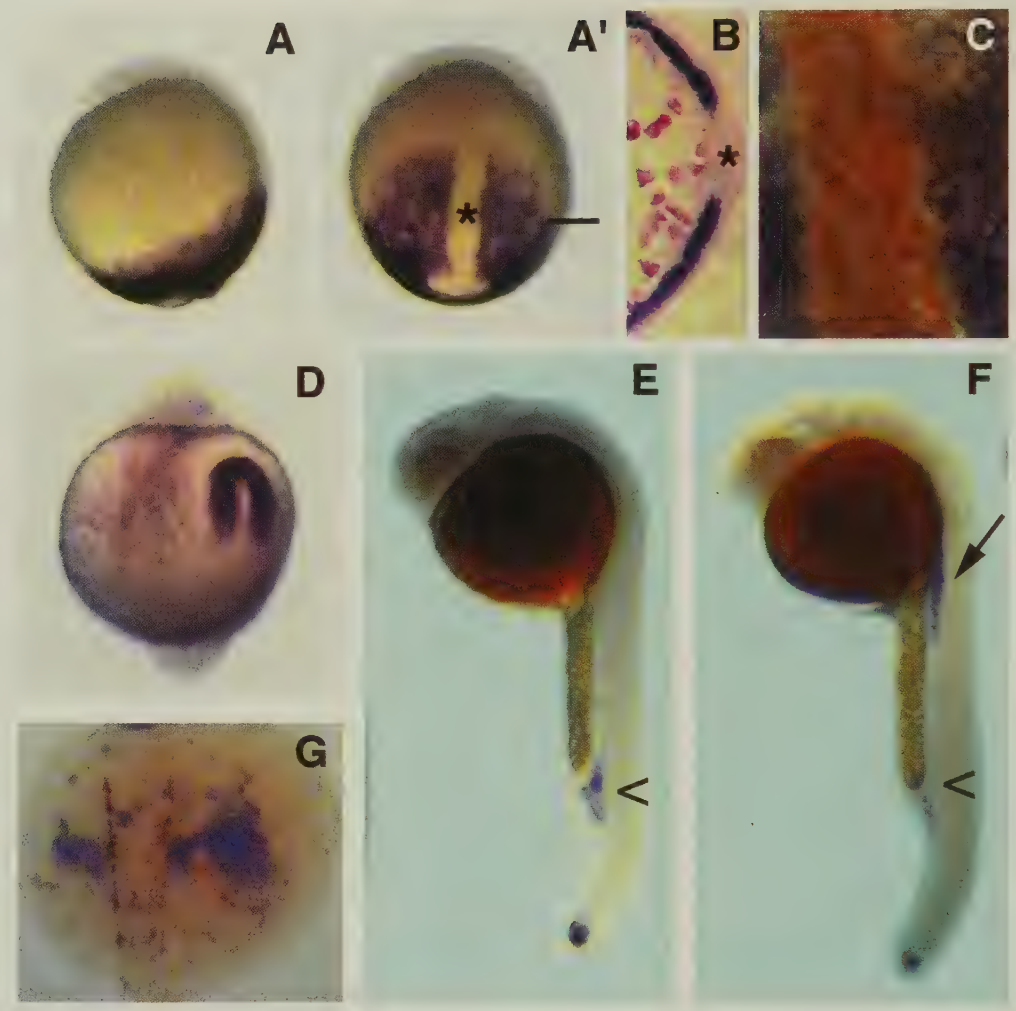

FIG. 5. *tbx6* expression is maintained in undifferentiated derivatives of the ventrolateral mesendodermal precursors. (A and A') Lateral (A, dorsal is right) and dorsal (A') views of *tbx6* expression in late gastrulae (95% epiboly, 9.5 h). During gastrulation, *tbx6* continues to be expressed at the margin of the blastoderm and is maintained in recently involuted cells as they move rostrally and converge dorsally toward the developing chordamesoderm (*). (B) A transverse section through the axis (at the level indicated by the bar in A') of a late gastrula (95% epiboly) embryo indicates that *tbx6* is specifically expressed in involuting hypoblast cells. The presumptive notochord (*, dorsal) is to the right. (C) A dorsal view of the midaxial region of a two-somite (11 h) embryo in which *tbx6*-expressing cells (blue staining) are identified by *in situ* hybridization and No Tail protein-expressing cells (brown) are identified by immunohistochemistry. The domain of *tbx6* expression lies immediately adjacent to the axial mesoderm identified by its expression of the No Tail protein. (D) A ventral view of a 15-h embryo shows that *tbx6* is expressed in the region of the early developing tail as an arc of cells whose apex is located at the posterior tip of the tail and whose wings extend anteriorly, bordering the axial mesoderm. A lateral view of a similar embryo (Fig. 6G) shows that *tbx6* expression is confined to the ventrolateral aspects of the developing tail at this stage. (E and F) Lateral views of two approximately 24-h embryos show the changing expression of *tbx6* in the developing tail and in the blood precursors. The embryo in D is slightly younger than the embryo in E. As tail development proceeds, *tbx6* expression becomes progressively restricted to smaller domains at the posterior tip of the tail. In the 24-h embryo, *tbx6* is also expressed in blood precursor cells that originate in the intermediate cell mass (arrowhead) and that move rostrally along the ventral midline (arrow) prior to entering the circulation. (G) A dorsal view (anterior to the top) of the midtrunk region of a 26-h embryo shows that blood precursor cells maintain expression of *tbx6* as they move laterally over the yolk cell to enter the circulation. Expression of *tbx6* among circulating blood cells has not been detected.

FIG. 6. Expression of *tbx6* in sibling wild-type and *no tail* embryos. Staged embryos from matings between *no tail*/+ heterozygotes were processed to detect *tbx6* transcripts (blue–black) by *in situ* hybridization. 6 and 9 h *no tail* mutant embryos were identified following immunohistochemical staining (brown) to detect the No Tail protein. At subsequent developmental stages, the *no tail* embryos could be identified unambiguously by morphological criteria. (A and B) Animal pole views of early gastrulae (6 h; * indicates dorsal) illustrate that *tbx6* is initially expressed normally in *no tail* mutant embryos. (C and D) Dorsal views (animal pole up) of late gastrulae (90% epiboly, 9 h) show that the overall pattern of *tbx6* expression in the hypoblast is normal. (E and F) Soon after the tail bud stage (12 h, posterior view), the domain of cells that express *tbx6* and the extent of *tbx6* expression appear diminished in *no tail* embryos. (G–J) As tail development proceeds, *tbx6* expression is dramatically down-regulated in *no tail* embryos. Only a small population of cells near the yolk cell of mutant embryos continues to express *tbx6* at 15–16 h. By 18 h, only cells in the region of the intermediate cell mass continue to express the gene in mutant embryos.

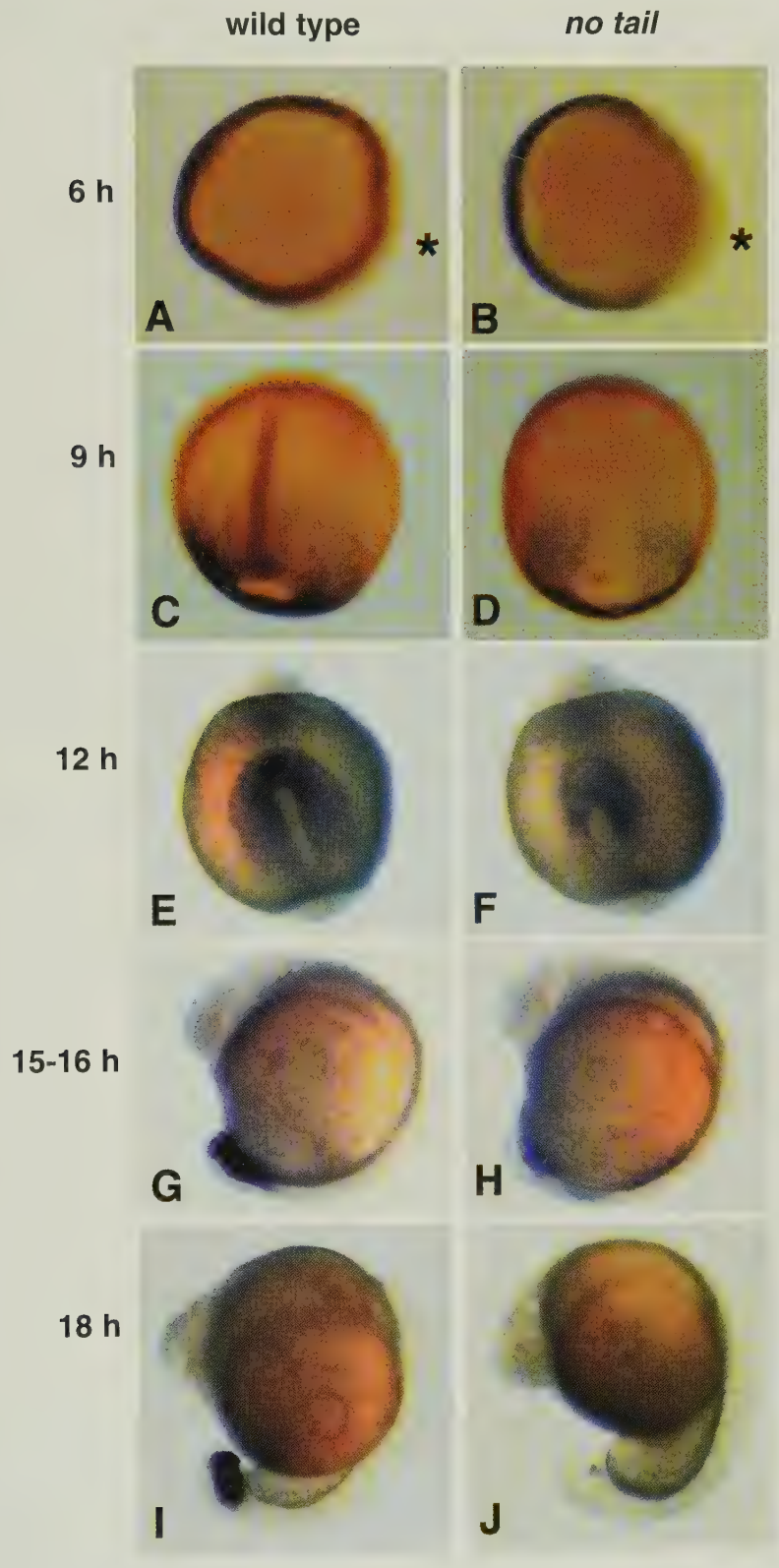

Copyright © 1997 by Academic Press. All rights of reproduction in any form reserved.

stained for expression of *tbx6* transcripts by *in situ* hybridization. Mutant and wild-type progeny were distinguished at early stages by antibody staining to detect the No Tail protein and at later stages by morphological examination of the posterior portion of the axis. As illustrated in Figs. 6A and 6B, the initial pattern of *tbx6* expression appears normal in 6-h *ntl* mutant embryos and thus is established independently of *no tail* gene function. The overall pattern of *tbx6* expression continues to appear normal in mutant embryos throughout gastrulation (Figs. 6C and 6D, 9-h embryos) and into the tailbud stage. However, after the tail begins to extend off the yolk cell, mutant embryos clearly have fewer *tbx6*-expressing cells than their wild-type siblings (Figs. 6E–6H, 12- and 15- to 16-h embryos). By 18 h (Figs. 6I and 6J), *tbx6* expression has been dramatically down-regulated in the tail of mutants so that the only remaining staining in the tail region likely reflects the presence of the blood precursor cells. *tbx6* transcripts have never been detected in the tails of older mutant embryos (data not shown). In sum, *no tail* gene function is not required for the establishment of *tbx6* expression, but may contribute directly or indirectly to the maintenance of *tbx6* expression.

DISCUSSION

tbx6 Gene Expression as a Marker of Ventral-Type Mesoderm Specification

Experiments performed in amphibian embryos have suggested that only two types of mesoderm are initially specified in the vertebrate embryo, a dorsal type (organizer tissue) and a ventral type (Dale and Slack, 1987b; Gerhart *et al.*, 1989). These experiments led to the notion that ventral mesoderm is initially a homogeneous population and that the set of gene activities expressed by ventral mesoderm becomes modified in response to the influence of dorsalizing signaling factors. Dorsalization of ventral mesoderm would lead to the establishment of precursor populations specific for many intermediate kinds of mesodermal tissue, including somites, heart, and kidney (Smith *et al.*, 1985; Dale and Slack, 1987b). Whereas several mesoderm-specific genes have been identified whose expression patterns correlate with the establishment of organizer tissue, *tbx6* is unique in that its expression marks the putative ventral mesoderm population. The expression pattern of *tbx6* gives support to the idea that such a uniformly specified population might exist. The finding that *tbx6*-related genes in zebrafish, mouse, and chicken display strikingly similar developmental patterns of expression (Chapman *et al.*, 1997; Knezevic *et al.*, 1997) is consistent with an essential role for *tbx6* in the development of the ventral mesoderm precursor population.

tbx6 is expressed exclusively by ventral mesendodermal tissue in the early gastrula. At the onset of gastrulation *tbx6* is expressed by ventrolateral *no tail*-expressing cells at the margin of the blastoderm. As indicated by the ability of bFGF or activin to induce *tbx6* transcription in isolated animal caps, the expression of *tbx6* is a component of the response to mesoderm induction. Restriction of *tbx6* expression to ventral mesendoderm is indicated by its absence from organizer tissue in unperturbed embryos and its down-regulation in embryos that have been dorsalized following exposure to lithium ions.

During gastrulation, *tbx6* appears to mark the presumptive nonaxial mesoderm. Upon the down-regulation of *no tail* in the dorsalmost *goosecoid*-expressing cells, the mesoderm consists of at least three distinct domains of gene expression, which appear to correlate with domains of mesodermal fate: a dorsalmost domain that expresses *goosecoid*, a dorsal domain that expresses only *no tail*, and a ventral domain that expresses *tbx6* and *no tail*. It is not yet clear whether all of the ventral mesoderm of the gastrula expresses *tbx6*. In addition, it will be interesting to determine whether the *no tail*-expressing cells that do not express either *goosecoid* or *tbx6* are the specific precursors of the notochord.

tbx6 expression appears to be a characteristic of early stages in the differentiation of ventral mesendoderm. *tbx6* is expressed by cells of the nascent hypoblast, but not in rostral regions of the hypoblast. Similarly, *tbx6* transcripts are found in undifferentiated regions of the mesendoderm of the developing tail and in blood precursors that have not entered circulation, but transcripts are absent from mature forms of these tissues. It is not yet clear what aspect of tissue differentiation correlates with down-regulation of *tbx6* expression. In the nascent hypoblast, adaxial cells continue to express *tbx6* (Fig. 5C) at a time when they also express the tissue-specific gene markers *MyoD* (Weinberg *et al.*, 1996) and *snail1* (Hammerschmidt and Nusslein-Volhard, 1993; Thisse *et al.*, 1993). In the case of blood development, the period of *tbx6* expression overlaps with the period in which lineage-restricted genes are expressed (Detrich *et al.*, 1995). Although we are unable to identify unambiguously all of the derivatives of the hypoblast cells that initially express *tbx6*, given the broad distribution of *tbx6* transcripts in late gastrulae (Fig. 5), it appears that these cells give rise to many, if not all, nonaxial mesodermal tissues. Further experiments will be required to determine whether endodermal precursors of the hypoblast also maintain *tbx6* expression.

Potential Role of tbx6 in Posterior Mesoderm Development

It seems possible that *Brachyury* and *tbx6* play similar but complementary roles in regulating the differentiation of trunk and posterior mesoderm. Previous studies have prompted several investigators to predict the existence of a gene whose expected characteristics appear to be met by *tbx6*. First, Herrmann (1995b) has speculated that the somitic defects seen in T^{Wis}/T^{Wis} homozygotes arise from a dominant negative effect exerted by the T^{Wis} product on a putative T-domain protein that normally contributes to somite formation. Tbx6 is a candidate for a protein whose

Copyright © 1997 by Academic Press. All rights of reproduction in any form reserved.

activity might be perturbed by expression of the T^{Wis} product in ventral mesendodermal precursors. Second, Griffin *et al.* (1995) have suggested the existence of a yet unidentified gene that is required for the development of nonaxial mesoderm in the trunk and that is dependent on FGF signaling. Their proposal was based on the observation that suppression of FGF signaling by the expression of dominant negative FGF receptors leads to severe deficits of mesoderm in *Xenopus* and zebrafish (Amaya *et al.*, 1991, 1993; Griffin *et al.*, 1995), which include but exceed those observed in *no tail* and *T* mutants. Our studies indicate that FGF signaling can lead to *tbx6* transcription. It will be interesting to determine whether *tbx6* expression is dependent on FGF signaling.

Relation of tbx6 and No Tail and Possible Interactions between the Genes

One possible basis for the different functions of *Brachyury* in axial and nonaxial mesodermal precursors could be that *Brachyury* interacts in some way with *tbx6* in the ventrolateral marginal cells. *tbx6* encodes a protein whose amino-terminal half is closely related to the T-domain of No Tail, which is necessary and sufficient for site-specific DNA binding (Kispert and Herrmann, 1993; Conlon *et al.*, 1996). Moreover, recent data (B. Hug, unpublished observations) indicate that *in vitro* synthesized Tbx6 protein is capable of binding DNA sequences that are specifically recognized by No Tail (Kispert and Herrmann, 1993).

We imagine three plausible scenarios for how the products of *tbx6* and *no tail* might interact. First, the two proteins may cooperate to modify the expression of specific target genes. Binding of Brachyury to multiple sites upstream of a reporter gene has more than an additive effect on reporter gene expression (Kispert, 1995), indicating that T-domain proteins can functionally interact to affect the expression of target genes. Second, *tbx6* and *no tail* function may be largely redundant in the ventrolateral marginal cells. Third, Tbx6 protein may compete with No Tail for some binding sites, effectively eliminating some or all of *no tail* activity in the ventrolateral margin of the blastoderm. The kinds of interactions invoked here have been exhibited by Hox genes (Davis *et al.*, 1995) and could help account for the modest effect of *no tail* null mutations on the development of the nonaxial mesoderm.

Timing of tbx6 Gene Expression and Its Potential Regulation

The patterning of mesoderm is thought to be an early embryonic event that is critical for the subsequent patterning and development of the embryo. Therefore, it is intriguing that *tbx6*, a gene specific to ventral mesoderm, is activated significantly later than many other regulatory genes that are expressed within the mesoderm (Fig. 4). A trivial explanation for this is that *tbx6* may be a relatively late marker of ventral-type specification. Alternatively, ventral mesoderm identity may emerge later than dorsal mesoderm identity. If maternally supplied inducing factors are sufficient for both dorsal and ventral mesoderm specification, then it seems likely that they operate with independent timing. Another possibility is that the specification of ventral mesoderm, including the transcription of *tbx6*, is dependent on the zygotic transcription of genes encoding modifying (competence) factors (Kimelman *et al.*, 1992; Moon and Christian, 1992). Hence, it may be relevant that secreted ventralizing factors, such as BMP4 (Koster *et al.*, 1991; Jones *et al.*, 1992; Dale *et al.*, 1992), which are capable of modifying the character of mesoderm formed in response to inductive factors (Dale *et al.*, 1992; Graff *et al.*, 1994; Suzuki *et al.*, 1994; Schmidt *et al.*, 1995), are also transcribed with some delay after the midblastula transition. The expression domain of *bmp4* in the marginal zone of the *Xenopus* embryo (Fainsod *et al.*, 1994; Schmidt *et al.*, 1995) appears to be analogous to the domain in which zebrafish *tbx6* is activated. Similar to *tbx6*, these genes are activated early in gastrulation, but later than the organizer-specific genes (Fainsod *et al.*, 1994). It seems possible either that the signals that trigger ventral-specific gene expression act on both *bmp4* and *tbx6* or that a set of zygotically transcribed ventral genes, perhaps including *bmp4*, are responsible for the activation of *tbx6* transcription (De Robertis and Sasai, 1996; Piccolo *et al.*, 1996; Zimmerman *et al.*, 1996). Experiments are underway to distinguish these possibilities.

ACKNOWLEDGMENTS

We thank Sharon Johnson for excellent assistance with the fish stocks. We thank our colleagues in the field for supplying many reagents required for these studies: anti-Ntl antibody (S. Schulte-Merker), *eve1* plasmid (J.-S. Joly), *ntl* plasmid (S. Schulte-Merker), *snail1* plasmid (J. Postlethwait), activinA (W. Fischer and W. Vale), and mutant lines of zebrafish (C. Kimmel). We thank D. Chapman, S. Mackem, G. Papaioannou, and L. Silver for sharing unpublished results regarding the expression of *tbx6* in the mouse and the chick embryo and C. Sagerstrom, Y. Grinblat, and H. Sive for advice on culturing animal caps. We thank our Utah colleagues, including B. Bisgrove, C. Cretekos, B. Riley, C. Thummel, E. Wilson, and Y. Zhu, for their insights, advice, and criticism. B.H. was supported by a predoctoral fellowship from an NIH Genetics Training Grant. This work was supported by grants from the NIH (1 RO1 RR10253-01) and NSF (MCB-9420984).

REFERENCES

Agulnik, S. I., Bollag, R. J., and Silver, L. M. (1995). Conservation of the T-box gene family from *Mus musculus* to *Caenorhabditis elegans*. *Genomics* **25,** 214–219.

Agulnik, S. I., Garvey, N., Hancock, S., Ruvinsky, I., Chapman, D. L., Agulnik, I., Bollag, R., Papaioannou, V., and Silver, L. M. (1996). Evolution of mouse T-box genes by tandem duplication and cluster dispersion. *Genetics* **144,** 249–254.

Amaya, E., Musci, T. J., and Kirschner, M. W. (1991). Expression of a dominant negative mutant of the FGF receptor disrupts mesoderm formation in Xenopus embryos. *Cell* **66,** 257–270.

Copyright © 1997 by Academic Press. All rights of reproduction in any form reserved.

Amaya, E., Musci, T. J., and Kirschner, M. W. (1993). FGF signalling in the early specification of mesoderm in Xenopus. *Development* **118,** 477–487.

Beddington, R. S. P., Rashbass, P., and Wilson, V. (1992). Brachyury—A gene affecting mouse gastrulation and early organogenesis. *Development* **1992 Suppl.,** 157–165.

Beddington, R. S., and Smith, J. C. (1993). Control of vertebrate gastrulation: Inducing signals and responding genes. *Curr. Opin. Genet. Dev.* **3,** 655–661.

Bollag, R. J., Siegfried, Z., Cebra-Thomas, J. A., Garvey, N., Davison, E. M., and Silver, L. M. (1994). An ancient family of embryonically expressed mouse genes sharing a conserved protein motif with the T locus. *Nature Genet.* **7,** 383–389.

Chapman, D. L., Agulnik, I., Hancock, S., Silver, L. M., and Papaioannou, V. E. (1996). *Tbx6,* a mouse T-box gene implicated in paraxial mesoderm formation at gastrulation. *Dev. Biol.* **180,** 534–542.

Chesley, P. (1935). Development of the short-tailed mutation in the house mouse. *J. Exp. Zool.* **70,** 429–459.

Conlon, F. L., Sedgwick, S. G., Weston, K. M., and Smith, J. C. (1996). Inhibition of Xbra transcription activation causes defects in mesodermal patterning and reveals autoregulation of Xbra in dorsal mesoderm. *Development* **122,** 2427–2435.

Cunliffe, V., and Smith, J. C. (1992). Ectopic mesoderm formation in Xenopus embryos caused by widespread expression of a Brachyury homologue. *Nature* **358,** 427–430.

Dale, L., Howes, G., Price, B. M. J., and Smith, J. C. (1992). Bone morphogenetic protein 4: A ventralizing factor in early Xenopus development. *Development* **115,** 573–585.

Dale, L., and Slack, J. M. W. (1987a). Fate map for the 32-cell stage of Xenopus laevis. *Development* **99,** 527–551.

Dale, L., and Slack, J. M. W. (1987b). Regional specification within the mesoderm of early embryos of Xenopus laevis. *Development* **100,** 279–295.

Davis, A. P., Witte, D. P., Hsieh-Li, H. M., Potter, S. S., and Capecchi, M. R. (1995). Absence of radius and ulna in mice lacking *hoxa-11* and *hoxd-11. Nature* **375,** 791–795.

De Robertis, E. M. (1995). Dismantling the organizer. *Nature* **374,** 407–408.

De Robertis, E. M., Blum, M., Niehrs, C., and Steinbesser, H. (1992). goosecoid and the organizer. *Development* **1992 Suppl.,** 167–171.

De Robertis, E. M., and Sasai, Y. (1996). A common plan for dorsoventral patterning in Bilateria. *Nature* **380,** 37–40.

Detrich, H. W., III, Kieran, M. W., Chan, F. Y., Barone, L. M., Yee, K., Rundstadler, J. A., Pratt, S., Ransom, D., and Zon, L. I. (1995). Intraembryonic hematopoietic cell migration during vertebrate development. *Proc. Natl. Acad. Sci. USA* **92,** 10713–10717.

Fainsod, A., Steinbesser, H., and De Robertis, E. M. (1994). On the function of BMP-4 in patterning the marginal zone of the Xenopus embryo. *EMBO J.* **13,** 5015–5025.

Gerhart, J., Danilchik, M., Doniach, T., Roberts, S., Rowning, B., and Stewart, R. (1989). Cortical rotation of the Xenopus egg: Consequences for the anteroposterior pattern of embryonic dorsal development. *Development* **1989 Suppl.,** 37–51.

Gerhart, J., Doniach, T., and Stewart, R. (1991). Organizing the Xenopus organizer. *In* "Gastrulation: Movements, Patterns and Molecules" (W. H. Clark, Jr. and F. Griffin, Eds.), pp. 57–77. Plenum Press, New York.

Gont, L. K., Steinbesser, H., Blumberg, B., and De Robertis, E. M. (1993). Tail formation as a continuation of gastrulation: The multiple cell populations of the Xenopus tailbud derive from the late blastopore lip. *Development* **119,** 991–1004.

Graff, J. M., Thies, R. S., Song, J. J., Celeste, A. J., and Melton, D. A. (1994). Studies with a Xenopus BMP receptor suggest that ventral mesoderm-inducing signals override dorsal signals in vivo. *Cell* **79,** 169–179.

Green, J. B. A., New, H. V., and Smith, J. C. (1992). Responses of embryonic Xenopus cells to activin and FGF are separated by multiple dose thresholds and correspond to distinct axes of the mesoderm. *Cell* **71,** 731–739.

Griffin, K., Patient, R. K., and Holder, N. (1995). Analysis of FGF function in normal and no tail zebrafish embryos reveals separate mechanisms for formation of the trunk and the tail. *Development* **121,** 2983–2994.

Halpern, M. E., Ho, R. K., Walker, C., and Kimmel, C. B. (1993). Induction of muscle pioneers and floor plate is distinguished by the zebrafish no tail mutation. *Cell* **75,** 99–111.

Hammerschmidt, M., and Nusslein-Volhard, C. (1993). The expression of a gene homologous to Drosophila *snail* suggests a conserved function in invertebrate and vertebrate gastrulation. *Development* **119,** 1107–1118.

Hauptmann, G., and Gerster, T. (1994). 2-color whole-mount in situ hybridization to vertebrate and Drosophila embryos. *Trends Genet.* **10,** 266.

Helde, K. A., and Grunwald, D. J. (1993). The DVR-1 (Vg1) transcript of zebrafish is maternally supplied and distributed throughout the embryo. *Dev. Biol.* **159,** 418–426.

Herrmann, B. G. (1991). Expression pattern of the Brachyury gene in whole-mount T^{Wis}/T^{Wis} mutant embryos. *Development* **113,** 913–917.

Herrmann, B. G. (1995a). Introduction: The Brachyury gene. *Semin. Dev. Biol.* **6,** 381–384.

Herrmann, B. G. (1995b). The mouse Brachyury (T) gene. *Semin. Dev. Biol.* **6,** 385–394.

Herrmann, B. G., and Kispert, A. (1994). The T genes in embryogenesis. *Trends Genet.* **10,** 280–286.

Ho, R. K., and Kimmel, C. B. (1993). Commitment of cell fate in the early zebrafish embryo. *Science* **261,** 109–111.

Joly, J-S., Joly, C., Schulte-Merker, S., Boulekbache, H., and Condamine, H. (1993). The ventral and posterior expression of the zebrafish homeobox gene eve1 is perturbed in dorsalized and mutant embryos. *Development* **119,** 1261–1275.

Jones, C. M., Lyons, K. M., Lapan, P. M., Wright, C. V. E., and Hogan, B. L. M. (1992). DVR-4 (bone morphogenetic protein-4) as a posterior-ventralizing factor in Xenopus mesoderm induction. *Development* **115,** 639–647.

Kane, D. A., and Kimmel, C. B. (1993). The zebrafish midblastula transition. *Development* **119,** 447–456.

Keller, R., and Danilchik, M. (1988). Regional expression, pattern and timing of convergence and extension during gastrulation of Xenopus laevis. *Development* **103,** 193–209.

Kimelman, D., Christian, J. L., and Moon, R. T. (1992). Synergistic principles of development: Overlapping patterning systems in *Xenopus* mesoderm induction. *Development* **116,** 1–9.

Kimmel, C. B., Ballard, W. M., Kimmel, S. R., Ullmann, B., and Schilling, T. F. (1995). Stages of embryonic development of the zebrafish. *Dev. Dyn.* **203,** 253–310.

Kimmel, C. B., Kane, D. A., Walker, C., Warga, R. M., and Rothman, M. B. (1989). A mutation that changes cell movement and cell fate in the zebrafish embryo. *Nature* **337,** 358–362.

Kimmel, C. B., Warga, R. M., and Schilling, T. F. (1990). Origin and organization of the zebrafish fate map. *Development* **108,** 581–594.

Kispert, A. (1995). The Brachyury protein: A T-domain transcription factor. *Semin. Dev. Biol.* **6,** 395–403.

Copyright © 1997 by Academic Press. All rights of reproduction in any form reserved.

Kispert, A., and Herrmann, B. G. (1993). The Brachyury gene encodes a novel DNA binding protein. *EMBO J.* **12,** 3211–3220.

Kispert, A., Koschorz, B., and Herrmann, B. G. (1995). The T protein encoded by Brachyury is a tissue-specific transcription factor. *EMBO J.* **14,** 4763–4772.

Knezevic, V., De Santo, R., and Mackem, S. (1997). Two novel chick T-box genes related to mouse *Brachyury* are expressed in different, non-overlapping mesodermal domains during gastrulation. *Development* **124,** 411–419.

Koster, M., Plessow, S., Clement, J. H., Lorenz, A., Tiedemann, H., and Knochel, W. (1991). Bone morphogenetic protein 4 (BMP-4), a member of the TGF-beta family in early embryos of *Xenopus laevis:* Analysis of mesoderm inducing activity. *Mech. Dev.* **33,** 191–200.

Lawson, K. A., and Pedersen, R. A. (1992). Clonal analysis of cell fate during gastrulation and early neurulation in the mouse. *In* "Postimplantation Development in the Mouse" (D. J. Chadwick and J. Marsh, Eds.), pp. 3–26. Wiley, Chichester.

Moon, R. T., and Christian, J. L. (1992). Competence modifiers synergize with growth factors during mesoderm induction and patterning in *Xenopus. Cell* **71,** 709–712.

Nieuwkoop, P. D. (1973). The "organizer center" of the amphibian embryo: Its origin, spatial organization, and morphogenetic action. *Adv. Morphogenet.* **10,** 1–39.

Piccolo, S., Sasai, Y., Lu, B., and De Robertis, E. M. (1996). Dorsoventral patterning in Xenopus: Inhibition of ventral signals by direct binding of chordin to BMP-4. *Cell* **86,** 589–598.

Schmidt, J. E., Suzuki, A., Ueno, N., and Kimelman, D. (1995). Localized BMP-4 mediates dorsal/ventral patterning in the early Xenopus embryo. *Dev. Biol.* **169,** 37–50.

Schulte-Merker, S. (1995). The zebrafish no tail gene. *Semin. Dev. Biol.* **6,** 411–416.

Schulte-Merker, S., Hammerschmidt, M., Beuchle, D., Cho, K., De-Robertis, E. M., and Nusslein-Volhard, C. (1994a). Expression of zebrafish goosecoid and no tail gene products in wild-type and mutant no tail embryos. *Development* **120,** 843–852.

Schulte-Merker, S., Ho, R. K., Herrmann, B. G., and Nusslein-Volhard, C. (1992). The protein product of the zebrafish homologue of the mouse T gene is expressed in nuclei of the germ ring and the notochord of the early embryo. *Development* **116,** 1021–1032.

Schulte-Merker, S., van Eeden, F. M., Halpern, M. E., Kimmel, C. B., and Nusslein-Volhard, C. (1994b). no tail (ntl) is the zebrafish homologue of the mouse T (Brachyury) gene. *Development* **120,** 1009–1015.

Slack, J. M. W. (1994). Inducing factors in Xenopus early embryos. *Curr. Biol.* **4,** 116–126.

Smith, J. C. (1993). Mesoderm-inducing factors in early vertebrate development. *EMBO J.* **12,** 4463–4470.

Smith, J. C., Cunliffe, V., O'Reilly, M-A. J., Schulte-Merker, S., and Umbhauer, M. (1995). Xenopus Brachyury. *Semin. Dev. Biol.* **6,** 405–410.

Smith, J. C., Dale, L., and Slack, J. M. W. (1985). Cell lineage labels and region-specific markers in the analysis of inductive interactions. *J. Embryol. Exp. Morphol.* **89 Suppl.,** 317–331.

Smith, J. C., Price, B. M. J., Green, J. B. A., Weigel, D., and Herrmann, B. G. (1991). Expression of a *Xenopus* homolog of *Brachyury* (*T*) is an immediate-early response to mesoderm induction. *Cell* **67,** 79–87.

Spemann, H., and Mangold, H. (1924). Uber Induktion von Embryonalanlagen durch Implantation artfremder Organisatoren. *Arch. Mikr. Anat. Entwicklungsmech. Org.* **100,** 599–638.

Stachel, S. E., Grunwald, D. J., and Myers, P. Z. (1993). Lithium perturbation and *goosecoid* expression identify a dorsal specification pathway in the pre-gastrula zebrafish. *Development* **117,** 1261–1274.

Streit, A., Thiery, C., and Stern, C. D. (1994). Of mice and frogs. *Trends Genet.* **10,** 181–183.

Suzuki, A., Thies, R. S., Yamaji, N., Song, J. J., Wozney, J. M., Murakami, K., and Ueno, N. (1994). A truncated bone morphogenetic receptor affects dorsal–ventral patterning in the early *Xenopus* embryo. *Proc. Natl. Acad. Sci. USA* **91,** 10255–10259.

Tam, P. P. L., and Quinlan, G. A. (1996). Mapping vertebrate embryos. *Curr. Biol.* **6,** 104–106.

Thisse, C., Thisse, B., Schilling, T. F., and Postlethwait, J. H. (1993). Structure of the zebrafish snail1 gene and its expression in wild-type, spadetail and no tail mutant embryos. *Development* **119,** 1203–1215.

Weinberg, E. S., Allende, M. L., Kelly, C. S., Abdelhamid, A., Murakami, T., Andermann, P., Doerre, O. G., Grunwald, D. J., and Riggleman, B. (1996). Developmental regulation of zebrafish *MyoD* in wild-type, *no tail* and *spadetail* embryos. *Development* **122,** 271–280.

Westerfield, M. (1993). "The Zebrafish Book. A Guide for the Laboratory Use of Zebrafish." Univ. Oregon Press, Eugene, OR.

Wilkinson, D. G., Bhatt, S., and Herrmann, B. G. (1990). Expression pattern of the mouse T gene and its role in mesoderm formation. *Nature* **343,** 657–659.

Wilson, V., Manson, L., Skarnes, W. C., and Beddington, R. S. P. (1995). The T gene is necessary for normal mesodermal morphogenetic cell movements during gastrulation. *Development* **121,** 877–886.

Wilson, V., Rashbass, P., and Beddington, R. S. P. (1993). Chimeric analysis of T (Brachyury) gene function. *Development* **117,** 1321–1331.

Zimmerman, L. B., De Jesus-Escobar, J. M., and Harland, R. M. (1996). The Spemann organizer signal noggin binds and inactivates bone morphogenetic protein 4. *Cell* **86,** 599–606.

Received for publication September 17, 1996
Accepted December 6, 1996

Copyright © 1997 by Academic Press. All rights of reproduction in any form reserved.

DEVELOPMENTAL BIOLOGY 183, 74–85 (1997)
ARTICLE NO. DB968481

Characterisation of Amphioxus HNF-3 Genes: Conserved Expression in the Notochord and Floor Plate

Sebastian M. Shimeld
School of Animal and Microbial Sciences, The University of Reading, Whiteknights, Reading, RG6 6AJ United Kingdom

The *fork head/HNF-3* genes form a subclass of a family of transcription factors united by the possession of a conserved DNA binding domain known as the fork head domain. Most vertebrate HNF-3 class genes show several conserved sites of expression during development, including the dorsal lip/Hensen's node, notochord and floor plate, all structures known to organise adjacent tissues. In this paper I report the characterisation of HNF-3 class genes from the cephalochordate amphioxus. I show that amphioxus has two HNF-3 class genes, named *AmHNF-3-1* and *AmHNF-3-2*; molecular phylogenetic analysis reveals that these derive from an independent duplication in the cephalochordate lineage. The expression of both genes in early development appears identical and shows striking similarities to that of vertebrates. In neurulae, transcripts of both genes were detected in the presumed organiser, endoderm, and notochord, supporting morphological and embryological evidence that these are homologous between vertebrates and amphioxus. This expression pattern overlaps considerably with that of amphioxus *brachyury*, suggesting that the functional relationship between these genes in vertebrates is conserved with amphioxus. Expression of both genes was maintained in the endoderm and notochord up to the 6 somite stage. After the 6 somite stage no expression of *AmHNF-3-2* was detected and expression of *AmHNF-3-1* began to decrease in the notochord, such that by the 10 somite stage transcripts were only detected in the terminal regions. At this stage, however, a column of *AmHNF-3-1*-expressing cells was detected at the ventral midline of the neural tube, a position occupied by the floor plate in vertebrates. This is the first evidence that amphioxus has a floor plate which is specified by a mechanism conserved with vertebrates. Taken together these data support two conclusions: Firstly, that the role of the dorsal lip/Hensen's node, notochord, and floor plate as organisers of the vertebrate body plan evolved prior to the separation of the vertebrate and cephalochordate lineages, at least 520 million years ago. Secondly, that the role of HNF-3 genes in these structures predates the origin of the multiple HNF-3 genes found in vertebrates. © 1997 Academic Press

INTRODUCTION

Families of genes encoding conserved protein domains play prominent roles during the development of metazoans. One such gene family is that initially defined by the conservation of an 110-amino-acid protein domain between the *Drosophila* gene *fork head* (*fkh*) and the rat liver factors *HNF-3α*, *β*, and *γ* (Weigel and Jäckle, 1990). This conserved domain, termed the fork head domain, forms a structure known as a winged helix and has been shown to be involved in DNA binding (Clarke *et al.*, 1993; Kauffman *et al.*, 1994). This suggests that proteins possessing a fork head domain are capable of acting as transcription factors.

The abundance of genes encoding fork head domains has been investigated in mice, humans, *Xenopus*, zebrafish, and *Drosophila* (Hacker *et al.*, 1992; Clevidence *et al.*, 1993; Hromas *et al.*, 1993; Kaestner *et al.*, 1993; King and Moore, 1994; Pierrou *et al.*, 1994; Dirksen and Jamrich, 1995). Current data indicate that, while there are numerous fork head domain genes in the genomes of these organisms, the *Drosophila fkh/HNF-3* group of genes (which includes *HNF-3α*, *β*, and *γ* in the mouse, *HNF-3β* in the chick, *HNF-3β*, *XFKH2*, and *pintallavis* in *Xenopus*, and *axial* in zebrafish) are more similar to each other than to other fork head domain-encoding genes. Therefore, the HNF-3/fkh genes can be considered a separate class within the fork head domain family and are hereafter termed the HNF-3 class.

The expression of *HNF-3β* has been examined in rat, mouse, chick, *Xenopus*, and zebrafish embryos (Ang *et al.*, 1993; Monaghan *et al.*, 1993; Ruiz i Altaba *et al.*, 1993b, 1995; Sasaki and Hogan, 1993; Strähle *et al.*, 1993). Comparison of these expression patterns reveals several common

0012-1606/97 $25.00
Copyright © 1997 by Academic Press
All rights of reproduction in any form reserved.

sites of expression; the endoderm, the embryonic organiser, the floor plate of the neural tube, and, with the exception of *Xenopus*, the notochord express *HNF-3β* in all these species. Similarly, rat and mouse *HNF-3α* and their probable orthologue in *Xenopus*, *XFKH2*, are also expressed in these tissues; differences in timing and in regional endoderm expression distinguish them from the *HNF-3β* expression pattern (Ang *et al.*, 1993; Bolce *et al.*, 1993; Monaghan *et al.*, 1993; Ruiz i Altaba *et al.*, 1993b; Sasaki and Hogan, 1993). Two other HNF-3 class genes, *HNF-3γ* and *pintallavis*, have also been characterised in vertebrates. *HNF-3γ* has been isolated from mouse and rat and has been found to be expressed only in a subset of endoderm-derived tissues (Monaghan *et al.*, 1993; Ruiz i Altaba *et al.*, 1993b). *pintallavis* is a *Xenopus* gene which has not been directly assigned to any particular mouse gene the basis of sequence. *pintallavis* expression is confined to the dorsal lip, hypochord, notochord, and floor plate (Dirksen and Jamrich, 1992; Knöchel *et al.*, 1992; Ruiz i Altaba and Jessell, 1992). The observation that the sum of the expression patterns of *Xenopus pintallavis* and *HNF-3β* were similar to that of mouse *HNF-3β* alone led Ruiz i Altaba *et al.* (1995) to propose that *pintallavis* is specific to *Xenopus* and that an orthologous gene does not exist in the mouse or chick genome.

There are species-specific and conserved features of the expression patterns of vertebrate HNF-3 class genes. Particularly striking is the conserved expression in the organiser and in the midline structures of the notochord and floor plate, all tissues which have been shown to organise adjacent tissues during development (Spemann and Mangold, 1924; Placzek *et al.*, 990; Yamada *et al.*, 1993). There is also evidence to suggest that the functions of some HNF-3 class genes in these tissues are conserved. The early role of *HNF-3β* in the mouse and *pintallavis* in *Xenopus* appears to involve the control of notochord specification/differentiation, a function which may involve synergy with *Brachyury* (Ang and Rossant, 1994; Weinstein *et al.*, 1994; O'Reilley *et al.*, 1995). Later in development, gain-of-function experiments in *Xenopus* and mouse have shown that expression of *pintallavis* or *HNF-3β* can cause ectopic differentiation of floor plate in inappropriate areas of the neural tube (Ruiz i Altaba and Jessell, 1992; Ruiz i Altaba *et al.*, 1993a; Sasaki and Hogan 1994). These results indicate that expression of these HNF-3 class genes does not just mark these organising structures but has a role in their specification and/or function. The role of other HNF-3 class genes in mesoderm and neurectoderm and the role of all HNF-3 class genes in embryonic endoderm is yet to be determined.

The comparison of gene expression patterns between taxa can provide insight into the evolution and development of both conserved and derived body structures (for example, see Akam *et al.*, 1994). To apply such comparison to the Vertebrata, the most appropriate taxa for study are the two other subphlya in phylum Chordata, the Urochordata and Cephalochordata. Thus, to increase our understanding of the role of HNF-3 class genes in vertebrate development and the evolution of the structures in which they are expressed, I have characterised HNF-3 class genes from the cephalochordate amphioxus. I show that amphioxus has at least two HNF-3 class genes, named *AmHNF-3-1* and *AmHNF-3-2*, which are more closely related to each other than to any vertebrate gene, suggesting they have arisen from an independent duplication in the cephalochordate lineage. The expression of these genes in amphioxus neurulae is strikingly similar to that of the vertebrate HNF-3 class genes: Transcripts were first detected in the presumptive organiser of gastrulating embryos and in invaginating presumptive notochord and endoderm cells. Subsequently, transcripts of both genes were detected in the notochord and endoderm. Transcripts of *AmHNF-3-1* were also detected in the ventral midline of the neural tube, providing the first molecular evidence that the amphioxus neural tube has a distinct floor plate. These data suggest that the role of the node, notochord, and floor plate as organisers in chordate embryos evolved before the divergence of the cephalochordate and vertebrate lineages.

MATERIALS AND METHODS

DNA Extraction and in Vitro Fertilisation of Amphioxus

Adult amphioxus (*Branchiostoma floridae*) were collected from Old Tampa Bay, Florida, in August 1994 and 1995. Individual adults for DNA extraction were homogenised in 1 ml of guanidinium isothiocyanate solution (4 *M* guanidinium isothiocyanate, 50 m*M* Tris–HCl, pH 7.6, 10 m*M* EDTA, 2% Sarcosyl with 1% β-mercaptoethanol added immediately prior to use) and stored at −20°C. For genomic DNA extraction, 1 ml of phenol (saturated with TE, pH 7.6), 0.2 ml of chloroform:isoamyl alcohol (49:1), and 0.1 ml of 2 *M* sodium acetate, pH 5.4, were added and the mixture was gently shaken and left on ice for 15 min. The samples were then centrifuged at 5000*g* for 20 min, and the aqueous layer was extracted once with TE-equilibrated phenol and once with chloroform and precipitated with ethanol. The resulting precipitate of genomic DNA was washed in 70% ethanol, dried, and resuspended in 400 μl of TE.

Ripe adults were used for *in vitro* fertilisation as described by Holland and Holland (1993). Embryos and larvae were reared in filtered seawater at 24°C and fixed overnight at 4°C in Mops-buffered paraformaldehyde (4% paraformaldehyde in 0.5 *M* NaCl, 1 m*M* $MgSO_4$, 2 m*M* EGTA, 0.1 *M* morpholinopropanesulfonic acid, pH 7.5) before transfer to 70% ethanol and storage at −20°C.

PCR Amplification of Amphioxus HNF-3 Homologues

Degenerate oligonucleotide primers corresponded to the amino acid sequences TL(SN)EIYQW (FK1, sense primer) and QKRFK-(DCL)E (FK3, antisense primer). The corresponding DNA sequences were: FK1 (5′ to 3′): ACGCTGAGTGA(AG)AT(ATC)TA(TC)-CA(AG)TGG and FK3 (5′ to 3′): CCTCTCACACTTGAA(ACT-G)C(CG)(TC)TT(CT)TG.

These sequences are highly conserved between vertebrate HNF-3 genes and *Drosophila fork head* but less conserved in other genes containing fork head-related domains. PCR amplification was per-

Copyright © 1997 by Academic Press. All rights of reproduction in any form reserved.

formed for 35 cycles of 94°C (60 sec), 52°C (45 sec), 72°C (60 sec) preceded by an initial denaturation at 94°C (90 sec) and followed by a final extension at 72°C (120 sec). PCR products were blunt ended (Holland 1993) and cloned into *Sma*1-cut pUC-18 (Pharmacia).

Isolation and Characterization of Genomic and cDNA Clones of Amphioxus HNF3

An amphioxus genomic library in LambdaFIXII (Garcia-Fernàndez and Holland, 1994) and two cDNA libraries in LambdaZAPII (one made from 3- to 5-day larvae and a gift from L. Z. Holland, Scripps Oceanographic Institute, the second made from 5- to 24-hr embryos and a gift from J. Langeland, University of Oregon) were screened with PCR-derived fragments. Hybridisations were carried out in the buffer described by Church and Gilbert (1984) at 65°C and hybridising clones plaque purified. cDNA's were rescued in pBSII(SK+) (according to Stratagene's instructions) and sequenced in both directions by a combination of subcloning and walking with specific oligonucleotide primers. DNA from genomic clones was prepared according to Sambrook *et al.* (1989) and mapped by Southern blotting. Fragments hybridising to the amphioxus HNF3 PCR-derived probe were cloned into pBSII(SK+) (Stratagene) and sequenced with primers FK1 and FK3.

Genomic Southern Analysis

DNA prepared from individual adult amphioxus of known sex was digested with *Eco*RI or *Hin*dIII and electrophoresed on a 0.7% agarose gel. After staining with ethidium bromide to visualise the DNA, the gel was depurinated, denatured, and neutralised according to Sambrook *et al.* (1989) and transferred onto Hybond N (Amersham). Southern blots were hybridised as described for library screening.

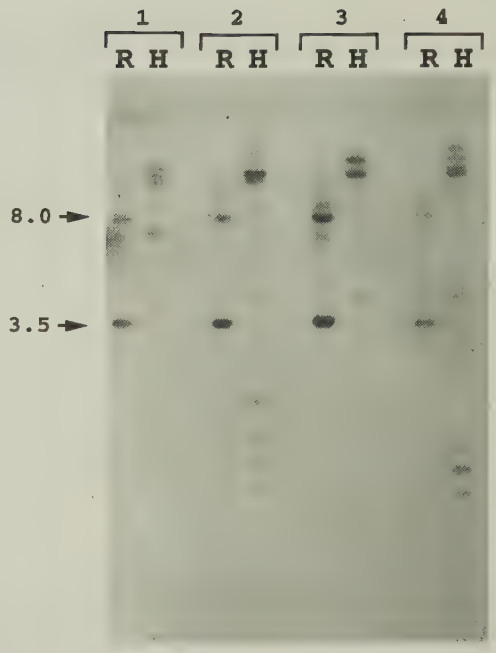

FIG.1. Southern blot of genomic DNA extracted from four individual adult amphioxus, digested with *Eco*RI (R) or *Hin*dIII (H) and hybridised to the *AmHNF-3-1* PCR probe at reduced stringency. In the *Eco*RI digest lanes two major bands are seen at approximately 8.0 and 3.5 kb, matching the sizes of *AmHNF-3-1* and *AmHNF-3-2* predicted from analysis of genomic clones. Multiple weaker bands are also present, suggesting that the amphioxus genome contains other genes encoding fork head domains distantly related to *AmHNF-3-1*.

Molecular Phylogeny of HNF-3 Genes

Alignments of vertebrate and amphioxus HNF-3 and *Drosophila* fork head protein sequences were assembled using the CLUSTAL V program (Higgins *et al.*, 1991). Phylogenies were constructed using the SEQBOOT, PROTDIST, NEIGHBOR, PROTPARS, and CONSENSE subprograms of the PHYLIP 3.5 package (Felsenstein, 1993), implemented by the human genome mapping project computers at Hinxton Hall, Cambridge. Confidence in the phylogeny was assessed by performing 100 bootstrap resamplings of the data.

Whole-Mount in Situ Hybridisation

Whole-mount *in situ* hybridisation was carried out as described by Holland *et al.* (1995). RNA antisense to *AmHNF-3-1* was synthesised from the entire *AmHNF-3-1* cDNA or from a 0.8-kb subclone containing only 3' untranslated sequence. The latter probe gave identical results to the entire cDNA, although with higher background level. RNA antisense to *AmHNF-3-2* was synthesised from the entire *AmHNF-3-2* cDNA. Since the two genes share only 72% similarity in the 300 bp forming the most conserved region, no cross-hybridisation should occur at the stringency used. Stained embryos were stored in 4% formaldehyde in PBS and mounted under coverslips in 100% glycerol for photography using Kodak 100T or Fuji 64T film. For sectioning, embryos were dehydrated in ethanol, stained in 1% eosin in ethanol or 1% poinceau S in 1% acetic acid for 30 min, and then set in LR White medium resin (TAAB Laboratory Supplies). Sections were cut at 3.5 μm.

RESULTS

Isolation of Amphioxus HNF-3 PCR and Genomic Clones

PCR amplification of amphioxus genomic DNA with primers FK1 and FK3 identified a fragment of a single gene which contained a fork head domain most closely related to the HNF-3 class. This fragment was used to isolate hybridising phage clones from an amphioxus genomic library; however, mapping of these phage resolved them into two distinct sets of overlapping clones (data not shown). To determine if these sets represented two independent HNF-3 class genes, the relevant fragments were subcloned and the fork head domains sequenced. This revealed two different HNF-3 class fork head domain-encoding sequences with 72% similarity and 81% identity to each other. These were named *AmHNF-3-1* and *AmHNF-3-2*. To confirm that these were separate loci and did not represent different alleles of the same gene, a Southern blot of genomic DNA extracted from individual amphioxus was probed with the PCR-derived HNF-3 domain fragment (Fig. 1). This revealed two

Copyright © 1997 by Academic Press. All rights of reproduction in any form reserved.

major hybridising bands for each individual, the sizes of which matched that predicted from the two sets of genomic phage. These data indicate that the amphioxus genome contains two HNF-3 class genes.

Isolation of AmHNF-3-1 cDNA Clones

Screening of amphioxus embryonic cDNA libraries with the *AmHNF-3* PCR clone identified eight hybridising clones. Sequencing the fork head domains of these clones resolved them into two groups, with three clones having identical sequence to *AmHNF-3-1* and five to *AmHNF-3-2.* The longest representative of each gene was fully sequenced and found to encode 404-amino-acid (AmHNF-3-1) and 442-amino-acid (AmHNF-3-2) proteins. Comparison of the deduced protein sequences with those encoded by the vertebrate HNF-3 class genes conclusively identified them as amphioxus HNF-3 class genes; important distinguishing features included two conserved domains found only in HNF-3 class genes, including *Drosophila* fork head, which were present at the carboxy end of the protein (Fig. 2). There is also limited conservation at the amino terminus; however, outside of these conserved domains the proteins bear no relationship to any specific vertebrate HNF-3 class protein.

Molecular Phylogenetic Reconstruction of HNF-3 Class Genes

Molecular phylogenetic reconstruction was performed using the 110-amino-acid fork head domain of characterised HNF-3 class genes; *zf-FKH-1* and *zf-FKH-2,* which are probably also HNF-3 class genes, were not included since only partial sequence of the fork head domain is available (Dirksen and Jamrich, 1995). A phylogenetic tree constructed by Neighbor Joining is shown in Fig. 3. Analysis of the same data by maximum parsimony produced a tree with the same topography but higher bootstrap values (not shown). Neither of these two programs assume a root to the tree; however, on the basis of the conventional classification of these taxa, I place the root between *Drosophila* and amphioxus.

The results strongly support the hypothesis that the two amphioxus HNF-3 class genes are derived form an independent duplication in the cephalochordate lineage; thus, neither can be considered closer than the other to any single vertebrate HNF-3 gene. The tree also supports the hypothesis that there have been two separate duplications in the lineage leading to vertebrates, the first creating *HNF-3β* and an *HNF-3α/γ* hybrid, the second affecting only this hybrid and creating *HNF-3α* and *HNF-3γ*. The exact position of *pintallavis* in this phylogeny is uncertain; the bootstrap value of 80 strongly suggests it clusters with *HNF-3α* and *HNF-3γ*, but its exact relationship to these genes is unresolved.

Expression of AmHNF-3-1 and AmHNF-3-2 in Amphioxus Gastrulae and Neurulae

Whole-mount *in situ* hybridisation was used to examine the expression of *AmHNF-3-1* and *AmHNF-3-2* between 7 and 36 hr of development, encompassing a period from gastrulation through to the early larva (Hatschek, 1881). In early gastrulae, no expression of *AmHNF-3-1* or *-AmHNF-3-2* was detected. By 10 hr of development, amphioxus embryos reach the early neurula stage. In these embryos transcripts of both genes were detected around the blastopore (Figs. 4A and 4B). Transcripts were also detected in invaginated dorsal mesodermal cells which are fated to form the notochord and in the invaginating endoderm (Figs. 4A–4D and 5A). No qualitative differences were detected between the expression patterns of *AmHNF-3-1* and *AmHNF-3-2* at these stages. However, despite the use of equivalent reaction conditions and similar length probes, embryos hybridised to *AmHNF-3-2* took four to five times longer to stain than embryos hybridised to *AmHNF-3-1.* This suggests a significant quantitative difference between the expression levels of the two genes, with *AmHNF-3-1* expressed at higher levels than *AmHNF-3-2.*

Expression of AmHNF-3-1 and AmHNF-3-2 between the Neurula and Larval Stages

By the late neurula stage the essentials of the chordate body plan, the dorsal to ventral ordering of the neural plate, notochord, and endoderm, are established. The subsequent 18 hr of amphioxus development are apparent externally by the anterior–posterior lengthening of the body and by the sequential formation of the somites (Hatschek, 1881; Willey, 1894).

Early during this period, in embryos with approximately six somites, expression of *AmHNF-3-1* and *AmHNF-3-2* was detected throughout the notochord (Figs. 4E and 4F) Expression of both genes was also detected in the endoderm, with an anterior boundary separating nonexpressing cells in the pharyngeal region with expressing cells to the posterior. Sectioning of embryos at this stage confirmed the tissue localisations described above and failed to identify any expressing cells in the neural tube (Figs. 5B–5D). Detection of *AmHNF-3-2* at this stage required extreme lengthening of the staining process (to greater than 48 hr).

By the 8 somite stage expression of *AmHNF-3-2* could no longer be detected (data not shown). Expression of *AmHNF-3-1* was still detected in the endoderm and the notochord, although expression in all but the terminal regions of the notochord had begun to decrease (Fig. 4G). This reduction in expression in the centre of the notochord continued such that by the 10 somite stage it was confined to the extreme anterior and posterior cells (Figs. 4H, 6A, and 6D). Expression of *AmHNF-3-1* in the posterior endoderm of 10 somite embryos began to decrease, leaving a central block of cells maintaining strong *AmHNF-3-1* expression (Fig. 4H). At this stage expression was also detected in midline endoderm beneath the anterior notochord.

Copyright © 1997 by Academic Press. All rights of reproduction in any form reserved.

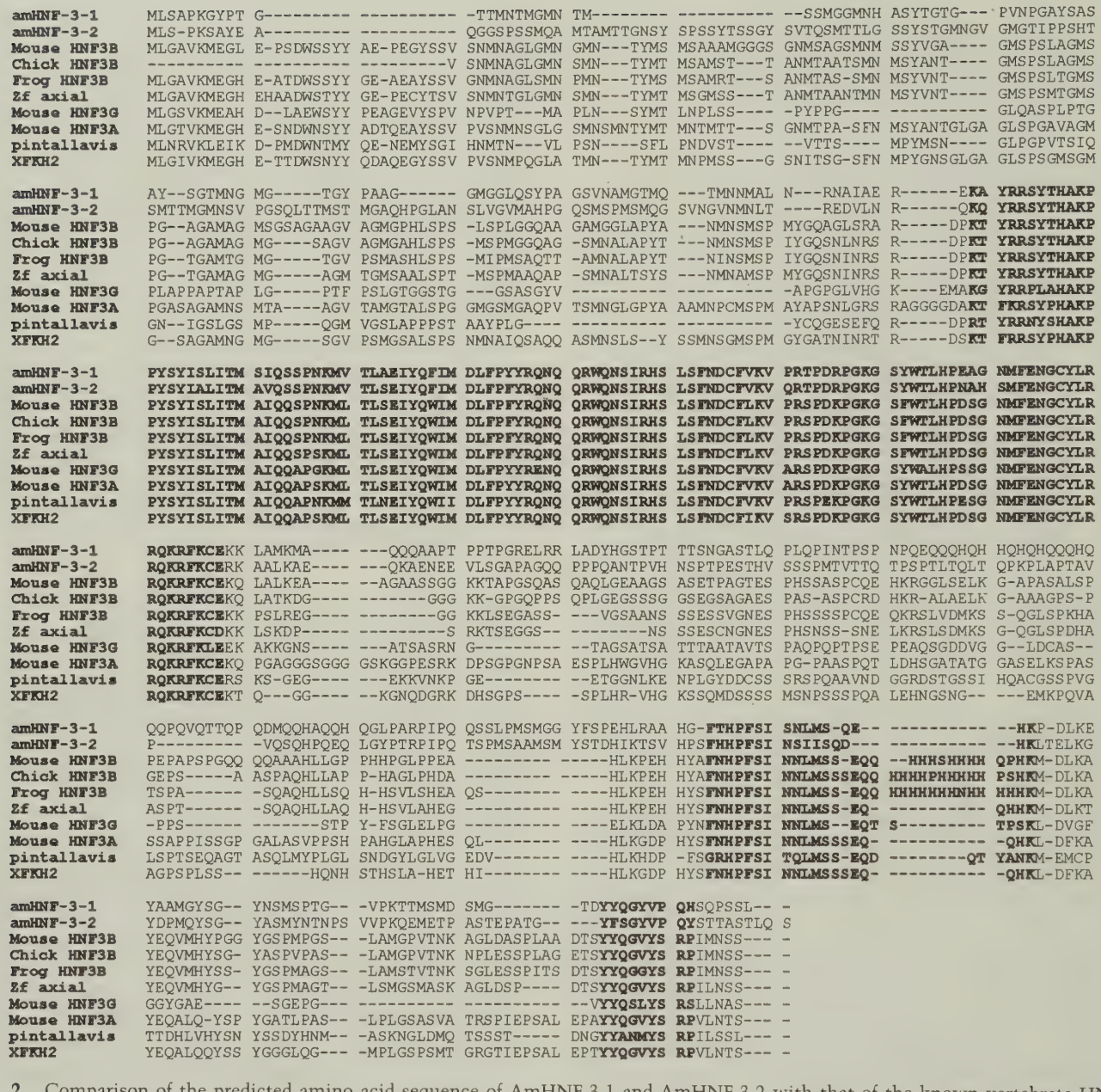
amHNF-3-1 MLSAPKGYPT G--------- ---------- -TTMNTMGMN TM-------- ---------- --SSMGGMNH ASYTGTG---PVNPGAYSAS
amHNF-3-2 MLS-PKSAYE A--------- ---------- QGGSPSSMQA MTAMTTGNSY SPSSYTSSGY SVTQSMTTLG SSYSTGMNGV GMGTIPPSHT
Mouse HNF3B MLGAVKMEGL E-PSDWSSYY AE-PEGYSSV SNMNAGLGMN GMN---TYMS MSAAAMGGGS GNMSAGSMNM SSYVGA---- GMSPSLAGMS
Chick HNF3B ---------- ---------- ---------V SNMNAGLGMN SMN---TYMT MSAMST---T ANMTAATSMN MSYANT---- GMSPSLAGMS
Frog HNF3B MLGAVKMEGH E-ATDWSSYY GE-AEAYSSV GNMNAGLSMN PMN---TYMS MSAMRT---S ANMTAS-SMN MSYVNT---- GMSPSLTGMS
Zf axial MLGAVKMEGH EHAADWSTYY GE-PECYTSV SNMNTGLGMN SMN---TYMT MSGMSS---T ANMTAANTMN MSYVNT---- GMSPSMTGMS
Mouse HNF3G MLGSVKMEAH D--LAEWSYY PEAGEVYSPV NPVPT---MA PLN---SYMT LNPLSS---- -PYPPG---- ---------- GLQASPLPTG
Mouse HNF3A MLGTVKMEGH E-SNDWNSYY ADTQEAYSSV PVSNMNSGLG SMNSMNTYMT MNTMTT---S GNMTPA-SFN MSYANTGLGA GLSPGAVAGM
pintallavis MLNRVKLEIK D-PMDWNTMY QE-NEMYSGI HNMTN---VL PSN----SFL PNDVST---- --VTTS---- MPYMSN---- GLPGPVTSIQ
XFKH2 MLGIVKMEGH E-TTDWSNYY QDAQEGYSSV PVSNMPQGLA TMN---TYMT MNPMSS---G SNITSG-SFN MPYGNSGLGA GLSPSGMSGM

amHNF-3-1 AY--SGTMNG MG-----TGY PAAG------ GMGGLQSYPA GSVNAMGTMQ ---TMNNMAL N---RNAIAE R------EKA YRRSYTHAKP
amHNF-3-2 SMTTMGMNSV PGSQLTTMST MGAQHPGLAN SLVGVMAHPG QSMSPMSMQG SVNGVNMNLT ----REDVLN R------QKQ YRRSYTHAKP
Mouse HNF3B PG--AGAMAG MSGSAGAAGV AGMGPHLSPS -LSPLGGQAA GAMGGLAPYA ---NMNSMSP MYGQAGLSRA R-----DPKT YRRSYTHAKP
Chick HNF3B PG--AGAMAG MG----SAGV AGMGAHLSPS -MSPMGGQAG -SMNALAPYT ---NMNSMSP IYGQSNLNRS R-----DPKT YRRSYTHAKP
Frog HNF3B PG--TGAMTG MG-----TGV PSMASHLSPS -MIPMSAQTT -AMNALAPYT ---NINSMSP IYGQSNINRS R-----DPKT YRRSYTHAKP
Zf axial PG--TGAMAG MG-----AGM TGMSAALSPT -MSPMAAQAP -SMNALTSYS ---NMNAMSP MYGQSNINRS R-----DPKT YRRSYTHAKP
Mouse HNF3G PLAPPAPTAP LG-----PTF PSLGTGGSTG ---GSASGYV ---------- ---------- -APGPGLVHG K----EMAKG YRRPLAHAKP
Mouse HNF3A PGASAGAMNS MTA----AGV TAMGTALSPG GMGSMGAQPV TSMNGLGPYA AAMNPCMSPM AYAPSNLGRS RAGGGGDAKT FKRSYPHAKP
pintallavis GN--IGSLGS MP-----QGM VGSLAPPPST AAYPLG---- ---------- ---------- -YCQGESEFQ R-----DPRT YRRNYSHAKP
XFKH2 G--SAGAMNG MG-----SGV PSMGSALSPS NMNAIQSAQQ ASMNSLS--Y SSMNSGMSPM GYGATNINRT R-----DSKT FRRSYPHAKP

amHNF-3-1 PYSYISLITM SIQSSPNKMV TLAEIYQFIM DLFPYYRQNQ QRWQNSIRHS LSFNDCFVKV PRTPDRPGKG SYWTLHPEAG NMFENGCYLR
amHNF-3-2 PYSYIALITM AVQSSPNKMV TLSEIYQFIM DLFPFYRQNQ QRWQNSIRHS LSFNDCFVKV QRTPDRPGKG SYWTLHPNAH SMFENGCYLR
Mouse HNF3B PYSYISLITM AIQQSPNKML TLSEIYQWIM DLFPFYRQNQ QRWQNSIRHS LSFNDCFLKV PRSPDKPGKG SFWTLHPDSG NMFENGCYLR
Chick HNF3B PYSYISLITM AIQQSPNKML TLSEIYQWIM DLFPFYRQNQ QRWQNSIRHS LSFNDCFLKV PRSPDKPGKG SFWTLHPDSG NMFENGCYLR
Frog HNF3B PYSYISLITM AIQQSPNKML TLSEIYQWIM DLFPFYRQNQ QRWQNSIRHS LSFNDCFLKV PRSPDKPGKG SFWTLHPDSG NMFENGCYLR
Zf axial PYSYISLITM AIQQSPSKML TLSEIYQWIM DLFPFYRQNQ QRWQNSIRHS LSFNDCFLKV PRSPDKPGKG SFWTLHPDSG NMFENGCYLR
Mouse HNF3G PYSYISLITM AIQQAPGKML TLSEIYQWIM DLFPYYRENQ QRWQNSIRHS LSFNDCFVKV ARSPDKPGKG SYWALHPSSG NMFENGCYLR
Mouse HNF3A PYSYISLITM AIQQAPSKML TLSEIYQWIM DLFPYYRQNQ QRWQNSIRHS LSFNDCFVKV ARSPDKPGKG SYWTLHPDSG NMFENGCYLR
pintallavis PYSYISLITM AIQQAPNKMM TLNEIYQWII DLFPYYRQNQ QRWQNSIRHS LSFNDCFVKV PRSPEKPGKG SYWTLHPESG NMFENGCYLR
XFKH2 PYSYISLITM AIQQAPSKML TLSEIYQWIM DLFPYYRQNQ QRWQNSIRHS LSFNDCFIKV SRSPDKPGKG SYWTLHPDSG NMFENGCYLR

amHNF-3-1 RQKRFKCEKK LAMKMA---- ---QQQAAPT PPTPGRELRR LADYHGSTPT TTSNGASTLQ PLQPINTPSP NPQEQQQHQH HQHQHQQQHQ
amHNF-3-2 RQKRFKCERK AALKAE---- ---QKAENEE VLSGAPAGQQ PPPQANTPVH NSPTPESTHV SSSPMTVTTQ TPSPTLTQLT QPKPLAPTAV
Mouse HNF3B RQKRFKCEKQ LALKEA---- --AGAASSGG KKTAPGSQAS QAQLGEAAGS ASETPAGTES PHSSASPCQE HKRGGLSELK G-APASALSP
Chick HNF3B RQKRFKCEKQ LATKDG---- -------GGG KK-GPGQPPS QPLGEGSSSG GSEGSAGAES PAS-ASPCRD HKR-ALAELK G-AAAGPS-P
Frog HNF3B RQKRFKCEKK PSLREG---- ---------GG KKLSEGASS- ---VGSAANS SSESSVGNES PHSSSSPCQE QKRSLVDMKS S-QGLSPKHA
Zf axial RQKRFKCDKK LSKDP----- ---------S RKTSEGGS-- --------NS SSESCNGNES PHSNSS-SNE LKRSLSDMKS G-QGLSPDHA
Mouse HNF3G RQKRFKLEEK AKKGNS---- ---ATSASRN G--------- --TAGSATSA TTTAATAVTS PAQPQPTPSE PEAQSGDDVG G--LDCAS--
Mouse HNF3A RQKRFKCEKQ PGAGGGSGGG GSKGGPESRK DPSGPGNPSA ESPLHWGVHG KASQLEGAPA PG-PAASPQT LDHSGATATG GASELKSPAS
pintallavis RQKRFKCERS KS-GEG---- ---EKKVNKP GE-------- --ETGGNLKE NPLGYDDCSS SRSPQAAVND GGRDSTGSSI HQACGSSPVG
XFKH2 RQKRFKCEKT Q---GG---- --KGNQDGRK DHSGPS---- -SPLHR-VHG KSSQMDSSSS MSNPSSSPQA LEHNGSNG-- ---EMKPQVA

amHNF-3-1 QQPQVQTTQP QDMQQHAQQH QGLPARPIPQ QSSLPMSMGG YFSPEHLRAA HG-FTHPFSI SNLMS-QE-- ---------- --HKP-DLKE
amHNF-3-2 P--------- -VQSQHPQEQ LGYPTRPIPQ TSPMSAAMSM YSTDHIKTSV HPSFHHPFSI NSIISQD--- ---------- --HKLTELKG
Mouse HNF3B PEPAPSPGQQ QQAAAHLLGP PHHPGLPPEA --------- -----HLKPEH HYAFNHPFSI NNLMSS-EQQ --HHHSHHHH QPHKM-DLKA
Chick HNF3B GEPS-----A ASPAQHLLAP P-HAGLPHDA --------- -----HLKPEH HYAFNHPFSI NNLMSSSEQQ HHHHPHHHHH PSHKM-DLKA
Frog HNF3B TSPA------ -SQAQHLLSQ H-HSVLSHEA QS-------- ----HLKPEH HYSFNHPFSI NNLMSS-EQQ HHHHHHNHH HHHKM-DLKA
Zf axial ASPT------ -SQAQHLLAQ H-HSVLAHEG ---------- ----HLKPEH HYSFNHPFSI NNLMSS-EQ- ---------- QHHKM-DLKT
Mouse HNF3G -PPS------ -------STP Y-FSGLELPG ---------- ----ELKLDA PYNFNHPFSI NNLMS--EQT S--------- TPSKL-DVGF
Mouse HNF3A SSAPPISSGP GALASVPPSH PAHGLAPHES QL-------- ----HLKGDP HYSFNHPFSI NNLMSSSEQ- ---------- -QHKL-DFKA
pintallavis LSPTSEQAGT ASQLMYPLGL SNDGYLGLVG EDV------- ----HLKHDP -FSGRHPFSI TQLMSS-EQD --------QT YANKM-EMCP
XFKH2 AGPSPLSS-- ------HQNH STHSLA-HET HI-------- ----HLKGDP HYSFNHPFSI NNLMSSSEQ- ---------- -QHKL-DFKA

amHNF-3-1 YAAMGYSG-- YNSMSPTG-- -VPKTTMSMD SMG------- -TDYYQGYVP QHSQPSSL-- -
amHNF-3-2 YDPMQYSG-- YASMYNTNPS VVPKQEMETP ASTEPATG-- ---YFSGYVP QYSTTASTLQ S
Mouse HNF3B YEQVMHYPGG YGSPMPGS-- -LAMGPVTNK AGLDASPLAA DTSYYQGVYS RPIMNSS--- -
Chick HNF3B YEQVMHYSG- YASPVPAS-- -LAMGPVTNK NPLESSPLAG ETSYYQGVYS RPIMNSS--- -
Frog HNF3B YEQVMHYSS- YGSPMAGS-- -LAMSTVTNK SGLESSPITS DTSYYQGGYS RPIMNSS--- -
Zf axial YEQVMHYG-- YGSPMAGT-- -LSMGSMASK AGLDSP---- DTSYYQGVYS RPILNSS--- -
Mouse HNF3G GGYGAE---- --SGEPG--- ---------- ---------- --VYYQSLYS RSLLNAS--- -
Mouse HNF3A YEQALQ-YSP YGATLPAS-- -LPLGSASVA TRSPIEPSAL EPAYYQGVYS RPVLNTS--- -
pintallavis TTDHLVHYSN YSSDYHNM-- -ASKNGLDMQ TSSST----- DNGYYANMYS RPILSSL--- -
XFKH2 YEQALQQYSS YGGGLQG--- -MPLGSPSMT GRGTIEPSAL EPTYYQGVYS RPVLNTS--- -

FIG. 2. Comparison of the predicted amino acid sequence of AmHNF-3-1 and AmHNF-3-2 with that of the known vertebrate HNF-3 class genes. Rat HNF-3α, β, and γ sequences are not included due to their close identity to the mouse HNF-3α, β, and γ sequences (95, 98, and 97%, respectively). The 110-amino-acid fork head domain is shown in bold, as are two conserved domains of unknown function at the carboxy terminus. Sources of sequences: Rat HNF-3α, Lai *et al.* (1990); rat HNF-3β and γ, Lai *et al.* (1991); mouse HNF-3α, β, and γ, Kaestner *et al.* (1994); chick HNF-3β, Ruiz i Altaba *et al.* (1995); frog HNF-3β, Ruiz i Altaba *et al.* (1993b); zebrafish axial, Strähle *et al.* (1993); XFKH2, Bolce *et al.* (1993); pintallavis, Ruiz i Altaba and Jessell (1992), Dirksen and Jamrich (1992), Knockel *et al.* (1992).

Prolonged staining and subsequent sectioning of 10 somite embryos revealed that expression of *AmHNF-3-1* could also be detected in the neural tube (Fig. 6). Expression was detected in the ventral-most cells along the length of the neural tube to an anterior limit at approximately the start of the swelling that defines the anterior cerebral vesicle. Serial sections of embryos stained in this manner confirmed these tissue locations, showing that only ventral neural cells were expressing *AmHNF-3-1* (Figs. 6B and 6C). Sections also confirmed that cells of the anterior cerebral vesicle, despite contacting the notochord, did not express *AmHNF-3-1* (Fig. 6D). Similar analysis of later embryonic

Copyright © 1997 by Academic Press. All rights of reproduction in any form reserved.

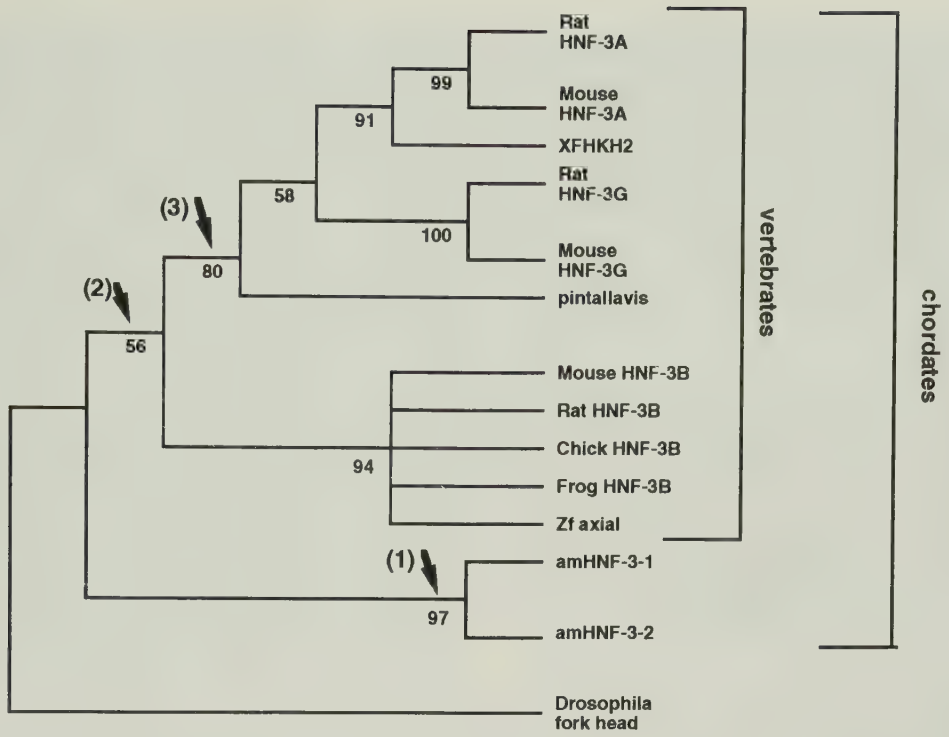

FIG. 3. Phylogenetic tree of HNF-3 class genes based on analysis of the amino acid sequence of the fork head domains by Neighbor Joining, which does not assume a root. Values adjacent to the nodes represent the score from 100 bootstrap resamplings of the data and provide a level of confidence in the tree. The tree indicates that the two amphioxus genes are most closely related to each other and were formed by a duplication specific to the cephalochordate lineage marked at (1). The HNF-3β proteins form a monophyletic group with axial, a grouping supported by a bootstrap value of 94. This supports the suggestion that *axial* is the zebrafish orthologue of *HNF-3β* (Strähle *et al.*, 1993). pintallavis groups with the HNF-3α and γ proteins; however, the node separating these three groups is only supported by a low bootstrap value. Thus, two separate duplications of HNF-3 genes have occurred in vertebrates: The first at (2) gave rise to the *HNF-3β* gene and to the branch leading to the *HNF-3α* and γ genes. The second at (3) occurred more recently and gave rise to distinct *HNF-3α* and γ genes. There is no measure of evolutionary distance in this tree; thus, the branch lengths do not indicate relative difference between genes.

stages also failed to detect expression of *AmHNF-3-1* in the anterior cerebral vesicle (data not shown).

Expression of AmHNF-3-1 in Amphioxus Larvae

At approximately 36 hr of development the mouth breaks through the wall of the pharynx and the larva, now fully motile, begins to feed. At this stage, expression of *AmHNF-3-1* was confined to three areas; a small area of cells in the pharynx, a region of central endoderm and the tail bud (Fig. 4I and data not shown).

DISCUSSION

In this paper I describe the characterisation and expression of amphioxus homologues of the HNF-3 class of transcription factors. Comparison of the sequence and expression of *AmHNF-3-1* and *AmHNF-3-2* with those of the vertebrate HNF-3 class genes allows deductions to be made concerning the evolution of this gene family and of the tissues in which its genes are expressed, several of which play key roles in the organisation of the vertebrate body plan.

Characterisation of Amphioxus HNF-3 Class Genes

The characterisation of amphioxus HNF-3 genomic clones suggested that amphioxus has at least two HNF-3 class genes. This finding was further investigated in three ways: Firstly, fragments from both clones were sequenced, revealing similar but distinct HNF-3 class fork head domains. Secondly, Southern analysis of genomic DNA from individual amphioxus identified two strongly hybridising bands with sizes corresponding to those predicted from the genomic clones. Thirdly, screening of amphioxus embryonic cDNA libraries identified clones corresponding to the two genomic phage sequences. This confirms that the am-

Copyright © 1997 by Academic Press. All rights of reproduction in any form reserved.

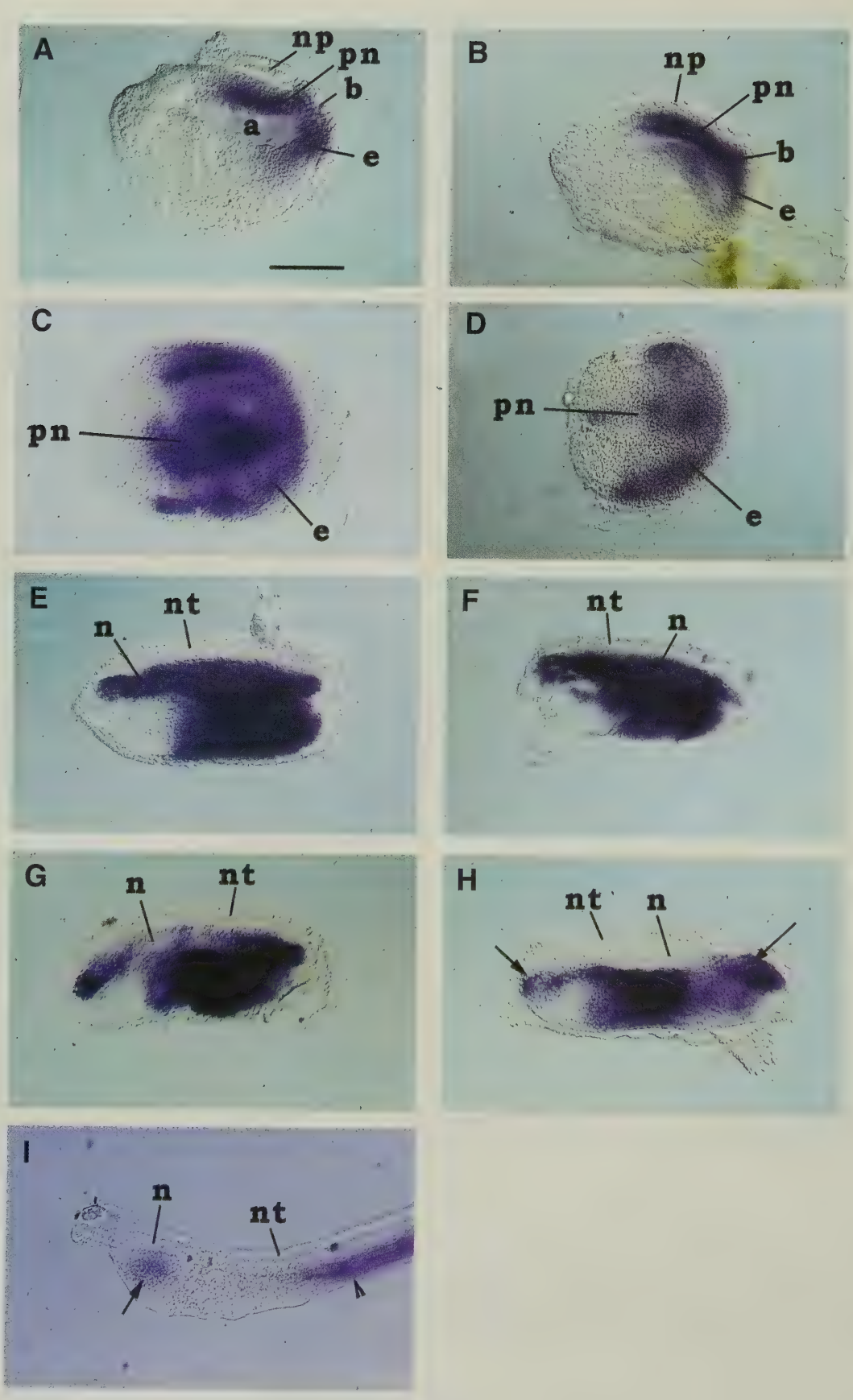
A
np
pn
b
a
e
B
np
pn
b
e
C
pn
e
D
pn
e
E
nt
n
F
nt
n
G
n
nt
H
nt
n
I
n
nt

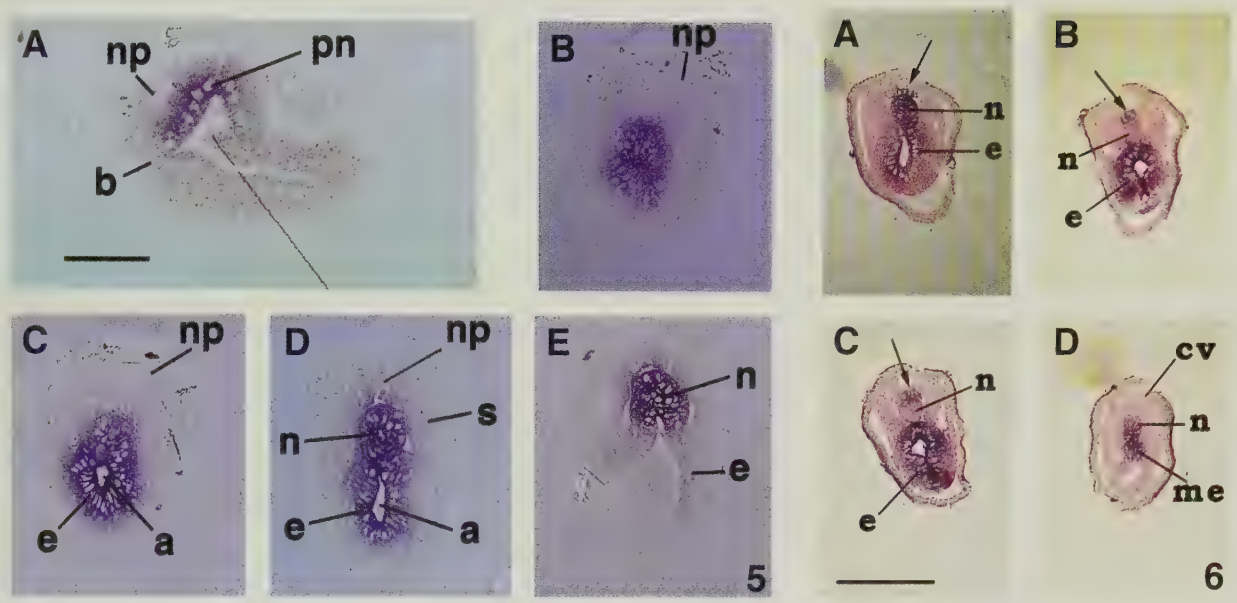

FIG. 5. (A) Sagittal section through an amphioxus neurula stained in whole-mount for *AmHNF-3-2*, showing expression in the presumptive notochord. Anterior is to the left. (B–E) Serial transverse sections from posterior (B) to anterior (E) through a 6 somite amphioxus embryo stained in whole-mount for *AmHNF-3-1*. (B) In the posterior of the embryo a central mass of stained cells is seen, with no clear delineation between notochord and endoderm. (C) More rostrally the archenteron is seen surrounded by endoderm to the bottom and sides and notochord above. The distinction between the two is more obvious in D. (E) In more anterior regions expression in the endoderm is much reduced. The delayed development of the notochord in the anterior is apparent in this section, since it is still not fully separated from the endoderm. No expression of *AmHNF-3-1* was detected in the neural plate of 6 somite embryos. The scale bar is equivalent to 40 μm for A and to 20 μm for B to E. a, archenteron; e, endoderm; n, notochord; np, neural plate; pn, presumptive notochord; s, somite.

FIG. 6. Serial sections from posterior (A) to anterior (D) through a 10 somite embryo after extensive staining for *AmHNF-3-1*. The scale bar on C is equivalent to 40 μm and is applicable to the other sections. (A) Section through the posterior, showing expression in endoderm and notochord and in neural cells overlying the notochord (arrow). (B, C) Progressively more anterior sections. Expression is lost in the notochord but maintained in the ventral neural tube (arrows) and endoderm. (D) In the anterior the cerebral vesicle is apparent as a swelling of the neural tube. No expression is present in the ventral neural tube; however, expression can be seen in the notochord and the dorsal midline of the endoderm. cv, cerebral vesicle; e, endoderm; me, midline endoderm; n, notochord.

phioxus genome encodes at least two HNF-3 class genes. It does not, however, fully rule out the possibility that other, as yet undiscovered, HNF-3 class genes are also present. Analysis of the evolution of the HNF-3 class genes showed that the two amphioxus genes are more closely related to each other than to HNF-3 genes in other species. This indicates that they are derived from a relatively recent duplication in the lineage leading to amphioxus, after its separation from that leading to vertebrates (Fig. 3). The *AmHNF-3* genes are not unique in this respect since the transcription factor *Brachyury* also appears to have undergone an independent duplication in amphioxus (Holland *et al.*, 1995b).

FIG. 4. Expression of *AmHNF-3-1* and *-2* as detected by whole-mount *in situ* hybridisation. Anterior is to the left in all cases. The scale bar in A is equivalent to 50 μm and is applicable to the other specimens. (A–D) Lateral (A,B) and dorsal (C,D) views of amphioxus neurulae stained for *AmHNF-3-1* (A,C) and *AmHNF-3-2* (B,D). Expression of both genes is visible in the presumptive notochord and invaginating endoderm. (E) Expression of *AmHNF-3-1* and (F) of *AmHNF-3-2* in 6 somite embryos. Expression can be seen throughout the notochord and in much of the endoderm, excluding that of the pharyngeal region. Detection of *AmHNF-3-2* expression at this stage required extensive staining and was not detected in older embryos. (G) Expression of *AmHNF-3-1* in an 8 somite embryo. Intense expression is maintained in the endoderm; however, expression in the centre of the notochord has begun to diminish. (H) Expression of *AmHNF-3-1* in a 10 somite embryo. Expression in the notochord is now restricted to the extreme anterior and posterior cells (arrows). (I) Anterior of an amphioxus larvae at 36 hr of development. Expression of *AmHNF-3-1* is seen in a small region of the pharynx (arrow) and in a wider region of more posterior endoderm (arrowhead). a, archenteron; b, blastopore; e, invaginating endoderm; pn, presumptive notochord; n, notochord; np, neural plate; nt, neural tube.

Copyright © 1997 by Academic Press. All rights of reproduction in any form reserved.

The Evolution of Chordate HNF-3 Genes

Molecular phylogenetic analysis of the fork head domains of HNF-3 class genes suggests that at least three independent duplications of HNF-3 genes have occurred during the evolution of the chordates (Fig. 3). One duplication, as discussed above, was specific to the lineage leading to present day cephalochordates and has resulted in the two closely related genes, *AmHNF-3-1* and *-2*. From this result we can hypothesise that the common ancestor of cephalochordates and vertebrates had a single HNF-3 class gene.

The second two gene duplications have occurred in the vertebrate lineage after its divergence from that leading to amphioxus (Fig 3). The first gave rise to *HNF-3β* and an *HNF-3α/γ* hybrid. This duplication must have occurred prior to the separation of the teleost and tetrapod lineages, since both these taxa possess distinct *HNF-3β* genes. Later in evolution the *HNF-3α/γ* hybrid underwent a further duplication, resulting in the *HNF-3α* and *γ* genes. Holland *et al.* (1994) and Sharman and Holland (1996) have observed that several gene families show evidence of two separate duplications during vertebrate evolution, one occurring prior to the divergence of the agnathan and gnathostome lineages, the second after this divergence. It is likely that the two duplications in the HNF-3 gene class occurred at the same time; this hypothesis is directly testable since it predicts that extant agnathans will possess two HNF-3 genes, one orthologous to *HNF-3β*, the second an *HNF-3α/γ* hybrid.

The position of *pintallavis* in this phylogeny is unresolved, although it groups with the *HNF-3α* and *γ* genes. Ruiz i Altaba *et al.* (1995) suggested that *pintallavis* may not have a direct homologue (orthologue) in amniotes. Since, however, *Xenopus* and mice have orthologues of *HNF-3α*, the duplication creating *HNF-3α* and *γ* must have occurred prior to the separation of these two lineages. Therefore, *Xenopus* should also possess an orthologue of *HNF-3γ*. One interpretation of the phylogeny is that *pintallavis* is orthologous to mouse *HNF-3γ*, with the difference in their patterns of expression resulting from divergent utilisation of HNF-3 genes in the lineages leading to *Xenopus* and mammals.

Similarity of Expression of AmHNF-3-1 and AmHNF-3-2

In early development the expression of *AmHNF-3-1* and *-2* was spatially identical, although the level of expression of *AmHNF-3-2* was lower than that of *AmHNF-3-1*. Later the expression patterns appeared to differ, since after about the 6 somite stage, *AmHNF-3-2* could no longer be detected. The similarity in early expression suggests that the duplication creating *AmHNF-3-1* and *-2* was accompanied by duplication of the control elements responsible for the early expression pattern. It also raises the question of why does amphioxus has two genes at all, if the expression patterns are identical? Possible explanations include biochemical differences between the two proteins and the potential for differences in expression in the larva or adult.

Conserved Expression of AmHNF-3-1 and AmHNF-3-2 during Early Development

The vertebrate HNF-3 genes have a conserved, characteristic pattern of expression during early development: With some exceptions, expression is seen in the organiser, endoderm, and notochord. The early expression of *AmHNF-3-1* and *-2* is strikingly similar to this pattern. Transcripts were first detected around the blastopore of gastrulating embryos, specifically in the dorsal region and endoderm. This supports the hypothesis that the dorsal region of the amphioxus embryo blastopore is homologous to the organiser of vertebrates, as indicated by their similar position in the embryo (Hatschek, 1881; Willey, 1894). Subsequently, high levels of *AmHNF-3-1* were detected in the notochord and in central and posterior endoderm.

In *Xenopus*, it has been shown that *pintallavis* and *Xbra*, a homologue of the mouse *Brachyury* gene, synergise during the specification of dorsal mesoderm, including notochord (O'Reilley *et al.*, 1995). This is supported by the study of naturally occurring mutants of *Brachyury* and of targeted mutants of *HNF-3β*, all of which show a reduction or lack of notochord (Hermann *et al.*, 1990; Ang and Rossant, 1994; Schulte-Merker *et al.*, 1994; Weinstein *et al.*, 1994). The amphioxus homologues of *Brachyury*, *Ambra-1* and *Ambra-2*, also have a conserved pattern of expression, with transcripts detected around the blastopore and in the notochord and posterior mesoderm (Holland *et al.*, 1995b). The expression of both *AmHNF-3* and the *AmBra*-genes around the blastopore of gastrulating amphioxus embryos suggests that the regulatory pathway involving these two gene families may be conserved between cephalochordates and vertebrates, lineages which last shared a common ancestor over 520 million years ago (Sansom *et al.*, 1992). It is curious that these functionally related transcription factors, *AmHNF-3* and *AmBra*, are to date the only two to also show independent duplications in amphioxus. Does this represent a functional coduplication of genes? This intriguing hypothesis is unfortunately untestable with the current level of genetics and embryology in amphioxus.

Expression of AmHNF-3-1 in the Anterior Notochord

Between the 6 and 10 somite stages expression of *AmHNF-3-1* in the centre of the notochord was seen to diminish, leaving isolated areas of expression in the anterior and posterior extremes. The anterior of the amphioxus notochord is atypical amongst chordates since it extends to the anterior limit of the neural tube. This is often considered a derived feature of amphioxus, specifically adapted to strengthen the head for burrowing into sediment. An alternative view, however, is that the rostrally expanded notochord is the ancestral state in chordates but has only been

Copyright © 1997 by Academic Press. All rights of reproduction in any form reserved.

retained in amphioxus. Thus far, palaeontology has failed to discern between these two possibilities, providing examples of Cambrian cephalochordates with both rostrally expanded and truncated notochords (Chen *et al.*, 1995, and references therein). The continued expression of *AmHNF-3-1* in the anterior notochord would suggest that there is a delay in the differentiation of these cells, which correlates with their delayed separation from the endoderm (Willey, 1894). This supports the view that the rostrally expanded notochord is a derived feature of amphioxus, since it suggests continued morphogenesis of the anterior notochord despite the overall anterior to posterior development of amphioxus.

Expression of AmHNF-3-1 in the Floor Plate of the Neural Tube

Amphioxus is distinguished from most vertebrates in that throughout its adult life it retains a distinct, differentiated notochord which acts as an endoskeleton on which the axial musculature may act. In many vertebrates, however, the notochord is a transient structure, present only during embryogenesis, where it performs a different role: Here the notochord acts as an organiser, inducing the floor plate in the ventral neural tube, then cooperating with the floor plate in establishing the dorsoventral pattern of the neural tube and somites (Yamada *et al.*, 1993; Fan and Tessier-Lavigne, 1994; Johnson *et al.*, 1994). Is this patterning system conserved with amphioxus? In vertebrates, a consistent feature of the floor plate is its expression of HNF-3 class genes. Extended staining and sectioning of 24-hr amphioxus embryos hybridised to an *AmHNF-3-1* probe positively identified expressing cells in the ventral midline of the neural tube. Electron microscope studies of amphioxus larvae have previously suggested that cells of the ventral midline of the neural tube may be considered as floor plate on histological grounds (Lacalli *et al.*, 1994). The expression of HNF-3 class genes by these cells in both vertebrates and amphioxus strongly supports this contention. Furthermore, the observation that only neural cells overlying the notochord express *AmHNF-3-1* suggests that the amphioxus floor plate may be induced by direct contact with notochord cells, as has been shown in vertebrates (Placzek *et al.*, 1990). We can thus conclude that the evolution of the floor plate as a distinct structure in the neural tube occurred prior to the separation of the amphioxus and vertebrate lineages, and therefore prior to the duplication of HNF-3 class genes seen during chordate evolution.

The anterior of the amphioxus neural tube forms a distinct swelling known as the cerebral vesicle. Historically, much discussion has centred on the relationship of the cerebral vesicle to the vertebrate neural tube; however, recent molecular and anatomical evidence suggests homology to the vertebrate brain, particularly the diencephalon (Lacalli *et al.*, 1994; Holland and Garcia-Fernàndez, 1996; Lacalli 1996). In vertebrates, the exact anterior limit of the floor plate has been a matter of some debate, with a recent model placing this limit adjacent to the anterior end of the notochord (reviewed by Shimamura *et al.*, 1995). Anterior to this is a region with some (but not all) of the characteristics of the floor plate which reaches approximately the level of the infundibulum. The exact anterior limit of *AmHNF-3-1* in the amphioxus neural tube has not been precisely determined since the neural tube at this stage lacks definitive anatomical markers, although it appears to coincide with the swelling marking the anterior cerebral vesicle. Lacalli *et al.* (1994), however, place the anterior limit of floor plate cells just posterior to the infundibulum, approximately in keeping with that observed for vertebrates. This raises an interesting question: If, as discussed above, the amphioxus notochord extends under the anterior of the cerebral vesicle, why are floor plate and *AmHNF-3-1* expression not also induced here? One possibility is that the signal inducing floor plate is absent, a second that cells of the cerebral vesicle are not competent to respond to the signal. Examination in amphioxus of members of the hedgehog family of signaling molecules should help distinguish between these possibilities.

Expression of AmHNF-3-1 in the Endoderm

Between the 10 and 13 somite stages, expression of *AmHNF-3-1* was seen in the midline cells of the endoderm, which in vertebrates also express HNF-3 class genes (Ruiz i Altaba and Jessell, 1992; Ang *et al.*, 1993; Monaghan *et al.*, 1993). Thus, conserved expression of HNF-3 genes was found in the midline cells of all three germ layers. The function of midline endoderm in development is not known. However, its presence in urochordate embryos (Satoh, 1994), plus this demonstration that it exists as a molecularly distinct structure in amphioxus, suggests that it is a conserved ancestral tissue in chordates. Therefore, it may also have a conserved function in the development of the chordate body plan.

Expression of *AmHNF-3-1* was also detected in other areas of endoderm. In vertebrates, several organs derived from endoderm also express HNF-3 class genes, including the liver, lungs, and gut (Ang *et al.*, 1993; Monaghan *et al.*, 1993; Sasaki and Hogan, 1993; Ruiz i Altaba *et al.*, 1995). Assignment of homology between these tissues and specific areas of amphioxus endoderm is, however, tenuous until confirmed by further molecular, morphological, or functional studies.

Conclusions

In this study I provide evidence that the expression of HNF-3 genes in the neurectoderm, mesoderm, and endoderm has been conserved between amphioxus and vertebrates, lineages which have been diverging for at least 520 million years (Sansom *et al.*, 1992). From this I have made three main deductions: Firstly, that the genetic pathway involving *Brachyury* and HNF-3 genes and leading to the specification of dorsal mesoderm evolved prior to the sepa-

Copyright © 1997 by Academic Press. All rights of reproduction in any form reserved.

ration of the amphioxus and vertebrate lineages. Secondly, that the role of the notochord in inducing floor plate in the ventral neural tube also evolved prior to this separation. Finally, that these roles evolved prior to the duplications of HNF-3 genes in the vertebrate lineage that gave rise to *HNF-3α, β* and *γ*.

ACKNOWLEDGMENTS

I am especially grateful to Peter W. H. Holland for numerous stimulating discussions on the evolution and development of vertebrates and in whose laboratory this work was undertaken. I am also grateful to Linda Holland and Jim Langeland for cDNA libraries, to Graham Luke and Liz Wheeler for technical assistance, to Kouzou Terazawa and Noriyuki Satoh for sharing unpublished data, and to anonymous referees for suggesting improvements to an earlier version of the manuscript. John M. Lawrence of the University of South Florida generously provided laboratory space during my stay in Tampa. This work was supported by a Career Development Award from the Medical Research Council and by the Wellcome Trust.

REFERENCES

Akam, M., Holland, P. W. H., Ingham, P. W., and Wray, G. A. (1994). The Evolution of Developmental Mechanisms. *Development Suppl.* 1994.

Ang, S-L., Wierda, A., Wong, D., Stevens, K. A., Cascio, S., Rossant, J., and Zaret, K. S. (1993). The formation and maintenance of the definitive endoderm lineage in the mouse: Involvement of HNF3/forkhead proteins. *Development* **119,** 1301–1315.

Ang, S-L., and Rossant, J. (1994). *HNF3B* is essential for node and notochord formation in mouse development. *Cell* **78,** 561–574.

Bolce, M. E., Hemmati-Brivanlou, A., and Harland, R. M. (1993). *XFKH2,* a *Xenopus HNF3A* homologue, exhibits both activin-inducible and autonomous phases of expression in early embryos. *Dev. Biol.* **160,** 413–423.

Chen, J.-Y., Dzik, J., Edgecombe, G. D., Ramsköld, L., and Zhou, G.-Q. (1995). A possible early Cambrian chordate. *Nature* **377,** 720–722.

Church, G. M., and Gilbert, W. (1984). Genomic sequencing. *Proc. Natl. Acad. Sci. USA* **81,** 1991–1995.

Clark, K. L., Halay, E. D., Lai, E., and Burley, S. K. (1993). Co-crystal structure of the HNF-3/fork head DNA-recognition motif resembles histone H5. *Nature* **364,** 412–420.

Clevidence, D. E., Overdier, D. G., Tao, W., Qian, X., Pani, L., Lai, E., and Costa, R. H. (1993). Identification of nine tissue-specific transcription factors of the hepatocyte nuclear factor 3/forkhead DNA-binding-domain family. *Proc. Natl. Acad. Sci. USA* **90,** 3948–3952.

Dirksen, M-L., and Jamrich, M. (1992). A novel activin-inducible blastopore lip-specific gene of *Xenopus laevis* contains a fork head DNA-binding domain. *Genes Dev.* **6,** 599–608.

Dirksen, M-L., and Jamrich, M. (1995). Differential expression of fork head genes during early *Xenopus* and zebrafish development. *Dev. Genet.* **17,** 107–116.

Fan, C.-M., and Tessier-Lavigne, M. (1994). Patterning of mammalian somites by surface ectoderm and notochord: Evidence for schlerotome induction by a *hedgehog* homolog. *Cell* **79,** 1175–1186.

Felsenstein, J. (1993). PHYLIP version 3.5c. University of Washington, Seattle.

Hacker, U., Grossniklaus, U., Gehring, W. J., and Jäckle, H. (1992). Developmentally regulated *Drosophila* gene family encoding the fork head domain. *Proc. Natl. Acad. Sci. USA* **89,** 8754–8758.

Hatschek, B. (1881). Studien uber entwicklun des amphioxus. *Arb. Zool. Inst. Wien* **IV,** 1–88.

Herrmann, B. G., Labeit, S., Poustka, A., King, T. R., and Lehrach, H. (1990). Cloning of the *T* gene required in mesoderm formation in the mouse. *Nature* **343,** 617–622.

Higgins, D. G., Bleasby, A. J., and Fuchs, R. (1991). CLUSTAL V: Improved software for multiple sequence alignment. *CABIOS,* **8,** 189–191.

Holland, P. W. H. (1993). Cloning genes using the polymerase chain reaction. *In* "Essential Developmental Biology: A Practical Approach" (C. D. Stern and P. W. H. Holland, Eds.), pp. 243–255. IRL Press at Oxford Univ. Press, Oxford.

Holland, N. D., and Holland, L. Z. (1993). Embryos and larvae of invertebrate deuterostomes. *In* "Essential Developmental Biology: A Practical Approach" (C. D. Stern and P. W. H. Holland, Eds.), pp. 21–32. IRL Press at Oxford Univ. Press, Oxford.

Holland, N. D., Holland, L. Z., and Kozmik, Z. (1995a). An amphioxus Pax gene, *AmphiPax-1,* is expressed in embryonic endoderm, but not in mesoderm: Implications for the evolution of class I paired box genes. *Mol. Mar. Biol. Biotec.* **4,** 206–214.

Holland, P. W. H., and Garcia-Fernàndez, J. (1996). Hox genes and chordate evolution. *Dev. Biol.* **173,** 382–395.

Holland, P. W. H., Garcia-Fernàndez, J., Williams, N. A., and Sidow, A. (1994). Gene duplications and the origin of vertebrate development. *Development Suppl.* 125–133.

Holland, P. W. H., Koschorz, B., Holland, L. Z., and Herrmann, B. G. (1995b). Conservation of *Brachyury* (*T*) genes in amphioxus and vertebrates: Developmental and evolutionary implications. *Development* **121,** 4283–4291.

Hromas, R., Moore, J., Johnstone, T., Socha, C., and Klemsz, M. (1993). *Drosophila fork head* homologues are expressed in a lineage-restricted manner in human haematopoetic cells. *Blood* **81,** 2854–2859.

Johnson, R. D., Laufer, E., Riddle, R. D., and Tabin, C. J. (1994). Ectopic expression of *Sonic hedgehog* alters dorsal-ventral patterning of somites. *Cell* **79,** 1166–1174.

Kaufmann, E., Hoch, M., and Jäckle, H. (1994). The interaction of DNA with the DNA-binding domain encoded by the *Drosophila* gene *fork head. Eur. J. Biochem.* **223,** 329–337.

Kaestner, K. H., Lee, K-H., Schlondorff, J., Hiemisch, H., Monaghan, A. P., and Schütz, G. (1993). Six members of the mouse fork head gene family are developmentally regulated. *Proc. Natl. Acad. Sci. USA* **90,** 7628–7631.

Kaestner, K. H., Hiemisch, H., Luckow, B., and Schütz, G. (1994). The HNF-3 family of transcription factors in mice: Gene structure, cDNA sequence and mRNA distribution. *Genomics* **20,** 377–385.

King, M. W., and Moore, M. J. (1994). Novel HOX, POU and FKH genes expressed during bFGF-induced mesodermal differentiation in *Xenopus. Nucleic Acids Res.* **22,** 3990–3996.

Knöchel, S., Lef, J., Clement, J., Klocke, B., Hille, S., Köster, M., and Knöchel, W. (1992). Activin-A induced expression of a fork-head related gene in posterior chordamesoderm (notochord) of *Xenopus laevis* embryos. *Mech. Dev.* **38,** 157–165.

Lacalli, T. C. (1996). Frontal Eye circuitry, rostral sensory pathways

Copyright © 1997 by Academic Press. All rights of reproduction in any form reserved.

and brain organization in amphioxus larvae: Evidence from 3D reconstructions. *Philos. Trans. R. Soc. London Ser. B* **351,** 243–263.

Lacalli, T. C., Holland, N. D., and West, J. E. (1994). Landmarks in the anterior central-nervous-system of amphioxus larvae. *Philos. Trans. R. Soc. London Ser. B.* **344,** 165–185.

Lai, E., Prezioso, V. R., Smith, E., Litvin, O., Costa, R. H., and Darnell, J. E. (1990). *HNF-3A,* a hepatocyte-enriched transcription factor of novel structure is regulated transcriptionally. *Genes Dev.* **4,** 1427–1436.

Lai, E., Prezioso, V. R., Tao, W., Chen, W. S., and Darnell, J. E. (1991). Hepatocyte nuclear factor 3A belongs to a gene family in mammals that is homologous to the *Drosophila* homeotic gene *fork head. Genes Dev.* **5,** 416–427.

Monaghan, A. P., Kaestner, K. H., Grau, E., and Schütz, G. (1993). Postimplantation expression patterns indicate a role for the mouse forkhead/*HNF-3 A, B* and *G* genes in determination of the definitive endoderm, chordamesoderm and neurectoderm. *Development* **119,** 567–578.

O'Reilley, M.-A. J., Smith, J. C., and Cunliffe, V. (1995). Patterning of the mesoderm in *Xenopus*: Dose-dependent and synergistic effects of *Brachyury* and *Pintallavis. Development* **121,** 1351–1359.

Pierrou, S., Hellqvist, M., Samuelsson, L., Enerback, S., and Carlsson, P. (1994). Cloning and characterisation of seven human forkhead proteins: Binding site specificity and DNA bending. *EMBO J.* **13,** 5002–5012.

Placzek, M., Tessier-Lavigne, M., Yamada, T., Jessell, T. M., and Dodd, J. (1990). Mesodermal control of neural cell identity: floor plate induction by the notochord. *Science* **250,** 985–988.

Ruiz i Altaba, A., and Jessell, T. M. (1992). *Pintallavis,* a gene expressed in the organiser and midline cells of frog embryos: Involvement in the development of the neural axis. *Development* **116,** 81–93.

Ruiz i Altaba, A., Cox, C., Jessell, T. M., and Klar, A. (1993a). Ectopic neural expression of a floor plate marker in frog embryos injected with the midline transcription factor *pintallavis. Proc. Natl. Acad. Sci. USA* **90,** 8268–8272.

Ruiz i Altaba, A., Prezioso, V. R., Darnell, J. E., and Jessell, T. M. (1993b). Sequential expression of *HNF3-β* and *HNF3-α* by embryonic organising centres: The dorsal lip/node, notochord and floorplate. *Mech. Dev.* **44,** 91–108.

Ruiz i Altaba, A., Placzek, M., Baldassare, M., and Jessell, T. M. (1995). Early stages of notochord and floorplate development in the chick embryo defined by normal and induced expression of *HNF-3β. Dev. Biol.* **170,** 299–313.

Sambrook, J., Fritsch, E. F., and Maniatis, T. (1989). "Molecular Cloning: A Laboratory Manual." Cold Spring Harbor Laboratory Press, Cold Spring Harbor, NY.

Sansom, I. J., Smith, M. P., Armstrong, H. A., and Smith, M. M. (1992). Presence of the earliest vertebrate hard tissues in conodonts. *Science* **256,** 1308–1311.

Sasaki, H., and Hogan, B. L. M. (1993). Differential expression of multiple fork head related genes during gastrulation and axial pattern formation in the mouse embryo. *Development* **118,** 47–59.

Sasaki, H., and Hogan, B. L. M. (1994). HNF-3B as a regulator of floor plate development. *Cell* **76,** 103–115.

Satoh, N. (1994). "Developmental Biology of Ascidians." Cambridge Univ. Press, Cambridge, UK.

Schulte-Merker, S., van Eeden, F., Halpern, M. E., Kimmel, C. B., and Nüsslein-Volhard, C. (1994). *No tail (ntl)* is the zebrafish homologue of the mouse *T (Brachyury)* gene. *Development* **120,** 1009–1015.

Sharman, A. C., and Holland, P. W. H. (1996). Conservation, duplication and divergence of developmental genes during chordate evolution. *Netherlands J. Zool.* **46,** 47–67.

Shimamura, K., Hartigan, D. J., Martinez, S., Puelles, L., and Rubenstein, J. L. R. (1995). Longitudinal organization of the anterior neural plate and neural tube. *Development* **121,** 3923–3933.

Spemann, H., and Mangold, H. (1924). Uber Induktion von embryonalanlangen durch implantation artfremder organisatoren. *Wilhelm Roux Arch. Entwicklungsmech. Org.* **100,** 599–638.

Strähle, U., Blader, P., Henrique, D., and Ingham, P. W. (1993). *Axial,* a zebrafish gene expressed along the developing body axis, shows altered expression in cyclops mutant embryos. *Genes Dev.* **7,** 1436–1446.

Weigel, D., Jurgens, G., Kuttner, K., Seifert, E., and Jäckle, H. (1989). The homeotic gene *fork head* encodes a nuclear protein and is expressed in the terminal regions of the *Drosophila* embryo. *Cell* **57,** 645–658.

Weigel, D., and Jäckle, H. (1990). Fork head: A new eukaryotic DNA-binding motif? *Cell* **63,** 455–456.

Weigel, D., Seifert, E., Reuter, D., and Jäckle, H. (1990). Regulatory elements controlling expression of the *Drosophila* homeotic gene *fork head. EMBO J.* **9,** 1119–1207.

Weinstein, D. C., Ruiz i Altaba, A., Chen, W. S., Hoodless, P., Prezioso, V. R., Jessell, T. M., and Darnell, J. E. (1994). The winged-helix transcription factor *HNF-3B* is required for notochord development in the mouse embryo. *Cell* **78,** 575–588.

Willey, A. (1894). "Amphioxus and the Ancestry of the Vertebrates." Macmillan Co., London.

Yamada, T., Pfaff, S. L., Ediund, T., and Jessell, T. M. (1993). Control of cell pattern in the neural tube: Motor neuron induction by diffusible factors from the notochord and floor plate. *Cell* **73,** 673–686.

Received for publication May 9, 1996
Accepted November 26, 1996

Copyright © 1997 by Academic Press. All rights of reproduction in any form reserved.

DEVELOPMENTAL BIOLOGY 183, 86–94 (1997)
ARTICLE NO. DB968498

Regeneration of *Sarcophaga* Imaginal Discs *in Vitro:* Implication of 20-Hydroxyecdysone

Takekazu Kunieda, Shoichiro Kurata, and Shunji Natori[1]
Faculty of Pharmaceutical Sciences, University of Tokyo, Bunkyo-ku, Tokyo 113, Japan

When the 3/4 sectors of leg imaginal discs of *Sarcophaga* were cultured *in vitro* in the presence of 2.5×10^{-8} *M* 20-hydroxyecdysone, wound healing and restoration of their morphology occurred. This concentration of ecdysone was critical for wound healing and was 40 times lower than that necessary for inducing differentiation of imaginal discs *in vitro*. Lost positional values revealed by expression of the *wingless* gene were found to show partial recovery under these conditions. These results suggest that a low titer of ecdysone is essential for the regeneration of imaginal discs. © 1997 Academic Press

INTRODUCTION

The molecular mechanisms involved in regeneration of lost tissues or organs are among the most intriguing topics of developmental biology. Several studies have been done on the regeneration of newt lenses (Itoh and Eguchi, 1986; Hyuga *et al.*, 1993), amphibian limb blastemas (Onda *et al.*, 1990), mammalian livers (Nakamura *et al.*, 1989; Kinoshita *et al.*, 1991) and the appendages of the cockroach (Bohn, 1974; Kunkel, 1977; Kunkel, 1985). However, their molecular mechanisms are complex and not well understood. In particular, the mechanisms involved in the restoration of lost positional values are totally unknown.

Fragmented imaginal discs of *Drosophila* have been shown to regenerate their lost parts when cultured in the abdomen of adult females (Schubiger, 1971; Russell, 1974; Karlsson, 1980). The boundary model (Meinhardt, 1983), which is a modified version of the polar coordinate model (French *et al.*, 1976), can account satisfactorily for the patterns of regeneration, duplication, and intercalary regeneration reported for various fragments of *Drosophila* imaginal discs (Schubiger, 1971; Dale and Bownes, 1985). When manipulated discs are transplanted into the adult abdomen, contact between usually nonadjacent cells takes place as a result of wound healing (Dale and Bownes, 1981, 1985). This unusual cell–cell contact is thought to generate a new compartment boundary which acts as a local organizer and stimulates cell growth at the junction, and during this growth of new tissue the positional values which normally exist between the apposed locations are generated by interaction.

To investigate the molecular mechanism of wound healing and regeneration in imaginal discs, we attempted to devise an *in vitro* culture system for imaginal discs which would allow these processes to take place. For this purpose, we used imaginal discs of *Sarcophaga peregrina* (flesh fly), because they are much larger than those of *Drosophila* and thus easier to handle. We found that 2.5×10^{-8} *M* 20-hydroxyecdysone (20-HE) was needed for wound healing of the cultured imaginal discs.

MATERIALS AND METHODS

In Vitro Culture of Sarcophaga Leg Discs

Third instar larvae of *Sarcophaga* were kept in contact with water for 2 days to synchronize their physiological ages (Ohtaki, 1966). Imaginal mesothoracic leg discs were dissected from the ecdysone-free larvae and rinsed successively with insect saline and culture medium. For all experiments, we used Grace's insect medium, but modified it before use by adding Hepes at a final concentration of 10 m*M*, adjusting the pH to 6.8 with a 1:1 mixture of 1 *M* NaOH and 1 *M* KOH and adding penicillin and streptomycin to give final concentrations of 120 units/ml and 0.5 mg/ml, respectively. Fragmentation of the discs was carried out with fine scissors under a binocular microscope. Usually, about 10 disc fragments were cultured in a single well containing 300 μl of culture medium at 25°C in a water-saturated atmosphere. When needed, 20-HE was added at a final concentration of 2.5×10^{-8} *M*.

Incorporation of [^{3}H]Thymidine

DNA synthesis in disc fragments was monitored by measuring their incorporation of [^{3}H]thymidine (Komano *et al.*, 1991). Thirty

[1] To whom correspondence should be addressed. Fax: +81-3-3813-5099. E-mail: fnatori@hongo.ecc.u-tokyo.ac.jp.

0012-1606/97 $25.00
Copyright © 1997 by Academic Press
All rights of reproduction in any form reserved.

disc fragments were cultured in 500 μl of culture medium for 2 days with or without 20-HE and then labeled for 2 hr by adding 2 μCi [^{3}H]thymidine. The disc fragments were collected, washed well, and lysed in 0.5 *N* NaOH. Then trichloroacetic acid was added to the lysate at a final concentration of 30% (v/v). The acid-insoluble material was trapped on a glass-fiber filter and its radioactivity was measured.

Immunofluorescence Analysis of Bromodeoxyuridine (BrdU) Incorporation

Culture and labeling of disc fragments was done as described above, except that 10 μM BrdU was used instead of [^{3}H]thymidine. Incorporated BrdU was detected by immunofluorescence essentially as described by Bryant and Fraser (1988). For this, disc fragments were fixed in Carnoy's fixative and blocked with 1% fetal calf serum before treatment with anti-BrdU antibody.

Isolation of Sarcophaga wingless cDNA and Sequencing

A probe for screening a *Sarcophaga* cDNA library was obtained by RT-PCR from total RNA of *Sarcophaga* leg discs. Primers were designed from amino acid sequences conserved in the *wingless/wnt-1* gene product of various animals (Baker, 1987; Rijsewijk *et al.*, 1987; Cabrera *et al.*, 1987; Noordermeer *et al.*, 1989; Nusse *et al.*, 1990). These were IESCTCDY and CWMRL-A/P-N/T/P for the initial PCR and QECKCHGM for the 3′ primer of nested PCR. After each PCR, the target product was detected by Southern blot analysis with the probe corresponding to GGCSDNI-G/D/E-FG. The target PCR product was cloned and used as probe. Two positive clones were isolated from 1.2×10^6 clones of a *Sarcophaga* leg disc ZAP cDNA library by plaque hybridization. These were the same clones, as judged from their restriction maps. The molecular size of the isolated cDNA was about 2.8 kb. For sequencing, a series of nested deletion derivatives was generated by digestion with exonuclease III and mung bean nuclease, and each derivative was sequenced by the dideoxy chain-termination method (Sanger *et al.*, 1977) using a DNA sequencer. The putative amino acid sequence of *Sarcophaga wingless* was determined in comparison with that of *Drosophila*. The nucleotide sequence data will appear in the DDBJ, EMBL, and GenBank nucleotide sequence databases with the Accession No. D85687.

Whole-mount in Situ Hybridization

Whole-mount *in situ* hybridization was carried out essentially as described in *Drosophila* (Phillips *et al.*, 1990; Poeck *et al.*, 1993; Tautz and Pfeifle, 1989). After fixation, discs were decolored in a mixture of methanol and 30% H_2O_2 (5:1 by volume) for 1 hr, washed three times in methanol for 5 min each time, and then rehydrated in a series of methanol solutions (methanol:phosphate-buffered saline containing 0.1% Tween 20 = 3:1, 1:1, and 1:3). Digestion with protease K at 4 μg/ml was carried out for 5 min. Digoxigenin-labeled probes were synthesized by a PCR DIG labeling kit using primers of ATC GAA ACG ATC TTT AAG ATT ATC GCC and GTT ACC CAT TCG ATA GCA CGG GCC TGC, respectively, for the antisense and sense probes.

RESULTS

Establishment of an in Vitro Culture System for Induction of Wound Healing in Imaginal Discs

To investigate wound healing *in vitro*, we used leg discs from *Sarcophaga* third instar larvae. According to the fate map of *Sarcophaga* leg discs (Kamai and Ohtaki, 1987), we removed the quadrant of a mature leg disc containing the boundary between the antero-ventral and posterior compartments using fine scissors under a binocular microscope (Fig. 1A). Then the remaining 3/4 sector of the injured disc was cultured in Grace's insect medium. Essentially no morphological change was detected when the disc fragment alone was cultured for 2 days (Fig. 1B). However, when the culture medium was supplemented with 2.5×10^{-8} *M* 20-HE, wound healing occurred and normally nonadjacent cells at the wound edge made contact with each other to form a round disc (Fig. 1C). We found that only 20-HE was effective for wound healing, and no appreciable morphological change in the 3/4 sectors was detected when they were cultured in the presence of 10 ng/ml each of bFGF, EGF, TGF-β, IGF-I, IGF-II, insulin, or 5% fetal calf serum. Coculture with NIH-Sape-4 cells (an embryonic cell line of *Sarcophaga*, 2×10^6 cells/well), fat body (total tissue from one larva/well) or hemocytes (2.5×10^4 cells/well) also did not induce wound healing of the 3/4 sectors.

It is known that *Sarcophaga* imaginal discs differentiate into adult structures in the presence of 1×10^{-6} *M* 20-HE *in vitro*, and that most anlages reach the stage of elongation when cultured for 2 days in Grace's insect medium (Kawaguchi *et al.*, 1991). This concentration of 20-HE was clearly higher than that which induces wound healing. We found that 2.5×10^{-8} *M* was the optimal concentration of 20-HE for induction of wound healing *in vitro*, and that the wound healing rate was greatly decreased upon treatment with 20-HE at concentrations above and below this. In other words, no appreciable morphological change in the 3/4 sectors was induced by 1×10^{-8} *M* 20-HE, whereas premature eversion (partial extension of the distal tip) was induced in some sectors by 5×10^{-8} *M* 20-HE, although no clear wound healing was detected.

The results of five independent experiments are summarized in Table 1. The average wound healing rate was 32% upon culture in the presence of 2.5×10^{-8} *M* 20-HE. About 20% of intact discs changed their morphology under these conditions, but no clear eversion defined by Milner (1977) was induced.

Detection of DNA Synthesis at the Contact Site

To examine whether cell division was needed to make the 3/4 sectors round, we examined DNA synthesis by the cultured discs. As shown in Fig. 2A, incorporation of [^{3}H]-thymidine by 3/4 sectors cultured in the presence of 20-HE was clearly higher than that in the absence of 20-HE and was also clearly higher than that obtained with intact discs

Copyright © 1997 by Academic Press. All rights of reproduction in any form reserved.

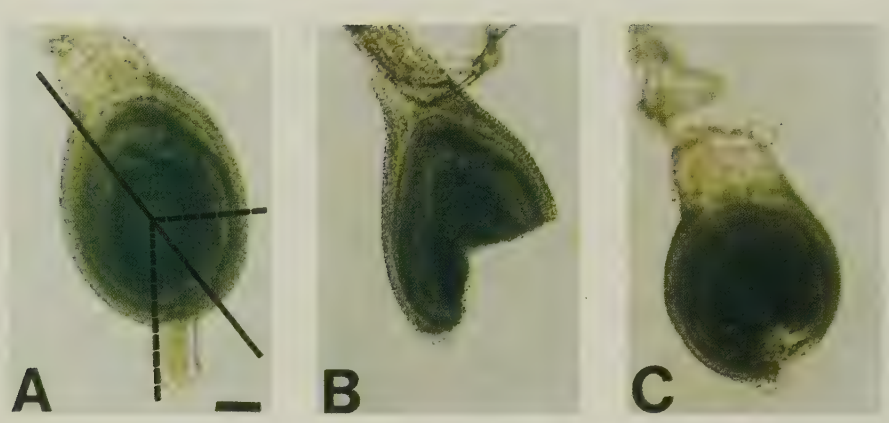

FIG. 1. Morphological change in imaginal disc fragments cultured *in vitro*. (A) Intact leg disc with location of cuts indicated by dashed lines. The postulated antero-posterior compartment boundary is indicated by the solid line. Disc fragments cultured for 2 days in the absence and presence of 2.5×10^{-8} *M* 20-HE are shown in (B) and (C), respectively. All discs are oriented dorsal side up, posterior to the left. The bar indicates 100 μm. Wound healing was detected only when the disc fragments were cultured in the presence of 20-HE.

cultured in the presence of 20-HE, suggesting that significant cell division occurs only in those sectors where wound healing is taking place. To identify the region of cell division in the sectors, we performed immunofluorescence experiments using a monoclonal antibody against BrdU. For this, we cultured the 3/4 sectors in the presence of 20-HE. After they had become round, we labeled them with BrdU and visualized their BrdU-labeled DNA by immunofluorescence. As shown in Figs. 2B and 2C, immunofluorescence was detected only in the vicinity of the junction of the wound edges where normally nonadjacent cells made contact to form a new boundary (magnified views are shown in Figs. 2D and 2E, respectively). These results indicated that cell division occurred exclusively at the junction of the wound edges when the 3/4 sectors were cultured in the presence of 20-HE.

Restoration of Positional Values during Wound Healing

After wound healing, the manipulated discs showed apparent restoration of their normal morphology. In *Drosophila* leg discs, it is known that expression of *wingless* (*wg*) is restricted to the sector of the antero-ventral compartment along the antero-posterior boundary (Baker, 1988). As we had surgically removed the quadrant containing this region from *Sarcophaga* leg discs to examine wound healing, we investigated the reexpression of *wg* in the morphologically restored leg discs by *in situ* hybridization. For this, we first isolated a cDNA for the *Sarcophaga wg* gene from a leg disc cDNA library of *Sarcophaga* and determined its sequence (Fig. 3A). As shown in Fig. 3B, the primary sequence of *Sarcophaga wg* was very similar to that of *Drosophila wg*, with 76% overall sequence identity between the two proteins.

Using this cDNA as a probe, we performed *in situ* hybridization of leg discs. As is evident from Fig. 4A, expression of *wg* in the intact leg disc was restricted to a narrow region along the antero-posterior boundary like that in the *Drosophila* leg disc. After removing the quadrant containing this region, we cultured the 3/4 sectors in the presence or absence of 20-HE for 2 days and then performed *in situ* hybridization. As shown in Fig. 4B, the expression of *wg* was detected only in those sectors whose morphology had been restored. No expression of *wg* was detected in the sectors cultured in the absence of 20-HE (Fig. 4C). The region reexpressing *wg* was restricted to the site of contact of normally nonadjacent cells, suggesting that a new antero-ventral and posterior boundary is generated at this contact site. It is possible that the wound healing of the 3/4 sectors in the presence of 20-HE occurred in a manner that restored the lost positional values. However, the region expressing *wg* was clearly smaller than that in the intact discs. These results suggest that the lost positional values are not fully restored, and thus regeneration is not completed, even though the 3/4 sectors show morphological restoration under these conditions.

TABLE 1
Summary of Data for Leg Disc Fragment Wound Healing *in Vitro*

Experiment:	1	2	3	4	5	Total
	$N = 11$	30	80	50	10	181
Wound healed	3	11	29	13	3	59
% of wound healing	27	36	36	26	30	32

Note. Results of five independent experiments. *N*, number of imaginal disc fragments tested.

Copyright © 1997 by Academic Press. All rights of reproduction in any form reserved.

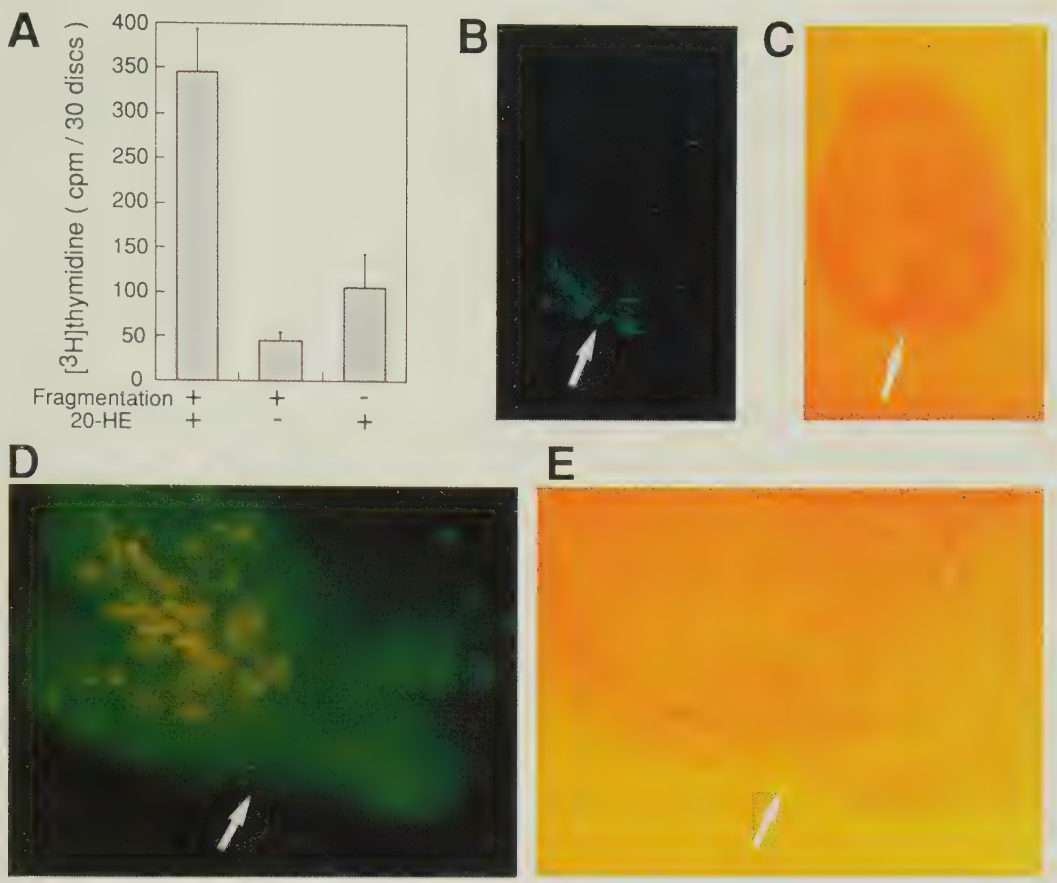

FIG. 2. Effect of 20-HE on DNA synthesis. (A) Fragmented or intact discs were cultured in the presence or absence of 2.5×10^{-8} *M* 20-HE for 2 days, and then incorporation of [^{3}H]thymidine into their DNA was examined for 2 h. Only fragmented discs showed significant DNA synthesis in the presence of 20-HE. To identify the region where DNA synthesis occurred, fragmented discs were labeled with BrdU instead of [^{3}H]thymidine, and the incorporated BrdU was visualized by immunofluorescence (B). Morphology of the disc in (B) is shown in (C). (D and E) Higher-magnification view of (B) and (C), respectively. Fluorescence was detected only around the healed wound shown by the arrow.

DISCUSSION

Imaginal discs are a fascinating material with which to study the molecular mechanisms of determination and differentiation. Although the cells constituting each disc are undifferentiated, their fates are predetermined, and positional information is believed to be important for this (Gehring and Nöthiger, 1973; Schubiger, 1968; Kamai and Ohtaki, 1987). It is known that *Drosophila* imaginal discs have the ability to regenerate lost segments when cultured in the abdomen of an adult after they have been removed surgically (Schubiger, 1971; Bryant, 1971). A scanning electron microscopy study (Reinhardt *et al.*, 1977; Reinhardt and Bryant 1981) has substantiated the polar coordinate model of French *et al.* (1976) in the wound healing of *Drosophila* wing discs.

Using *Sarcophaga* leg discs, we succeeded in inducing wound healing *in vitro*. We found that 2.5×10^{-8} *M* 20-HE was essential for the wound healing and regeneration of lost positional values. This concentration of 20-HE was very critical for the induction of wound healing and was 40 times lower than that necessary for inducing the differentiation of imaginal discs *in vitro*.

In a classical transplantation experiment using *Drosophila*, it was demonstrated that the growth of transplanted discs in the abdomen of the adult female is better than that in the abdomen of the male. The growth of discs in the male abdomen was accelerated by cotransplantation of the ring-gland or injection of a low-titer 20-HE, but a high-titer 20-HE induced their metamorphosis (Bodenstein, 1943; Postlethwait and Schneiderman, 1968). Later studies revealed that a low level of ecdysteroid does exist in the adult fly (Hodgetts, 1977; Handler, 1982) and that the titer in the female is higher than in the male (Schwartz *et al.*, 1985, 1989; but see Bownes *et al.*, 1984; Bownes, 1989). Similar results have been reported for *Sar-*

Copyright © 1997 by Academic Press. All rights of reproduction in any form reserved.

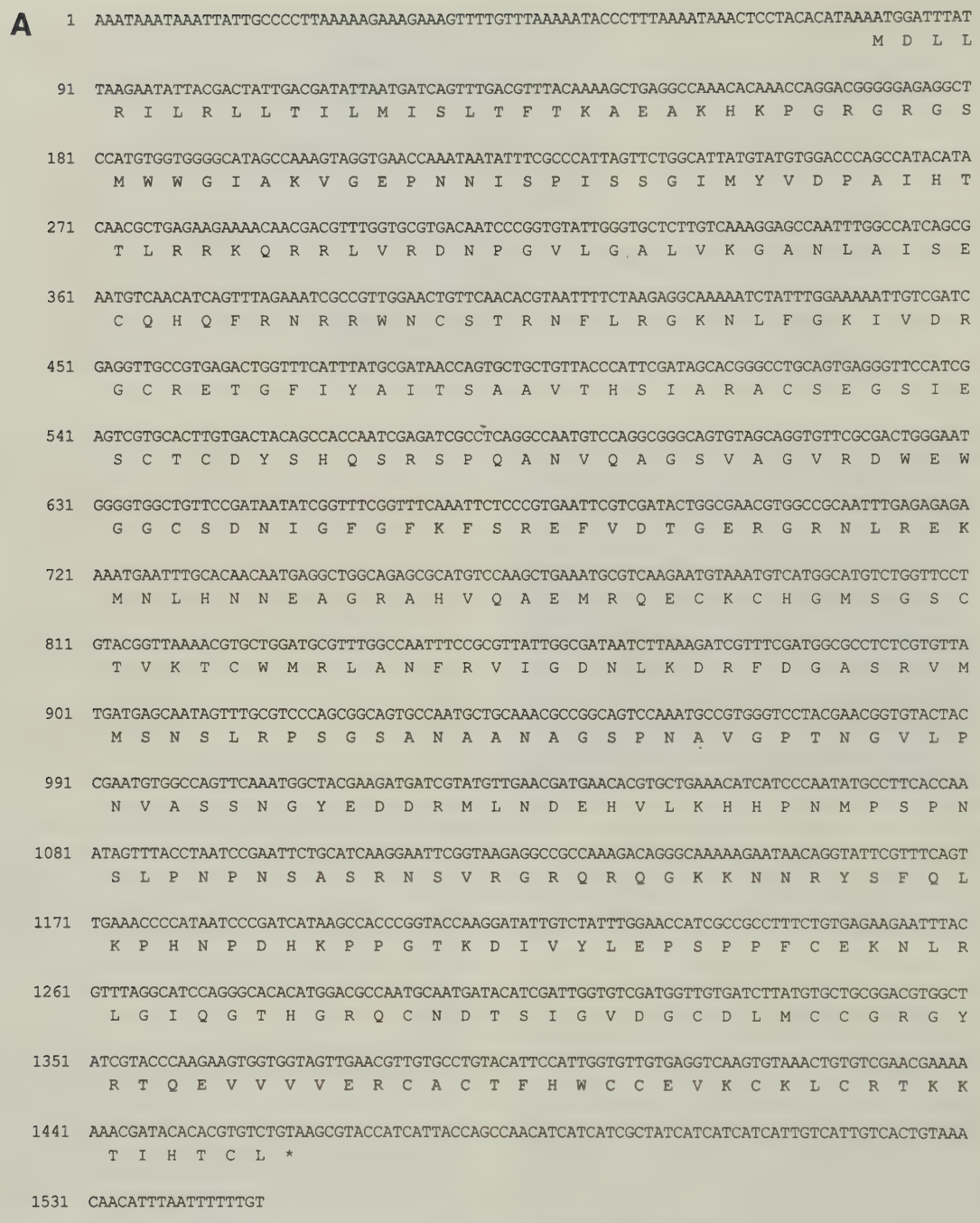
A
1 AAATAAATAAATTATTGCCCCTTAAAAAGAAAGAAAGTTTTGTTTAAAAATACCCTTTAAAATAAACTCCTACACATAAAATGGATTTAT
M D L L
91 TAAGAATATTACGACTATTGACGATATTAATGATCAGTTTGACGTTTACAAAAGCTGAGGCCAAACACAAACCAGGACGGGGGAGAGGCT
R I L R L L T I L M I S L T F T K A E A K H K P G R G R G S
181 CCATGTGGTGGGGCATAGCCAAAGTAGGTGAACCAAATAATATTTCGCCCATTAGTTCTGGCATTATGTATGTGGACCCAGCCATACATA
M W W G I A K V G E P N N I S P I S S G I M Y V D P A I H T
271 CAACGCTGAGAAGAAAACAACGACGTTTGGTGCGTGACAATCCCGGTGTATTGGGTGCTCTTGTCAAAGGAGCCAATTTGGCCATCAGCG
T L R R K Q R R L V R D N P G V L G A L V K G A N L A I S E
361 AATGTCAACATCAGTTTAGAAATCGCCGTTGGAACTGTTCAACACGTAATTTTCTAAGAGGCAAAAATCTATTTGGAAAAATTGTCGATC
C Q H Q F R N R R W N C S T R N F L R G K N L F G K I V D R
451 GAGGTTGCCGTGAGACTGGTTTCATTTATGCGATAACCAGTGCTGCTGTTACCCATTCGATAGCACGGGCCTGCAGTGAGGGTTCCATCG
G C R E T G F I Y A I T S A A V T H S I A R A C S E G S I E
541 AGTCGTGCACTTGTGACTACAGCCACCAATCGAGATCGCCTCAGGCCAATGTCCAGGCGGGCAGTGTAGCAGGTGTTCGCGACTGGGAAT
S C T C D Y S H Q S R S P Q A N V Q A G S V A G V R D W E W
631 GGGGTGGCTGTTCCGATAATATCGGTTTCGGTTTCAAATTCTCCCGTGAATTCGTCGATACTGGCGAACGTGGCCGCAATTTGAGAGAGA
G G C S D N I G F G F K F S R E F V D T G E R G R N L R E K
721 AAATGAATTTGCACAACAATGAGGCTGGCAGAGCGCATGTCCAAGCTGAAATGCGTCAAGAATGTAAATGTCATGGCATGTCTGGTTCCT
M N L H N N E A G R A H V Q A E M R Q E C K C H G M S G S C
811 GTACGGTTAAAACGTGCTGGATGCGTTTGGCCAATTTCCGCGTTATTGGCGATAATCTTAAAGATCGTTTCGATGGCGCCTCTCGTGTTA
T V K T C W M R L A N F R V I G D N L K D R F D G A S R V M
901 TGATGAGCAATAGTTTGCGTCCCAGCGGCAGTGCCAATGCTGCAAACGCCGGCAGTCCAAATGCCGTGGGTCCTACGAACGGTGTACTAC
M S N S L R P S G S A N A A N A G S P N A V G P T N G V L P
991 CGAATGTGGCCAGTTCAAATGGCTACGAAGATGATCGTATGTTGAACGATGAACACGTGCTGAAACATCATCCCAATATGCCTTCACCAA
N V A S S N G Y E D D R M L N D E H V L K H H P N M P S P N
1081 ATAGTTTACCTAATCCGAATTCTGCATCAAGGAATTCGGTAAGAGGCCGCCAAAGACAGGGCAAAAAGAATAACAGGTATTCGTTTCAGT
S L P N P N S A S R N S V R G R Q R Q G K K N N R Y S F Q L
1171 TGAAACCCCATAATCCCGATCATAAGCCACCCGGTACCAAGGATATTGTCTATTTGGAACCATCGCCGCCTTTCTGTGAGAAGAATTTAC
K P H N P D H K P P G T K D I V Y L E P S P P F C E K N L R
1261 GTTTAGGCATCCAGGGCACACATGGACGCCAATGCAATGATACATCGATTGGTGTCGATGGTTGTGATCTTATGTGCTGCGGACGTGGCT
L G I Q G T H G R Q C N D T S I G V D G C D L M C C G R G Y
1351 ATCGTACCCAAGAAGTGGTGGTAGTTGAACGTTGTGCCTGTACATTCCATTGGTGTTGTGAGGTCAAGTGTAAACTGTGTCGAACGAAAA
R T Q E V V V V E R C A C T F H W C C E V K C K L C R T K K
1441 AAACGATACACACGTGTCTGTAAGCGTACCATCATTACCAGCCAACATCATCATCGCTATCATCATCATCATTGTCATTGTCACTGTAAA
T I H T C L *
1531 CAACATTTAATTTTTTGT

FIG. 3. (A) Nucleotide sequence of cDNA encoding *Sarcophaga wingless* and the predicted amino acid sequence. The open reading frame of the *Sarcophaga* cDNA was determined on the basis of that of *Drosophila* cDNA. Asterisk indicates termination codon. (B) Alignment of the deduced *wingless* amino-acid sequences for *Sarcophaga* (Sar) and *Drosophila* (Dro). Gaps have been inserted for optimal matching (76% identity on the basis of the *Drosophila* sequence). Asterisks indicate identical residues. All 23 Cys residues conserved among *Drosophila, Xenopus,* and mouse *wingless/wnt-1* are also conserved in *Sarcophaga wingless* (underlined).

cophaga bullata (Briers and De Loof, 1980). Thus, a low level of ecdysone seems to be required for the growth of discs both *in vivo* and *in vitro,* and this may enhance the wound healing and subsequent regeneration of the 3/4 sectors cultured *in vivo.*

The concentration of ecdysteroid in the hemolymph of

Copyright © 1997 by Academic Press. All rights of reproduction in any form reserved.

B

```
Sar   1 :  MDLLRI---- LRLLTILMIS LTFTKAEAKH KPGRGRGSMW WGIAKVGEPN NISPISSGIM
           **   *     *  *     * *     * *  * ******** ********** ** *    **
Dro   1 :  MDISYIFVIC LMALCSGGSS L--SQVEGKQ KSGRGRGSMW WGIAKVGEPN NITP----IM

Sar  57 :  YVDPAIHTTL RRKQRRLVRD NPGVLGALVK GANLAISECQ HQFRNRRWNC STRNFLRGKN
           * ***** ** ********** ********** ********** ********** ***** ****
Dro  55 :  YMDPAIHSTL RRKQRRLVRD NPGVLGALVK GANLAISECQ HQFRNRRWNC STRNFSRGKN

Sar 117 :  LFGKIVDRGC RETGFIYAIT SAAVTHSIAR ACSEGSIESC TCDYSHQSRS PQANVQAGSV
           ********** *** ****** ********** ***** **** ********** **** *****
Dro 115 :  LFGKIVDRGC RETSFIYAIT SAAVTHSIAR ACSEGTIESC TCDYSHQSRS PQANHQAGSV

Sar 177 :  AGVRDWEWGG CSDNIGFGFK FSREFVDTGE RGRNLREKMN LHNNEAGRAH VQAEMRQECK
           ********** ********** ********** ********** ********** **********
Dro 175 :  AGVRDWEWGG CSDNIGFGFK FSREFVDTGE RGRNLREKMN LHNNEAGRAH VQAEMRQECK

Sar 237 :  CHGMSGSCTV KTCWMRLANF RVIGDNLKDR FDGASRVMMS NSLRPSGSAN A--ANAGSPN
           ********** ********** ******** * **** **    ****           **   *
Dro 235 :  CHGMSGSCTV KTCWMRLANF RVIGDNLKAR FDGATRVQVT NSLRATNALA PVSPNAAGSN

Sar 295 :  AVGPTNGVLP NVASSNGYED DRMLND---- ------EHVL K-HHPNMPSP NSLPNPNSAS
            **      *       * *   *****                * ******** ****
Dro 295 :  SVGSNGLIIP QSGLVYGEEE ERMLNDHMPD ILLENSHPIS KIHHPNMPSP NSLP--QAGQ

Sar 344 :  RNSVRGRQRQ GKKNNRYSFQ LKPHNPDHKP PGTKDIVYLE PSPPFCEKNL RLGIQGTHGR
           *    ** ** * * *** ** * **** *** ** ** **** *** ****** * ** *****
Dro 352 :  RGGRNGR-RQ GRKHNRYHFQ LNPHNPEHKP PGSKDLVYLE PSPSFCEKNL RQGILGTHGR

Sar 404 :  QCNDTSIGVD GCDLMCCGRG YRTQEVVVVE RCACTFHWCC EVKCKLCRTK KTIHTCL
           *** ** *** ** ******* **  ****** ********** ********** * * ***
Dro 412 :  QCNETSLGVD GCGLMCCGRG YRRDEVVVVE RCACTFHWCC EVKCKLCRTK KVIYTCL
```

FIG. 3—*Continued*

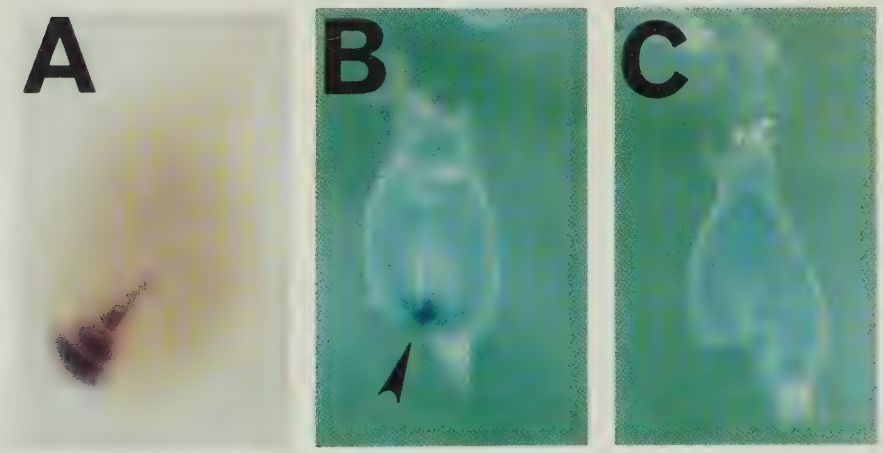

FIG. 4. Reexpression of *wingless* in a regenerated disc fragment revealed by *in situ* hybridization. (A) The *wingless* of *Sarcophaga* expressed in the antero-ventral sector of the intact leg disc, which is included in the quadrant to be removed (see Fig. 1A). Reexpression of the *wingless* was detected only in the disc fragment cultured in the presence of 20-HE (B) and not in its absence (C). Arrow in (B) indicates reexpression of *wingless*.

Copyright © 1997 by Academic Press. All rights of reproduction in any form reserved.

adult female of *Sarcophaga* has been found to remain constant at 2×10^{-8} *M*, although the total content of ecdysteroid varies from 30 to 70 ng/g, depending upon the rearing conditions of flies (Briers and De Loof, 1980). It is noteworthy that the concentration of ecdysteroid in hemolymph is close to the optimal concentration of 20-HE for inducing wound healing of 3/4 sectors *in vitro*.

Madhavan and Schneiderman (1969) documented clearly the relationship between a low titer of ecdysone and disc regeneration *in vivo* using ligated *Galleria mellonella* larvae. However, an *in vivo* experiment cannot exclude the possibility of indirect participation of other tissues stimulated by ecdysone in the regeneration of transplanted discs.

Fain and Schneiderman (1979) demonstrated that about 19% of *Drosophila* imaginal disc fragments regenerated *in vitro* when they were cultured in a medium designated XCS, which contained juvenile hormone analogue, insulin, and larval fat body, but no 20-HE. However, in their system, the disc fragments had to be transplanted into the adult abdomen to allow initial wound healing *in vivo* prior to *in vitro* culture. Slightly wounded discs were found to proliferate in this medium (Davis and Shearn, 1977), and *in vitro* transdetermination of leg discs was found to occur in this medium (Shearn *et al.*, 1978). Shearn *et al.* (1978) also pointed out that the extensively wounded discs disintegrated if cultured *in vitro* in this medium. Taking these results and our present ones together, it is possible to conclude that low-titer 20-HE is essential for wound healing, and that other components of XCS medium, such as juvenile hormone analogue, insulin, or fat body, may support cell proliferation rather than wound healing or regeneration.

In mammals, Lefebvre *et al.* (1993) have demonstrated that the regeneration of auditory hair cells can be stimulated by retinoic acid *in vitro*. The signals of both 20-HE and retinoic acid are thought to be transduced through heterodimeric nuclear receptors (Yao *et al.*, 1992, 1993; Leid *et al.*, 1992), and it is possible that the members of the nuclear receptor family are common molecules that participate in the regeneration process in both vertebrates and invertebrates. Although enhancer trap lines showing altered expression during regeneration in *Drosophila* have been isolated (Brook *et al.*, 1993), the genes related to regeneration have not yet been identified.

We found that the lost positional values revealed by *wg* expression were generated again after wound healing, and also that DNA synthesis occurred in the area where cells at the wound edge made contact, as in the case of disc fragments of *Drosophila* cultured in the adult abdomen (Adler, 1984; Bryant and Fraser 1988). Normally, *wg* is expressed only in a restricted portion of the antero-ventral sector along antero-posterior boundary (Baker, 1988). An ectopic expression experiment using *hedgehog* (*hh*) has revealed that all cells in the antero-ventral sector of the leg disc can express *wg* in response to *hh* (Basler and Struhl, 1994; Diaz-Benjumea *et al.*, 1994). Thus, *hh* normally expressed in the posterior half of the disc (Lee *et al.*, 1992; Mohler and Vani, 1992; Tabata *et al.*, 1992) induces and defines the *wg*-expressing cells in antero-ventral sector. In our work, we surgically removed the quadrant containing the *wg* zone and the boundary between the antero-ventral and posterior compartments. As a result, cells at the anterior wound edge of the 3/4 sectors were antero-ventral cells which did not express *wg*, while cells at the posterior wound edge were posterior cells expressing *hh*. As the antero-ventral cells confronted *hh*-expressing posterior cells after wound healing, the former cells would receive *hh* from their new neighbors and thus start to express *wg*. This is one possible molecular mechanism that could explain the reexpression of *wg* along the new boundary between the antero-ventral cells and posterior cells of wound-healed discs.

Ectopic expression of *wg* in *Drosophila* discs is known to induce an extra ventral structure (Struhl and Basler, 1993). On the other hand, suppression of *wg* function in the early patterning of imaginal discs results in loss of the ventral structure and mirror-image duplication of the dorsal structure (Couso *et al.*, 1993). Thus, *wg* not only has ventro-organizing activity, but also is responsible for the formation of the dorso-ventral (D/V) axis of imaginal discs. Its participation in the formation of the proximo-distal (P/D) axis has also been suggested (Campbell *et al.*, 1993; Diaz-Benjumea *et al.*, 1994; Campbell and Tomlinson, 1995). Thus, our system that induces reexpression of *wg* in the 3/4 sectors of *Sarcophaga* discs *in vitro* may be useful for studying the formation of D/V and P/D axes in the development of imaginal discs.

Recently, Maves and Schubiger (1995) reported that *wg* induced transdetermination when it was expressed ectopically in the dorsal region of intact *Drosophila* leg discs by the *flp*-out technique. Therefore, it would be interesting to clarify whether *trans*-determination is induced in the regenerated 3/4 sectors of *Sarcophaga* leg discs.

Cell proliferation was detected locally in the vicinity of the junction of the wound edges. However, it is not clear whether contact between usually nonadjacent cells occurred first and then cell division started between the apposed locations to regenerate the positional values, or whether cells at the wound edges started to divide in the presence of 20-HE, recovering their morphology and subsequently their positional values. In any event, although the morphology and positional values of 3/4 sectors are apparently restored when cultured *in vitro* in the presence of 20-HE, the restoration of positional values is only partial. These results suggest that 20-HE initiates, but is not sufficient for, completion of imaginal disc regeneration *in vitro*.

Nonetheless, it is clear that 20-HE induces the apposition of cells belonging to different compartments of disc fragments *in vitro*, and that the expression of *wg* is detectable only in these disc fragments. This suggests that a new boundary is generated by the interaction of different compartments, a process which perhaps involves the *hh* signaling pathway. This *in vitro* system may provide clues for clarifying the molecular mechanism of new boundary generation and subsequent regeneration.

Copyright © 1997 by Academic Press. All rights of reproduction in any form reserved.

ACKNOWLEDGMENT

This work was supported by a Grant-in-Aid for Specifically Promoted Research from the Ministry of Education, Science, Sports and Culture of Japan.

REFERENCES

Adler, P. N. (1984). DNA replication and pattern regulation in the imaginal wing disc of *Drosophila*. *Dev. Biol.* **102,** 300–308.

Baker, N. E. (1987). Molecular cloning of sequences from *wingless*, a segment polarity gene in *Drosophila:* The spatial distribution of a transcript in embryos. *EMBO J.* **6**(6), 1765–1773.

Baker, N. E. (1988). Transcription of the segment-polarity gene *wingless* in the imaginal discs of *Drosophila*, and the phenotype of a pupal-lethal *wg* mutation. *Development* **102,** 489–497.

Basler, K., and Struhl, G. (1994). Compartment boundaries and the control of *Drosophila* limb pattern by *hedgehog* protein. *Nature* **368,** 208–214.

Bodenstein, D. (1943). Hormones and tissue competence in the development of *Drosophila*. *Biol. Bull.* **84,** 34–59.

Bohn, H. (1974). Extent and properties of the regeneration field in the larval legs of cockroaches (*Leucophaer amaderae*). *J. Embryol. Exp. Morphol.* **31,** 557–572.

Bownes, M., Dübendorfer, A., and Smith, T. (1984). Ecdysteroids in adult males and females of *Drosophila melanogaster*. *J. Insect Physiol.* **30**(10), 823–830.

Bownes, M. (1989). The roles of juvenile hormone, ecdysone and the ovary in the control of *Drosophila* vitellogenesis. *J. Insect Physiol.* **35**(5), 409–413.

Briers, T., and De Loof, A. (1980). The molting hormone activity in *Sarcophaga bullata* in relation to metamorphosis and reproduction. *Int. J. Invertebr. Reprod.* **2,** 363–372.

Brook, W. J., Ostafichuk, L. M., Piorecky, J., Wilkinson, M. D., Hodgetts, D. J., and Russel, M. A. (1993). Gene expression during imaginal disc regeneration detected using cnhancer-sensitive P-elements. *Development* **117,** 1287–1297.

Bryant, P. J. (1971). Regeneration and duplication following operations *in situ* on the imaginal discs of *Drosophila melanogaster*. *Dev. Biol.* **26,** 606–615.

Bryant, P. J., and Fraser, S. E. (1988). Wound healing, cell communication, and DNA synthesis during imaginal disc regeneration in *Drosophila*. *Dev. Biol.* **127,** 197–208.

Cabrera, C. V., Alonso, M. C., Johnson, P., Phillips, R. G., and Lawrence, P. A. (1987). Phenocopies induced with antisense RNA identify the *wingless* gene. *Cell* **50,** 659–663.

Campbell, G., Weaver, T., and Tomlinson, A. (1993). Axis specification in the developing *Drosophila* appendage: The role of *wingless, decapentaplegic,* and the homeobox gene *aristaless*. *Cell* **74,** 1113–1123.

Campbell, G., and Tomlinson, A. (1995). Initiation of the proximodistal axis in insect legs. *Development* **121,** 619–628.

Couso, J. P., Bate, M., and Martinez-Arias, A. (1993). A *wingless*-dependent polar coordinate system in *Drosophila* imaginal discs. *Science* **259,** 484–489.

Dale, L., and Bownes, M. (1981). Wound healing and regeneration in the imaginal wing disc of *Drosophila*. *Roux's Arch. Dev. Biol.* **190,** 185–190.

Dale, L., and Bownes, M. (1985). Pattern regulation in fragments of *Drosophila* wing discs which show variable wound healing. *J. Embryol. Exp. Morphol.* **85,** 95–109.

Davis, K. T., and Shearn, A. (1977). *In vitro* growth of imaginal disks from *Drosophila melanogaster*. *Science* **196,** 438–440.

Diaz-Benjumea, F. J., Cohen, B., and Cohen, S. M. (1994). Cell interaction between compartments establishes the proximal–distal axis of *Drosophila* legs. *Nature* **372,** 175–179.

Fain, M. J., and Schneiderman, H. A. (1979). Wound healing and regenerative response of fragments of the *Drosophila* wing imaginal disc cultured *in vitro*. *J. Insect Physiol.* **25,** 913–924.

French, V., Bryant, P. J., and Bryant, S. V. (1976). Pattern regulation in epimorphic fields. *Science* **193,** 969–981.

Gehring, W. J., and Nöthiger, R. (1973). The imaginal discs of *Drosophila*. *In* "Developmental Systems: Insects" (S. Counce and C. G. Waddington, Eds.), pp. 212–290. Academic Press, New York.

Handler, A. M. (1982). Ecdysteroid titers during pupal and adult development in *Drosophila melanogaster*. *Dev. Biol.* **923,** 73–82.

Hodgetts, R. B., Sage, B., and O'Connor, J. D. (1977). Ecdysone titers during postembryonic development of *Drosophila melanogaster*. *Dev. Biol.* **60,** 310–317.

Hyuga, M., Kodama, R., and Eguchi, G. (1993). Basic fibroblast growth factor as one of the essential factors regulating lens transdifferentiation of pigmented epithelial cells. *Int. J. Dev. Biol.* **37,** 319–326.

Itoh, Y., and Eguchi, G. (1986). *In vitro* analysis of cellular metaplasia from pigmented epithelial cells to lens phenotypes: A unique model system for studying cellular and molecular mechanisms of "transdifferentiation." *Dev. Biol.* **115,** 353–362.

Kamai, H., and Ohtaki, T. (1987). Pattern regulation of the leg disc of the fleshfly, *Sarcophaga peregrina*. *Dev. Growth Differ.* **29**(1), 71–83.

Karlsson, J. (1980). Distal regeneration in proximal fragments of the wing disc of *Drosophila*. *J. Embryol. Exp. Morphol.* **59,** 315–323.

Kawaguchi, N., Komano, H., and Natori, S. (1991). Involvement of *Sarcophaga* lectin in the development of imaginal discs of *Sarcophaga peregrina* in an autocrine manner. *Dev. Biol.* **144,** 86–93.

Kinoshita, T., Hirao, S., Matsumoto, K., and Nakamura, T. (1991). Possible endocrine control by hepatocyte growth factor of lever regeneration after partial hepatectomy. *Biochem. Biophys. Res. Commun.* **177,** 330–335.

Komano, H., Homma, K., and Natori, S. (1991). Involvement of sapecin in embryonic cell proliferation of *Sarcophaga peregrina* (flesh fly). *FEBS Lett.* **289**(2), 167–170.

Kunkel, J. G. (1977). Cockroach molting. II. The nature of regeneration-induced delay of molting hormone secretion. *Biol. Bull.* **153,** 145–162.

Kunkel, J. G. (1985). Regeneration. *In* "The American Cockroach" (W. J. Bell and K. G. Adiyodi, Eds.), pp. 425–443. Chapman and Hall, London.

Lee, J. J., von Kessler, D., Parks, S., and Beachy, P. A. (1992). Secretion and localized transcription suggests a role in positional signaling for products of the segmentation gene *hedgehog*. *Cell* **71,** 33–50.

Lefebvre, P. P., Malgrange, B., Staecker, H., Moonen, G., and Van De Water, T. R. (1993). Retinoic acid stimulates regeneration of mammalian auditory hair cells. *Science* **260,** 692–695.

Leid, M., Kastner, P., Lyons, R., Nakshari, H., Saunders, M., Zacharewski, T., Chen, J.-Y., Staub, A., Garnier, J.-M., Mader, S., and

Copyright © 1997 by Academic Press. All rights of reproduction in any form reserved.

Chambon, P. (1992). Purification, cloning, and RXR identity of the HeLa cell factor with which RAR or TR heterodimerizes to bind target sequences efficiently. *Cell* **68,** 377–395.

Madhavan, K., and Schneiderman, H. A. (1969). Hormonal control of imaginal disc regeneration in *Galleria Mellonella* (Lepidoptera). *Biol. Bull.* **137,** 321–331.

Maves, L., and Schubiger, G. (1995). *wingless* induces transdetermination in developing *Drosophila* imaginal discs. *Development* **121,** 1263–1272.

Meinhardt, H. (1983). Cell determination boundaries as organizing regions for secondary embryonic fields. *Dev. Biol.* **96,** 375–385.

Milner, M. J. (1977). The eversion and differentiation of *Drosophila melanogaster* leg and wing imaginal discs cultured *in vitro* with an optimal concentration of b-ecdysone. *J. Embryol. Exp. Morphol.* **37,** 105–117.

Mohler, J., and Vani, K. (1992). Molecular organization and embryonic expression of the *hedgehog* gene involved in cell–cell communication in segmental patterning of *Drosophila. Development* **115,** 957–971.

Nakamura, T., Nishizawa, T., Hagiya, M., Seki, T., Shimonishi, M., Sugimura, A., Tashiro, K., and Shimizu, S. (1989). Molecular cloning and expression of human hepatocyte growth factor. *Nature* **342,** 440–443.

Noordermeer, J., Meijlink, F., Verrijzer, P., Rijsewijk, F., and Destree, O. (1989). Isolation of the *Xenopus* homolog of *int-1/wingless* and expression during neurula stages of early development. *Nucleic Acids Res.* **17,** 11–18.

Nusse, R., Theunissen, H., Wagenaar, E., Rijsewijk, F., Gennissen, A., Otte, A., Schuuring, E., and van Ooyen, A. (1990). The *wnt-1* (*int-1*) oncogene promoter and its mechanism of activation by insertion of proviral DNA of the mouse mammary tumor virus. *Mol. Cell. Biol.* **10,** 4170–4179.

Ohtaki, T. (1966). On the delayed pupation of the flesh fly, *Sarcophaga peregrina,* Robineau–Desvoidy. *Jpn. J. Med. Sci. Biol.* **19,** 97–104.

Onda, H., Goldhamer, D. J., and Tassawa, R. A. (1990). An extracellular matrix molecule of newt and axolotl regeneration limb blastemas and embryonic limb buds: Immunological relationship of MT1 antigen with tenascin. *Development* **108,** 657–668.

Phillips, R. G., Roberts, I. J. H., Ingham, P. W., and Whittle, J. R. S. (1990). The *Drosophila* segment polarity gene *patched* is involved in a position-signalling mechanism in imaginal discs. *Development* **110,** 105–114.

Poeck, B., Hofbauer, A., and Pflugfelder, G. O. (1993). Expression of the *Drosophila optomotor-blind* gene transcript in neuronal and glial cells of the developing nervous system. *Development* **117,** 1017–1029.

Postlethwait, J. H., and Schneiderman, H. A. (1968). Effects of an ecdysone on growth and cuticle formation of *Drosophila* imaginal discs cultured *in vivo. Biol. Bull.* **135,** 431–432.

Reinhardt, C. A., Hodgkin, N. M., and Bryant, P. J. (1977). Wound healing in the imaginal discs of *Drosophila.* I. Scanning electron microscopy of normal and healing wing discs. *Dev. Biol.* **60,** 238–257.

Reinhardt, C. A., and Bryant, P. J. (1981). Wound healing in the imaginal discs of *Drosophila.* II. Transmission electron microscopy of normal and healing wing discs. *J. Exp. Zool.* **216,** 45–61.

Rijsewijk, F., Schuermann, M., Wagenaar, E., Parren, P., Weigel, D., and Nusse, R. (1987). The *Drosophila* homolog of the mouse mammary oncogene *int-1* is identical to the segment polarity gene *wingless. Cell* **50,** 649–657.

Russell, M. A. (1974). Pattern formation in the imaginal discs of a temperature-sensitive cell-lethal mutant of *Drosophila melanogaster. Dev. Biol.* **40,** 24–39.

Sanger, F., Nicklen, S., and Coulson, R. R. (1977). DNA sequencing with chain-terminating inhibitors. *Proc. Natl. Acad. Sci. USA* **74**(12), 5463–5467.

Schubiger, G. (1968). Anlageplan, Determinationszustand und Transdeterminationslestungen der maennlichen Vorderbeinscheibe von *Drosophila melanogaster. Wilhelm Roux' Arch. Entwicklungsmech.* **160,** 9–40.

Schubiger, G. (1971). Regeneration, duplication and *trans*-determination in fragments of the leg disc of *Drosophila melanogaster. Dev. Biol.* **26,** 277–295.

Schwartz, M. B., Kelly, T. J., Imberski, R. B., and Rubenstein, E. C. (1985). The effects of nutrition and methoprene treatment on ovarian ecdysteroid synthesis in *Drosophila melanogaster. J. Insect Physiol.* **31**(12), 947–957.

Schwartz, M. B., Kelly, T. J., Woods, C. W., and Imberski, R. B. (1989). Ecdysteroid fluctuations in adult *Drosophila melanogaster* caused by elimination of pupal reserves and synthesis by early vitellogenic ovarian follicles. *Insect Biochem.* **19**(3), 243–249.

Shearn, A., Davis, K. T., and Hersperger, E. (1978). Transdetermination of *Drosophila* imaginal discs cultured *in vitro. Dev. Biol.* **65,** 536–540.

Struhl, G., and Basler, K. (1993). Organizing activity of *wingless* protein in *Drosophila. Cell* **72,** 527–540.

Tabata, T., Eaton, S. E., and Kornberg, T. B. (1992). The *Drosophila hedgehog* gene is expressed specifically in posterior compartment cells and is a target of *engrailed* expression. *Genes Dev.* **6,** 2635–2645.

Tautz, D., and Pfeifle, C. (1989). A non-radioactive *in situ* hybridization method for the localization of specific RNAs in *Drosophila* embryos reveals translational control of the segmentation gene *hunchback. Chromosoma* **98,** 81–85.

Yao, T. P., Segraves, W. A., Oro, A. E., McKeown, M., and Evans, R. M. (1992). *Drosophila ultraspiracle* modulates ecdysone receptor function via heterodimer formation. *Cell* **71,** 63–72.

Yao, T. P., Forman, B. M., Jiang, Z., Cherbas, L., Chen, J., -D., McKeown, M., Cherbas, P., and Evans, R. M. (1993). Functional ecdysone receptor is the product of *EcR* and *Ultraspiracle* genes. *Nature* **366,** 476–479.

Received for publication July 15, 1996
Accepted December 23, 1996

Copyright © 1997 by Academic Press. All rights of reproduction in any form reserved.

DEVELOPMENTAL BIOLOGY **183,** 95–107 (1997)
ARTICLE NO. DB968467

Steroid Hormones Act Directly to Trigger Segment-Specific Programmed Cell Death of Identified Motoneurons *in Vitro*

Laura C. Streichert,[1] Jonathan T. Pierce, Julie A. Nelson, and Janis C. Weeks

Institute of Neuroscience, University of Oregon, Eugene, Oregon 97403-1254

In larvae of the hawkmoth, *Manduca sexta,* accessory planta retractor (APR) motoneurons undergo a segment-specific pattern of programmed cell death at pupation. APR death is triggered hormonally by the prepupal peak of the ecdysteroid, 20-hydroxyecdysone (20-HE). Previous studies found no evidence that cellular interactions regulate the segmental pattern of APR death *in vivo.* To test the hypothesis that 20-HE acts directly on APRs to trigger a cell-autonomous, segment-specific pattern of death, APRs were labeled with the fluorescent dyes DiI or DiA, removed from the nervous system before the prepupal peak, and placed in low-density cell culture. Physiological levels of 20-HE triggered the same segment-specific pattern of APR death *in vitro* as seen *in vivo,* both in cultures containing a single APR and in cultures containing two APRs removed from the same donor animal. The presence or absence of contact with other cells did not influence the APRs' responses to 20-HE. The death of APRs in culture was characterized by fragmentation or rounding up of the cell body and fragmentation of the neurites. These findings suggest that intrinsic segmental identity regulates whether these motoneurons live or die when exposed to a steroid hormone during development. © 1997 Academic Press

INTRODUCTION

The nervous systems of many animals, including arthropods and vertebrates, are organized in repeating units along the anterior–posterior body axis. This organization is manifested by segmental patterns of gene expression and the development of segmented structures (Akam *et al.,* 1994; Keynes and Krumlauf, 1994; Lawrence and Morata, 1994; Wilkinson, 1995). In some instances, neurons and other cell types acquire intrinsic segmental identities that regulate particular aspects of their development, even if normal cues from the environment are missing (Shankland and Martindale, 1992). One phenotype often expressed during segmental specialization of the nervous system is programmed cell death, which sculpts the final number of neurons to match the functional requirements of the body segment (Bate *et al.,* 1981; Jeffs *et al.,* 1992; Thompson and Siegler, 1993). Programmed cell death is a widespread developmental phenomenon that can be triggered by extrinsic cues, but results ultimately from an autonomous program of self-destruction undertaken by the dying cell (White and Steller, 1995). Among the many extrinsic factors that regulate programmed cell death are steroid hormones, as illustrated by the development of sexually dimorphic neural populations in vertebrates (Breedlove, 1992; Mills and Sengelaub, 1993; Nordeen *et al.,* 1985) and the elimination of outmoded neurons during insect metamorphosis (see below; Truman *et al.,* 1992). Steroid hormones typically have access to all cells in an organism via the circulatory system, yet the responses of individual cells can be remarkably specific. An important issue relevant to the development of both vertebrate and invertebrate nervous systems is how segmental identity and steroid responsiveness interact to regulate neuronal phenotype, including the expression of programmed cell death.

During metamorphosis, the insect nervous system undergoes a hormonally mediated reorganization that includes dendritic and axonal remodeling, the generation of new neurons, and programmed cell death of outmoded neurons (Levine *et al.,* 1995; Weeks and Levine, 1992). Programmed cell death in the hawkmoth, *Manduca sexta,* has been best characterized in abdominal motoneurons. These motoneurons undergo two waves of death: one following entry into

[1] Current Address: Department of Biological Structure, University of Washington, Seattle, WA 98195-7420.

0012-1606/97 $25.00
Copyright © 1997 by Academic Press
All rights of reproduction in any form reserved.

the pupal stage and one following emergence of the adult moth, paralleling the progressive simplification of the abdominal musculature (Giebultowicz and Truman, 1984; Levine and Truman, 1985; Taylor and Truman, 1974; Truman, 1983; Weeks and Truman, 1985). Metamorphic changes in the *Manduca* nervous system, including programmed cell death, are regulated by juvenile hormone (JH) and ecdysteroids [ecdysone and its biologically active hydroxylation product, 20-hydroxyecdysone (20-HE)]. Specific changes in the circulating levels of these hormones trigger the two waves of motoneuron death (see below; Bennett and Truman, 1985; Truman and Schwartz, 1984; Weeks, 1987; Weeks and Truman, 1985, 1986; Weeks *et al.*, 1992).

Among motoneurons that die after pupation, the best-studied are those that innervate larval proleg muscles. The prolegs are locomotory appendages located on abdominal segments three through six (A3–A6) and the terminal abdominal segment (Fig. 1). The musculature of each proleg in segments A3–A6 includes the accessory planta retractor muscle (APRM), which is innervated by two accessory planta retractor (APR) motoneurons located in the ganglion of the same segment (Sandstrom and Weeks, 1996; Weeks and Truman, 1984). During the larval stage, APR homologs in segments A3–A6 [termed APR(3), APR(4), etc.] are indistinguishable by many electrophysiological and morphological criteria, and their behavioral roles are well characterized (Sandstrom, 1993; Sandstrom and Weeks, 1996; Streichert and Weeks, 1995; Weeks and Jacobs, 1987; Weeks and Truman, 1984). In contrast to their similarities during the larval stage, APR homologs in different segments exhibit markedly different fates at pupation: the APR(3)s and APR(4)s survive and are respecified for new functions, while the APR(5)s and APR(6)s undergo programmed cell death (Lubischer *et al.*, 1995; Sandstrom, 1993; Weeks and Ernst-Utzschneider, 1989; Weeks *et al.*, 1992). The death of APR(5)s and APR(6)s occurs within 48 hr after entry into the pupal stage.

Previous studies have investigated the hormonal cues for APR death and possible causes of the segment-specific pattern by which APRs die. After entry into the final larval instar, JH levels drop, followed by a small elevation of ecdysteroids in the absence of JH (the *commitment pulse;* Fig. 1). The commitment pulse acts as a developmental switch that commits cells to express pupal phenotypes during the subsequent *prepupal peak* of ecdysteroids, which triggers the larval–pupal molt (Bollenbacher, 1988; Riddiford, 1985). The prepupal peak of ecdysteroids also triggers the death of proleg motoneurons, as shown by experimental manipulations of hormone levels (Weeks, 1987; Weeks and Truman, 1985, 1986; Weeks *et al.*, 1992). For example, elimination of the prepupal peak prevents the death of APR(5)s and APR(6)s, and reinstatement of the prepupal peak by infusing 20-HE into the hemolymph (blood) triggers the death of APR(5)s and APR(6)s (Weeks *et al.*, 1992). In either case, the APR(3)s and APR(4)s survive. Tests of the possible role of interactions with other cells in regulating the segmental pattern of the APRs' responses to the prepupal peak have been uniformly negative. Cues from the target muscle have been ruled out by observations that the segmental pattern of APRM degeneration at pupation does not match the segmental pattern of APR death, and ablation of APRMs does not influence which APRs live or die (Lubischer and Weeks, 1996; Sandstrom, 1993). Likewise, deafferentation of APRs by amputating the proleg or severing the proleg sensory nerve (to eliminate a major source of monosynaptic excitatory input to APRs), or neural isolation of individual ganglia by severing the adjacent interganglionic connectives, do not alter the segment-specific pattern of APR death (Lubischer and Weeks, 1996; Weeks and Davidson, 1994).

These observations suggested that each APR may respond directly to the prepupal peak of ecdysteroids, with the motoneuron's segmental identity determining whether the death program is initiated. Most *Manduca* motoneurons, including the APRs, express ecdysteroid receptors (EcRs) during the prepupal peak (J. Ewer and J. C. Weeks, unpublished results; Fahrbach, 1992; Truman *et al.*, 1994), consistent with the possibility of direct hormone action. A powerful technique for testing whether the expression of a particular phenotype is cell autonomous is to place the cells of interest in a different environment by the use of transplantation or cell culture. The hypothesis that ecdysteroids act directly on APRs to trigger a cell-autonomous, segment-specific pattern of programmed cell death was tested in the present experiments by removing APRs from the nervous system and exposing them to 20-HE *in vitro.* APRs exhibited the same segment-specific pattern of programmed cell death *in vitro* as *in vivo,* supporting this hypothesis. Some of these results appeared previously in an abstract (Streichert and Weeks, 1994).

MATERIALS AND METHODS

Experimental Animals

M. sexta larvae were reared on artificial diet (modified from Bell and Joachim, 1976) in a colony maintained on a 17 hr light, 7 hr dark photoperiod and a 27:25°C temperature cycle. Larvae were staged by characteristic developmental events (Fig. 1) and anesthetized in CO_2 gas or by chilling on ice before dye injections or dissections.

Labeling of APR Motoneurons

APRs were retrogradely labeled *in situ* by application of the lipophilic carbocyanine dyes, DiI or DiA (Molecular Probes), to APRMs of intermolt 4th instar larvae (Fig. 1). APRM, which runs dorsoventrally from the body wall adjacent to the spiracle (respiratory opening) to the lateral wall of the proleg, is an external muscle that lies immediately beneath the body wall (Weeks and Ernst-Utzschneider, 1989; Weeks and Truman, 1984). Approximately 5 μl of DiI or DiA (10 mg/ml in petroleum jelly) was injected into the space between APRM and the body wall, using a Hamilton syringe.

Copyright © 1997 by Academic Press. All rights of reproduction in any form reserved.

Injection of dye into this region minimized potential contact with other muscles. For singly cultured APRs (see Results), DiI was injected bilaterally in segments A4 and/or A6. For cocultures of two APRs from the same larva, DiA was injected bilaterally in segment A4 and DiI was injected bilaterally in segment A6. On Day W0 (5 to 7 days postinjection; Fig. 1) ganglia from injected segments were removed in filter-sterilized physiological saline (in mM: NaCl, 140; KCl, 5; $CaCl_2$, 4; glucose, 28; Hepes, 5; pH 7.4; Trimmer and Weeks, 1989). The ganglia were then placed in serum-free, hormone-free control culture medium [modified Leibovitz's L15 (Gibco); Prugh *et al.*, 1992], desheathed without enzymatic pretreatment, mounted in control culture medium between coverslips, and examined under epifluorescent illumination for labeled APRs. APRs are the only proleg motoneurons with cell bodies on the ventral surface of the ganglion and hence can be identified unambiguously by soma location (Weeks and Davidson, 1994; Weeks and Truman, 1984). Labeled APRs exhibited punctate, cytoplasmic fluorescence under rhodamine (for DiI) or fluorescein (for DiA) optics (Figs. 2, 3, and 5). The cytoplasmic location of the label has been reported previously for other *Manduca* motoneurons labeled by this technique (Prugh *et al.*, 1992). Two APRs innervate each APRM (Sandstrom and Weeks, 1996), so as many as four APRs were labeled per ganglion (Fig. 2). Other motoneurons that innervate internal muscles near APRM have cell bodies on the dorsal surface of the ganglion (Levine and Truman, 1985; Weeks and Truman, 1984). Infrequently, these motoneurons were labeled, in which case they were excised before the ganglion was dissociated.

Culture Procedures

Methods for culturing APRs were adapted from those used previously to culture *Manduca* interneurons (Hayashi and Hildebrand, 1990) and thoracic motoneurons (Prugh *et al.*, 1992). Ganglia containing labeled APRs were treated with 1 mg/ml collagenase (Sigma) and 4 mg/ml dispase (Boehringer-Mannheim) in Ca^{2+}-free and Mg^{2+}-free Hanks' balanced salt solution (30–60 min, 23–26°C), rinsed twice in control culture medium, and dissociated by trituration using fine tungsten needles and a fire-polished micropipet tip. In experiments with one APR per culture dish, a single DiI-labeled APR was transferred to a drop of control medium in a glass-bottomed well in a UV-sterilized, 35-mm plastic petri dish coated with concanavilin A (Sigma) and laminin (Gibco; Prugh *et al.*, 1992). A small number (<20) of additional, unidentified cells were also transferred to the dish. The same procedures were used for cocultured APRs (see Results), except that each culture dish contained one DiA-labeled APR(4) and one DiI-labeled APR(6) which had been removed from the same larva. A small number of additional cells from the two ganglia were also added. Covered culture dishes were placed within larger, covered petri dishes, each containing a small open dish of dH_2O to maintain humidity. The cultures were kept in a 26°C incubator with ambient air. After 1 day, the culture dishes were flooded with 2 ml of control medium. APRs that adhered to the substratum and extended one or more neurites within 3 to 7 days after being placed in culture were accepted for the study, and the culture dish was treated with medium containing 1 or 10 μg/ml 20-HE (Sigma), or control medium containing no hormone. The day of this medium change was designated Experimental Day 0 (Fig. 1). Half the medium was exchanged twice weekly with medium of the same composition.

Assessment of APR Survival

Cultured APRs were viewed under a Zeiss Axiovert inverted microscope equipped with epifluorescence optics. APRs were photographed under epifluorescence and phase contrast optics on Day 0 and under phase contrast optics at approximately 3-day intervals for at least 20 days, unless an APR was scored as dead (see Results) before this time. APRs were readily reidentifiable on subsequent days *in vitro* by their individual morphologies and patterns of neurite outgrowth. Reidentification was facilitated by the low density of cells in each dish. Brief fluorescent illumination to visualize the DiI or DiA label was used only as needed to reconfirm APR identity. No deleterious effects have been reported for long-term labeling of *Manduca* motoneurons with carbocyanine dyes (Kent and Levine, 1988; Prugh *et al.*, 1992) and we likewise observed no ill effects.

APRs were scored as dead by specific morphological criteria (see Results). The specificity of APR death was verified by the presence of other live cells in each dish. For each cultured APR included in this paper (n = 87), the series of photographs taken during the culture period was coded and scored blindly and independently by two to six observers. The presence of contact with other cells was also scored in each photographic series.

The viability of some APRs was examined at the end of the culture period by staining with Trypan blue (Sigma), which is excluded from living cells, or MTT (3-(4,5-dimethylthiazol-2-yl)-2,5-diphenyltetrazolium bromide; Sigma), a positive marker of mitochondrial dehydrogenase activity in living cells. For Trypan blue staining, the culture medium was replaced with 0.4% Trypan blue in physiological saline for 10 min, followed by repeated saline rinses. The presence of positive blue staining of the cell body (or its fragmented remnants) indicated cell death. For MTT staining, cells were incubated in 0.125 mg/ml MTT in culture medium for 40 min and examined for dark purple reaction product, indicating cell viability. Both types of staining were performed at room temperature (24–26°C).

Statistical Analyses

All statistical comparisons were by χ^2 analysis (BMDP Statistical Software, Inc., Los Angeles, CA).

RESULTS

Effect of 20-HE on the Survival of Singly Cultured APR(4)s and APR(6)s

To test the hypothesis that 20-HE triggers a cell-autonomous, segment-specific pattern of APR death, we placed APR(4)s and APR(6)s in culture and examined their responses to 20-HE. The APR(4)s and APR(6)s survive and die, respectively, after pupation, and APRMs degenerate in both segments (Sandstrom, 1993; Weeks and Ernst-Utzschneider, 1989). Figure 1 summarizes the experimental protocol for singly cultured APRs. APR(4)s and APR(6)s were retrogradely labeled *in situ* with the fluorescent marker, DiI (see Materials and Methods). On Day W0, following the commitment pulse but prior to the prepupal peak, ganglia from segments A4 or A6 were removed and examined for labeled APRs (Fig. 2). Ganglia that contained DiI-labeled APRs were

Copyright © 1997 by Academic Press. All rights of reproduction in any form reserved.

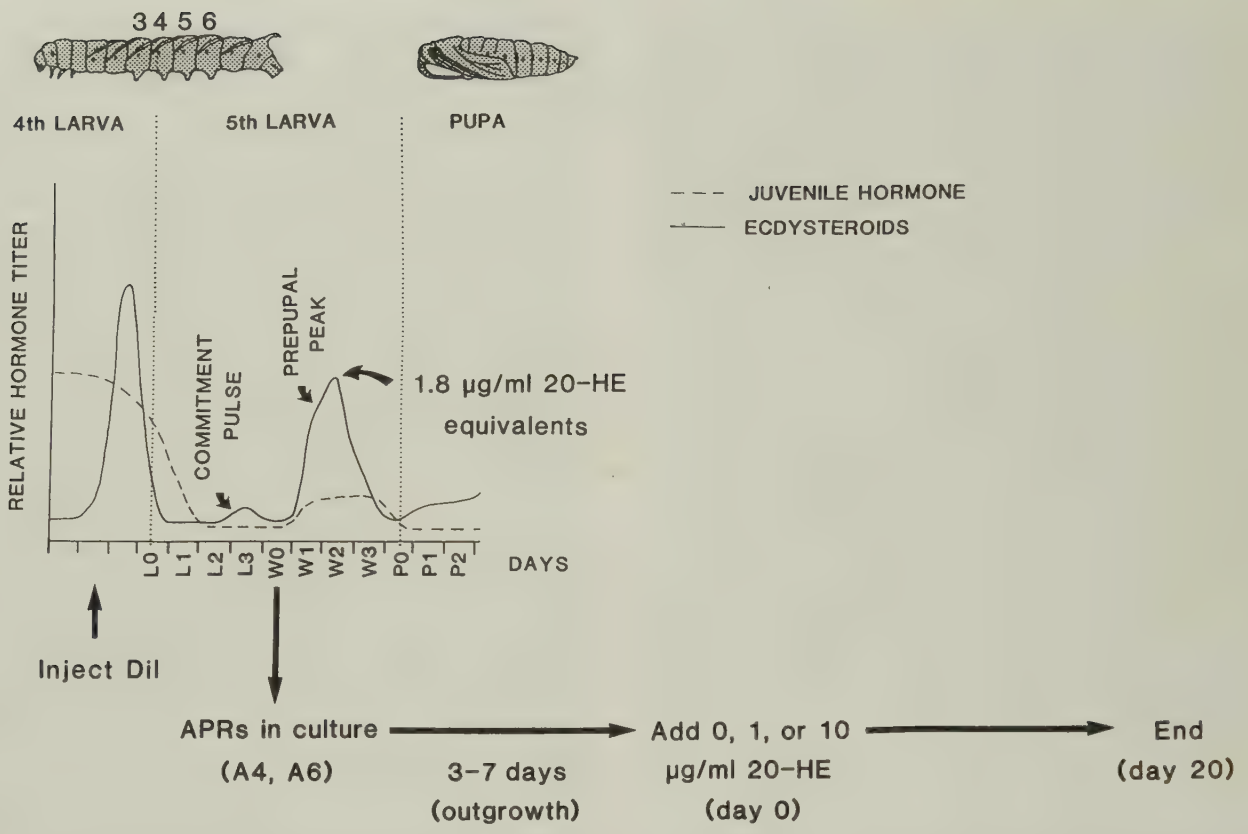

FIG. 1. Experimental protocol for singly cultured APRs. A timeline of development is shown, spanning the 4th larval instar to early pupal stage. Days of development are numbered relative to the following developmental events: L0, day of entry into the 5th larval instar; W0, day of onset of wandering behavior (marked by pigmentation changes and gut purge); P0, day of entry into the pupal stage. Other days are numbered with respect to these events. The relative levels of ecdysteroids and juvenile hormone (JH) are shown, and the commitment pulse and prepupal peak of ecdysteroids are indicated (hormone titers redrawn from Riddiford and Truman, 1994). The value for the maximum 20-HE concentration in the hemolymph during the prepupal peak is from Bollenbacher *et al.* (1981). The protocol for singly cultured APRs is summarized beneath the timeline. See text for details.

dissociated and one DiI-labeled APR(4) or APR(6), along with a small number of additional cells, was placed in each culture dish in hormone-free, serum-free control medium (see Materials and Methods). Because the dissociation procedure eliminated neuronal processes, each APR had only a cell body and, in some cases, a short length of primary neurite when placed in culture. The DiI label persisted for the entire culture period.

APRs that adhered to the substratum and initiated process outgrowth within 3 to 7 days after being placed in culture entered the study. This waiting period eliminated APRs that were damaged during dissociation and ensured that APRs in the study were viable and hence more likely to exhibit physiologically appropriate responses. Similar proportions of APR(4)s and APR(6)s met these acceptance criteria (see below). On the day that an APR entered the study (Day 0; Fig. 1), the culture dish was treated with medium containing 1 or 10 μg/ml 20-HE or with control medium containing no 20-HE. These concentrations of 20-HE bracket endogenous levels during the prepupal peak (Fig. 1). The same hormonal conditions were maintained for the remainder of the culture period (which was 20 days, unless an APR died earlier; see below).

Live and dead APRs were easily distinguished by obvious morphological criteria. The cell bodies of live APRs were ovoid and flattened and adhered firmly to the substratum (Figs. 3A, 3B, and 5A). The cell bodies were continuous with the neurites, which were flattened, extensively branched, and continued to undergo morphological remodeling throughout the culture period. The transformation from live to dead was characterized by a profound loss of cellular integrity (Figs. 3C and 5B). The neurites fragmented and became discontinuous with each other and the cell body (Fig. 3C, Days 4 and 7). Concomitantly, the cell body either fragmented (Fig. 3C, Day 7) or rounded up into a spherical shape that was poorly attached to the substratum (Fig. 5B,

Copyright © 1997 by Academic Press. All rights of reproduction in any form reserved.

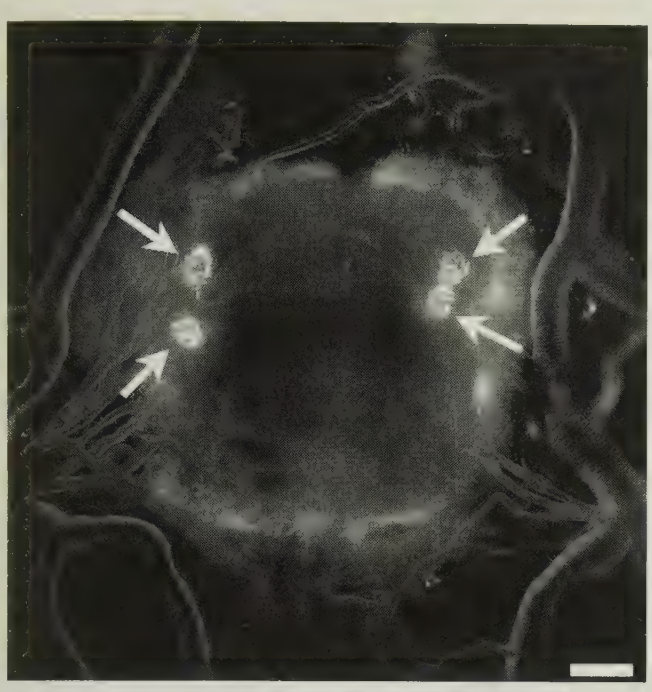

FIG. 2. Labeled APRs *in situ*. Four APR(6)s (arrows) labeled with DiI are shown in a living ganglion on Day W0, prior to dissociation. The DiI label consisted of bright, punctate fluorescence in the somatic cytoplasm. Background fluorescence in connective tissue around the periphery of the ganglion is also apparent. Anterior is up. Scale bar = 100 μm.

Day 20). Because of our acceptance criteria (see above), 100% of APR(4)s and APR(6)s were alive when they entered the study on Day 0. An APR was scored as dead when the following two morphological criteria were met: (1) the neurites were fragmented and (2) the soma was either fragmented or rounded up. The specificity of APR death was verified by the presence of other live cells in each dish. In some instances, APRs were stained at the end of the culture period with either Trypan blue or MTT, which are markers of cell viability (see Materials and Methods). These stains confirmed the scoring of APRs as dead or alive by the above morphological criteria (data not shown). A more recent study has likewise confirmed these morphological criteria for APR death by the use of additional staining methods (Hoffman and Weeks, 1996 and unpublished results).

Figure 3 shows representative APRs from different 20-HE treatment groups, and Fig. 4 summarizes the findings. Figure 3A shows an APR(4) cultured in 1 μg/ml 20-HE. This APR(4) underwent substantial neuritic growth during the culture period and was still alive on Day 21, as indicated by the above morphological criteria including intact cell body and neurites. Conspicuous lamellipodia, indicating active growth, were apparent on each day shown. Figure 4 shows that nearly all APR(4)s survived through Day 20, regardless of whether they were cultured with or without 20-HE. The proportion of surviving APR(4)s did not differ significantly among the three treatment groups ($P > 0.05$).

In contrast, the proportion of surviving APR(6)s did differ significantly among the three treatment groups ($P < 0.01$). Nearly all APR(6)s cultured without 20-HE survived, as illustrated by the cell shown in Fig. 3B. This APR(6) was still alive on Day 26, at which time its cell body and neurites were intact and remodeling of neuritic processes was still ongoing. Neuritic growth in APR(6)s cultured without 20-HE appeared similar to that of APR(4)s cultured with or without 20-HE. As shown in Fig. 4, the survival of APR(6)s did not differ significantly from the survival of APR(4)s when cultured in the absence of 20-HE ($P > 0.05$). Treatment with 20-HE, however, caused APR(6)s to die. Figure 3C illustrates the death of an APR(6) cultured in 1 μg/ml 20-HE. On Day 2, the cell was alive. By Day 4 its neurites had begun to fragment, and by Day 7 the cell body had also undergone complete fragmentation. As in all cases in which an APR was scored as dead, other cells in the same culture dish were still alive (not shown). Figure 4 shows that, in both the 1 and 10 μg/ml 20-HE treatment groups, the proportion of surviving APR(4)s and APR(6)s differed significantly ($P < 0.002$).

In summary, 20-HE evoked the same segment-specific pattern of APR death *in vitro* as seen *in vivo:* APR(4)s survived in the presence or absence of 20-HE, whereas APR(6)s survived in the absence of 20-HE but died when exposed to physiological levels of 20-HE.

Effect of 20-HE on the Survival of Cocultured APR(4)s and APR(6)s

Two sources of uncontrolled variability in the previous experiments were that APRs were removed from different larvae and cultured in different dishes. Although these factors were unlikely to account for the segmental specificity with which 20-HE triggered APR death, we performed another set of experiments that eliminated both sources of variability. The same protocol shown in Fig. 1 was followed, with the following modifications. In individual larvae, the APR(4)s were labeled with DiA while the APR(6)s were labeled with DiI. This labeling technique permitted the two APRs to be unequivocally distinguished throughout the culture period. On Day W0, cocultures were prepared in which one APR(4) and one APR(6) from the *same* larva were placed in the *same* dish. When both APRs met the acceptance criteria and a culture entered the study (Day 0), it was treated with 10 μg/ml 20-HE for the remainder of the culture period.

Figure 5 shows a representative coculture. On Day 0, the distinguishing fluorescent labels of the two APRs are shown. On Day 6, both APRs were alive and active growth cones were apparent at the distal tips of growing neurites. However, by Day 20, the APR(6) had died (note rounded-up

Copyright © 1997 by Academic Press. All rights of reproduction in any form reserved.

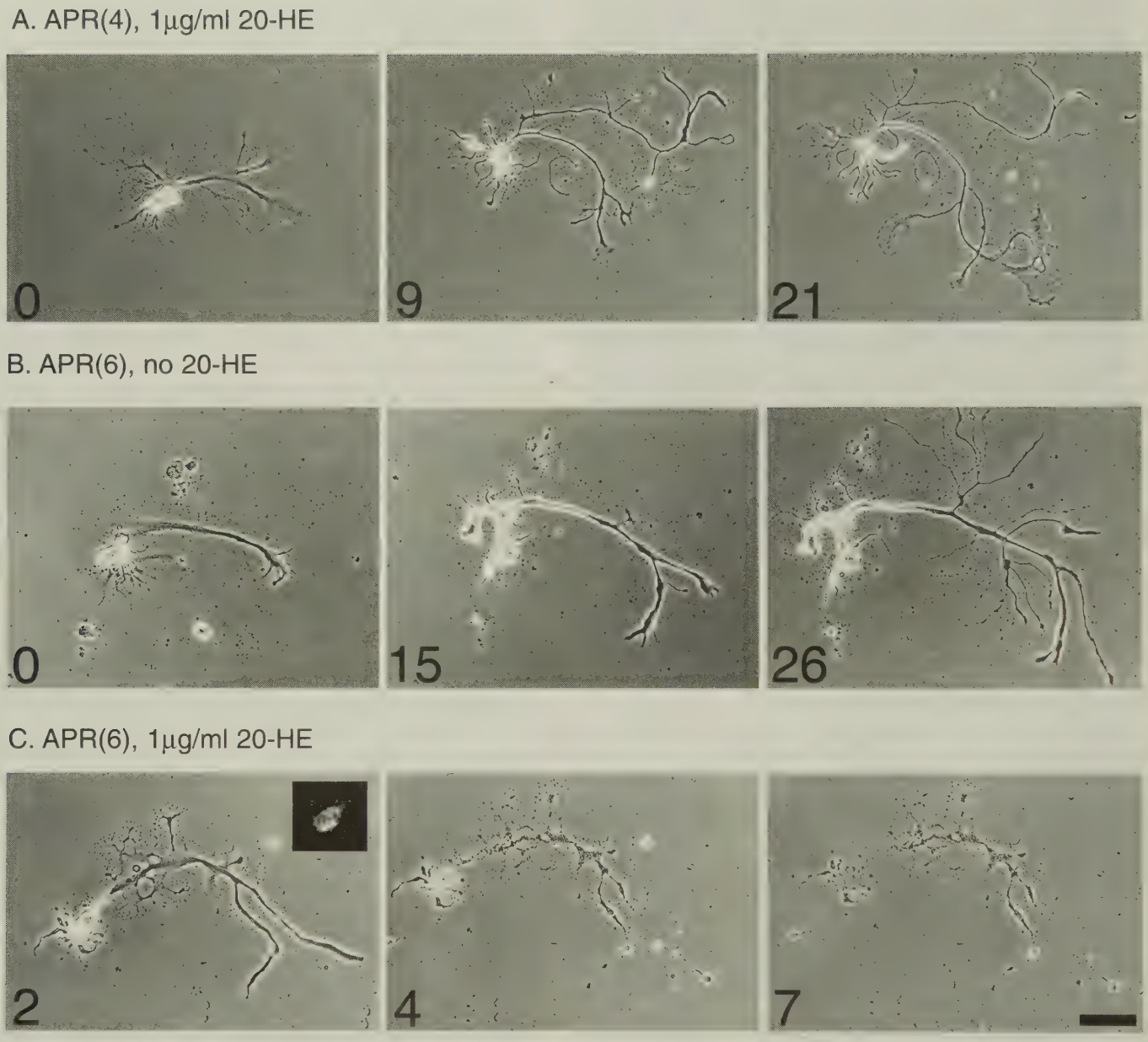

FIG. 3. Effects of 20-HE on singly cultured APRs. Photomicrographic series of singly cultured APRs from the indicated segment and hormonal condition are shown. Experimental day is indicated in each panel. (A) APR(4) treated with 1 μg/ml 20-HE. (B) APR(6) cultured without 20-HE. (C) APR(6) treated with 1 μg/ml 20-HE; the inset shows DiI labeling of the same APR. The APR(4) in 1 μg/ml 20-HE (A) and the APR(6) cultured without 20-HE (B) survived more than 20 days. The APR(6) in 1 μg/ml 20-HE (C) was dead by Day 7, as indicated by fragmented neurites and cell body. Note in A and B that, over the culture period, some neurites ceased growth and took on a "beaded" appearance while other neurites continued active growth. This beaded appearance, which was characteristic of neuritic remodeling, was quite distinct from fragmentation (e.g., C, Days 4 and 7). Scale bar = 50 μm except Days 9 and 21 in A, where bar = 75 μm.

cell body and fragmented neurites), whereas the APR(4) was still alive. The same result was obtained in each of five cocultures: the APR(4) survived while the APR(6) died. This difference in the survival of cocultured APR(4)s and APR(6)s was significant ($P < 0.002$). Thus, APRs isolated from the same donor animal, differing only in segment of origin, ex-

Copyright © 1997 by Academic Press. All rights of reproduction in any form reserved.

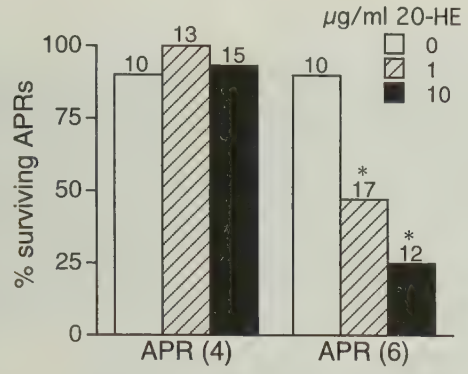

FIG. 4. Segment-specific death of singly cultured APRs in response to 20-HE. The percentage of APRs alive on Day 20 is shown by segment and hormone treatment (*n* above each bar). The proportion of surviving APR(4)s did not differ significantly among the three hormone treatment groups (0, 1, or 10 μg/ml 20-HE), whereas the survival of APR(6)s did. Comparison of APR(4)s and APR(6)s showed no significant difference in survival between the two no-hormone groups. In contrast, the proportion of surviving APR(4)s and APR(6)s did differ significantly in both the 1 and 10 μg/ml 20-HE groups (*). See text for details.

hibited different responses when exposed to an identical hormonal environment in culture.

Proportion of APRs Meeting Acceptance Criteria

As described above, acceptance criteria were used to ensure that APRs that entered the study were viable. Because previous studies found no segmental differences among APRs on Day W0 (Sandstrom, 1993; Streichert and Weeks, 1995; Weeks *et al.*, 1992), and all APRs were treated identically during culturing procedures, we expected that similar proportions of APR(4)s and APR(6)s would meet the criteria. This expectation was borne out. The percentage of singly cultured APRs that met acceptance criteria was 41% (45 of 109) for APR(4)s and 31% (49 of 159) for APR(6)s. For cocultured APRs, these percentages were 67% (12 of 18) for APR(4)s and 58% (11 of 19) for APR(6)s. In both cases, the proportions of APR(4)s and APR(6)s that met the acceptance criteria did not differ significantly ($P > 0.05$). The percentage of accepted APRs was higher for cocultures than single cultures, reflecting improvements in culturing techniques over the course of this study. The number of APRs that passed acceptance criteria was greater than the final number for which data are reported due to factors such as occasional loss of cultures from contamination and the elimination of some cocultures when only one APR of the pair met the acceptance criteria.

Time to Death

In vivo, 5 days separate the onset of the prepupal peak and the death of APR(6)s (Weeks *et al.*, 1992). In culture, the mean time from the addition of 20-HE on Day 0 to the death of APR(6)s was 12.4 ± 3.2 (SD) days ($n = 24$; combined data from singly cultured and cocultured APRs). The mean time to death was similar in the 1 and 10 μg/ml 20-HE groups. Thus, the interval from the onset of hormone exposure to the time at which an APR(6) was scored as dead was approximately twice as long in culture as *in vivo*.

Role of Contact

In all experiments each culture dish contained fewer than 20 cells. Some APRs remained physically isolated from other cells while other APRs had contact with one or more cells of unknown identity. No APR(4)s and APR(6)s contacted each other in cocultures. Because the presence or absence of contact could potentially influence the responses of APRs to 20-HE, we scored the incidence of contacts. Table 1 presents the number of APRs with or without contact and indicates whether APRs in these two categories were alive or dead at the end of the culture period. In total, 45% of the APRs (39 of 87; combined data from singly cultured and cocultured APRs) showed contact with another cell during the culture period. However, the proportion of APRs with contact did not differ significantly among the six experimental groups shown in Table 1 ($P > 0.05$), so this factor could not explain the observed effects of 20-HE on APR survival. The lack of relationship between cell contact and APR survival is underscored by specific examples. For example, among the 23 APR(6)s that died in the 1 and 10 μg/ml 20-HE treatment groups, 12 had contact and 11 did not. Likewise, of the 11 APR(6)s in the 1 and 10 μg/ml 20-HE groups that survived, 4 had contact and 7 did not. Of the 41 of 43 APR(4)s that survived, 17 had contact and 24 did not. Thus, segment of origin and exposure to 20-HE were the key determinants of APR survival rather than whether cell contact occurred.

As a specific test of the hypothesis that 20-HE acts *directly* on APRs to trigger segment-specific death, we examined the effect of 20-HE treatment on the survival of the subset of 48 APRs that had no contact during the culture period (Table 1). In this group, the proportions of surviving APR(4)s and APR(6)s cultured without 20-HE did not differ significantly ($P > 0.05$). In contrast, in the presence of 1 or 10 μg/ml 20-HE, the proportions of surviving APR(4)s and APR(6)s were significantly different ($P < 0.02$). Thus, even in the absence of contact with other cells, APRs showed the correct segment-specific pattern of programmed cell death in response to 20-HE.

DISCUSSION

Segment-Specific Death of APRs Is Triggered Directly by 20-HE in Vitro

This study provides compelling evidence for the hypothesis that ecdysteroids act directly on APRs to trigger a cell-

Copyright © 1997 by Academic Press. All rights of reproduction in any form reserved.

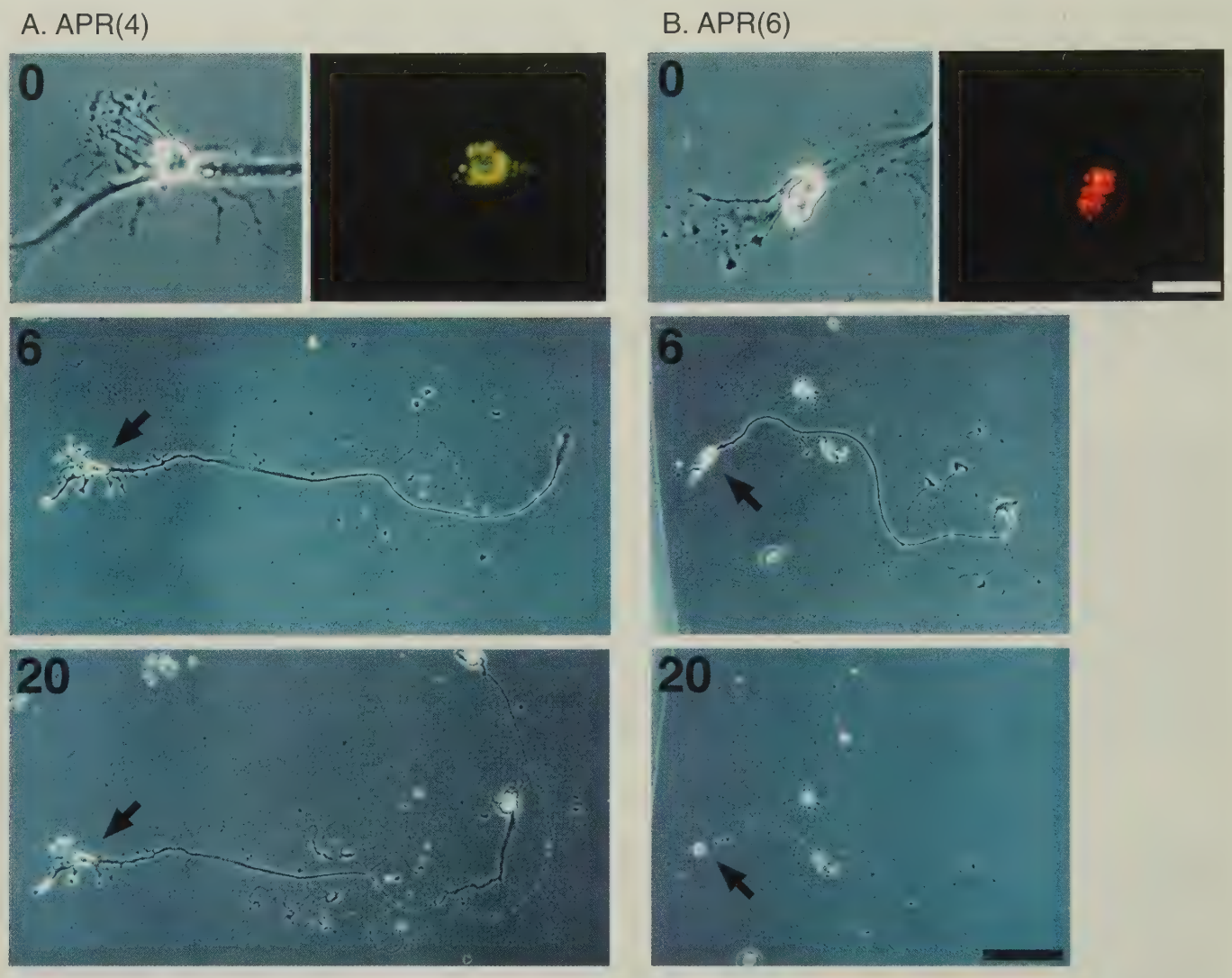

FIG. 5. Effects of 20-HE on cocultured APRs. Photomicrographic series show an APR(4) (A) and an APR(6) (B) removed from a single larva and cocultured in a dish treated with 10 μg/ml 20-HE beginning on Day 0. Experimental day is indicated in each panel. Fluorescent DiA labeling of APR(4) (A) and DiI labeling of APR(6) (B) are shown on Day 0. APR somata are marked by arrows on Days 6 and 20. The APR(4) remained alive through Day 20, whereas the APR(6) was dead by Day 20 (indicated by fragmented neurites and rounded-up cell body). This APR(6) was first scored dead on Day 9 (not shown). Note that the most distal neurite in A initially extended (Day 6) but then became beaded as a more proximal branch extended (Day 20). Scale bar: Day 0, 50 μm; other days, 200 μm.

autonomous, segment-specific pattern of programmed cell death. APR homologs in larval abdominal segments A3–A6 are indistinguishable by a number of criteria (Sandstrom, 1993; Streichert and Weeks, 1995), yet show strikingly different responses to the hormonal environment of pupation: the prepupal peak of ecdysteroids triggers the death of APR(5)s and APR(6)s while APR(3)s and APR(4)s survive and are respecified for new functional roles. The present experiments demonstrate that APRs continue to express the correct segment-specific pattern of programmed cell death when removed from the nervous system and exposed to 20-HE *in vitro*. When the prepupal peak is prevented *in vivo*, the APR(6)s survive (Weeks *et al.*, 1992) and, similarly, APR(6)s cultured in the absence of 20-HE survived (Fig. 4). Treatment with physiological levels of 20-HE that bracket the hemolymph concentration of 20-HE during the prepupal peak (Fig. 1) caused a significant proportion of APR(6)s to die. The ability of 20-HE to trigger the death of APR(6)s could not be explained by nonspecific toxic effects of the hormone because other cells in each dish remained alive

Copyright © 1997 by Academic Press. All rights of reproduction in any form reserved.

TABLE 1
Comparison of Cell Contact and APR Survival[a]

	20-HE (μg/ml)	n^b	APRs with contact		APRs without contact	
			Alive	Dead	Alive	Dead
APR(4)	0	10	3	1	6	0
	1	13	6	0	7	0
	10	20	8	0	11	1
APR(6)	0	10	5	0	4	1
	1	17	4	3	4	6
	10	17	0	9	3	5

[a] Whether or not an APR had contact with other cells during the culture period was scored (see Materials and Methods) for each APR in the different treatment groups. The table shows the number of APRs with or without contact that were alive or dead at the end of the culture period. See text for details.

[b] Number of APRs. Data combined from singly cultured and co-cultured APRs.

and, furthermore, APR(4)s exposed to the same 20-HE treatments survived (Fig. 4), just as they do *in vivo* (Weeks *et al.*, 1992). The most striking demonstration of the selective effect of 20-HE in inducing APR death was provided by cocultures in which the hormone triggered the death of APR(6)s but not APR(4)s taken from the same donor larva (Fig. 5). The present experiments utilized only APR(4)s and APR(6)s, which are representative of the subsets of APRs that survive and die, respectively, at pupation: we assume that APRs from other segments would express their segment-specific responses to 20-HE in culture, as well. Previous studies have similarly demonstrated the specificity of 20-HE action in promoting neurite outgrowth of cultured *Manduca* thoracic leg motoneurons, which mimics the stage- and cell-specificity of 20-HE effects *in vivo* (Prugh *et al.*, 1992; Witten and Levine, 1991).

All APRs examined in this study were removed from larvae on Day W0, following the commitment pulse of ecdysteroids and prior to the prepupal peak (Fig. 1). The relative roles of the commitment pulse and prepupal peak in regulating the expression of pupal phenotypes in proleg motoneurons have been identified by manipulating hormone levels experimentally (Weeks and Truman, 1985, 1986; Weeks, 1987; Weeks *et al.*, 1992). Treatment with JH during the commitment pulse prevents expression of pupal phenotypes during the prepupal peak, whereas treatment with JH during the prepupal peak has no effect. The quantitative relationship between the dose and time of 20-HE exposure, and the efficacy of the exposure in triggering the programmed cell death of APRs, has also been determined (Weeks *et al.*, 1992). These *in vivo* studies have generated a number of hypotheses about hormonal effects on neuronal phenotype in *Manduca* that now can be further tested *in vitro* at the level of individual neurons. As an example of this approach, Prugh *et al.* (1992) have shown that JH blocks the ability of 20-HE to promote neurite outgrowth in cultured *Manduca* thoracic leg motoneurons, just as it does *in vivo* (Truman and Reiss, 1988).

Two aspects of the 20-HE exposure *in vitro* differed from the *in vivo* conditions, but could not account for the segmental specificity of APR responses. First, after APRs were placed in culture on Day W0, there was a 3- to 7-day hormone-free period before they were treated with 20-HE. This protocol delayed the onset of 20-HE exposure relative to the normal onset of the prepupal peak on Day W1 (Fig. 1). A previous study showed that, following exposure to the commitment pulse, proleg motoneurons retain the ability to express pupal phenotypes *in vivo* when the prepupal 20-HE exposure is delayed by 4 days (Weeks and Truman, 1985). The present results confirm this finding *in vitro*. Another difference between culture conditions and the *in vivo* situation was that APRs were cultured in a constant 20-HE concentration for an extended period of time and did not experience the normal decline in 20-HE levels at the end of the prepupal peak (Fig. 1). A decline in ecdysteroid levels is required for some developmental events (Ashburner and Richards, 1976; Woodard *et al.*, 1994; Truman and Schwartz, 1984), but prevention of the falling phase of the prepupal peak *in vivo* by infusing 20-HE into the hemolymph does not prevent the death of proleg motoneurons (Weeks and Truman, 1985). Thus, both *in vivo* and *in vitro* experiments indicate that the rising phase of the prepupal peak of ecdysteroids triggers the death of APR(5)s and APR(6)s and that the decline is not required. At adult emergence, the death of a group of *Manduca* abdominal motoneurons that innervate intersegmental muscles is triggered by an ecdysteroid decline (Truman and Schwartz, 1984). Although the hormonal trigger for the death of APR(3)s and APR(4)s at emergence has not been tested directly, it is likely to be the same as for the other motoneurons. If this is the case, then different aspects of the 20-HE profile—a rise in 20-HE at pupation and a fall in 20-HE at emergence—trigger the death of APR homologs in different segments. As discussed elsewhere (Weeks and Levine, 1992), the response of a cell to a particular hormonal event during metamorphosis depends critically on the cell's past history of hormonal exposure. In the case of the APRs, segmental identity further refines the specificity of the response. One of the key questions raised by these experiments is how segmental identity regulates the interpretation of hormonal events such that the death program is activated in APR homologs in different segments at different developmental times.

Most *Manduca* motoneurons express EcRs during the prepupal peak (Fahrbach, 1992; Truman *et al.*, 1994), including the APRs in segments A3–A6 (J. Ewer and J. C. Weeks, unpublished results). However, this observation is not, by itself, sufficient to conclude that 20-HE triggers the death of APR(6)s by a direct action. Previous experiments ruled out interactions with muscles, sensory afferents and other

Copyright © 1997 by Academic Press. All rights of reproduction in any form reserved.

ganglia as being necessary for the segment-specific pattern of APR death (Lubischer and Weeks, 1996; Weeks and Davidson, 1994), but it was still possible that 20-HE acted on other cells (e.g., interneurons or glia in the same ganglion) to trigger death indirectly through contact or a diffusible factor (e.g., Forger *et al.*, 1992). However, the finding that cultured APRs removed from their normal cellular environment nevertheless exhibited the correct segment-specific pattern of programmed cell death in response to 20-HE provides compelling evidence that 20-HE acts directly on APRs and that this direct action is sufficient to produce the characteristic segment-specific pattern of death. In the low-density cultures used in this study, some APRs had contact with other unidentified cells but the presence or absence of contact was unrelated to the responses of APRs to 20-HE (Table 1). Most strikingly, the subset of APRs that had no contact for the entire culture period showed the correct segment-specific pattern of death. Because other cells were present in the culture dishes we cannot exclude the possibility of indirect influences of 20-HE on APRs, but it seems highly unlikely that the small number (<20) of cells could have had a conditioning effect on the medium that affected APR survival; the volume of the medium was 2 ml, of which half was exchanged twice weekly with fresh medium. Furthermore, cocultured APR(4)s and APR(6)s shared the dish with additional cells derived from both segments, yet expressed the correct segment-specific phenotypes.

The most parsimonious interpretation of our results is that 20-HE acts directly on APR(6)s via EcRs to trigger an intrinsic cell death program. Although APR(4)s also have EcRs during the prepupal peak, exposure to 20-HE does not activate the death program. Interestingly, APRs in all segments respond to the prepupal peak *in vivo* by undergoing dendritic regression (Sandstrom, 1993; Streichert and Weeks, 1995), but it is not known whether regression is a direct or indirect response to 20-HE. 20-HE does appear to act directly in promoting neurite outgrowth in cultured *Manduca* thoracic leg motoneurons (Prugh *et al.*, 1992; Witten and Levine, 1991). It should be noted that more complex scenarios could underlie the death of APR(6)s and survival of APR(4)s at pupation. The molecular pathways for programmed cell death are subject to both positive and negative regulation at multiple levels and it is possible, for example, that EcRs activate cell death pathways in both APR(4)s and APR(6)s but concurrently trigger the synthesis of survival-promoting factors in APR(4)s that override the death-promoting effect (see Steller, 1995). Further characterization of the molecular pathways involved in APR death would be required to address this issue.

Time Course of APR Death in Culture

In this study, the mean time to death of APR(6)s following addition of 20-HE to the culture medium was approximately 12 days (see Results). *In vivo*, the death of APR(6)s is complete by Day P2 (Weeks *et al.*, 1992), which is 5 days following the onset of the prepupal peak (Fig. 1). The death of APR(6)s *in vivo* is indicated by the loss of the ability to be stained retrogradely with cobalt chloride (Weeks *et al.*, 1992) and, when examined *in situ* on Day P2, the somata of DiI-labeled APR(6)s are shrunken and rounded up (Hoffman and Weeks, 1996 and unpublished results). The DiI label subsequently becomes dispersed, presumably due to fragmentation and glial engulfment of the dead APR(6)s.

Several factors may have contributed to the lengthened time to death of cultured APR(6)s. First, cultured APRs were photographed at approximately 3-day intervals, which introduced delays between the time some APRs died and when they were scored as dead. This factor would contribute, at most, approximately 3 days to the measured time to death. Second, the criteria for death used in the study—fragmentation of the neurites and rounding-up or fragmentation of the soma—are late morphological stages in programmed cell death. Studies of other neurons undergoing programmed cell death have shown that breakdown of the plasma membrane is a relatively late event that follows other terminal events including condensation of the chromatin and DNA fragmentation (*in vitro* examples: Deckwerth and Johnson, 1993; Edwards and Tolkovsky, 1994). Recent studies of cultured APR(6)s confirm this sequence of events (Hoffman and Weeks, 1996, and unpublished results), indicating that the measured latency to APR death would have been shorter had an earlier marker of death been chosen. A third factor relevant to the use of fragmentation as a death marker is the absence in culture of interactions with other cells such as glia that might normally accelerate the degradation process (Batistatou and Greene, 1991; Thanos *et al.*, 1993; Sonetti *et al.*, 1994). Glial association with dying *Manduca* motoneurons *in vivo* has been reported (Stocker *et al.*, 1978). Finally, it is possible that biosynthetic processes were slowed in culture. The cultures were incubated at a temperature (26°C) similar to that in the *Manduca* colony (25–27°C; see Materials and Methods), but the culture medium or other aspects of the culture conditions may have been suboptimal. Although the use of fragmentation as a marker of APR death increased the measured time to death, it had several advantages for this initial characterization of programmed cell death *in vitro*. In particular, fragmentation is an unambiguous, easily scored phenotype that is apparent without the use of histological stains (most of which terminate the culture). Characterization of the programmed cell death of cultured APRs by the use of various histological markers of cell viability will be described elsewhere (Hoffman and Weeks, 1996 and unpublished results).

Molecular Mechanisms of Segmental Identity, Ecdysteroid Action, and Programmed Cell Death

The present experiments demonstrate that segmental identity intrinsically regulates whether APR motoneurons live or die when exposed to a developmentally appropriate

Copyright © 1997 by Academic Press. All rights of reproduction in any form reserved.

steroid hormone signal. These findings raise numerous questions regarding the molecular mechanisms involved in segmental identity, ecdysteroid action and programmed cell death in this system. The expression of different EcR isoforms is correlated with differences in cellular responses to ecdysteroids (Truman *et al.*, 1994; Robinow *et al.*, 1993), and it is possible that APRs from different segments express different EcR isoforms or differ in the regulation of events downstream of hormone–receptor binding (see above; Thummel, 1995; Zelhof *et al.*, 1995). Genes involved in segmental patterning, such as homeotic genes (reviewed in Carroll, 1995) could regulate the ability of EcRs to activate the molecular pathways for programmed cell death or, conversely, inhibit the expression of genes that promote neuronal survival (Evans-Storms and Cidlowski, 1995; White and Steller, 1995). Experiments performed *in vivo* have shown that treatment with cycloheximide to inhibit protein synthesis blocks the death of APRs (Weeks *et al.*, 1993) and other *Manduca* motoneurons (Fahrbach *et al.*, 1993), and recent experiments demonstrate that the death of APR(6)s *in vitro* is likewise blocked by cycloheximide treatment (K. L. Hoffman and J. C. Weeks, unpublished results). Rapid progress is being made in identifying molecules involved in programmed cell death pathways, many of which are conserved in invertebrate and vertebrate animals (White and Steller, 1995). The potential role of these molecules in the death of APRs remains to be investigated. Steroid hormone receptors and homeotic genes are also remarkably conserved between invertebrates and vertebrates (Carroll, 1995; Koelle *et al.*, 1991) and their actions in the developing nervous system may share common features. The present study suggests that it will be feasible to investigate molecular and cellular mechanisms that underlie the coordinate regulation of neuronal survival by segmental identity and hormonal signals, at the level of individually identified neurons with known behavioral roles.

ACKNOWLEDGMENTS

This research was supported by NIH NRSA F32 NS08966 to L.C.S., NIH T32 GM07257 to J.T.P., and NIH Grants R01 NS23208 and K04 NS01473 and an NSF Presidential Young Investigator Award to J.C.W. We thank Dr. R. B. Levine (University of Arizona) for insightful discussions and assistance in setting up the culture system, K. L. Hoffman for sharing unpublished results and the MTT staining protocol, R. Williams for assistance with graphics, and numerous colleagues for comments on the manuscript.

REFERENCES

Akam, M., Averof, M., Castelli-Gair, J., Dawes, R., Falciani, F., and Ferrier, D. (1994). The evolving role of Hox genes in arthropods. *Development* (Suppl.), 209–215.

Ashburner, M., and Richards, G. (1976). Sequential gene activation by ecdysone in polytene chromosomes of *Drosophila melanogaster.* III. Consequences of ecdysone withdrawal. *Dev. Biol.* **54,** 241–55.

Bate, M., Goodman, C. S., and Spitzer, N. C. (1981). Embryonic development of identified neurons: Segment-specific differences in the H cell homologues. *J. Neurosci.* **1,** 103–106.

Batistatou, A., and Greene, L. A. (1991). Aurintricarboxylic acid rescues PC12 cells and sympathetic neurons from cell death caused by NGF-deprivation: Correlation with suppression of endonuclease activity. *J. Cell Biol.* **115,** 461–471.

Bell, R. A., and Joachim, F. A. (1976). Techniques for rearing laboratory colonies of tobacco hornworms and pink bollworms. *Ann. Entomol. Soc. Am.* **69,** 365–373.

Bennett, K. L., and Truman, J. W. (1985). Steroid-dependent survival of identifiable neurons in cultured ganglia of the moth *Manduca sexta. Science* **229,** 58–60.

Bollenbacher, W. E. (1988). The interendocrine regulation of larval–pupal development in the tobacco hornworm, *Manduca sexta:* A model. *J. Insect Physiol.* **34,** 941–947.

Bollenbacher, W. E., Smith, S. L., Goodman, W., and Gilbert, L. I. (1981). Ecdysteroid titer during larval–pupal–adult development of the tobacco hornworm, *Manduca sexta. Gen. Comp. Endocrinol.* **44,** 302–306.

Breedlove, S. M. (1992). Sexual dimorphism in the vertebrate nervous system. *J. Neurosci.* **12,** 4133–4142.

Carroll, S. B. (1995). Homeotic genes and the evolution of arthropods and chordates. *Nature* **376,** 479–485.

Deckwerth, T. L., and Johnson, E. M., Jr. (1993). Temporal analysis of events associated with programmed cell death (apoptosis) of sympathetic neurons deprived of nerve growth factor. *J. Cell Biol.* **123,** 1207–1222.

Edwards, S. N., and Tolkovsky, A. M. (1994). Characterization of apoptosis in cultured rat sympathetic neurons after nerve growth factor withdrawal. *J. Cell Biol.* **124,** 537–546.

Evans-Storms, R. B., and Cidlowski, J. A. (1995). Regulation of apoptosis by steroid hormones. *J. Steroid Biochem. Mol. Biol.* **53,** 1–8.

Fahrbach, S. E. (1992). Developmental regulation of ecdysteroid receptors in the nervous system of *Manduca sexta. J. Exp. Zool.* **261,** 245–253.

Fahrbach, S. E., Choi, M. K., and Truman, J. W. (1993). Inhibitory effects of actinomycin D and cycloheximide on neuronal death in adult *Manduca sexta. J. Neurobiol.* **25,** 59–69.

Forger, N. G., Hodges, L. L., Roberts, S. L., and Breedlove, S. M. (1992). Regulation of motoneuron death in the spinal nucleus of the bulbocavernosus. *J. Neurobiol.* **23,** 1192–1203.

Giebultowicz, J. M., and Truman, J. W. (1984). Sexual differentiation in the terminal ganglion of the moth *Manduca sexta:* Role of sex-specific neuronal death. *J. Comp. Neurology* **226,** 87–95.

Hayashi, J. H., and Hildebrand, J. G. (1990). Insect olfactory neurons *in vitro:* Morphological and physiological characterization of cells from the developing antennal lobes of *Manduca sexta. J. Neurosci.* **10,** 848–859.

Hoffman, K. L., and Weeks, J. C. (1996). Segment-specific, steroid-mediated programmed cell death of identified motoneurons in cell culture. *Soc. Neurosci. Abstr.* **22,** 1720.

Jeffs, P., Jagues, K., and Osmond, M. (1992). Cell death in cranial neural crest development. *Anat. Embryol.* **185,** 583–588.

Kent, K. S., and Levine, R. B. (1988). Dendritic reorganization of an identified neuron during metamorphosis of the moth *Manduca sexta:* The influence of interactions with the periphery. *J. Neurobiol.* **24,** 1–22.

Copyright © 1997 by Academic Press. All rights of reproduction in any form reserved.

Keynes, R., and Krumlauf, R. (1994). Hox genes and regionalization of the nervous system. *Annu. Rev. Neurosci.* **17,** 109–132.

Koelle, M. R., Talbot, W. S., Segraves, W. A., Bender, W. A., Cherbas, P., and Hogness, D. S. (1991). The *Drosophila* EcR gene encodes an ecdysone receptor, a new member of the steroid receptor superfamily. *Cell* **67,** 59–78.

Lawrence, P. A., and Morata, G. (1994). Homeobox genes: Their function in *Drosophila* segmentation and pattern formation. *Cell* **78,** 181–189.

Levine, R. B., and Truman, J. W. (1985). Dendritic reorganization of abdominal motoneurons during metamorphosis of the moth, *Manduca sexta*. *J. Neurosci.* **5,** 2424–2431.

Levine, R. B., Morton, D. B., and Restifo, L. L. (1995). Remodeling of the insect nervous system. *Curr. Opin. Neurobiol.* **5,** 28–35.

Lubischer, J. L., and Weeks, J. C. (1996). Target muscles and sensory afferents do not influence steroid-regulated, segment-specific death of identified motoneurons in *Manduca sexta*. *J. Neurobiol.* **31,** 449–460.

Lubischer, J. L., Verhegge, L. D., and Weeks, J. C. (1995). Evidence that larval *Manduca* proleg muscles are respecified for hemolymph circulation in pupae. *Soc. Neurosci. Abstr.* **21,** 426.

Mills, A. C., and Sengelaub, D. R. (1993). Sexually dimorphic neuron number in lumbosacral dorsal root ganglia of the rat: Development and steroid regulation. *J. Neurobiol.* **24,** 1543–1553.

Nordeen, E. J., Nordeen, K. W., Sengelaub, D. R., and Arnold, A. P. (1985). Androgens prevent normally occurring cell death in a sexually dimorphic spinal nucleus. *Science* **229,** 671–673.

Prugh, J., Della Croce, K., and Levine, R. B. (1992). Effects of the steroid hormone, 20-hydroxyecdysone, on the growth of neurites by identified insect motoneurons *in vitro*. *Dev. Biol.* **154,** 331–347.

Riddiford, L. M. (1985). Hormone action at the cellular level. *In* "Comprehensive Insect Physiology, Biochemistry, and Pharmacology" (G. A. Kerkut and L. I. Gilbert, Eds.), Vol. 8, pp. 37–84. Pergamon, New York.

Riddiford, L. M., and Truman, J. W. (1994). Hormone receptors and the orchestration of development during insect metamorphosis. *In* "Perspectives in Comparative Endocrinology," pp. 389–394. National Research Council of Canada.

Robinow, S., Talbot, W. S., Hogness, D. S., and Truman, J. W. (1993). Programmed cell death in the *Drosophila* CNS is ecdysone-regulated and coupled with a specific ecdysone receptor isoform. *Development* **119,** 1251–1259.

Sandstrom, D. J. (1993). "Respecification of Identified Larval Muscles, Motor Neurons and Interneurons to Pupal Functions in *Manduca sexta*." Doctoral Dissertation, University of California, Berkeley.

Sandstrom, D. J., and Weeks, J. C. (1996). Novel dual innervation of a larval proleg muscle by two similar motoneurons in the tobacco hornworm, *Manduca sexta*. *J. Exp. Biol.* **199,** 775–791.

Shankland, M., and Martindale, M. Q. (1992). Segmental differentiation of lineally homologous neurons in the central nervous system of the leech. *In* "Determinants of Neuronal Identity" (M. Shankland and E. R. Macagno, Eds.), pp. 45–77. Academic Press, San Diego.

Sonetti, D., Ottaviani, E., Bianchi, F., Rodriguez, M., Stefano, M. L., Scharrer, B., and Stefano, G. B. (1994). Microglia in invertebrate ganglia. *Proc. Natl. Acad. Sci. USA* **91,** 9180–9184.

Steller, H. (1995). Mechanisms and genes of cellular suicide. *Science* **267,** 1445–1449.

Stocker, R. F., Edwards, J. S., and Truman, J. W. (1978). Fine structure of degenerating moth motoneurons after eclosion. *Cell Tissue Res.* **191,** 317–331.

Streichert, L. C., and Weeks, J. C. (1994). Selective death of identified *Manduca sexta* motoneurons is induced by ecdysteroids *in vitro*. *Soc. Neurosci. Abstr.* **20,** 461.

Streichert, L. C., and Weeks, J. C. (1995). Decreased monosynaptic sensory input to an identified motoneuron is associated with steroid-mediated dendritic regression during metamorphosis in *Manduca sexta*. *J. Neurosci.* **15,** 1484–1495.

Taylor, H. M., and Truman, J. W. (1974). Metamorphosis of the abdominal ganglia of the tobacco hornworm, *Manduca sexta:* Changes in populations of identified motor neurons. *J. Comp. Physiol.* **90,** 367–388.

Thanos, S., Mey, J., and Wild, M. (1993). Treatment of the adult retina with microglia-suppressing factors retards axotomy-induced neuronal degration and enhances axonal regeneration *in vivo* and *in vitro*. *J. Neurosci.* **13,** 455–466.

Thompson, K. J., and Siegler, M. V. S. (1993). Development of segment-specificity in identified lineages of the grasshopper CNS. *J. Neurosci.* **13,** 3309–3381.

Thummel, C. S. (1995). From embryogenesis to metamorphosis: The regulation and function of *Drosophila* nuclear receptor superfamily members. *Cell* **83,** 871–877.

Truman, J. W. (1983). Programmed cell death in the nervous system of an adult insect. *J. Comp. Neurol.* **216,** 445–452.

Trimmer, B. A., and Weeks, J. C. (1989). Effects of nicotinic and muscarinic agents on an identified motoneurone and its direct afferent inputs in larval *Manduca sexta*. *J. Exp. Biol.* **144,** 303–337.

Truman, J. W., and Reiss, S. E. (1988). Hormonal regulation of the shape of identified motor neurons in *Manduca sexta*. *J. Neurosci.* **8,** 765–775.

Truman, J. W., and Schwartz, L. M. (1984). Steroid regulation of neuronal death in the moth nervous system. *J. Neurosci.* **4,** 274–280.

Truman, J. W., Talbot, W. S., Fahrbach, S. E., and Hogness, D. S. (1994). Ecdysone receptor expression in the CNS correlates with stage-specific responses to ecdysteroids during *Drosophila* and *Manduca* development. *Development* **120,** 219–234.

Truman, J. W., Thorn, R. S., and Robinow, S. (1992). Programmed neuronal death in insect development. *J. Neurobiol.* **23,** 1295–1311.

Weeks, J. C. (1987). Time course of hormonal independence for developmental events in neurons and other cell types during insect metamorphosis. *Dev. Biol.* **124,** 163–176.

Weeks, J. C., and Jacobs, G. A. (1987). A reflex behavior mediated by monosynaptic connections between hair afferents and motoneurons in the larval tobacco hornworm, *Manduca sexta*. *J. Comp. Physiol. A* **160,** 315–29.

Weeks, J. C., and Davidson, S. K. (1994). Influence of interganglionic interactions on steroid-mediated dendritic reorganization and death of proleg motor neurons during metamorphosis in *Manduca sexta*. *J. Neurobiol.* **25,** 535–554.

Weeks, J. C., Davidson, S. K., and Debu, B. H. G. (1993). Effects of a protein synthesis inhibitor on the hormonally-mediated regression and death of motor neurons in the tobacco hornworm, *Manduca sexta*. *J. Neurobiol.* **24,** 125–140.

Weeks, J. C., and Ernst-Utzschneider, K. (1989). Respecification of larval proleg motoneurons during metamorphosis of the tobacco hornworm, *Manduca sexta:* Segmental dependence and hormonal regulation. *J. Neurobiol.* **20,** 569–592.

Copyright © 1997 by Academic Press. All rights of reproduction in any form reserved.

Weeks, J. C., and Levine, R. B. (1992). Endocrine influences on the postembryonic fates of identified neurons during insect metamorphosis. *In* "Determinants of Neuronal Identity" (M. Shankland and E. Macagno, Eds.), pp. 293–322. Academic Press, San Diego.

Weeks, J. C., and Truman, J. W. (1984). Neural organization of peptide-activated ecdysis behaviors during the metamorphosis of *Manduca sexta*. II. Retention of the proleg motor pattern despite loss of the prolegs at pupation. *J. Comp. Physiol.* **155,** 423–433.

Weeks, J. C., and Truman, J. W. (1985). Independent steroid control of the fates of motoneurons and their muscles during insect metamorphosis. *J. Neurosci.* **5,** 2290–2300.

Weeks, J. C., and Truman, J. W. (1986). Hormonally mediated reprogramming of muscles and motoneurones during the larval–pupal transformation of the tobacco hornworm, *Manduca sexta*. *J. Exp. Biol.* **125,** 1–13.

Weeks, J. C., Roberts, W. M., and Trimble, D. L. (1992). Hormonal regulation and segmental specificity of motoneuron phenotype during metamorphosis of the tobacco hornworm, *Manduca sexta*. *Dev. Biol.* **149,** 185–196.

White, K., and Steller, H. (1995). The control of apoptosis in *Drosophila*. *Trends Cell Biol.* **5,** 74–78.

Wilkinson, D. G. (1995). Genetic control of segmentation in the vertebrate hindbrain. *Perspect. Dev. Neurobiol.* **3,** 29–38.

Witten, J. L., and Levine, R. B. (1991). Cellular specificity of steroid influences on process outgrowth of identified motoneurons in culture. *Soc. Neurosci. Abstr.* **21,** 426.

Woodard, C., Baehrecke, E. H., and Thummel, C. S. (1994). A molecular mechanism for the stage specificity of the *Drosophila* prepupal genetic response to ecdysone. *Cell* **79,** 607–615.

Zelhof, A. C., Yao, T. P., Chen, J. D., Evans, R. M., McKeown, M. (1995). Seven-up inhibits ultraspiracle based signaling pathways *in vitro* and *in vivo*. *Mol. Cell Biol.* **15,** 6736–6745.

Received for publication September 4, 1996
Accepted November 8, 1996

Copyright © 1997 by Academic Press. All rights of reproduction in any form reserved.

DEVELOPMENTAL BIOLOGY 183, 108–121 (1997)
ARTICLE NO. DB968487

SOX9 Binds DNA, Activates Transcription, and Coexpresses with Type II Collagen during Chondrogenesis in the Mouse

Ling-Jim Ng,*,[1] Susan Wheatley,†,[1] George E. O. Muscat,† John Conway-Campbell,† Jo Bowles,† Edwina Wright,† Donald M. Bell,* Patrick P. L. Tam,‡ Kathryn S. E. Cheah,* and Peter Koopman†,§

**Department of Biochemistry, Hong Kong University, Sassoon Road, Hong Kong; †Centre for Molecular and Cellular Biology and §Department of Anatomical Sciences, The University of Queensland, Brisbane 4072, Australia; and ‡Children's Medical Research Institute, Locked Bag 23, Wentworthville 2145, Australia*

Two lines of evidence suggest that the *Sry*-related gene *Sox9* is important for chondrogenesis in mammalian embryos. *Sox9* mRNA is expressed in chondrogenic condensations in mice, and mutations in human *SOX9* are known to cause skeletal dysplasia. We show here that mouse SOX9 protein is able to bind to a SOX/SRY consensus motif in DNA and contains a modular transcriptional activation domain, consistent with a role for SOX9 as a transcription factor acting on genes involved in cartilage development. One such gene is *Col2a1*, which encodes type II collagen, the major structural component of cartilage. We have compared, in detail, the expression of *Sox9* and *Col2a1* during mouse development. In chondrogenic tissues the expression profiles of the two genes were remarkably similar. Coexpression was detected in some nonchondrogenic tissues such as the notochord, otic vesicle, and neural tube, but others such as heart and lung differed in their expression of the two genes. Immunohistochemistry using an antibody specific for SOX9 revealed that expression of SOX9 protein mirrored the distribution of *Sox9* mRNA. Our results suggest that SOX9 protein is involved in the regulation of *Col2a1* during chondrogenesis, but that this regulation is likely to depend on additional cofactors.
© 1997 Academic Press

INTRODUCTION

During the development of the vertebrate skeleton, endochondral bone formation is initiated when mesenchymal cells condense and differentiate to form chondrocytes. These cells synthesize a framework of cartilage matrix in the approximate shape of future bones. The recent identification of gene defects responsible for skeletal abnormalities in mouse and man has shown that not only structural components of the cartilage extracellular matrix, but also growth and differentiation factors, signaling molecules, and transcription factors are important for proper morphogenesis during skeletal development (reviewed by Erlebacher *et al.*, 1995). However details of the mechanisms involved and the identities of many of the interacting molecules regulating chondrogenesis remain unknown.

Sox9 is a recently identified gene that may have a role in regulating chondrogenesis in mammals. This gene encodes one of a family of proteins that includes the mammalian Y-linked testis-determining factor, SRY (Gubbay *et al.*, 1990). Several SOX proteins have been shown to bind to DNA and activate transcription *in vitro* (van de Wetering *et al.*, 1993; Dubin and Ostrer, 1994; Hosking *et al.*, 1995; Kamachi *et al.*, 1995; Kanai *et al.*, 1996). This property and the tissue-specific expression pattern of some *Sox* genes (Koopman *et al.*, 1990; Stevanovic *et al.*, 1993; van de Wetering *et al.*, 1993; Uwanogho *et al.*, 1994; Connor *et al.*, 1995; Dunn *et al.*, 1995; Hosking *et al.*, 1995; Jay *et al.*, 1995; Kamachi *et al.*, 1995; Kanai *et al.*, 1996) indicate that they may regulate gene expression in specific cell lineages. A preliminary survey in which *Sox9* expression was examined in whole-mount mouse embryos has shown this gene to be expressed strongly in mesenchymal condensations before and during chondrogenesis, and in other tissues such as the central

[1] These two authors contributed equally to this work.

0012-1606/97 $25.00
Copyright © 1997 by Academic Press
All rights of reproduction in any form reserved.

TABLE 1
Primers Used in the Construction of *Sox9* Deletion Mutants

Construct	Primers (5′–3′)	Primer position[a]
pGSox9p	Sox9A1 (GCGAATTCATGAATCTCCTGGACCCCTT)	302–321
	g10b (TTCCGTGGCCTCTTCGGCCTC)	863–882
pGR990	Sox9A3 (GGGAATTCGTGAAGAACGGACAAGCGG)	845–863
	Sox9B2 (CTTCTAGAAGGGTCTGGTGACCTGTGT)	1823–1805
pGR560	Sox9A2 (CCGAATTCGCGACCGCGGGCCACG)	1286–1301
	Sox9B2	
pGR300	Sox 9A2	
	Sox9B1 (AGTCTAGATGAAGGGGCTGTAGGAGAT)	1565–1547
pGR260	Sox9A4 (ACGAATTCCACTACAGGCCCTCCTAC)	1574–1591
	Sox9B2	

[a] Position shown relative to *Sox9* cDNA sequence described by Wright *et al.* (1995).

nervous system, otocysts, heart, and vibrissae (Wright *et al.*, 1995). The human *SOX9* gene is also expressed in differentiating chondrocytes, and mutation of the gene is associated with the skeletal malformation disorder campomelic dysplasia (CD; Foster *et al.*, 1994; Wagner *et al.*, 1994).

To delineate the potential role of *Sox9* in cartilage and bone development, it is important to determine its functional properties and identify molecules with which it may interact. The timing and sites of *Sox9* expression during mouse development (Wright *et al.*, 1995), and the skeletal dysmorphology associated with SOX9 mutations in CD patients (Lee *et al.*, 1972; Hovmoller *et al.*, 1977; Houston *et al.*, 1983; Foster *et al.*, 1994; Wagner *et al.*, 1994), indicate that a major function of SOX9 is to regulate a gene or genes important for chondrocyte differentiation and skeletal development. Candidates include genes expressed early in chondrocyte differentiation, such as those encoding cartilage extracellular matrix components (e.g., collagens, proteoglycans, cartilage matrix protein, and cartilage oligomeric matrix protein), growth factors (e.g., fibroblast growth factors, bone morphogenetic proteins, cartilage-derived growth factors, and parathyroid hormone-related peptide) and their receptors, signaling molecules (e.g., members of the hedgehog family), and other transcription factors.

The major extracellular matrix component of cartilage is type II collagen, which constitutes up to 60% of the total protein content. Type II collagen is a homotrimer of identical α1(II) chains, encoded in the mouse by the *Col2a1* gene. Transcription of *Col2a1* in mesenchymal cells precedes chondrocyte differentiation and is one of the hallmarks of chondrogenesis (von der Mark and von der Mark, 1977; Kravis and Upholt, 1985; Kosher *et al.*, 1986; Swalla *et al.*, 1988, Cheah *et al.*, 1991; Ng *et al.*, 1993). Type II collagen is important in maintaining the integrity of cartilaginous structures, and disruptions of its synthesis due to mutations of the *COL2A1* gene have been linked to human chondrodysplasias (reviewed by Vikkula *et al.*, 1994; Ritvaniemi *et al.*, 1995). Abnormal skeletal formation is also found in transgenic mice that express mutated type II collagen genes (Garofalo *et al.*, 1991; Vandenberg *et al.*, 1991; Metsäranta *et al.*, 1992; Li *et al.*, 1995).

In this study we show that SOX9 protein can bind to a SOX/SRY consensus sequence, copies of which are present in the regulatory regions of the human *COL2A1* gene. In addition, we identified a modular activation domain in the protein, suggesting a role for SOX9 as a transcriptional activator. Further, we have compared in detail the timing and sites of expression of the *Sox9* and *Col2a1* genes during mouse embryogenesis. We show, by *in situ* hybridization, a concordance of expression of these two genes at sites of chondrogenesis, consistent with a role for *Sox9* as a direct or indirect regulator of *Col2a1*.

MATERIALS AND METHODS

Cloning of Sox9 Deletion Mutants

A construct (pGSox9p) containing the *Sox9* open reading frame and the 3′ untranslated region was cloned as a fusion of a 583-bp PCR fragment generated using the primers Sox9A1 and g10b (Table 1) and a 1.6-kb *Bss*HII/*Xho*I fragment of *Sox9* cDNA (Wright *et al.*, 1995) into the expression vector pGAL0 (Kato *et al.*, 1990). *Sox9* deletion mutants were generated by cloning PCR fragments generated from the *Sox9* cDNA in frame into the same vector. PCR primers used for this purpose are described in Table 1. Inserts of constructs other than pGR990 were sequenced completely, and all insert/vector junctions were sequenced using a GAL4-specific primer (5′-CGACATCATCATCGGAAGAG-3′) to verify the reading frame.

Electrophoretic Mobility Shift Assay (EMSA)

To generate a source of SOX9 protein suitable for EMSA analysis, 20 μg of a plasmid containing the coding sequence for the first 147 amino acids of the yeast transcriptional activator GAL4 (GAL0; Kato *et al.*, 1990) fused to the *Sox9* coding sequence (Wright *et al.*, 1995) was transfected into COS-1 cells using Lipofectamine (Gibco BRL) as described (Kent *et al.*, 1996). Nuclear extracts were prepared from GAL0-transfected and GALSOX9-transfected cells using a

Copyright © 1997 by Academic Press. All rights of reproduction in any form reserved.

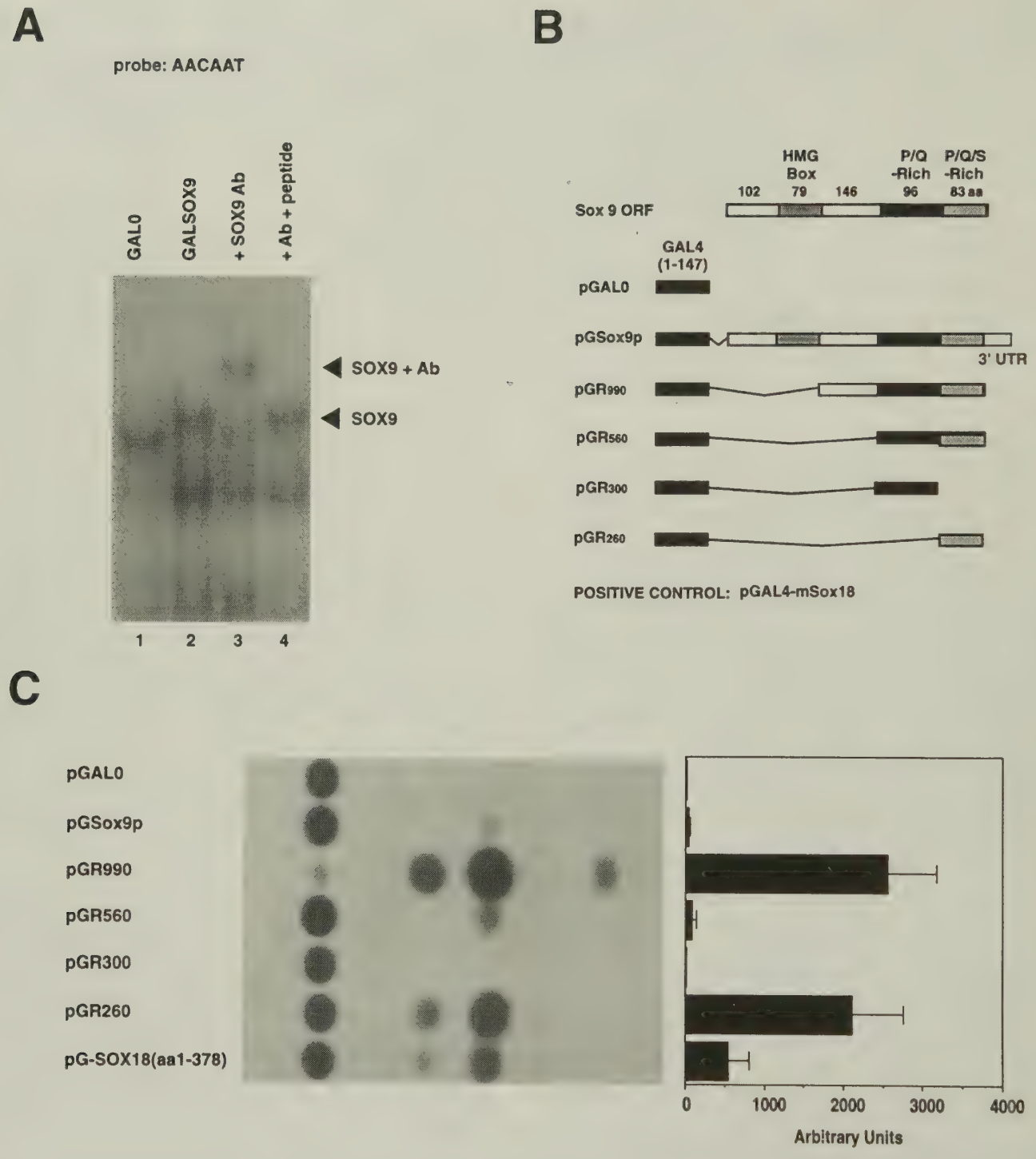

FIG. 1. DNA binding and transcriptional activation by SOX9 protein. (A) SOX9 binds to the SOX/SRY consensus AACAAT. EMSA analysis: lane 1, an extract from GAL0-transfected COS-1 cells incubated with the probe does not produce a specific retarded band; lane 2, an extract from GALSOX9-transfected cells produces a retarded band specific for SOX9; lane 3, the identity of the SOX9 band is confirmed using anti-SOX9 polyclonal antiserum, which produces a "supershift"; lane 4, this supershift is abolished by incubating the probe, extract, and antibody with the immunogenic peptide which competes for binding to the antibody and prevents it binding to SOX9 and producing the supershift. The positions of the SOX9 band and the "supershifted" band are indicated. (B, C) Activation of transcription by SOX9. (B) Constructs for GAL4 transcriptional activation assays containing the full-length *Sox9* open reading frame or fragments thereof fused to the GAL4 DNA-binding domain. (C) The extent of transcriptional activation by each construct is indicated by the CAT assay results and the mean of triplicate assays is shown with bars indicating standard error.

Copyright © 1997 by Academic Press. All rights of reproduction in any form reserved.

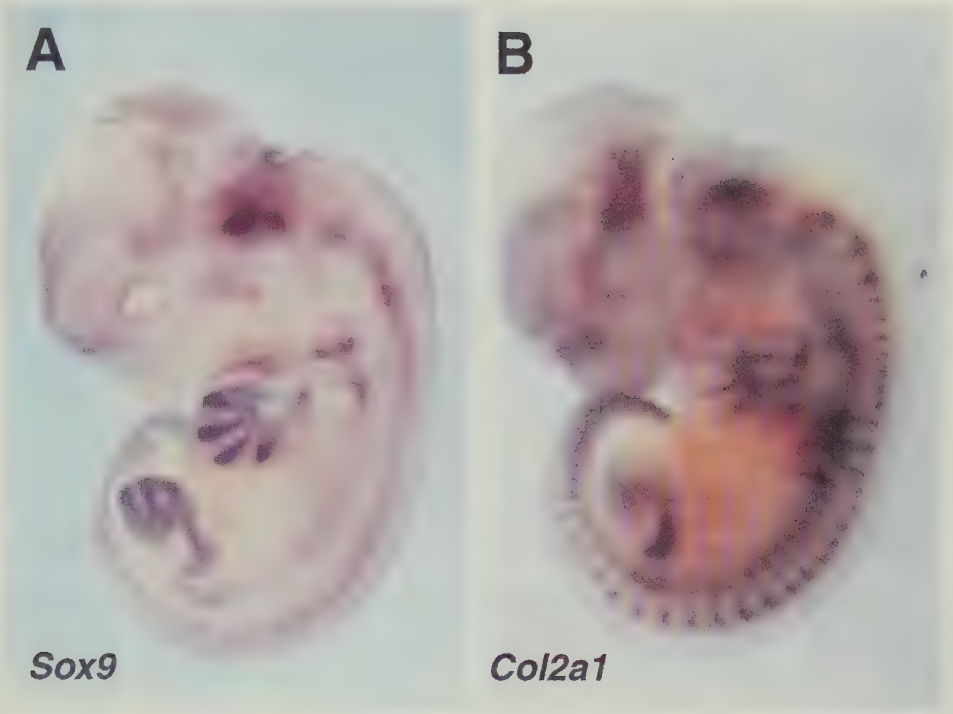

FIG. 2. Whole-mount *in situ* hybridization of 12.5 dpc fetuses showing the similarity of expression of *Sox9* (A) and *Col2a1* (B) in skeletal structures.

method based on that described by Osborn *et al.* (1989). Briefly, after washing the cells in buffer A, 10^7 cells were resuspended in 500 μl buffer A and 1 ml buffer A/0.1% NP-40 was added. After mixing gently, nuclei were collected by centrifugation at 2500 rpm for 3 min at 4°C in a microfuge and then resuspended in 100 μl buffer C. After vortexing, incubation on ice for 10 min, and centrifugation at 13,000 rpm for 10 min at 4°C in a microfuge, the supernatant containing nuclear proteins was stored at −70°C. Binding reactions (Schreiber *et al.*, 1989) were performed in the presence of 2 μg salmon sperm DNA and 1 μg/μl BSA. An extract from GAL0-transfected cells was used as a background DNA-binding activity control. Briefly, 4 μg of nuclear extract was incubated initially with all components except probe for 30 min on ice. After the addition of 1 ng gel-purified, double-stranded probe (sense strand: 5′-GATCCGGACTAATAAACAATAAAGTCGACG-3′), the reactions were incubated on ice for a further 30 min and loaded onto a nondenaturing 5% polyacrylamide, 0.8× TBE gel. Sixteen-centimeter gels were run at 10 V/cm and the dried gels were exposed to Fuji RX X-ray film. Variations to this standard procedure included adding 0.5 μg affinity-purified anti-SOX9 polyclonal antiserum (Kent *et al.*, 1996) or adding antibody plus 1 μg of the immunogenic SOX9 peptide.

Transfection of Mammalian Cells and Chloramphenicol Acetyl Transferase (CAT) Assays

COS-1 cells at 60–70% confluence were transiently transfected with 1.5 μg of chimeric *GAL4-Sox9* plasmids and 3.5 μg of reporter plasmid (pG5E1bCAT, containing five GAL4 binding sites upstream of the CAT gene) per well of a six-well plate, using DOTAP (Boehringer-Mannheim). Between 40 and 48 hr after transfection, cells were harvested and the ability of SOX9 to activate transcription was assayed by measuring CAT activity (Gorman *et al.*, 1982). Constructs were assayed in three independent experiments.

In Situ Hybridization

Antisense and sense probes for *in situ* hybridization were generated from clones pNJ61, pEL111, and pSox9.5a. pNJ61 is a 500-bp fragment covering exon 1 to exon 5B of *Col2a1* obtained by RT-PCR using oligonucleotides 5′-TCTCCTGCCTCCTCCTGCTC-3′ and 5′-CTCCATCTCTGCCACGGGGT-3′ subcloned in pBluescribe (Stratagene). pEL111 is a 0.6-kb genomic fragment of *Col2a1* containing exon 1 (Cheah *et al.*, 1991). pSox9.5a (Wright *et al.*, 1995) contained 500-bp of sequence 3′ to the HMG box of *Sox9* not including the poly(A) sequence, subcloned in pBSKSII$^-$ (Stratagene).

Whole-mount *in situ* hybridization was carried out using 12.5 days post coitum (dpc) Swiss outbred mouse embryos as described by Wright *et al.* (1995), using pSox9.5a and pEL111 probes. For *in situ* hybridization to sections, CBA/n mouse embryos at 7.5 to 18.5 days were fixed in 4% paraformaldehyde and processed as described (Cheah *et al.*, 1991). pNJ61 and pSox9.5a RNA probes labeled with [α-^{35}S]UTP (1000 Ci/mmol, Amersham) were generated by *in vitro* transcription and used to localize transcripts in embryonic tissues. The number of UTP molecules per strand of antisense RNA probe generated from pNJ61 and pSox9.5a are 110 and 119, respectively; therefore, the intensities of hybridization signals of the two riboprobes are comparable. pNJ61 and pSox9.5a were hybridized to consecutive adjacent sections covering 24–48 μm. Specific hybridization was achieved by treating the sections with 20 μg/ml RNase

Copyright © 1997 by Academic Press. All rights of reproduction in any form reserved.

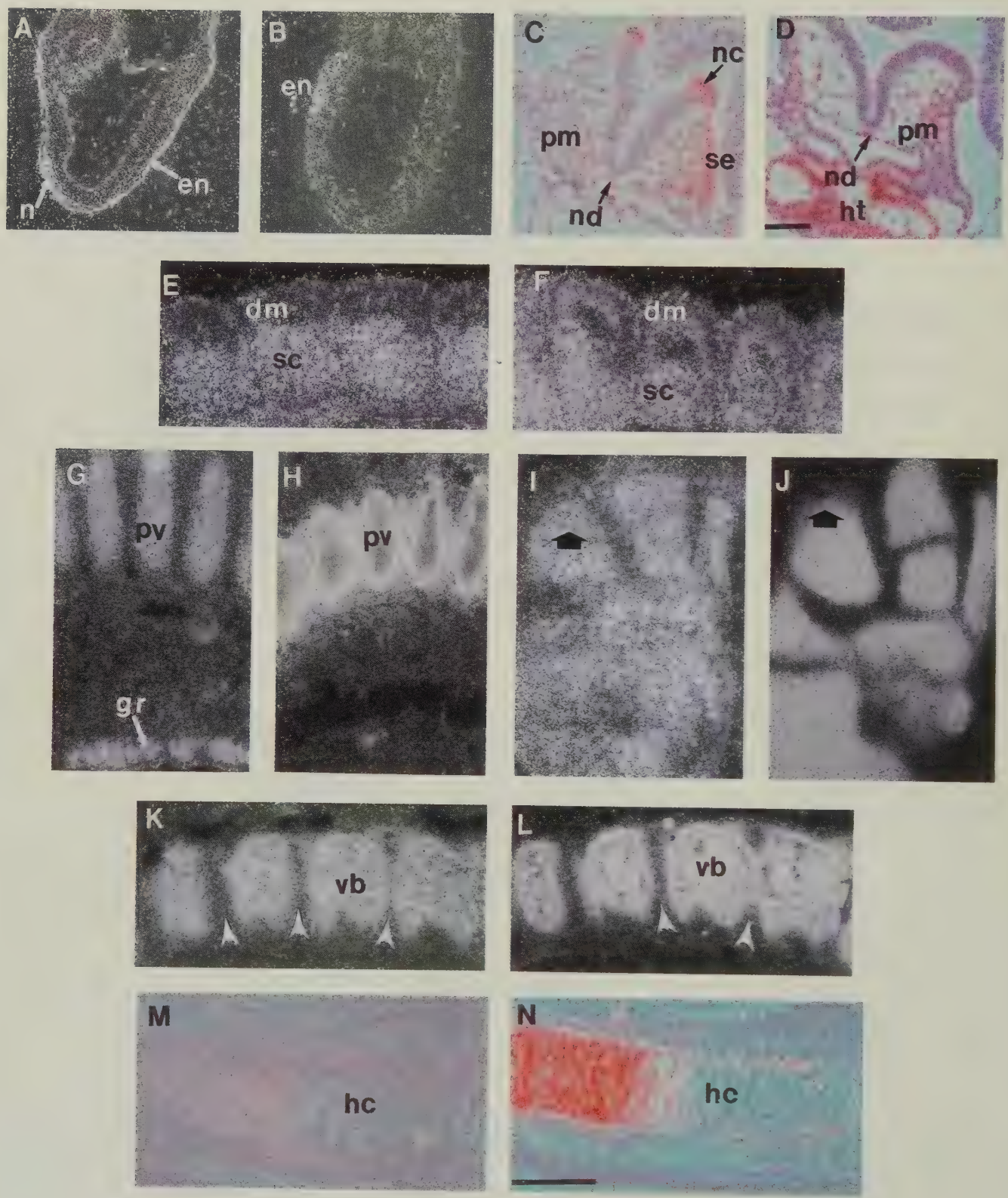

FIG. 3. Coexpression of *Sox9* and *Col2a1* in the early embryo and chondrogenic tissues. *Sox9* expression is shown in A, C, E, G, I, K, and M (left-hand side of each pair of photomicrographs) and *Col2a1* in B, D, F, H, J, L, and N (right-hand side of each pair). Each pair of illustrations was taken from sections approximately 24–48 μm apart within the same specimen. (A) *Sox9* expression in the notochordal plate (n) at 7.5 dpc. (B) 7.5 dpc embryo hybridized with *Col2a1* probe showing expression limited to a small patch of primitive endoderm

Copyright © 1997 by Academic Press. All rights of reproduction in any form reserved.

A and 50 u/ml RNase T_1 at 37°C for 45 min and washing at 65°C in 2× SSC, 50% formamide, 20 m*M* dithiothreitol. Autoradiography and photography of sections were as described previously (Cheah *et al.*, 1991).

Immunohistochemistry

Immunohistochemistry was performed on frozen sections of mouse embryos. Embryos were dissected into PBS, fixed in 4% paraformaldehyde for 4 hr or overnight at 4°C, and saturated with 15% glucose in PBS overnight at 4°C. After incubation in graded mixtures of 15% glucose/PBS and OCT compound (Tissuetek), embryos were embedded in OCT in cryomoulds (Tissuetek) and frozen on dry ice for 30 min. Ten-micrometer sections were cut on a cryostat at −20°C. Sections were applied to SuperFrost/Plus slides (Menzel Glaser, Germany) and allowed to dry thoroughly before staining.

All steps in the staining procedure were performed in a humidified chamber at 4°C. Sections were first rinsed 2× with PBS then bleached with 0.6% H_2O_2 in PBS for 20 min. Sections were then blocked with 10% fetal calf serum/0.1% Triton X-100 in PBS for 30 min. The specificity of the anti-SOX9 antibody has been established previously (Kent *et al.*, 1996). Affinity-purified anti-SOX9 antiserum was diluted to 10 μg/ml in PBS/Triton X-100 and applied to the sections overnight. The sections were then washed in PBS/Triton X-100 and a biotinylated anti-rabbit Ig (Amersham) was diluted to 10 μg/ml and applied to the sections overnight. After washing in PBS/Triton X-100 then PBS alone, a horseradish peroxidase (HRP)-conjugated avidin/biotin complex (ABC) reagent (Vector Laboratories) was applied to the sections for 30 min. After washing in PBS, HRP was developed using 2.5 μg/ml 3,3′-diaminobenzidine, 0.08% $NiCl_2$, and 0.03% H_2O_2. Sections were dehydrated, cleared, and mounted in DPX mounting medium. Photomicrographs were taken on an Olympus AX70 microscope using Kodak 64T Ektachrome film.

RESULTS

SOX9 Can Bind DNA and Is a Transcriptional Trans-Activator

The sequence AACAAT has been determined as the optimal binding site for SRY (Harley *et al.*, 1994), SOX5 (Denny *et al.*, 1992), and SOX17 (Kanai *et al.*, 1996), and it has been shown that this sequence can bind SOX2 (Kamachi *et al.*, 1995) and SOX6 (Connor *et al.*, 1995). Copies of this sequence are present in the regulatory regions of the human *COL2A1* gene (Metsäranta *et al.*, 1991), suggesting that it might mediate binding of SOX9 to this gene and activate transcription. EMSA analysis was carried out to investigate whether SOX9 can bind to this consensus. Specific binding activity with this probe was observed with extracts of GAL-SOX9-transfected COS-1 cells, but not with extracts of GAL0-transfected cells (Fig. 1A). The identity of the SOX9-specific band was confirmed by including affinity-purified anti-SOX9 polyclonal antiserum (Kent *et al.*, 1996) in some binding reactions. This produced a "supershift" of the SOX9 band, which was abolished by incubating the binding reaction plus antibody with the immunogenic peptide used to raise the antibody (Fig. 1A). These results demonstrate that SOX9 binds to the consensus sequence AACAAT.

Eukaryotic transcription factors usually consist of modular DNA binding and transcriptional activation or repression domains (Ptashne, 1988; Mitchell and Tjian, 1989). Consistent with a role as a transcriptional activator, the SOX9 protein contains two domains which are rich in proline, glutamine, or serine residues and which are distinct from the HMG box DNA binding domain (Wright *et al.*, 1995). To determine whether SOX9 is able to activate transcription and to define the domains of activation, distinct SOX9 protein domains were assayed using the GAL4 hybrid system in transfected mammalian cells (Lillie and Green, 1989).

A full-length SOX9 construct (pGSox9p; Fig. 1B) was able to activate transcription, albeit weakly (Fig. 1C), raising the possibility that the presence in this construct of a second DNA binding domain, the HMG box, affected the assay. To examine this possibility, the HMG box was excluded by assaying only the 3′ coding sequence (pGR990; Fig. 1B). This construct was able to stimulate the transcription of the reporter gene to a very high level (Fig. 1C), indicating that SOX9 contains at least one activation domain downstream of the HMG box.

Further experiments were performed to delimit the activation domain(s). A region exceptionally rich in proline and glutamine residues (amino acids 329–421) was considered most likely to be responsible for the transcriptional activation, by analogy with the composition of activation domains in the B-cell-specific factor OTF-2 (Clerc *et al.*, 1988), the human Sp1 transcription factor (Courey and Tjian, 1988), and members of the CTF/NF-I family (Santoro *et al.*,

---

cells in the anterior region (en). (C, D) Expression of both genes is detected in the cranial paraxial mesenchyme (pm) and notochord (nd) of 8.5 dpc embryos (see also coexpression in 9.5 dpc notochord, Figs. 6A and 6B). The *in situ* hybridization signal for *Sox9* transcripts is strong in the crest of the neural plate (nc), the surface ectoderm (se, presumptive placodal epithelium), and the subjacent neural crest cells (C). Cardiogenic mesoderm (ht) shows strong *Col2a1* expression (D). (E, F) Coexpression in the sclerotome (sc) of the lower trunk somites of a 9.5 dpc embryo. Weaker *Sox9* expression is found in the dermamyotome (dm). (G, H) Mesenchymal condensation for prevertebrae (pv) expresses both *Sox9* and *Col2a1* mRNAs. Strong *Sox9* expression is found in the urogenital ridge (gr) of this 11.5 dpc embryo (sex unknown). (I, J) Expression of *Sox9* and *Col2a1* in the chondrogenic mass of the tarsals and metatarsals in the hind limb of a 15.5 dpc fetus. The arrows point distally. (K, L) Coexpression of both genes in the chondrocytes of the lower trunk vertebrae (vb) of a 14.5 dpc embryo and diminished level of expression in the intervertebral tissues (arrowheads). (M, N) Relatively stronger expression of *Col2a1* compared to *Sox9* in the proliferating chondrocytes of the basioccipital bone at 16.5 dpc. In hypertrophic chondrocytes (hc) *Col2a1* mRNAs were diminished and *Sox9* transcripts were almost at background levels. Bar = 50 μm (A–D) and 100 μm (E–N).

Copyright © 1997 by Academic Press. All rights of reproduction in any form reserved.

1988). Present within this region is a stretch of 39 amino acids composed exclusively of proline (15), glutamine (17), and arginine residues (7). Surprisingly, this region was able to transactivate only weakly (pGR300; Figs. 1B and 1C). Instead, the C-terminal fragment (pGR260, amino acids 424–507; Fig. 1B) was able to stimulate transcription to a very high level, comparable to the strong transcriptional activators SOX18 (Hosking *et al.*, 1995; Fig. 1C) and Sp1 (Courey and Tjian, 1988; data not shown). These results demonstrate the presence of a potent modular activation domain within the terminal 83 amino acids of the SOX9 protein.

Sox9 and Col2a1 Are Coexpressed in Skeletogenic Tissues

A comparison of the distribution of the *Sox9* and *Col2a1* transcripts by whole-mount *in situ* hybridization of midgestation mouse fetuses revealed a widespread concordance of gene expression in cartilaginous tissues (Fig. 2). Expression of these two genes was examined in detail by *in situ* hybridization on sections of mouse embryos of various stages. The presence of SOX9 protein was confirmed at many *Sox9* mRNA expression sites by immunohistochemistry on cryosections of mouse embryos. Coexpression of *Sox9* and *Col2a1* was first noted in the cranial mesenchyme of embryos at the early somite stage (8.5 dpc). *Sox9* was expressed strongly in the mesenchyme subjacent to the surface ectoderm and the epidermal placodes at the mid- and hindbrain level, which presumably consists of migrating neural crest cells that contribute to the facial skeleton (Fig. 3C). Moderate expression was also found in the paraxial mesoderm (Fig. 3C). *Col2a1* expression in the cranial mesenchyme was mostly confined to the paraxial mesoderm with lower levels of expression in the neural crest cell population (Fig. 3D). Both *Sox9* and *Col2a1* were expressed at later stages in the frontonasal mesenchyme, cranial paraxial mesenchyme, branchial arch mesenchyme, and the dispersing sclerotome of the somites (Figs. 3E and 3F). SOX9 protein was also observed in the dispersing sclerotome of the somites at 10.5 dpc (Fig. 4A).

Sox9 and *Col2a1* were strongly expressed when the prechondrogenic mesenchyme condensed into cartilage primordia throughout the developing skeleton (Fig. 2). For example, the prevertebrae derived from the condensation of sclerotomal cells clearly expressed both genes (Figs. 3G and 3H) and SOX9 protein expression was also confirmed in these structures (Figs. 4B and 4C). Transcription of both genes and expression of SOX9 protein (Fig. 4D) were maintained as the prechondrocytes differentiated into immature and proliferating chondrocytes. *In situ* hybridization revealed the presence of *Sox9* and *Col2a1* mRNAs in the perichondrium and the pre-hypertrophic chondrocytes of fetal cartilages such as the hind limb cartilages (Figs. 3I and 3J), vertebral bodies (Figs. 3K and 3L), cartilage in the skull, larynx, sternum, limb girdles, and Meckel's cartilage. Both transcripts and SOX9 protein were absent or at very diminished levels in hypertrophic chondrocytes in the centrum

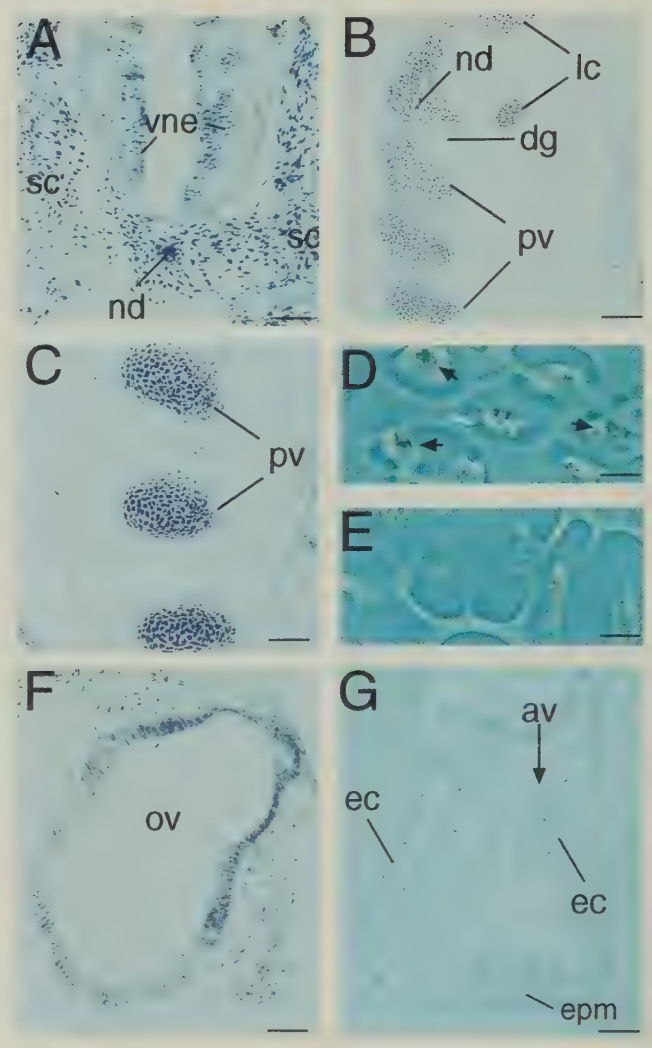

FIG. 4. Immunohistochemical analysis of SOX9 protein expression. (A) A transverse section of a 10.5 dpc mouse embryo. SOX9 protein is present in the notochord (nd), the sclerotome (sc) of the somites and the ventricular neuroepithelial layer of the spinal cord (vne). (B) A parasagittal section of a 13.5 dpc mouse embryo showing SOX9 protein in the prevertebrae (pv). The SOX9-expressing notochord (nd) is also seen, while the dorsal root ganglia (dg) between the prevertebrae are negative. SOX9 is also expressed in the mesenchymal condensations of the laryngeal cartilages (lc). (C) A parasagittal section through a 13.5 dpc embryo, more lateral to that in B, showing SOX9 expression in the vertebral bodies undergoing chondrocytic differentiation, but not yet hypertrophy. (D) High-power view showing the strong expression of SOX9 in proliferating chondrocytes from a hind limb bone of a 17.5 dpc embryo. Arrows show SOX9 protein in the nuclei of these cells. (E) High-power view of hypertrophic chondrocytes from the same bone as in D, showing that the expression of SOX9 protein is downregulated upon hypertrophy of the chondrocytes. (F) A parasagittal section through a 10.5 dpc embryo showing that SOX9 is expressed in the epithelium of the otic vesicle (ov). (G) A parasagittal section of a 10.5 dpc embryo showing SOX9 protein in the endocardial cushions of the developing heart (ec) flanking the atrioventricular canal (av). SOX9 protein is absent from the epimyocardium (epm). Bar = 100 μm (A, B), 50 μm (C, F, G), and 25 μm (D, E).

Copyright © 1997 by Academic Press. All rights of reproduction in any form reserved.

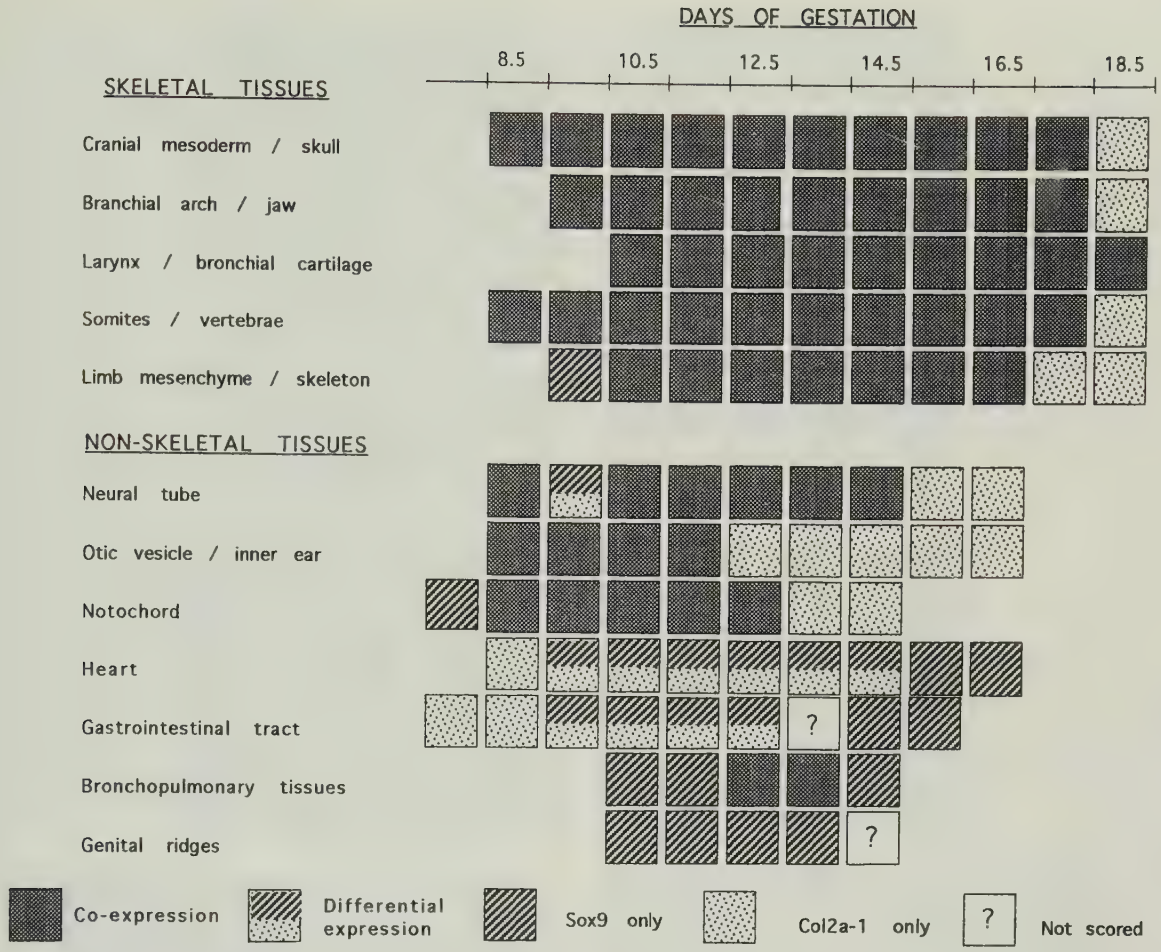

FIG. 5. Summary of the expression profiles of *Sox9* and *Col2a1* in skeletal and nonskeletal tissues during mouse development.

of the vertebrae and in the preossified regions of the cartilage in the chondrocranium, ribs, otic capsule, and limb bones (Figs. 3M and 3N, 4E, and data not shown). From 13.5 dpc onward, expression of *Sox9* and *Col2a1* was also found in some osteogenic tissues of membranous bones such as the cranium and the facial and jaw skeleton. *Sox9* mRNAs were concentrated mostly in the endocranium in contrast with the more uniformly distributed *Col2a1* transcripts. During late fetal development (17.5–18.5 dpc), *Sox9* expression progressively diminished in most skeletal tissues and by 18.5 days, *Sox9* expression was found only in small clusters of chondrocytes in the femur, vertebral bodies, larynx, and some osteoblasts in the mandible and maxilla. *Col2a1* expression continued during this period.

In summary, coexpression of *Sox9* and *Col2a1* mRNA and of SOX9 protein was observed during the differentiation and maturation of chondrocytes and osteogenic tissues (Fig. 5). However, during late fetal development, *Sox9* mRNA and protein expression in mature cartilage and membranous bones is downregulated in advance of *Col2a1*.

Sox9 and Col2a1 Are Coexpressed in a Subset of Nonskeletal Tissues

The concordant expression of *Sox9* and *Col2a1* mRNA and SOX9 protein was not found exclusively in chondrogenic and osteogenic tissues. Coexpression was also observed in the notochord and otic vesicles and at specific stages of central nervous system (CNS) development. In general, as in skeletogenic tissues, *Col2a1* was activated at the same stage as or shortly after *Sox9*, and *Col2a1* expression tended to persist beyond the extinction of *Sox9*.

Notochord. *Sox9* mRNA was first detected in the node, the early notochordal plate, and the mesoderm immediately lateral to the node of the late primitive streak-stage embryo, before the onset of expression of *Col2a1* (Figs. 3A and 3B). Expression of *Col2a1* lagged behind that of *Sox9* and was first detected in the nascent notochord of the early-somite-stage embryo (8.5 dpc; Fig. 3D). *Sox9* and *Col2a1* were coexpressed in the notochord until 12.5 dpc (Figs. 3C and 3D, 4A and 4B, 5, and 6A and 6B), after which time *Sox9* transcripts were not detected. However, SOX9 protein expres-

Copyright © 1997 by Academic Press. All rights of reproduction in any form reserved.

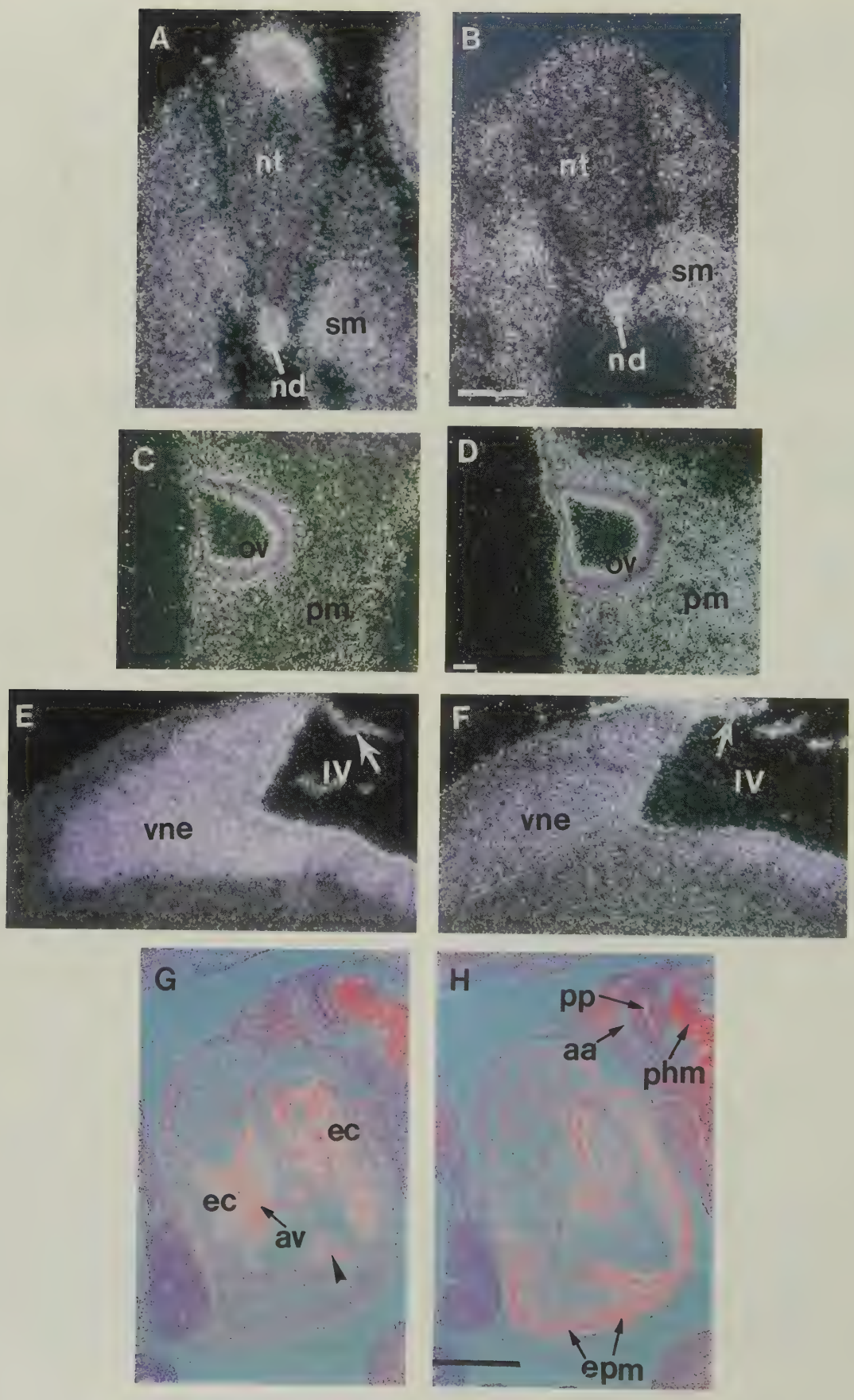

Copyright © 1997 by Academic Press. All rights of reproduction in any form reserved.

sion was confirmed in the notochord at 10.5 and 13.5 dpc (Figs. 4A and 4B), demonstrating that SOX9 protein expression persisted beyond that of *Sox9* mRNA.

Otic vesicles. Expression of *Sox9* was first detected in the epidermal placodes that precede the invagination of the otic vesicle (Fig. 3C). Once invagination has occurred, both *Sox9* and *Col2a1* mRNA and SOX9 protein were expressed in the epithelium of the vesicles (Figs. 4F and 6C and 6D). In contrast to *Col2a1, Sox9* transcripts were not detected in the sensory epithelium of the inner ear at 11.5–17.5 dpc (data not shown).

Central nervous system. *Sox9* and *Col2a1* were expressed in different dorsoventral regions of the early neural tube, but came to be coexpressed in later stages of CNS development. *Sox9* was first expressed in the crest region of the cephalic neural plate at 8.5 dpc (Fig. 3C). In the closed neural tube, *Sox9* expression was strongest in the roof plate and the alar plate (Fig. 6A), and *Col2a1* expression was generally low (Fig. 6B). Coexpression of these genes was found in the neuroepithelium of the forebrain at 8.5–9.5 dpc. At later stages (10.5–16.5 dpc), *Sox9* and *Col2a1* were coexpressed in the ventricular layer of the forebrain, midbrain, and hindbrain (Figs. 6E and 6F) and in the roof plate of the lower hindbrain and cervical spinal cord. SOX9 protein was also detected in the ventricular neuroepithelial layer of the spinal cord (Fig. 4A). Expression of *Sox9* was extinguished by 15.5–16.5 dpc but *Col2a1* transcripts persisted in the hindbrain neuroepithelium.

Differential Expression of Sox9 and Col2a1

Despite extensive coexpression of *Sox9* and *Col2a1* during development, particularly in skeletogenic tissues, many examples of differential expression of the two genes were found in other fetal tissues at various stages. These are summarized in Table 2 and Fig. 5. In some mesoendodermal organs, *Sox9* and *Col2a1* were expressed in tissue types derived from different germ layers. For example, *Sox9* was not expressed in the endoderm of the pharynx where *Col2a1* was expressed. In the respiratory tract, *Sox9* was expressed in the bronchial epithelium and the mesenchyme of the lung bud but *Col2a1* transcripts were found only in the bronchial epithelium and not in the mesenchyme at 12.5 dpc. A striking example of differential expression of the two genes was seen in the heart. At early somite stage (8.5 dpc), *Sox9* transcripts were absent when *Col2a1* was expressed strongly in the cardiogenic mesoderm (Figs. 3C and 3D). *Sox9* expression was found during the differentiation of the heart tissues and was restricted initially to the thin layer of endocardium in the atrium at 9.5 dpc. Subsequently, at 11.5 and 12.5 dpc *Sox9* was found in the endocardium of the heart chambers, in the endocardial cushions of the heart valves, and in the atrioventricular canal (Fig. 6G). Differential expression of these genes was confirmed by the observation that SOX9 protein is expressed only in the endocardial cushions of the heart at 10.5 dpc (Fig. 4G). In contrast, *Col2a1* was expressed in the epimyocardium of the heart (Fig. 6H). Expression of *Col2a1* was transient and was absent by 14.5 dpc. However, weak expression of *Sox9* mRNA persisted in the endocardial cushion of the heart as late as 16.5 dpc.

DISCUSSION

The human and mouse *SOX9/Sox9* genes encode highly conserved proteins with features of transcriptional regulators, including potential DNA binding and transcriptional activation domains (Foster *et al.*, 1994; Wagner *et al.*, 1994; Wright *et al.*, 1995). The ability to activate transcription has been demonstrated for the mouse proteins SRY, SOX2, SOX4, SOX17, and SOX18 (van de Wetering *et al.*, 1993; Dubin and Ostrer, 1994; Hosking *et al.*, 1995; Kamachi *et al.*, 1995; Kanai *et al.*, 1996), but it is not yet known whether this is a general feature of SOX proteins. We have demonstrated that mouse SOX9 protein can activate transcription of a reporter gene in mammalian cells. Unexpectedly, the strongest transactivation domain for SOX9 was located in the C-terminal 83 amino acid residues and not in the proline- and glutamine-rich domain typical of several known transcription factors. Our data confirm and extend those of Südbeck *et al.* (1996) who demonstrated that the carboxy-terminal 107 amino acids of human SOX9 can activate transcription. As the human and mouse SOX9 proteins show an overall amino acid identity of 96%, it is assumed that the two proteins are biochemically and functionally indistinguishable. It will be of interest to delimit further the region required for transcriptional activation. In this regard

FIG. 6. Expression of *Sox9* and *Col2a1* in nonchondrogenic tissues. *Sox9* expression is shown in A, C, E, and G (left-hand side picture of each pair) and *Col2a1* in B, D, F, and H (right-hand side pictures). (A, B) *Sox9* transcripts are localized to the dorsal region of the neural tube (nt) of a 9.5 dpc embryo and in the sclerotome of the somites (sm), whereas *Col2a1* expression is low in the neural tube but strong in the sclerotome. The notochord (nd) expresses both genes. (C, D) Coexpression in the otic vesicle (ov) at 9.5 dpc. Note the relatively weaker expression of *Sox9* in the paraxial mesoderm (pm). (E, F) Coexpression of both genes in the ventricular neuroepithelium (vne) of the hindbrain and the roof plate (arrows) of an 11.5 dpc embryo. IV marks the fourth ventricle of the hindbrain. (G, H) Differential expression of *Sox9* and *Col2a1* in the 11.5 dpc heart. *Sox9* is expressed in the endocardium (arrowhead) of the ventricle and in the endocardial cushions (ec) flanking the atrioventricular canals (av). *Col2a1*, in contrast, is expressed in the epimyocardium (epm) of the ventricular and the interatrial region. Strong expression of both genes is found in the pharyngeal mesenchyme (phm) but *Col2a1* is preferentially expressed in the pharyngeal pouch (pp) and the arch mesenchyme adjacent to the arch artery (aa). Bar = 50 μm (A, B, G, H) and 100 μm (C–F).

Copyright © 1997 by Academic Press. All rights of reproduction in any form reserved.

TABLE 2
Differential Expression of *Sox9* and *Col2a1* in Nonskeletal Tissues

Tissues	*Sox9*	*Col2a1*
7.5 dpc		
Trophoblast, ectoplacental cone	+	–
Visceral endoderm	–	Over cardiogenic mesoderm
Gut		
Foregut portal endoderm	Weak, patchy	+
Hindgut endoderm	Weak, patchy	–
Oesophagus		
Epithelium	+	–
Mesenchyme	+	–
Hepatic diverticulum, septum transversum	+	Patchy
Pancreas		
Ductal epithelium	+ (14.5, 15.5 dpc)	–
Islet	–	+ (14.5 dpc)
Intestine		
Mucosa	+ (11.5–16.5 dpc)	–
Submucosa	+ (16.5 dpc)	+
Root of mesentery	+	–
Branchial arches		
I and II arch mesenchyme	– (Later in maxillary prominence)	Weak
III–VI arch	+	–
Pharynx		
Endoderm	–	+
Surface ectoderm	+	+
Lower lip		
Mesenchyme	–	+
Alveolar ridge mesenchyme	–	+
Tongue mesoderm	–	+ (distal tip)
Submandibular gland (duct)	–	+
Respiratory tract		
Bronchial epithelium	+	+
Lung bud mesenchyme	+	
Limb bud		
Surface ectoderm	Weak	Strong
Mesenchyme	Preaxial > postaxial	Restricted to condensed mass
Urogenital structures[a]		
Genital ridge mesenchyme	+ (12.5 dpc)	–
Metanephric tubules	+ (12.5 dpc)	±
Genital tubercle mesenchyme	+ (14.5 dpc)	–
Others		
Tail tendon	–	+
Cornea	–	+ (17.54 dpc)
Umbilical cord (membrane)	+ (11.5, 12.5 dpc)	–
Heart		
Epimyocardium	–	+
Endocardium	+	–

[a] Sex unknown.

it may be significant that the terminal 20 amino acids of SOX9 from mouse (Wright *et al.*, 1995), human (Foster *et al.*, 1994; Wagner *et al.*, 1994), chicken (GenBank Accession No. U12533), and rainbow trout (N. Takamatsu, personal communication) show a higher degree of conservation than the remainder of the terminal 83-amino-acid domain. Further, the terminal 20 amino acids of mouse and human SOX9 show 60% identity to the rainbow trout SOX8 sequence (Ito *et al.*, 1995), whereas the remainder of the 83 amino acid region is only 18% identical. Many of the *SOX9* mutations in CD patients have been found to affect the composition of the HMG box or to lead to severe truncation

Copyright © 1997 by Academic Press. All rights of reproduction in any form reserved.

or missense translation of the region downstream from the HMG box (Foster *et al.*, 1994; Wagner *et al.*, 1994; Kwok *et al.*, 1995), confirming the importance of both domains for SOX9 function. Indeed, Südbeck *et al.* (1996) have demonstrated that a SOX9 protein with an intact HMG box but lacking an activation domain can act as a dominant negative regulator of transcription. In view of the present results it will be important to determine the effect on *Col2a1* transcription and the developmental consequences of mimicking similar CD mutations in transgenic mice.

While the gross pattern of expression of *Sox9* has been described previously (Wright *et al.*, 1995), a comprehensive survey of the timing and sites of *Sox9* mRNA and protein expression during development has not been reported. The results presented here suggest that, in addition to its major roles in chondrogenesis and skeletal development, *Sox9* is important for a variety of developmental processes, with expression observed in the developing CNS, notochord, lungs, heart, and urogenital system. The functional significance of these sites of expression is confirmed by the observation that *SOX9* mutations in CD patients commonly affect a variety of nonskeletal organs such as the brain, tracheopulmonary system, heart, and urinary tract (Lee *et al.*, 1972; Houston *et al.*, 1983; Rodriguez, 1993) and frequently result in XY sex reversal (Hovmoller *et al.*, 1977; Tommerup *et al.*, 1993). In addition to genes important for skeletal development, those involved in morphogenesis of other tissues affected by CD, and in the testis-determining pathway, must be considered potential targets for the SOX9 protein.

Given that SOX9 can activate transcription and may function as a transcription factor, it is necessary to identify target genes in order to clarify its developmental role. To date, the only SOX protein for which a target has been identified is SOX2. In the mouse, *Sox2* mRNA is expressed in the lens of the embryonic eye, and SOX2 protein was shown to activate the chicken δ1-crystallin gene encoding the major protein component of the lens (Kamachi *et al.*, 1995). To investigate the possibility of a regulatory relationship between SOX9 and *Col2a1*, the gene encoding the major structural component of cartilage, we have directly compared the expression of these two genes in a comprehensive series of adjacent sections of mouse embryos ranging from 7.5 to 18.5 dpc. Coexpression of these genes was extensive in skeletal tissues, as summarized in Fig. 5. The onset of expression of the two genes appeared to be tightly coupled. The precise relative timing of *Sox9* and *Col2a1* expression could not be resolved in all tissues by sampling of embryos at 1-day intervals, but appearance of *Sox9* mRNA was found to precede that of *Col2a1* transcripts in the chondrogenic mesenchyme of the limb and in the notochord. Both SOX9 protein and *Col2a1* mRNA are present in prechondrogenic mesenchyme and proliferating and maturing chondrocytes. *Sox9* and *Col2a1* also continue to be strongly expressed in cartilaginous tissues which do not ossify and where chondrocytes do not hypertrophy, such as the larynx and bronchial cartilages. The temporal and spatial similarity of these expression patterns suggests that SOX9 is a regulator of *Col2a1* in differentiating chondrocytes, either directly or indirectly. The coexpression of SOX9 protein and *Col2a1* mRNA in some nonchondrogenic tissues such as notochord, otic vesicle, and the developing CNS suggests that positive regulation of *Col2a1* by SOX9 may also occur in these other tissues.

Despite the simplicity of a model in which SOX9 directly or indirectly activates transcription of the *Col2a1* gene, several observations indicate that the transcriptional regulation of *Col2a1* is likely to be more complex. First, *Sox9* expression was down-regulated in hypertrophic chondrocytes and at sites of endochondral ossification by 17.5–18.5 dpc, whereas *Col2a1* expression declined to a lesser degree. Second, *Col2a1* expression in mature cartilage persisted beyond that of *Sox9* mRNA and protein during later stages of fetal development, indicating that SOX9 is not required for the longer term maintenance of *Col2a1* expression. Third, the two genes show differential expression in several nonchondrogenic tissues such as the heart and lung. Fourth, transcriptional activation by other HMG proteins such as LEF-1 and SOX-2 requires cooperation of other factors (Carlson *et al.*, 1993; Giese and Grosschedl, 1993; Kamachi *et al.*, 1995; Yuan *et al.*, 1995). These observations, and the known involvement of multiple factor interactions in transcriptional regulation (Tjian and Maniatis, 1994), suggest that SOX9 also requires other tissue-specific cofactors for transactivation of its target genes. The involvement of *Sox9* in unrelated processes such as sex determination (Kent *et al.*, 1996; Morais da Silva *et al.*, 1996) also points to varying combinations of SOX9 and other transcription factors to achieve different regulatory functions. The determination of the precise molecular mechanisms by which SOX9 regulates chondrogenesis and the identification of potential cooperating factors are important goals of future research.

ACKNOWLEDGMENTS

This work was supported by grants to K.S.E.C. from the Arthritis and Rheumatism Council (UK) and to P.K. and E.W. from the National Health and Medical Research Council of Australia. S.W. is supported by a Wellcome Trust fellowship, Grant 043765. We thank Andy Greenfield and Peter Rowe for critical reading of the manuscript Andrew McCormack for technical assistance, and Nobuhiko Takamatsu for sharing unpublished data.

REFERENCES

Carlson, P., Waterman, M., and Jones, K. (1993). The hLEF/TCF-1α HMG protein contains a context-dependent transcriptional activation domain that induces the TCRα enhancer in T cells. *Genes Dev.* **7,** 2418–2430.

Cheah, K. S. E., Lau, E. T., Au, P. K. C., and Tam, P. P. L. (1991). Expression of the mouse α1(II) collagen gene is not restricted to cartilage during development. *Development* **111,** 945–953.

Clerc, R., Corcoran, L., LeBowitz, J., Baltimore, D., and Sharp, D. (1988). The B-cell-specific Oct-2 protein contains POU-box and homeobox-type domains. *Genes Dev.* **2,** 1570–1581.

Connor, F., Wright, E., Denny, P., Koopman, P., and Ashworth, A.

Copyright © 1997 by Academic Press. All rights of reproduction in any form reserved.

(1995). The *Sry*-related HMG box-containing gene *Sox6* is expressed in the adult testis and developing nervous system of the mouse. *Nucleic Acids Res.* **23,** 3365–3372.

Courey, A., and Tjian, R. (1988). Analysis of Sp1 *in vivo* reveals multiple transcriptional activating domains, including a novel glutamine-rich activation motif. *Cell* **55,** 887–898.

Denny, P., Swift, S., Connor, F., and Ashworth, A. (1992). An *SRY*-related gene expressed during spermatogenesis in the mouse encodes a sequence-specific DNA-binding protein. *EMBO J.* **11,** 3705–3712.

Dubin, R. A., and Ostrer, H. (1994). Sry is a transcriptional activator. *Mol. Endocrinol.* **8,** 1182–1192.

Dunn, T. L., Mynett-Johnson, L., Hosking, B. M., Koopman, P. A., and Muscat, G. E. O. (1995). Sequence and expression of *Sox-18,* a new HMG-box transcription factor. *Gene* **161,** 223–225.

Erlebacher, A., Filvaroff, E. H., Gitelman, S. E., and Derynck, R. (1995). Toward a molecular understanding of skeletal development. *Cell* **80,** 371–378.

Foster, J. W., Dominguez-Steglich, M. A., Guioli, S., Kwok, C., Weller, P. A., Weissenbach, J., Mansour, S., Young, I. D., Goodfellow, P. N., Brook, J. D., and Schafer, A. J. (1994). Campomelic dysplasia and autosomal sex reversal caused by mutations in an *SRY*-related gene. *Nature* **372,** 525–530.

Garofalo, S., Vuorio, E., Metsäranta, M., Rosati, R., Toman, D., Vaughan, J., Lozano, G., Mayne, R., Ellard, J., Horton, W. A., and De Crombrugghe, B. (1991). Reduced amounts of cartilage collagen fibrils and growth plate anomalies in transgenic mice harboring a glycine-to-cysteine mutation in the mouse type II procollagen α1-chain gene. *Proc. Natl. Acad. Sci. USA* **88,** 9648–9652.

Giese, K., and Grosschedl, R. (1993). LEF-1 contains an activation domain that stimulates transcription only in a specific context of factor binding sites. *EMBO J.* **12,** 4667–4676.

Gorman, C. M., Moffat, L. F., and Howard, B. H. (1982). Recombinant genomes which express chloramphenicol acetyltransferase in mammalian cells. *Mol. Cell Biol.* **2,** 1044–1051.

Gubbay, J., Collignon, J., Koopman, P., Capel, B., Economou, A., Münsterberg, A., Vivian, N., Goodfellow, P., and Lovell-Badge, R. (1990). A gene mapping to the sex-determining region of the mouse Y chromosome is a member of a novel family of embryonically expressed genes. *Nature* **346,** 245–250.

Harley, V. R., Lovell-Badge, R., and Goodfellow, P. N. (1994). Definition of a concensus DNA binding site for SRY. *Nucleic Acids Res.* **22,** 1500–1501.

Hosking, B. M., Muscat, G. E. O., Koopman, P. A., Dowhan, D. H., and Dunn, T. L. (1995). *Trans*-activation and DNA-binding properties of the transcription factor, Sox-18. *Nucleic Acids Res.* **23,** 2626–2628.

Houston, C. S., Opitz, J. M., Spranger, J. W., Macpherson, R. I., Reed, M. H., Gilbert, E. F., Herrmann, J., and Schinzel, A. (1983). The campomelic syndrome: Review, report of 17 cases, and follow-up on the currently 17-year old boy first reported by Maroteaux *et al.* in 1971. *Am. J. Med. Genet.* **15,** 3–28.

Hovmoller, M. L., Osuna, A., Eklof, O., Fredga, K., Hjerpe, A., Lindsten, J., Ritzen, M., Stanescu, V., and Svenningsen, N. (1977). Camptomelic dwarfism. A genetically determined mesenchymal disorder combined with sex reversal. *Hereditas* **86,** 51–62.

Ito, M., Ishikawa, M., Suzuki, S., Takamatsu, N., and Shiba, T. (1995). A rainbow trout *SRY*-type gene expressed in pituitary glands. *FEBS Lett.* **377,** 37–40.

Jay, P., Gozé, C., Marsollier, C., Taviaux, S., Hardelin, J.-P., Koopman, P., and Berta, P. (1995). The human SOX11 gene: Cloning, chromosomal assignment and tissue expression. *Genomics* **29,** 541–545.

Kamachi, Y., Sockanathan, S., Liu, Q., Breitman, M., Lovell-Badge, R., and Kondoh, H. (1995). Involvement of SOX proteins in lens-specific activation of crystallin genes. *EMBO J.* **14,** 3510–3519.

Kanai, Y., Kanai-Azuma, M., Noce, T., Saido, T. C., Shiroishi, T., Hayashi, Y., and Yazaki, K. (1996). Identification of two Sox17 messenger RNA isoforms, with and without the high mobility group box region, and their differential expression in mouse spermatogenesis. *J. Cell Biol.* **133,** 1–15.

Katò, G. J., Barrett, J., Villa-Garcia, M., and Dang, C. V. (1990). An amino-terminal c-myc domain required for neoplastic transformation activates transcription. *Mol. Cell. Biol.* **10,** 5914–5920.

Kent, J., Wheatley, S. C., Andrews, J. E., Sinclair, A. H., and Koopman, P. (1996). A male-specific role for *SOX9* in vertebrate sex determination. *Development* **122,** 2813–2822.

Koopman, P., Münsterberg, A., Capel, B., Vivian, N., and Lovell-Badge, R. (1990). Expression of a candidate sex-determining gene during mouse testis differentiation. *Nature* **348,** 450–452.

Kosher, R. A., Kulyk, W. M., and Gay, S. W. (1986). Collagen gene expression during limb bud differentiation. *J. Cell Biol.* **102,** 1151–1156.

Kravis, D., and Upholt, W. B. (1985). Quantitation of type II procollagen mRNA levels during chick limb cartilage differentiation. *Dev. Biol.* **108,** 164–172.

Kwok, C., Weller, P., Guioli, S., Foster, J. W., Mansour, S., Zuffardi, O., Punnett, H. H., Dominguez-Steglich, M. A., Brook, J. D., Young, I. D., Goodfellow, P. N., and Schafer, A. J. (1995). Mutations in *SOX9,* the gene responsible for campomelic dysplasia and autosomal sex reversal. *Am. J. Hum. Genet.* **57,** 1028–1036.

Lee, F. A., Issacs, H., and Strauss, J. (1972). The 'camptomelic' syndrome. Short life-span dwarfism with respiratory distress, hypotonia, peculiar facies, and multiple skeletal and cartilaginous deformities. *Am. J. Dis. Child.* **124,** 485–496.

Li, S-W., Prockop, D. J., Helminen, H., Fassler, R., Lapvetelainen, T., Kiraly, K., Peltarri, A., Arokoski, J., Lui, H., Arita, M., and Khillan, J. S. (1995). Transgenic mice with a targeted inactivation of the Col2a1 gene for collagen II develop a skeleton with membranous and periosteal bone but no endochondral bone. *Genes Dev.* **9,** 2821–2830.

Lillie, J. W., and Green, M. R. (1989). Transcription activation by the adenovirus E1a protein. *Nature* **338,** 39–44.

Metsäranta, M., Garofalo, S., Decker, G., Rintala, M., De Crombrugghe, B., and Vuorio, E. (1992). Chondrodysplasia in transgenic mice harboring a 15-amino acid deletion in the triple helical domain of proα1(II) collagen chain. *J. Cell Biol.* **118,** 203–212.

Metsäranta, M., Toman, D., De Crombrugghe, B., and Vuorio, E. (1991). Mouse type II collagen gene. Complete nucleotide sequence, exon structure, and alternative splicing. *J. Biol. Chem.* **266,** 16862–16869.

Mitchell, P., and Tjian, R. (1989). Transcriptional regulation in mammalian cells by sequence-specific DNA binding proteins. *Science* **245,** 371–378.

Morais da Silva, S., Hacker, A., Harley, V., Goodfellow, P., Swain, A., and Lovell-Badge, R. (1996). *Sox9* expression during gonadal development implies a conserved role for the gene in testis differentiation in mammals and birds. *Nature Genet.* **14,** 62–68.

Ng, L. J., Tam, P. P. L., and Cheah, K. S. E. (1993). Preferential expression of alternatively spliced mRNAs encoding type II procollagen with a cysteine-rich amino-propeptide in differentiating cartilage and nonchondrogenic tissues during early mouse development. *Dev. Biol.* **159,** 403–417.

Osborn, L., Kunkel, S., and Nabel, G. J. (1989). Tumour necrosis factor α and interleukin 1 stimulate the human immunodefi-

Copyright © 1997 by Academic Press. All rights of reproduction in any form reserved.

ciency virus enhancer by activation of the nuclear fcator κB. *Proc. Natl. Acad. Sci. USA* **86,** 2336–2340.

Ptashne, M. (1988). How eukaryotic transcriptional activators work. *Nature* **335,** 683–689.

Ritvaniemi, P., Korkko, J., Bonaventure, J., Vikkula, M., Hyland, J., Paasilta, P., Kaitila, I., Kaariainen, H., Sokolov, B. P., Hakala, M., Mannismaki, P., Meerson, E. M., Klemola, T., Williams, C., Peltonen, L., Kivirikko, K. I., Prockop, D. J., and Ala-Kokko, L. (1995). Analysis of the COL2A1 gene detects mutations in over 20 percent of patients with chondrodysplasias and up to 2 percent of patients with familial osteoarthritis. *Arthritis Rheum.* **38,** 999–1004.

Rodriguez, J. I. (1993). Vascular anomalies in campomelic syndrome. *Am. J. Med. Genet.* **46,** 185–192.

Santoro, C., Mermod, N., Andrews, P., and Tjian, R. (1988). A family of human CCAAT-box-binding proteins active in transcription and DNA replication: Cloning and expression of multiple cDNAs. *Nature* **334,** 218–224.

Schreiber, E., Matthias, P., Muller, M. M., and Schaffner, W. (1989). Rapid detection of octamer binding proteins with 'mini-extracts,' prepared from a small number of cells. *Nucleic Acids Res.* **17,** 6419.

Stevanovic, M., Lovell-Badge, R., Collignon, J., and Goodfellow, P. N. (1993). *SOX3* is an X-linked gene related to *SRY*. *Hum. Mol. Genet.* **3,** 2013–2018.

Südbeck, P., Lienhard Schmitz, M., Baeuerle, P. A., and Scherer, G. (1996). Sex reversal by loss of the C-terminal transactivation domain of human SOX9. *Nature Genet.* **13,** 230–232.

Swalla, B. J., Upholt, W. B., and Solursh, M. (1988). Analysis of type II collagen RNA localization in chick wing buds by *in situ* hybridization. *Dev. Biol.* **125,** 51–58.

Tjian, R., and Maniatis, T. (1994). Transcriptional activation: A complex puzzle with few easy pieces. *Cell* **77,** 5–8.

Tommerup, N., Schempp, W., Mienecke, P., Pedersen, S., Bolund, L., Brandt, C., Goodpasture, C., Guldberg, P., Held, K. R., Reinwein, H., Saaugstad, O. D., Scherer, G., Skjeldal, O., Toder, R., Westvik, J., van der Hagen, C. B., and Wolf, U. (1993). Assignment of an autosomal sex reversal locus (SRA1) and campomelic dysplasia (CMPD1) to 17q24.3-q25.1. *Nature Genet.* **4,** 170–174.

Uwanogho, D., Rex, M., Cartwright, E. J., Pearl, G., Healy, C., Scotting, P., and Sharpe, P. T. (1994). Embryonic expression of the chicken Sox2, Sox3 and Sox11 genes suggests an interactive role in neural development. *Mech. Dev.* **49,** 23–36.

Vandenberg, P., Khillan, J. S., Prockop, D. J., Helminen, H., Kontusaari, S., and Ala-Kokko, L. (1991). Expression of a partially deleted gene of human type II procollagen (*COL2A1*) in transgenic mice produces a chondrodysplasia. *Proc. Natl. Acad. Sci. USA* **88,** 7640–7644.

van de Wetering, M., Oosterwegel, M., van Norren, K., and Clevers, H. (1993). Sox-4, an Sry-like HMG box protein, is a transcriptional activator in lymphocytes. *EMBO J.* **12,** 3847–3854.

Vikkula, M., Metsäranta, M., and Ala-Kokko, L. (1994). Type II collagen mutations in rare and common cartilage diseases. *Ann. Med.* **26,** 107–114.

Von der Mark, K., and Von der Mark, H., and Gay, S. (1977). Immunological and biochemical studies of collagen type transition during *in vitro* chondrogenesis of chick limb mesodermal. *J. Cell Biol.* **73,** 736–747.

Wagner, T., Wirth, J., Meyer, J., Zabel, B., Held, M., Zimmer, J., Pasantes, J., Bricarelli, F. D., Keutel, J., Hustert, E., Wolf, U., Tommerup, N., Schempp, W., and Scherer, G. (1994). Autosomal sex reversal and campomelic dysplasia are caused by mutations in and around the *SRY*-related gene *SOX9*. *Cell* **79,** 1111–1120.

Wright, E., Hargrave, M. R., Christiansen, J., Cooper, L., Kun, J., Evans, T., Gangadharan, U., Greenfield, A., and Koopman, P. (1995). The *Sry*-related gene *Sox-9* is expressed during chondrogenesis in mouse embryos. *Nature Genet.* **9,** 15–20.

Yuan, H., Corbi, N., Basilico, C., and Dailay, L. (1995). Developmental-specific activity of the FGF-4 enhancer requires the synergistic action of Sox2 and Oct-3. *Genes Dev.* **9,** 2635–3645.

Received for publication November 1, 1996
Accepted December 4, 1996

Copyright © 1997 by Academic Press. All rights of reproduction in any form reserved.

DEVELOPMENTAL BIOLOGY 183, f-1–f-2 (1997)
ARTICLE NO. DB978524

THE 13TH INTERNATIONAL CONGRESS OF DEVELOPMENTAL BIOLOGY

Jointly sponsored by the *International Society for Developmental Biologists* and the *Society for Developmental Biology*

July 5 - 10, 1997 Snowbird, Utah, U.S.A.

OPENING SYMPOSIUM Eric Wieschaus
Christiane Nuesslein–Volhard
Edward Lewis

PLENARY SESSIONS

Establishing Asymmetries: Judith Kimble, Ruth Lehmann, Hiroshi Hamada, Ira Herskowitz, David McClay, Ralph Quatrano

Pattern Formation in Development and Evolution: Elliott Meyerowitz, Steven Cohen, Rosa Beddington, Cliff Tabin, Walter Gehring, Paul Sternberg

Neural Development and Patterning: Friedrich Bonhoeffer, Marc Tessier–Lavigne, Linda Buck, Joe Culotti, Masotoshi Takeichi, Marianne Bronner-Fraser

Signalling Pathways in Development: Lee Niswander, Trudi Schupbach, Phil Ingham, Roel Nusse, Naoto Ueno, Joanne Chory

CONCURRENT SYMPOSIA

Lineage analysis and cell fate: Patrick Tam, Ben Scheres

Genetic regulation of organogenesis: Greg Dressler, Kathy Mahon, Richard Harvey

Gene regulation in development: Herbert Jackle, Mike Levine, Robb Krumlauf

Localization of determinants: Anne Ephrussi, Ken Kemphues, Hiroki Nishida

Eye development: Robert Grainger, Peter Gruss, Roderick McInnes

Signalling pathways in development: Patricia Simpson, Andy McMahon

Flower development and function: Detlef Weigel, June Nasrallah, George Coupland

Development and evolution: Rudolf Raff, Scott Poethig, Anne Burke

Inductive interactions in development: Hazel Sive, Jim Smith, Siew-Lan Ang

Patterning the developing body axes: Marysia Placzek, Kiyotaka Okada, Wolfgang Driever

Germ line development: Anne McLaren, Satori Kobayashi, Susan Strome

Cell type specification: Margaret Buckingham, Yuh Nung Jan

CONKLIN AWARD LECTURE To be announced

WORKSHOPS

Education issues: Gary Schoenwolf, Chair. One plenary session - speakers to be announced
Concurrent workshops: Susan Singer, Drew Node, Mary Tyler, Laurie Iten, Ida Chow, John Doctor

Techniques To be announced **Special topics** To be announced

POSTER SESSIONS Four dedicated sessions and exhibits

All speakers listed in the enclosed program have confirmed their participation. More invited speakers will be added, as well as talks chosen from submitted abstracts. SDB members will pay reduced registration fee. Electronic abstract submission will be available. Limited student dorm accommodation will be available on a first come first served basis.

For more information and registration/abstract package please mail or FAX request to:
Ida Chow, Ph.D., Executive Officer, Society for Developmental Biology, 9650 Rockville Pike, Bethesda, MD 20814–3998, U.S.A. FAX: 301–530–7049

You may also register your interest via SDB Web Page: http://sdb.bio.purdue.edu/

Copyright © 1997 by Academic Press
All rights of reproduction in any form reserved.

Symposium Announcement

8th International Center for Biotechnology Symposium on Cytoplasmic Protein Tyrosine Kinases

Novum Research Park—Huddinge, Stockholm, Sweden, May 23-25, 1997

The 8th International Center for Biotechnology Symposium on Cytoplasmic Protein Tyrosine Kinases will be held May 23-25, 1997, in Novum Research Park, Karolinska Institute, Huddinge, South of Stockholm, Sweden. The Symposium organizers are C.I.E. Smith and M. Vihinen. For further information, please contact:

Aila Holappa
Fax: 46-(0)-8-774-55-38
E-mail: aila.holappa@cbt.ki.se
http://www.cbt.ki.se/sts/

DEVELOPMENTAL BIOLOGY

Information for Authors

Developmental Biology publishes papers containing new and significant information bearing on developmental mechanisms of general interest. Areas of particular interest include experimental manipulation of embryos or tissues, genetic and transgenic approaches to studying gene expression, transcriptional control mechanisms, embryonic patterning, cell–cell interactions, fertilization, growth factors and signal transduction, regulatory hierarchies, and evolutionary mechanisms. Descriptive work, at either the anatomical or molecular level, will not be published unless it leads to new insights into developmental processes.

Articles usually do not exceed 15,000 words and must be preceded by an abstract of about 200 words.

Rapid Communications present findings that will have an immediate and significant impact and should therefore be made known to other researchers as quickly as possible. They are not meant as a forum for publishing short, preliminary studies. These reports will be reviewed within one week of receipt and, if accepted, will be published in the next available issue. Rapid Communications are generally limited to 1200 words, two tables or figures, and eight references. An abstract not exceeding 150 words should be included. Authors should indicate in a cover letter why the paper is of particular importance and needs to be considered rapidly rather than as a regular submission.. Rapid Communications may be submitted by fax if they do not include photographs. To expedite publication of such articles, authors will not receive proofs.

Review articles usually are solicited; however, the Editor-in-Chief invites inquiries and suggestions. Review articles are subject to the same review process as regular articles, but receive priority publication.

Submission of manuscripts. Manuscripts must be written in English. **Submit 1 original and 3 copies**, including illustrations, to *Developmental Biology*, Editorial Office, 525 B Street, Suite 1900, San Diego, CA 92101-4495. Phone: 619-699-6325, Facsimile: 619-699-6211, E-mail: db@acad.com. Authors may submit their papers directly to an Editor. Addresses for the Editors appear on the following page.

Original papers only will be considered. Submission of a manuscript implies the authors' assurance that the work has not been published nor is under consideration for publication elsewhere and that its submission for publication has been approved by all of the authors and by the institution where the work was carried out.

Authors submitting a manuscript do so on the understanding that if the manuscript is accepted for publication, copyright in the article, including the right to reproduce the article in all forms and media, shall be assigned exclusively to the Publisher. The Publisher will not refuse any reasonable requests by authors for permission to reproduce any of their contributions to the journal.

Preparation of manuscript. Manuscripts should be double-spaced throughout on one side of $8\frac{1}{2} \times 11$-inch or A4 paper. Pages should be numbered consecutively and organized as follows: title page (page 1), which should contain the article title, authors' names and complete affiliations, footnotes to the title, a running title of fewer than 50 characters, and the address for correspondence (including telephone and fax numbers and an e-mail address); abstract (page 2); introduction; materials and methods; results; discussion (results and discussion may be combined); acknowledgments; references; footnotes; tables; and figure legends. Most recommendations of the Council of Biology Editors should be followed; consult the *CBE Manual for Authors, Editors, and Publishers,* 6th ed. (Cambridge University Press). Nonstandard abbreviations should be defined at their initial appearance.

References should be cited in the text by name and date. Only articles that have been published or are in press should be included in the references. Unpublished results or personal communications should be cited as such in the text. Please use the following styles in the reference section:

Arcaro, K. F., and Lnenicka, G. A. (1995). Intrinsic differences in axonal growth from crayfish fast and slow motoneurons. *Dev. Biol.* **168,** 272–283.

Girard, S., and Clapham, D. E. (1994). Simultaneous near ultraviolet and visible excitation confocal microscopy of calcium transients in *Xenopus* oocytes. *In* "Methods in Cell Biology" (R. Nuccitelli, Ed.), Vol. 40, pp. 263–283. Academic Press, San Diego.

Figures should be in a finished form suitable for publication. Number figures consecutively with Arabic numerals and indicate the top and the authors on the back of each figure. Lettering on drawings should be professional quality or generated by high-resolution computer graphics and must be large enough to withstand appropriate reduction for publication.

Two color figures will be published *free* of charge in each article. **Additional color figures** will be published *free* of charge at the discretion of the Editors. Color figures *must* be submitted on flexible board due to the nature of the reproduction process.

Suggestions for **cover photographs** are welcome. Submit them as slides with $8\frac{1}{2} \times 11$-inch color or black-and-white prints to accompany specific articles. A short (one-line) legend should accompany each photograph.

Tables should be numbered consecutively with Arabic numerals in order of appearance in the text. Type each table double-spaced on a separate page with a short descriptive title typed directly above and with essential footnotes below. Authors should submit complex tables as camera-ready copy.

Proofs and reprints. Proofs will be sent to the authors with reprint order forms. Fifty reprints of each article are provided free of charge. Additional reprints may be ordered using the form provided.

Personal computer disks. Each manuscript should be submitted to *Developmental Biology* on a personal computer disk after the paper has been accepted and after all revisions have been incorporated into the text. Label the disk with the type of computer used, the type of software and the version number, and the disk format. A hard-copy printout of the manuscript that exactly matches the disk file must be supplied.

Distribution of material. Authors who publish a research article in *Developmental Biology* must be prepared to freely distribute to academic researchers for their own use any cell lines, DNA clones, monoclonal antibodies, or genetically engineered mice described in the article. All genetic sequence information published in *Developmental Biology* must also be deposited with GenBank.

For information about advertising in *Developmental Biology*, please contact Andrea Cowan, Advertising Coordinator, Academic Press, 525 B Street, Suite 1900, San Diego, California 92101-4495 (telephone: (619) 699-6825, fax: (619) 699-6380).

Editor-in-Chief

Eric N. Olson
Hamon Center for Basic Cancer Research
The University of Texas
Southwestern Medical Center at Dallas
5323 Harry Hines Blvd.
Dallas, TX 75235-9148 USA
phone: (214) 648-1187
fax: (214) 648-1140
email: eolson@hamon.swmed.edu

Editors

Marianne Bronner-Fraser
Beckman Institute
California Institute of Technology
Mail Code (139-74)
Pasadena, CA 91125 USA
fax: (818) 395-7717
email: mbronner@druggist.gg.caltech.edu

Eric H. Davidson
Division of Biology
California Institute of Technology
Mail Code 156-29
Pasadena, CA 91125 USA
phone: (818) 395-4937
fax: (818) 564-9685

Scott Fraser
Biological Imaging Center
California Institute of Technology
Mail Code (139-74)
Pasadena, CA 91125 USA
phone: (818) 395-2790
fax: (818) 564-9685
email: sefraser@gg.caltech.edu

Richard Harland
Department of Molecular and Cell Biology
University of California
Division of Biochemistry and Molecular Biology
410 Barker Hall, #3204
Berkeley, CA 94720-3204 USA
phone: (510) 643-6003
fax: (510) 643-1729
email: harland@mendel.berkeley.edu

Philip Ingham
Molecular Embryology Laboratory
Imperial Cancer Research Fund
P.O. Box 123, Lincoln's Inn Fields
London, WC2A 3PX UK
phone: 44-171-269-3393
fax: 44-171-269-3093
email: ingham@icrf.icnet.uk

Laurinda A. Jaffe
Department of Physiology
University of Connecticut
Health Center, Room L5004
Farmington, CT 06032 USA
phone: (203) 679-2661
fax: (860) 679-1661
email: ljaffe@neuron.uchc.edu

Robb Krumlauf
Laboratory of Developmental Neurobiology
National Institute for Medical Research
The Ridgeway, Mill Hill
London, NW7 1AA UK
phone: 44-181-913-8530
fax: 44-181-913-8658
email: r-krumla@nimr.mrc.ac.uk

Andrew P. McMahon
Department of Molecular and Cellular Biology
Harvard University
16 Divinity Avenue, Biological Laboratories
Cambridge, MA 02138 USA
phone: (617) 496-3757
fax: (617) 496-3763
email: amcmahon@Hubio2.harvard.edu

Gary Ruvkun
Department of Molecular Biology
Massachusetts General Hospital
Wellman 8
Boston, MA 02114 USA
phone: (617) 726-5959/5973
fax: (617) 726-6893
email: Ruvkun@Frodo.MGH.Harvard.edu

Matthew P. Scott
Department of Developmental Biology and Genetics
Stanford University
Howard Hughes Medical Institute
Stanford, CA 94305-5427 USA
phone: (415) 725-7680
fax: (415) 723-9878
email: scott@cmgm.stanford.edu

Cold Spring Harbor Laboratory

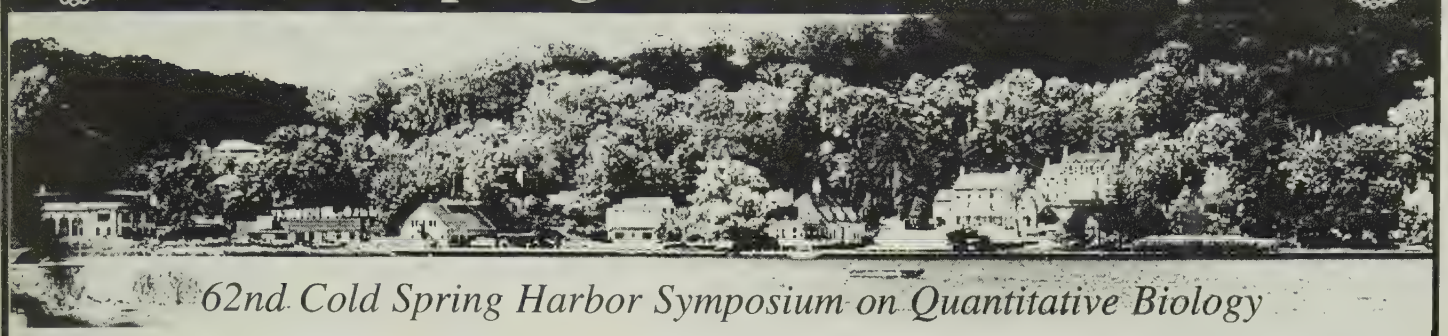

62nd Cold Spring Harbor Symposium on Quantitative Biology

Pattern Formation During Development

May 28th - June 2nd, 1997

Organized by **Bruce Stillman,** *Cold Spring Harbor Laboratory*

Topics Include:

- **Evolutionarily conserved mechanisms of pattern formation**
- **Establishing patterns - maternal effects, oocyte and egg patterning**
- **Early embryonic patterning and axis formation**
- **Organizers, morphogens**
- **Patterning during organogenesis**
- **Neural pathfinding, appendage formation, specifying tissue**
- **Cellular responses to signalling molecules**
- **Gene regulation**
- **RNA localization and translation control**
- **Pattern formation in plants**

Invited Speakers (Partial Listing)

Shinichi Aizawa, *Kumamoto University, Japan*
David J. Anderson, *California Institute of Technology*
Kathryn Anderson, *Sloan-Kettering Institute*
Michael Bate, *University of Cambridge*
Rosa Beddington, *National Institute for Medical Research, UK*
Richard Behringer, *University of Texas/ M.D. Anderson Cancer Center*
Mario Capecchi, *University of Utah*
Sean Carroll, *University of Wisconsin, Madison*
William Chia, *National University of Singapore*
Eddy DeRobertis, *University of California, Los Angeles*
Wolfgang Driever, *University of Freiburg*
Anne Ephrussi, *European Molecular Biology Laboratory, Germany*
John Fowler, *University of Carolina, Chapel Hill*
Corey Goodman, *University of California, Berkeley*
Ueli Grossniklaus, *Cold Spring Harbor Laboratory*
John Gurdon, *University of Cambridge, UK*
Richard Harland, *University of California, Berkeley*
Ira Herskowitz, *University of California, San Francisco*
Michael Hoffman, *University of Wisconsin Medical School*
Brigid Hogan, *Vanderbilt University Medical School*
H. Robert Horvitz, *Massachusetts Institute of Technology*
Philip Ingham, *Imperial Cancer Research Fund, UK*
Yuh-Nung Jan, *University of California, San Francisco*
Thomas Jessell, *Columbia University*
Cynthia Kenyon, *University of California, San Francisco*
Mark Krasnow, *Stanford University*
Robb Krumlauf, *National Institute for Medical Research, UK*
Andrew Lassar, *Harvard Medical School*
Ruth Lehmann, *New York University Medical Center*
Michael Levine, *University of California, Berkeley*
Richard Losick, *Harvard University*
Robert Martienssen, *Cold Spring Harbor Laboratory*
Gail Martin, *University of California, San Francisco*
Andrew McMahon, *Harvard University*
Douglas Melton, *Harvard Medical School*
Elliot Meyerowitz, *California Institute of Technology*
Jeremy Nathans, *Johns Hopkins Medical School*
Lee Niswander, *Sloan-Kettering Institute*
Roel Nusse, *Stanford University*
Christiane Nüsslein-Volhard, *Max-Planck-Institut für Entwicklungsbiologie, Germany*
Eric Olson, *University of Texas Southwestern Medical School*
Norbert Perrimon, *Harvard Medical School*
Alessandro Puoti, *University of Wisconsin, Madison*
Elizabeth Robertson, *Harvard University*
Janet Rossant, *University of Toronto*
Gerald M. Rubin, *University of California, Berkeley*
Noriyuki Satoh, *Kyoto University, Japan*
Matthew Scott, *Stanford University*
Ben-Zion Shilo, *Weizmann Institute of Science. Israel*
Hazel Sive, *Whitehead Institute*
Jim Smith, *National Institute for Medical Research, UK*
Allan Spradling, *Carnegie Institution of Washington*
Clifford Tabin, *Harvard Medical School*
Masatoshi Takeichi, *Kyoto University, Japan*
Patrick Tam, *Children's Medical Research Institute, Australia*
Marc Tessier-Levigne, *University of California, San Francisco*
Irma Thesleff, *University of Helsinki, Finland*
Christopher Wright, *Vanderbilt University*
Larry Zipursky, *University of California, Los Angeles*

Abstract Deadline: March 12th, 1997

Submission of abstracts for poster presentations is encouraged. Early registration and abstract submission is advisable since posters will be limited to 120 total. Limited funds for junior researchers may be available to support registration costs. Cold Spring Harbor Laboratory encourages you to register and submit abstracts online via the World Wide Web at ***http://www.cshl.org/meetings*** *or by email. Further information, registration and abstract materials are available from:*

Meetings & Courses Office, 1 Bungtown Rd., Cold Spring Harbor, NY 11724-2213
Email: meetings@cshl.org Phone: (516) 367-8346 Fax: (516) 367-8845 http://www.cshl.org/meetings

ASSISTANT PROFESSOR
Developmental Neurobiology
The Pennsylvania State University

The Department of Biology invites applications for a tenure-track faculty position in *developmental neurobiology*. We seek a developmental biologist with a strong research program focusing on any aspect of neurogenesis using genetic and/or molecular approaches that would complement existing strengths in developmental biology and neuroscience. The Pennsylvania State University has made a commitment to expanding research and education in biological sciences through a new, University-wide Life Sciences Consortium (see http://www.lsc.psu.edu). The successful candidate will be expected to develop an active research program and participate in undergraduate and graduate teaching.

Applicants should submit their *curriculum vitae*, reprints of three key publications, a brief statement of research goals (three pages maximum), and three letters of recommendation to:

Developmental Neurobiology Search Committee
Department of Biology
208 Mueller Laboratory
The Pennsylvania State University
University Park, PA 16802

Review of applications will begin immediately and continue until the position is filled.

An Affirmative Action/Equal Opportunity Employer.
Women and Minorities are Encouraged to Apply.

ACADEMIC PRESS JOURNALS

Excellence in Scientific Publishing

When you need the latest information, turn to Academic Press. We publish journals covering 30 disciplines. Respected in their fields, Academic Press journals have carried a reputation of quality for more than 50 years.

Journal Disciplines

Accounting and Management
Anthropology and Archaeology
Astronomy
Biochemistry and Molecular Biology
Biology
Biomedical Sciences and Basic Medical Research
Botany
Chemistry
Clinical Medicine
Clinical Psychology and Psychiatry
Computer Science
Earth Science
Economics
Education
Engineering
Environmental Sciences
Food Sciences and Nutrition
History
Immunology and Pathology
Language Sciences
Law
Library and Information Sciences
Mathematics
Neurosciences
Physics
Psychology
Social Sciences
Speech and Hearing Sciences
Toxicology and Pharmacology
Zoology

For information concerning a particular journal or discipline, please write or call:

ACADEMIC PRESS, INC., Journal Promotion Department
525 B Street, Suite 1900, San Diego, CA 92101-4495, U.S.A.
(800) 894-3434

S4128G

BIOMEDICAL SCIENCES AND BASIC MEDICAL RESEARCH

Academic Press Journals

Acta Virologica
Anaerobe
Analytical Biochemistry
Appetite
Archives of Biochemistry and Biophysics
Biochemical and Biophysical Research Communications
Biochemical and Molecular Medicine
Biochemistry and Molecular Biology International
Biologicals
Bioorganic Chemistry
Brain, Behavior, and Immunity
Cell Biology International
Cellular Immunology
Clinical Immunology and Immunopathology
Computers and Biomedical Research
Cryobiology
Cytokine
Developmental Biology
Environmental Research
Experimental Cell Research
Experimental Eye Research
Experimental and Molecular Pathology
Experimental Neurology
Food Microbiology
Frontiers in Neuroendocrinology
Fundamental and Applied Toxicology
Genomics
Journal of Autoimmunity
Journal of Food Composition and Analysis
Journal of Magnetic Resonance—Series B
Journal of Molecular Biology
Journal of Molecular and Cellular Cardiology
Journal of Structural Biology
Methods: A Companion to Methods in Enzymology
Microbial Pathogenesis
Microchemical Journal
Molecular and Cellular Neuroscience
Molecular and Cellular Probes
Neurodegeneration
NeuroImage
Pharmacological Research
Plasmid
Protein Expression and Purification
Pulmonary Pharmacology
Seminars in Cancer Biology
Seminars in Cell and Developmental Biology
Seminars in Immunology
Seminars in the Neurosciences
Seminars in Virology
Toxicology and Applied Pharmacology
Virology

For more information, please indicate the journals that interest you and write or call:

FIND US ON THE WEB!
AP NET
Academic Press
http://www.apnet.com/

Academic Press, Inc.
Marketing Department
525 B Street, Suite 1900
San Diego, CA 92101-4495, U.S.A.
1-800-894-3434 or 1-619-699-6742
e-mail: apsubs@acad.com

Academic Press, Limited
Marketing Department
24-28 Oval Road
London NW1 7DX, U.K.
In Europe call: 0181-300-3322

for a FREE SAMPLE
MAIL

BIOMED96E

Archives of Biochemistry AND Biophysics

Chairman of the Editorial Committee

J. Thomas August
The Johns Hopkins University
Baltimore, Maryland

Editorial Committee

A. H. Abeles, R. F. Colman
R. Croteau, A. Ginsburg
V. C. Hascall, A. Kobata
J. M. McCord , G. H. Reed
A. Scarpa, H. Sies
W.L. Smith, E. R. Stadtma
P.K. Vogt, M. R. Waterman

Archives of Biochemistry and Biophysics presents articles in the developing areas of biochemistry and biophysics, especially those related to molecular biology, cell biology, and developmental biology. The journal strives for the rapid publication of articles of high quality and significance in an international forum. The journal features research reports and a new rapid communications section.

Database coverage includes Biological Abstracts (BIOSIS), CABS, Chemical Abstracts, Current Contents/Life Sciences, Excerpta Medica (EMBASE), Genetics Abstracts, Index Medicus (MEDLINE), Research Alert, Science Citation Index, and SCISEARCH.

INCREASED FREQUENCY

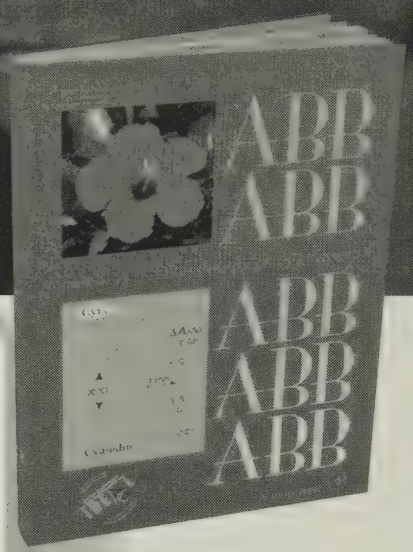

Research Areas Include

- Molecular biology and biochemistry of cell–surface and membrane proteins
- Proteases, protein turnover, and post-translational processing
- Enzyme structure, function, and regulation
- Plant molecular biology and biochemistry
- Protein structure and functions
- Glycobiology: Proteoglycans, extracellular matrices, glycoconjugates, and oligosaccharides
- Cytokines and cytokine receptors; hematopoietic transformation
- Transcriptional control; oncogenes and signal transduction; protein–DNA interaction
- Biological oxidations, free radical reactions, and oxygen toxicity
- Biophysical chemistry; spectroscopy of proteins and nucleic acids
- X-ray crystallography and high-resolution structure analysis
- Receptors, membrane transport, and intracellular signals
- Biological oxidations, oxidants, and antioxidants
- Lipids and lipid mediators; glycolipids
- Cellular regulation; phosphorylation and dephosphorylation
- Molecular biology of oxygenases and P450 reactions

The new journal ***Nitric Oxide: Biology and Chemistry*** (***Part B of Archives of Biochemistry and Biophysics***), will be provided free of charge in 1997.

Volumes 337–348 (1997), 24 issues
ISSN 0003-9861
In the U.S.A. and Canada: $2295.00
All other countries: $2750.00

FIND US ON THE WEB!
AP NET
Academic Press
www.apnet.com

Log in to the Academic Press Online Library
URL: http://www.idealibrary.com
URL: http://www.europe.idealibrary.com

IDEAL

Sample copies are available on request.
For more information, please write or call:

ACADEMIC PRESS, INC.
Marketing Department
525 B Street, Suite 1900
San Diego, CA 92101-4495, U.S.A.
1-800-894-3434/1-619-699-6742

ACADEMIC PRESS, LTD.
Marketing Department
24-28 Oval Road
London NW1 7DX, U.K.
In Europe call: 0181-300-3322

CALL FOR A FREE SAMPLE

All prices are in U.S. dollars and are subject to change without notice. Canadian customers: Please add 7% Goods and Services Tax to your order.

ARCH97A

Now Available Online!

GENOMICS

International Journal for Analyses of the Human and Other Genomes

Editors-in-Chief

Victor A. McKusick
The Johns Hopkins University, Baltimore, Maryland

Raju S. Kucherlapati
Albert Einstein College of Medicine, Bronx, New York

Frank H. Ruddle
Yale University, New Haven, Connecticut

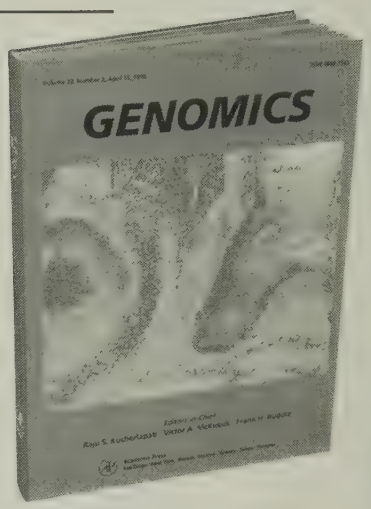

Genomics emphasizes the integration of basic and applied research in human and comparative gene mapping, molecular cloning, large-scale restriction mapping, and DNA sequencing and computational analysis. The journal provides a common meeting ground for those involved in molecular biology and genetics. Technologic and methodologic advances in genomic analysis and interpretation are described, and analyses of the human genome in hereditary and neoplastic diseases are reported. Full-length articles, short communications, brief reports, and reviews are included. In addition, ***Genomics*** promotes efficient communication with the major genetic databases.

RESEARCH AREAS INCLUDE

- Chromosomal assignments of genes and DNA fragments by Mendelian and physical mapping approaches
- Reports of nucleic acid sequences of cloned genes and other interesting genomic regions
- Descriptions of distributions of gene families and genes that share nucleic acid or amino acid sequence domains
- Comparative analyses of genomes to yield structural, functional, or evolutionary insights
- Patterns of genome organization that provide insights into gene regulation and development
- Methods for large-scale genomic cloning, restriction mapping, and DNA sequencing
- Computational methods and descriptions of algorithms for the manipulation of DNA and protein sequence data
- Analyses of genetic linkage data in pursuit of information on inherited disorders
- Development of experimental, computational, and database management techniques of broad applicability in genome research

Database coverage includes Biological Abstracts (BIOSIS), CABS, Current Contents/Life Sciences, Genetics Abstracts, Genome Abstracts, Index Medicus (MEDLINE), Research Alert, ISI's Science Citation Index, and SCISEARCH.

Volumes 39–46 (1997), 24 issues (including annual subject index)

	Institutional Rates	Personal Rates*
In the U.S.A. and Canada:	$1100.00	$295.00
All other countries:	1300.00	333.00

ISSN 0888-7543

Log in to the Academic Press Online Library
URL: http://www.idealibrary.com
URL: http://www.europe.idealibrary.com

IDEAL

Sample are available upon request. For more information, please write or call:

ACADEMIC PRESS, INC.
Marketing Department
525 B Street, Suite 1900
San Diego, CA 92101-4495, U.S.A.
800-894-3434 • 619-699-6742
e-mail: apsubs@acad.com

ACADEMIC PRESS, LTD.
Marketing Department
24-28 Oval Road
London NW1 7DX, U.K.
In Europe call: 0181-300-3322

FIND US ON THE WEB!
APNET
Academic Press
www.apnet.com

All prices are in U.S. dollars and are subject to change without notice. Canadian customers: Please add 7% Goods and Services Tax to your order.
*Personal rates are available only on orders placed directly with the Publisher and paid for with personal funds.

GENOM97A

Society for Developmental Biology

APPLICATION FOR MEMBERSHIP

January 1997 through December 1997

Excerpt from the Bylaws and the Code of the Society: "Self-nomination for full or student membership may be made by the applicant (voted on by the SDB Board of Trustees, January, 1995)." "A doctoral degree or its equivalent and an interest in development and growth in biological systems shall be prerequisites for full membership." "Students enrolled in a graduate program leading to an advanced degree in Developmental Biology or related fields shall be eligible for student membership."

Membership Category: [ ] Full $35.00 [ ] Student $15.00

Name of Candidate: _____

Department/Institution: _____

Street Address/P.O. Box: _____ City: _____

State: _____ Country: _____ Zip+4: _____

Telephone: _____ Fax: _____ E-Mail: _____

Degrees, Granting Institutions and Dates:

_____

Present Position: _____

Please check your area of research within each category:

A. RESEARCH THEME:

1. [ ] Fertilization
2. [ ] Early Development
3. [ ] Organogenesis
4. [ ] Pattern formation
5. [ ] Neurobiology
6. [ ] Genetics
7. [ ] Gene Regulation
8. [ ] Cell Lineage
9. [ ] Cytoskeleton and Cell Surface
10. [ ] Evolution

B. ORGANISMS:

1. [ ] Plant
2. [ ] Invertebrates
3. [ ] Vertebrates
4. [ ] Unicellular Organisms

C. METHODS:

1. [ ] Molecular Biology/Biochemistry
2. [ ] Physiology
3. [ ] Morphology

Signature: _____

Please return completed application with payment to:

Society for Developmental Biology, Inc.
9650 Rockville Pike
Bethesda, Maryland 20814-3998
U.S.A.
Telephone: (301) 571-0647
Fax: (301) 530-7049
E-Mail: sdb@faseb.org

CREDIT CARD INFORMATION (Please type or print clearly) [ ] VISA [ ] MasterCard [ ] American Express

Name on card: _____ Card Number: _____

Expiration Date: _____ Authorized Signature: _____

For information about subscriptions to **DEVELOPMENTAL BIOLOGY**, please contact the publisher: **Academic Press, Inc., Journal Division,** 525 B Street, Suite 1900, San Diego, California 92101-4495. Telephone: (619) 699-6742.

Protein Expression and Purification

Editor-in-Chief
Owen W. Griffith
Medical College of Wisconsin, Milwaukee
Executive Editors
Loran L. Bieber, Richard R. Burgess, John J. Dunn, Andrew P. Seddon, Max D. Summers, Paula Traktman

The power of modern molecular genetics to provide large quantities of proteins that were previously difficult to obtain has sparked an explosion of interest in both practical and theoretical aspects of protein purification.

Protein Expression and Purification is dedicated to providing a forum for information about protein isolation based on conventional fractionation as well as techniques employing various molecular biological procedures to increase protein expression.

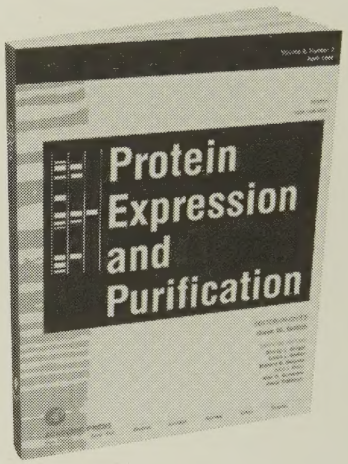

The following types of articles are published:

- Original articles reporting novel or significantly improved isolations of highly purified proteins
- Procedures for expressing and isolating proteins from genetically engineered sources
- Novel or improved molecular biological methods for overexpression of specific proteins
- Review articles that describe and evaluate important approaches to the expression and purification of proteins

Database coverage includes Biological Abstracts (BIOSIS), Chemical Abstracts, Current Contents/Life Sciences, Food Science and Technology Abstracts, Index Medicus (MEDLINE), Research Alert, and Science Citation Index.

Volumes 9–11 (1997), 9 issues
(including annual subject index)
ISSN 1046-5928

	Institutional Rates	Personal Rates*
In the U.S.A. and Canada:	$245.00	$122.50
All other countries:	280.00	147.50

Log in to the Academic Press Online Library
URL: http://www.idealibrary.com
URL: http://www.europe.idealibrary.com

IDEAL

FIND US ON THE WEB!
AP NET
Academic Press
www.apnet.com

Sample copies are available upon request. For more information, please write or call:

ACADEMIC PRESS, INC.
Marketing Department
525 B Street, Suite 1900
San Diego, CA 92101-4495, U.S.A.
1-800-894-3434/1-619-699-6742
e-mail: apsubs@acad.com

ACADEMIC PRESS, LTD.
Marketing Department
24-28 Oval Road
London NW1 7DX, U.K.
In Europe call: 0181-300-3322

for a FREE SAMPLE CALL

All prices are in U.S. dollars and are subject to change without notice.
Canadian customers: *Please add 7% Goods and Services Tax to your order.
Personal rates are available only on orders placed directly with the Publisher and paid for with personal funds.

PEP97A

ACADEMIC PRESS

SCIENCE

Start Your Day with inScight

Science and ***Academic Press*** invite you to start your day with **inScight,** the online information service devoted specifically to late-breaking science news.

Located at **www.apnet.com/inscight,** the site is a free service featuring daily topical news items of interest to researchers, practitioners, students, and anyone with an interest in current science issues. The experienced and preeminent news team of the weekly ***Science*** compiles and provides **inScight** with the day's primary science news stories which are then formatted and maintained online through the Academic Press electronic production services department.

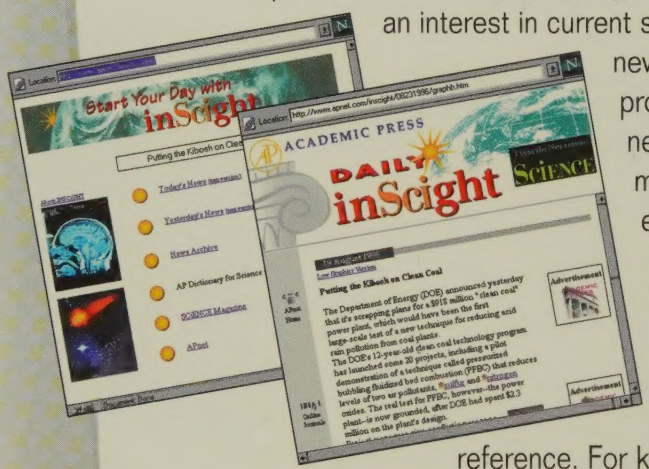

In addition to providing daily science news, **inScight** features a daily-updated network of links to related newsmakers, associations, and appropriate science subjects. Stories are archived for easy searchable reference. For key word descriptions, the service incorporates the **Academic Press Dictionary of Science and Technology,** a comprehensive reference of more than 130,000 entries.

Start your day off right, with inScight!

inScight–
www.apnet.com/inscight

Science–www.sciencemag.org

Academic Press–www.apnet.com/ or www.europe.apnet.com/

LK/KJ/FF 18116